

---

**30 MAY-1 JUNE 2022**  
i3S, PORTO, PORTUGAL  
AND ONLINE



**INSTITUTO  
DE INVESTIGAÇÃO  
E INOVAÇÃO  
EM SAÚDE**  
UNIVERSIDADE  
DO PORTO

The background of the entire page is a photograph of Porto, Portugal, taken during a golden sunset. The Douro River flows through the center, with the city's colorful buildings and the Dom Luís I Bridge visible. The scene is framed by large, semi-circular graphic elements in shades of orange and blue.

# 11<sup>th</sup> Arkadi M. Rywlin International Pathology Slide Seminar Symposium in Anatomic Pathology

.....  
**Course Directors: Saul Suster  
and Manuel Sobrinho Simões**

# Index

Case 1 .....	5
Case 2 .....	10
Case 3 .....	11
Case 4 .....	13
Case 5 .....	17
Case 6 .....	19
Case 7 .....	25
Case 8 .....	27
Case 9 .....	30
Case 10 .....	36
Case 11 .....	38
Case 12 .....	40
Case 14 .....	46
Case 15 .....	49
Case 16 .....	54
Case 17 .....	57
Case 19 .....	61
Case 21 .....	64
Case 22 .....	66
Case 23 .....	71
Case 24 .....	77

Case 25 .....81

Case 26 .....86

Case 27 .....88

Case 28 .....92

Case 29 .....95

Case 30 .....96

Case 32 .....98

Case 33 ..... 101

Case 34 ..... 104

Case 35 ..... 107

Case 36 ..... 111

Case 37 ..... 113

Case 38 ..... 117

Case 39 ..... 121

Case 40 ..... 126

Case 41 ..... 128

Case 42 ..... 130

Case 43 ..... 132

Case 44 ..... 136

Case 45 ..... 143

Case 46 ..... 149

Case 47 ..... 152

Case 48 ..... 157

Case 49 ..... 162

Case 50 ..... 164

Case 51 .....	168
Case 52 .....	171
Case 53 .....	174
Case 54 .....	176
Case 55 .....	180
Case 56 .....	185
Case 57 .....	191
Case 58 .....	202
Case 59 .....	207
Case 60 .....	217
Case 61 .....	222
Case 62 .....	231
Case 63 .....	237
Case 64 .....	240
Case 65 .....	251
Case 66 .....	252
Case 67 .....	257
Case 68 .....	260
Case 69 .....	272
Case 70 .....	273
Case 71 .....	286
Case 72 .....	290
Case 73 .....	294
Case 74 .....	300
Case 75 .....	303

Case 76 ..... 307

Case 77 ..... 310

Case 78 ..... 314

Case 79 ..... 319

Case 80 ..... 322

Case 81 ..... 326

# Case 1

## Ira J Bleiweiss, MD - Mucinous cystadenocarcinoma

---

### Brief clinical history:

A 68-year-old retired nurse presented with a large palpable left breast mass which measured 5cm by ultrasound. It was biopsied and excised. The slides are from the excision.

### Short summary of case:

A 68-year-old retired nurse presented with a large palpable left breast mass which measured 5cm by ultrasound. It was relatively well circumscribed but had slightly irregular margins and had both solid and cystic components on ultrasound. The lesion was initially core biopsied at an outside institution, and a diagnosis of low-grade mucinous carcinoma was rendered. After immunohistochemical results on the core biopsy showed that the tumor was negative for estrogen receptor (ER), progesterone receptor (PR), and Her2neu, neoadjuvant chemotherapy was recommended. The patient, being enterprising and web-savvy, researched her diagnosis and correctly concluded that there was a problem since low grade mucinous carcinoma (colloid carcinoma) should virtually always be positive for ER and PR. To be otherwise would therefore be, for all practical purposes, a contradiction in terms. She then sought a second opinion. The biopsy was reviewed and revealed detached fragments of carcinoma with papillary features and extracellular mucin. The tumor cells had grade II-III nuclear pleomorphism and were identical to lesions one might see in the pancreas or GYN tract; however, a small area of intraductal carcinoma was identified. Despite the presence of intraductal carcinoma, a panel of additional immunohistochemical stains was performed showing that the tumor cells were positive for CK7, focally positive for mammoglobin, and negative for CK-20, CDX-2, WT-1, PAX-8, GATA3, and breast antigen (BRST-2, GCDFP-15), indicating a breast primary. The patient did more research and refused neoadjuvant chemotherapy. Approximately 3 months after initial biopsy, the patient had a lumpectomy with sentinel node sampling, revealing a 6.2 cm mucinous cystadenocarcinoma without DCIS or lymphatic invasion and negative lymph nodes. The tumor was close to the deep margin. She refused chemotherapy and radiation therapy and the tumor recurred

approximately 6 months later as a 3.0 cm irregular mass which was again excised with more negative lymph nodes. As of this writing the patient is lost to follow up.

## **Diagnosis: Mucinous cystadenocarcinoma.**

### **Discussion:**

Mucinous cystadenocarcinoma (MCA) of the breast is a rare variant of invasive duct carcinoma

morphologically similar to MCAs of ovary, pancreas, and gastrointestinal tract. Since its first description

by Koenig and Tavassoli in the year 1998, only 25 cases (including this one) of MCA of breast have been reported in the literature (1-20). Since most consist of descriptive case reports, there is little data about long term prognosis and/or effective therapy.

Koenig and Tavassoli (1) considered this neoplasm a low-grade variant of invasive duct carcinoma based on negative myoepithelial immunohistochemical staining (smooth muscle actin) around the cystic mucinous ducts in their cases. All 4 cases in their study showed variably sized cystic spaces lined largely by a single layer of bland columnar cells with abundant intracellular mucin and basally placed nuclei. Foci of epithelial tufting and papillae formation were noted. The degree of cytologic atypia varied from region to region of the cases with increasing degrees of atypia associated with depletion of mucin. Three of their 4 cases demonstrated focal abrupt squamous differentiation. One of the 4 cases exhibited extravasation of mucin into the surrounding stroma without neoplastic cells. Two of the 4 had associated DCIS, one with a mucinous and micropapillary pattern, closely resembling the invasive carcinoma; the other case contained grade 2 cribriform DCIS without mucin production. One case showed a high-grade sarcomatous component admixed with the mucinous component, favoring metaplastic carcinoma.

All other cases reported to date conform to the original morphological description by Koenig and Tavassoli (1) with only minor variations (2-20). Extravasation of mucin into the adjacent stroma was not a constant feature, being present in 10 cases (1,2,4,8-11,14,20). Furthermore, 8 cases show single or clustered tumor cells floating in the extravasated mucin mimicking ordinary mucinous carcinoma of breast (2,4,9-11,14,20). DCIS with or without mucin production was noted in 14 cases (1,2,4,5,7,10-12,14,16,17,20), 5 of which had histological features in DCIS similar to the of invasive carcinoma, characterized by distended ducts lined by simple or stratified tall columnar cells with abundant intracellular mucin and variable cytologic atypia. In such

cases DCIS was distinguished from invasion by the presence of myoepithelial cells around the cystic ducts (1,4,5,9,11). Chen et al named this pattern of DCIS "MCA in situ" and postulated that it may be derived from mucinous metaplasia of ordinary DCIS (5). The reported size of these invasive tumors ranges from 0.8 to 19.0 cm with the majority larger than 2.0 cm (mean 4.6 cm). The incidence of lymph node involvement appears to be low with only 4 reported cases having ipsilateral axillary lymph node macrometastasis (1,3,12,19). One of our reported cases showed isolated cytokeratin positive tumor cells in one of the axillary lymph nodes dissected at the time of original lumpectomy; however, one cannot definitively exclude the possibility that these cells represented iatrogenically-displaced tumor cells instead of true metastases, given the papillary architecture and friable nature of MCA (20).

Immunohistochemically, almost all reported cases of mammary MCA are negative for estrogen receptor (ER), progesterone receptor (PR), and HER2 expression (1,3,5-9,11-15,17-20) with only 3 cases reported to be positive for HER2 either by IHC or FISH (10,16,18) and one case being positive for ER (8).

Interestingly, the Ki-67 proliferation index has been reportedly high with a range of 20.5% to 90% (5,7).

Despite having a high proliferation index and triple negative biomarker status, the biological behavior of MCA is reportedly favorable. However, most previously reported cases had a short clinical follow-up (ranging from 6 to 24 months) and were alive with no evidence of disease (1,2,5,7-9,11-17). Two cases with a relatively longer follow-up (48 months and 108 months) died of diseases other than MCA (3,4). Only one case presented with local recurrence 8 years (96 months) after lumpectomy with negative margins (20). Distant metastasis has not, to our knowledge, been reported.

From the standpoint of differential diagnosis, this tumor bears a strong histologic resemblance to mucinous and cystic neoplasms of ovary, pancreas, and gastrointestinal tract. Thus, comprehensive clinical and radiological workup should be performed to rule out primary cancer at the above sites.

A panel of IHC stains comprising of CK7, CK20, CDX2, Pax-8, WT-1, CA19-9, GCDFP-15, mammaglobin, GATA-3, ER, and PR will also be useful in this regard. Another equally important diagnostic pitfall is misdiagnosing MCA as primary invasive mucinous carcinoma of breast (colloid carcinoma), a far more common lesion than MCA. Histologically, unlike the cells of invasive mucinous carcinoma, cells of MCA possess abundant intracellular mucin, maintaining this feature in the extravasated stromal mucin. Also, MCA is essentially negative for ER and PR whereas, invasive mucinous carcinoma is fundamentally positive for ER and PR. In fact, in our

experience, in the current case and in several we have seen since, MCA only comes to diagnostic light when the pathologist is surprised that a mucinous carcinoma of breast is staining as negative for ER and PR. This is the moment that should indicate that something is amiss, and the working diagnosis should be reconsidered. The distinction is far from academic since in the light of its characteristic triple-negative profile and relatively larger tumor size at presentation, failing to correctly diagnose this tumor may potentially lead to inappropriate preoperative neoadjuvant chemotherapy. Most previously reported cases have been managed by lumpectomy/mastectomy alone with or without sentinel node biopsy (19). The role of adjuvant chemotherapy or radiation is currently undefined.

## Selected References:

1. Koenig C, Tavassoli FA. Mucinous cystadenocarcinoma of the breast. *Am J Surg Pathol*. 1998;22:698-703.
2. Domoto H, Terahata S, Eyamazaki T, Sato K, Takeo H, Tamai S. Mucinous cystadenocarcinoma of the breast showing sulfomucin production. *Histopathology*. 2000;36:567-569.
3. Honma N, Sakamoto G, Ikenaga M, Kuroiwa K, Younes M, Takubo K. Mucinous cystadenocarcinoma of the breast: a case report and review of the literature. *Arch Pathol Lab Med*. 2003;127:1031-1033.
4. Rosen PP, Scott M. Cystic hypersecretory carcinoma of breast. *Am J Surg Pathol*. 1984;8:31-41.
5. Chen WY, Chen CS, Chen HC, Hung YJ, Chu JS. Mucinous cystadenocarcinoma of the breast coexisting with infiltrating ductal carcinoma. *Pathol Int*. 2004;54:781-786.
6. Coyne JD, Irion L. Mammary mucinous cystadenocarcinoma. *Histopathology*. 2006;49:659-660.
7. Lee SH, Chaung CR. Mucinous metaplasia of breast carcinoma with macrocystic transformation resembling ovarian mucinous cystadenocarcinoma in a case of synchronous bilateral infiltrating ductal carcinoma. *Pathol Int*. 2008;58:601-605.
8. Rakici S, Gonullu G, Gursel SB, Yildiz L, Bayrak IK, Yucel I. Mucinous cystadenocarcinoma of the breast with estrogen receptor expression: a case report and review of the literature. *Case Rep Oncol*. 2009;2:210-216.
9. Gulwani H, Bhalla S. Mucinous cystadenocarcinoma: a rare primary malignant tumor of the breast. *Indian J Pathol Microbiol*. 2010;53:200-202.

10. Petersson F, Pang B, Thamboo TP, Putti TC. Mucinous cystadenocarcinoma of the breast with amplification of the HER2-gene confirmed by FISH: the first case reported. *Hum Pathol*. 2010;41:910-913.
11. Sentani K, Tashiro T, Uraoka N, et al. Primary mammary mucinous cystadenocarcinoma: cytological and histological findings. *Diagn Cytopathol*. 2012;40:624-628.
12. Deng Y, Xue D, Wang X, et al. Mucinous cystadenocarcinoma of the breast with a basal-like immunophenotype. *Pathol Int*. 2012;62:429-432.
13. Li X, Peng J, Zhang Z, Zhang Y. Mammary mucinous cystadenocarcinoma. *Breast J*. 2012;18:282-283.
14. Kim SE, Park JH, Hong S, Koo JS, Jeong J, Jung WH. Primary mucinous cystadenocarcinoma of the breast: cytologic finding and expression of MUC5 are different from mucinous carcinoma. *Korean J Pathol*. 2012;46:611-616.
15. Lin DL, Hu JL, Shao SH, Sun DM, Wang JG. Primary mucinous cystadenocarcinoma of the breast with endocervical-like mucinous epithelium. *Breast Care (Basel)*. 2013;8:445-447.
16. Kucukzeybek BB, Yigit S, Sari AA, Rezanko T, Durak E, Sadullahoglu C. Primary mucinous cystadenocarcinoma of the breast with amplification of the HER2 gene confirmed by FISH—case report and review of the literature. *Pol J Pathol*. 2014;65:70-73.
17. Witherspoon LE, Oxenhandler RW. A rare tumor:mucinous cystadenocarcinoma of the breast. *Am Surg*. 2015;81:E106-E108.
18. Seong M, Ko EY, Han BK, et al. Radiologic findings of primary mucinous cystadenocarcinoma of the breast: a report of two cases and a literature review. *J Breast Cancer*. 2016;19:330-333.
19. Koufopoulos N, Goudeli C, Syrios J, Filopoulos E, Khaldi L. Mucinous cystadenocarcinoma of the breast: the challenge of diagnosing a rare entity. *Rare Tumors*. 2017;9:7016.doi:10.4081/rt.2017.7016.
20. Nayak A, Bleiweiss IJ, Dumoff K, Bhuiya TA. Mucinous cystadenocarcinoma of the breast: report of 2 cases including one with long-term local recurrence. *Intl J Surg Pathol* 2018;26:749-757.

## Case 2

### Leiomyoma of breast (L. DiTommaso)

---

#### Clinical history:

Women, 68 yrs old. No previous oncological history.

#### Pathologic findings.

Left breast, upper external region; deep located, well circumscribed, 2,4 cm lesion; whitish colour, soft consistency. The lesion showed the following immunoprofile: SMA+, desmin+, CD10-, CD34-, bcl2-, p63-; Ki67:< 5%.

#### Diagnosis. Leiomyoma of the breast.

#### Discussion:

This is a rare lesion, the largest series reporting 7 deep leiomyomas (1,2). More frequent is the presence of scattered smooth muscle cells in the stroma of fibroadenomas and hamartomas (3). The origin of leiomyoma of the breast has been variously indicated in myoepithelium, mamillary muscle and vessels wall (4).

#### References.

1. Jones MW et al. Smooth muscle and nerve sheath tumors of the breast. A Clinicopathologic study of 45 cases. *Int J Surg pathol* 1994;2:85-92.
2. Diaz-Arias AA et al. Leiomyoma of the breast. *Hum Pathol*. 1989;20:396-9.
3. Di Tommaso L et al. Smooth muscle cell differentiation in mammary stromo-epithelial lesions with evidence of a dual origin: stromal myofibroblasts and myoepithelial cells. *Histopathology* 2003; 42:448-456
4. Krings G et al. Myofibroblastic, fibroblastic and myoid lesions of the breast. *Semin Diagn Pathol*. 2017; 34:427-437.

## Case 3

### Ira J Bleiweiss, MD - Solid Papillary Carcinoma, High Grade

---

#### Brief clinical history:

A 68 year old female palpated a right breast mass which was biopsied and excised by mastectomy. The slides are from the mastectomy specimen.

#### Short summary of case:

A 68 year old female palpated a right breast mass. Ultrasound revealed a lesion at 7:00, 5 cm from the nipple described as a heterogeneous microlobulated mass measuring 3.9 x 3.1 x 4.0 cm and highly suspicious. An ultrasound-directed core biopsy was read as papillary carcinoma which was ER and PR negative. A definitive diagnosis of invasion was deferred to excision. On physical examination the mass was felt to be ~6.0 cm. Because of the size of the lesion, she underwent a mastectomy with sentinel node biopsy four months later. Grossly the mass was described as well circumscribed with central necrosis and measured 6.5x5.2x3.5 cm. Microscopically there were multiple foci of infiltrating moderately differentiated duct carcinoma, the largest of which measured 6 mm, surrounding a large mass of intraductal carcinoma, solid, papillary, and cribriform types with necrosis involving intraductal papilloma with focal secondary cystic duct dilatation. No lymphatic invasion was present and two sentinel nodes were negative. Skeletal muscle (deep margin) was also negative, although 0.4 cm at closest extent. The invasive carcinoma was triple negative (ER, PR, Her2). Of note, the biopsy site was associated with intraductal carcinoma. Because of the triple negative nature of the tumor, she underwent 4 cycles of Taxotere/Cytoxan chemotherapy. Approximately 1.5 years later she presented with a tender palpable lateral chest wall mass. She refused intervention and the mass gradually enlarged until it was biopsied and resected after several months. The tumor was well circumscribed, purely invasive with areas of necrosis, measured 4.74 cm, and again was triple negative. Although focal residual breast tissue was present deep to the tumor, no intraductal carcinoma was present, and the tumor largely involved the prior surgical site with invasion of overlying skin. Repeat sentinel node biopsy yielded two negative lymph nodes. She is currently undergoing chemotherapy with Adriamycin/Cytoxan, and radiation therapy to the chest wall is likely to follow.

## Diagnosis: Solid Papillary Carcinoma, High Grade, focally Invasive

### Discussion:

Solid papillary carcinoma of the breast is a somewhat controversial diagnosis for a rare entity first described by Maluf and Koerner (1). Their initial findings were further elucidated by other authors, most notably Nassar, et al (2) and Guo, et al (3). The lesion is composed of multiple individually well-circumscribed nodules which resemble intraductal carcinoma. The proliferation is made up of low grade tumor cells which often grow around subtle, delicate vascular papillary structures. Extravasated mucin may be seen as well neuroendocrine differentiation, often accompanying the mucin. Typically, but not exclusively, the tumor occurs in an elderly population and, as might be expected it is positive for estrogen receptor and progesterone receptor and negative for Her2neu. Despite the lack of morphologic or immunohistochemical evidence of myoepithelial cells at the periphery, most, though by no means all, authors consider these intraductal lesions, in part because of their indolent behavior and relative lack of nodal spread. That being said, a large number of reported cases contain conventional areas of invasive carcinoma, and it is these cases that in large part are associated with lymph node metastasis and infrequent local recurrence (approx. 4%), distant metastasis (approx. 4.5%), and death due to carcinoma (approx. 3%). There are no other consistently described histologic predictors of adverse events. The current case is unusual in that it has the growth pattern of solid papillary carcinoma but is of high histologic grade and triple negative immunophenotype, factors which no doubt contributed to its rapid local recurrence despite adjuvant chemotherapy.

### Selected References:

1. Maluf H, Koerner FC/ Solid papillary carcinoma of the breast: a form of intraductal carcinoma frequently associated with mucinous carcinoma. *Am J Surg Pathol* 1995;19:1237-1244.
2. Nassar H, Qureshi H, Adsay NV, Visscher D. Clinicopathologic analysis of solid papillary carcinomas of the breast and associated invasive carcinomas. *Am J Surg Pathol* 2006;30:501-507.
3. Guo S, Wang Y, Rohr J, et al. Solid papillary carcinoma of the breast: a special entity needs to be distinguished from conventional invasive carcinoma avoiding over-treatment. *The Breast* 2016;26:67-72.

## Case 4

Anais Malpica, M.D.

---

### Clinical History:

A 56-year-old female, status-post left salpingo-oophorectomy presented to the emergency room with acute urinary retention. CT scan showed a 12.0 cm right pelvic mass. Her serum CA125 was 1,104 U/mL. She underwent a TAHRS and staging.

### Pathology Findings

#### Gross Features

The right ovary was totally replaced by a 13.5 x 9.0 x 6.5 cm firm, white mass

#### Microscopic Features

The tumor shows a proliferation of oval, round or irregular glands lined by columnar cells, with nuclei arranged perpendicularly to their lumens. The nuclei have an open chromatin and in some areas the nuclei appear clear with rare grooves. There are areas of squamous differentiation and an eosinophilic material in the luminal spaces.

#### Immunohistochemical Features

The tumor cells are positive for ER (>90%, strong) and PR (>90%, strong) while negative for TTF-1 and GATA-3.

**Diagnosis: Ovary, Endometrioid Carcinoma, Grade 2, with Squamous Differentiation.**

### Discussion

The presence of eosinophilic material in the luminal spaces and some of the nuclear features raise the possibility of mesonephric-like carcinoma. However, the presence of conspicuous squamous differentiation favors endometrioid carcinoma. As we have encountered a rare case of metastatic endometrial mesonephric-like carcinoma with focal squamous differentiation, a battery of immunohistochemical studies, hormone receptors (ER, PR), GATA-3 and TTF-1, was obtained to confirm the diagnosis. In this discussion, the following points are addressed:

**1. Mesonephric-like carcinoma of the ovary**

This is an uncommon tumor that shares histological and immunohistochemical features with mesonephric carcinoma of the cervix and mesonephric-like carcinoma of the endometrium. Patients have a wide age range, 29 to 81 years, and they usually present with pelvic/abdominal pain, pelvic mass or abdominal distention. Occasionally, the tumor is incidentally detected. CA125 levels have ranged from 12.2 U/mL to 108.8 U/mL. About 50% of the cases present with FIGO stage I disease. Tumor size ranges from 4.7 cm to 15 cm. Microscopically, there are several architectural patterns (tubular, glandular, solid, papillary, and trabecular) and a variable amount of eosinophilic material in the luminal spaces. Cells are typically columnar with amphophilic or basophilic cytoplasm, clear nuclei and nuclear grooves. In areas, the cells can be flattened, cuboidal or hobnail and with light eosinophilic or clear cytoplasm -mimicking clear cell carcinoma. Spindle cells can be seen. Atypia is usually mild to moderate, although it can be severe in certain areas. The mitotic index is variable. The association with endometriosis is frequent as it is the association with other ovarian tumors (i.e., low grade serous carcinoma, high grade serous carcinoma, borderline tumor -serous or endometrioid, clear cell carcinoma, mature teratoma, mixed germ cell tumor). Of note, we have encountered a case where the association with low grade serous carcinoma was metachronous.

Immunohistochemical studies show that typically the tumor cells are positive for PAX-8, GATA-3 and TTF-1 while negative for ER and PR; p53 shows a wild type expression pattern. Supplemental immunostains are CD10 (luminal expression) and calretinin. Some caveats are: 1) the expression of GATA-3 and TTF1 shows an inverse pattern, 2) an occasional case can have focal and weak/moderate expression of hormone receptors, and 3) this tumor can be positive for napsin A and HNF1. KRAS and PIK3CA mutations are commonly seen. This tumor is often misclassified and when compared with low grade endometrioid ovarian carcinoma, it shows a higher incidence of advanced stage disease and propensity to metastasis in lung and liver

**2. Endometrioid carcinoma of ovary, some relevant points, including immunohistochemical and molecular features**

Some of the features traditionally used to facilitate the recognition of ovarian endometrioid carcinoma are: the presence of squamous differentiation or an adenofibromatous background, an association with endometriosis or borderline tumor - endometrioid, mixed epithelia, seromucinous, in the context of glands like the ones seen in low grade endometrioid adenocarcinoma arising in the endometrium. Most cases are either grade 1 or 2. Immunohistochemically, this tumor is usually positive for ER and PR

and essentially negative for WT-1; p53 expression is wild type and p16 is focally or patchy positive. Low grade tumors, particularly those with squamous morules show nuclear expression of beta-catenin. Caveats: 1) WT-1 can be diffusely positive 2) other markers that can give an aberrant immunoreactivity are: CK20, CDX2, SATB2, TTF-1, and GATA-3 (focal), 3) occasional cases can be negative for CK7, PAX8, ER and PR. Loss of MMR proteins, most commonly MLH1 and PMS2, occurs in 10% to 20% of ovarian endometrioid carcinomas, in most cases due to MLH1 methylation. Of note, endometrioid carcinoma is the most common type of Lynch-syndrome associated ovarian cancer. A rare case can show Her2 amplification. Mutations seen in ovarian endometrioid carcinoma are: CTNNB1, PIK3CA, ARID1A, PTEN, KRAS, TP53, and SOX8. POLE mutation is uncommon (6%). Cases with CTNNB1 mutation are predominantly stage 1/2 with excellent outcome while cases with TP53 mutation are stage III/IV and have a poor survival.

## References:

### Mesonephric-like carcinoma

1. Pors J, Segura S, Chiu DS, et al. Clinicopathologic Characteristics of Mesonephric Adenocarcinomas and Mesonephric-like Adenocarcinomas in the Gynecologic Tract: A Multi-institutional Study. *Am J Surg Pathol*. 2021 Apr 1;45(4):498-506.
2. da Silva EM, Fix DJ, Sebastiao APM, et al. Mesonephric and mesonephric-like carcinomas of the female genital tract: molecular characterization including cases with mixed histology and matched metastases. *Mod Pathol*. 2021 Aug;34(8):1570-1587.
3. Chang CS, Carney ME, Killeen JL. Two Cases of Mesonephric-like Carcinoma Arising From Endometriosis: Case Report and Review of the Literature. *Int J Gynecol Pathol*. 2022 Feb 22. Epub ahead of print. PMID: 35191427.
4. Deolet E, Arora I, Van Dorpe J, et al. Extrauterine Mesonephric-like Neoplasms: Expanding the Morphologic Spectrum. *Am J Surg Pathol*. 2022 Jan 1;46(1):124-133.
5. Koh HH, Park E, Kim HS. Mesonephric-like Adenocarcinoma of the Ovary: Clinicopathological and Molecular Characteristics. *Diagnostics (Basel)*. 2022 Jan 27;12(2):326
6. Euscher ED, Marques-Piubelli ML, Ramalingam P, et al. Extra-Uterine Mesonephric-Like Carcinoma Is Associated with Endometriosis and May Behave Aggressively. *Mod Pathol* (35) Supp 2, March 2022: 743

### Endometrioid carcinoma

1. Lim D, Murali R, Murray MP, Veras E, Park KJ, Soslow RA. Morphological and Immunohistochemical Reevaluation of Tumors Initially Diagnosed as Ovarian Endometrioid Carcinoma With Emphasis on High-grade Tumors. *Am J Surg Pathol*. 2016 Mar;40(3):302-12.

2. Rajendran S, McCluggage, WG. WT1 Positive Ovarian Endometrioid Tumors: Observations From Consult Cases and Strategies for Distinguishing From Serous Neoplasms, *International Journal of Gynecological Pathology*: March 2022 - Volume 41 - Issue 2 - p 191-202
3. McMullen-Tabry, Emily R. M.D.; Sciallis, Andrew P. et al.. Unusual Ovarian Tumors With Endometrioid Proliferations Co-Expressing Estrogen Receptor and CDX-2 Arising in Cystadenofibromatous Background, *International Journal of Gynecological Pathology*: February 11, 2022 - Volume - Issue - doi: 10.1097/PGP.0000000000000862
4. Kubba LA, McCluggage WG, Liu J, et al. Thyroid transcription factor-1 expression in ovarian epithelial neoplasms. *Mod Pathol* 2008;21:485-90.
5. Rambau PF, Duggan MA, Ghatage P, et al. Significant frequency of MSH2/MSH6 abnormality in ovarian endometrioid carcinoma supports histotype-specific Lynch syndrome screening in ovarian carcinomas. *Histopathology* 2016;69:288-97.
6. Crosbie EJ, Ryan NAJ, McVey RJ, et al. Assessment of mismatch repair deficiency in ovarian cancer. *J Med Genet*. 2021 Oct;58(10):687-69
7. Bennett JA, Pesci A, Morales-Oyarvide V, et al. incidence of mismatch repair protein deficiency and associated clinicopathologic features in a cohort of 104 ovarian endometrioid carcinomas. *Am J Surg Pathol* 2019;43:235-43
8. Chau B, Balzer B, Maluf H, Medeiros F. HER2 Expression in Ovarian Endometrioid Carcinoma. *Mod Pathol* (35) Supp 2, March 2022: 728
9. Hollis, R.L., Thomson, J.P., Stanley, B. et al. Molecular stratification of endometrioid ovarian carcinoma predicts clinical outcome. *Nat Commun* 11, 4995 (2020)

# Case 5

Contributed by Delia Perez-Montiel, MD

---

## Clinical History:

A 21-year-old female with abdominal pain and abdominal distension of 2 months. Abdominal CT with ovarian mass. CA125: 244. Ascites and pleural effusion. Resection of abdominal mass and frozen section was performed. The rest of pelvic cavity with adhesions.

## Pathology findings:

Grossly a 16x9x8 cm multinodular soft mass was received in frozen section area. Surface was tan, soft. Internal surface was a multicystic mass with clear fluid. Internal surface of the cysts were smooth, without papillae. The walls of the cysts showed variable thickness of fibrous and edematous appearance. Microscopically, cystic walls showed areas with cellular stroma-endometrial type with areas of fibrosis with thick-walled blood vessels. The cystic lumens were lined by epithelium with tubaric, mucinous and endometrial features. Only, after an extensive sampling, areas with endometrial glands without atypia surrounded by endometrial stroma were found.

**Immunohistochemistry stains:** CD10 positive in cellular stroma, Estrogen receptors positive in glands and stromal cells.

**Diagnosis: Polypoid endometriosis.**

## Comment:

Endometriosis is an extremely common condition, particularly in women in the reproductive years. Many symptoms and sites involved have been described, some of them in uncommon regions and show uncommon histologic variants. One of these variants is the polypoid endometriosis. This disease is a rare presentation describe by Mostoufizadeh and Scully in 1980.

It has been described or could present as a mass in the colon and rectum (lumen and wall), cervical, uterine serosa, peritoneum, retroperitoneum, bladder, ureter, urethra,

ovary, salpinx, vagina, pouch of Douglas and periadrenal tissue. Some series have shown, unlike to classical endometriosis, a high prevalence in peri-menopausal and post-menopausal women, some of them associated to hormonal replacement treatment.

Grossly, lesions varied from 0.4 to 14 cm in size and were typically solid and fleshy, but also showed variable degrees of cystic change and hemorrhage. Histological findings include a spectrum of endometrial changes that varies from atrophic glands to atypical hyperplasia with practically all kind of metaplasias described as tubaric, mucinous, squamous and papillary. Stroma varies from inactive to proliferative with fibrous areas or polyp like and hemorrhagic.

Malignant transformation is rare but a few cases of adenocarcinomas and sarcomas related have also been described.

Main differential diagnoses include adenosarcoma, but prominent phyllodes like architecture and periglandular cuffing with mitosis are absent in polypoid endometriosis.

## Selected References:

1. McCluggage WG Endometriosis-related pathology: a discussion of selected uncommon benign, premalignant and malignant lesions..Histopathology. 2020 Jan;76(1):76-92. doi: 10.1111/his.13970.
2. Parker RL, Dadmanesh F, Young RH, Clement PB Polypoid endometriosis: a clinicopathologic analysis of 24 cases and a review of the literature. .Am J Surg Pathol. 2004 Mar;28(3):285-97. doi: 10.1097/00000478-200403000-00001.
3. Miyoshi S, Yamaguchi K, Chigusa Y, Sunada M, Yamanoi K, Horie A, Hamanishi J, Kondoh E, Mandai M Fertility preservation of polypoid endometriosis: Case series and literature review. J Obstet Gynaecol Res. 2022 Feb;48(2):502-509. doi: 10.1111/jog.15096. Epub 2021 Nov 11.PMID: 34766411 Review.
4. Clement PB The pathology of endometriosis: a survey of the many faces of a common disease emphasizing diagnostic pitfalls and unusual and newly appreciated aspects. Adv Anat Pathol. 2007 Jul;14(4):241-60. doi: 10.1097/PAP.0b013e3180ca7d7b.

## Case 6

Presented by Ricardo R. Lastra, University of Chicago

---

### Clinical History:

80-year-old woman with presenting with a 10.5 cm cystic and solid right ovarian mass and peritoneal tumor deposits. Submitted slides for the symposium were cut from the metastatic tumor deposits on the peritoneum. A previous peritoneal core needle biopsy showed metastatic adenocarcinoma with focal adenoid-cystic-like features. Hysterectomy, bilateral salpingo-oophorectomy, and omentectomy were performed.

### Pathology:

Gross findings: The external surface of the right ovarian mass showed areas of coarse granularity. The cut surface was predominantly solid, tan-gray with focal cystic components containing clear fluid. A subset of cysts showed papillary excrescences. The right fallopian tube and the left adnexal structures were grossly unremarkable. The omentum and the pelvic peritoneum showed numerous tumor nodules (0.5 – 2.5 cm), also involving the serosal aspect of the uterus.

*Microscopic:* The ovarian mass is composed of **two histologically distinct components**. The predominant tumor component (2/3<sup>rd</sup> of the ovarian mass) is a partly cystic, **low grade serous carcinoma** arising from a serous borderline tumor with ovarian surface involvement.

*Immunohistochemical study:* Diffuse positivity for CK7, EMA, PAX8, WT1, and PR but only focal staining for ER and p16. CK20, GATA3, and TTF-1 are negative. The p53 staining-pattern is “wild type” and Ki-67 indicates a low proliferation rate.

The second tumor component (1/3<sup>rd</sup> of the ovarian mass) mainly has a solid to microglandular appearance. It exhibits an unusual histologic pattern for a primary ovarian neoplasm but does show *close resemblance to mesonephric adenocarcinomas of the cervix*, which may also occur rarely in other parts of the gynecologic tract (vaginal wall and uterine corpus). This **mesonephric-like adenocarcinoma of the ovary**, similarly to its cervical counterpart, exhibits a variety of architectural patterns from solid islands to small tubular and papillary structures in a variably hyalinized stroma. Many of the tubules typically contain eosinophilic, colloid-like secretions. The tumor cells are relatively small,

cuboidal, non-mucinous epithelial cells having round to focally angulated nuclei containing small nucleoli. There is no significant nuclear pleomorphism but mitotic figures can easily be identified.

*Immunohistochemical study:* Diffuse immunoreactivity for CK7, EMA, PAX8, GATA3, and TTF-1, with focal/weak staining for p16, p63, and inhibin. CD10 immunoreactivity is seen within the luminal border of some of the neoplastic tubules. The following markers are negative: CK20, ER, PR, thyroglobulin, PTH, chromogranin, synaptophysin, calretinin, WT1, and CDX2. Ki-67 staining indicates low proliferative activity, but higher than that seen in the low-grade serous carcinomatous component. The p53 staining-pattern is "wild type".

The interface of the two histologically different components shows mingling.

Omental/peritoneal/uterine serosal tumor deposits: Most of the metastatic tumor nodules are composed of mesonephric-like adenocarcinoma, however some contain both tumors and a few only low grade serous carcinoma.

Uterus: The serosal deposits of mesonephric-like adenocarcinoma focally invade into the outer third of the myometrium. The endometrium is atrophic. The uterine cervix is free of tumor. Neither the cervix nor the uterine corpus contains mesonephric (Wolffian) remnants, on extensive sampling.

**Differential diagnosis** of the *mesonephric-like adenocarcinoma of the ovary* includes metastatic cervical mesonephric adenocarcinoma, microglandular endometrioid carcinoma, adenoid cystic carcinoma, thyroid carcinoma, FATWO, and sex-cord tumors.

**Key question:**

Is this biphenotypic neoplasm a *collision tumor* of a low-grade serous carcinoma with a mesonephric-like adenocarcinoma of the right ovary or *one neoplasm with dual differentiation*?

In order to answer the question, molecular study was performed. On molecular analysis, the serous borderline tumor, the primary and metastatic low-grade serous carcinoma, and the primary and metastatic mesonephric-like adenocarcinoma each harbored a shared *NRAS* p.Q61R hotspot mutation, shared gains in chromosome 1q and 18p, and shared losses in chromosomes 1p, 18q, and 22. *These shared molecular features indicate a clonal relationship between all morphologic elements of this ovarian adenocarcinoma, suggesting that at least some mesonephric adenocarcinomas may arise from Mullerian precursors* (Chapel DB et al. 2017).

## Final diagnosis: Ovarian adenocarcinoma with combined low-grade serous and mesonephric-like differentiation

### Comments:

Mesonephric adenocarcinoma is a rare but well-recognized subtype of adenocarcinomas of the uterine cervix (Clement PB et al, 1995; Howitt BE, Nucci MR, 2018). It is thought to arise from Wolffian (mesonephric) remnants located in the lateral wall of the cervix. Exceptionally rarely it may also occur in the vaginal wall and in the uterine corpus. McFarland et al (2016) described a series of hormone receptor-negative, TTF-1 positive ovarian and uterine adenocarcinomas, which they designated as “mesonephric-like adenocarcinomas” (5 ovarian and 7 uterine corpus). The authors point out that the histologic features of these mesonephric-like adenocarcinomas are comparable/identical to those that occur in the uterine cervix. However, they recommended the term mesonephric-like adenocarcinomas until their histogenesis is firmly established as no excess numbers of Wolffian (mesonephric) remnants were identified next to these tumors. Neither the ovarian nor the uterine “mesonephric-like” adenocarcinomas in McFarland’s series were associated with any other type of cancer. At the time of this case, this was the first described instance of a mesonephric-like carcinoma of the female genital tract with an adjacent distinct component (low-grade serous carcinoma), in which molecular studies indicated a clonal relationship (*NRAS* p.Q61R mutation) between all morphologic elements, suggesting that at least some mesonephric adenocarcinomas may arise from Mullerian precursors (Chapel DB et al, 2017). Subsequent publications have demonstrated similar associations of mesonephric-like carcinomas with adjacent histologically distinct neoplastic components, including mucinous and endometrioid components (da Silva et al. 2021). Studies demonstrating the molecular composition of mesonephric-like carcinomas of the female genital tract published in the recent years have demonstrated overlapping *KRAS* mutations (often seen in mesonephric carcinomas of the cervix) with molecular alterations more classically associated to Mullerian tumors (including *PTEN*, *NRAS*, and *BRAF*) (Mirkovic et al. 2018, McCluggage WG et al. 2018, and da Silva et al. 2021). In addition, mixed mesonephric adenocarcinoma and high-grade neuroendocrine carcinoma of the uterine cervix has been published with a conclusion of clonal origin of the 2 components, rather than a collision tumor (Cavalcanti MS et al, 2016). A recent retrospective, combined morphologic and molecular study identified *KRAS*-mutated mesonephric-like adenocarcinomas of the endometrium which represents ~1% of all endometrial carcinomas (Kolin DL et al. 2019). Mirkovic J et al 2018, reported

that mesonephric adenocarcinomas are commonly associated with *KRAS* and *NRAS* mutations as well as mutations in some chromatin remodeling genes (*ARID1A*, *ARID1B* or *SMARCA4*).

Mesonephric adenocarcinomas are assumed to arise from benign mesonephric (Wolffian) remnants. When they occur in the cervix, these remnants are often identified in the deep lateral cervical wall. Rarely mesonephric remnants are seen lateral to the uterine corpus and the vagina. These embryologic remnants can usually be identified in the para-ovarian region (paroophoron, epoophoron). Another neoplasm of presumed mesonephric origin, FATWO, may occur rarely in the ovary. One can speculate that, similar to FATWO, which arise most commonly in a para-ovarian/para-tubal location but which occur occasionally in the ovary, mesonephric-like adenocarcinomas could arise from mesonephric remnants around the ovary and get incorporated into the ovary. However, given the described morphologic and molecular findings, these are now favored to represent Mullerian derived carcinomas that demonstrate mesonephric-like differentiation.

Even though these tumors, independent of anatomic sites in the gynecologic tract, have typical histologic features and immunohistochemical profile, they can be confused with several primary and metastatic neoplasms. A number of immunohistochemical markers (negative CEA, and ER/PR), together with staining for PAX8, GATA3, CD10 are useful in the diagnosis of mesonephric carcinomas. (Silver SA et al, 2001; Howitt BA et al, 2015; Roma AA et al, 2015). The frequent immunoreactivity for TTF1, together with the tubular structures containing eosinophilic, colloid-like secretion, may lead to the erroneous diagnosis of thyroid carcinoma (Zhang PJ et al, 2009). Mesonephric adenocarcinomas, however, are negative for thyroglobulin. In addition, these tumors are HPV negative and express p16 only focally. For detailed discussion on the differential diagnosis and immunohistochemical profile, see the excellent paper by McFarland et al, 2016.

Although it is difficult to provide prognostic parameters on the basis of the limited number of published cases, recent data seems to suggest the potential for aggressive behavior, and clearly the tumor stage has an impact on prognosis (Euscher ED et al. 2019; Horn LC et al, 2020). The patients' ages, in the cited series, ranged from 36-76 years. Follow up data from the largest available series (da Silva et al. 2021) demonstrated metastatic disease in 78% of patients.

## References:

1. Da Silva EM et al. Mesonephric and mesonephric-like carcinomas of the female genital tract: molecular characterization including cases with mixed histology and matched metastasis. *Mod Pathol.* 2021 Aug;34(8):1570-1578

2. Horn LC et al. Mesonephric-like adenocarcinomas of the uterine corpus: report of a case series and review of the literature indicating poor prognosis for this type of endometrial adenocarcinoma. *J Cancer Res Clin Oncol*. 2020 Apr;146(4):971-983
3. Euscher ED et al. Mesonephric-like carcinoma of the endometrium. A subset of endometrial carcinoma with an aggressive behavior. *Am J Surg Pathol*. 2020 Apr;44(4):429-443
4. Kolin DL et al. A combine morphologic and molecular approach to retrospectively identify KRAS-mutated mesonephric-like adenocarcinomas of the endometrium. *Am J Surg Pathol*. 2019 Mar; 43(3):389-398
5. Howitt BE, Nucci MR. Mesonephric proliferations of the female genital tract. *Pathology*. 2018 Feb;50(2):141-150
6. McCluggage WG et al. Ovarian combined low-grade serous and mesonephric-like adenocarcinoma: further evidence for a Mullerian origin of mesonephric-like adenocarcinoma. *Int J Gyn Pathol*. 2020 Jan;39(1):84-92
7. Mirkovic J et al. Targeted genomic profiling reveals recurrent KRAS mutations in mesonephric-like adenocarcinomas of the female genital tract. *Am J Surg Pathol*. 2018 Feb;42(2):227-233
8. Chapel DB et al. An ovarian adenocarcinoma with combined low-grade serous and mesonephric morphologies suggests a Mullerian origin for some mesonephric carcinomas. *Int J Gyn Pathol*. 2018 Sep;37(5):448-459
9. McFarland M, Quick CM, McCluggage WG. Hormone receptor-negative, thyroid transcription factor 1-positive uterine and ovarian adenocarcinomas: report of a series of mesonephric-like adenocarcinomas. *Histopathology*. 2016 Jun;68(7):1013-1020
10. Cavalcanti MS, Schultheis AM, Ho C et al. Mixed mesonephric adenocarcinoma and high-grade neuroendocrine carcinoma of the uterine cervix: case description of a previously unreported entity with insights into its molecular pathogenesis. *Int J Gynecol Pathol*. 2017 Jan;36(1):78-89
11. Mirkovic J, Sholl LM, Garcia E et al. Targeted genomic profiling reveals recurrent KRAS mutations and gain of chromosome 1q in mesonephric carcinomas of the female genital tract. *Mod Pathol*. 2015 Nov;28(5):1504-1514
12. Howitt BE, Emori MM, Drapkin R et al. GATA3 is a sensitive and specific marker of benign and malignant mesonephric lesions in the lower female genital tract. *Am J Surg Pathol*. 2015 Oct; 39(10):1411-1419
13. Roma AA, Goyal A, Yang B. Differential expression patterns of GATA3 in uterine mesonephric and nonmesonephric lesions. *Int J Gynecol Pathol*. 2015 Sep;34(5):480-486
14. Zhang PJ, Gao HG, Pasha TL, Litzky L, Livolsi VA. TTF-1 expression in ovarian and uterine epithelial neoplasia and its potential significance, an immunohistochemical assessment with multiple monoclonal antibodies and different secondary detection systems. *Int J Gynecol Pathol*. 2009 Jan;28(1):10-18

15. Silver SA, Devouassoux-Shisheboran M, Mezzetti TP, Tavassoli FA. Mesonephric adenocarcinomas of the uterine cervix: a study of 11 cases with immunohistochemical findings. *Am J Surg Pathol.* 2001 Mar;25(3):379-387
16. Clement PB, Young RH, Keh P, Ostor AG, Scully RE. Malignant mesonephric neoplasms of the uterine cervix. Report of eight cases, including four with malignant spindle cell component. *Am J Surg Pathol* 1995 Oct;19(10):1158-1171

## Case 7

Masaharu Fukunaga, M.D. Shin-yurigaoka General Hospital,  
Kawasaki, Japan

---

### History:

A 46-year-old, gravida 1, para 1, female presented with a month history of abnormal vaginal bleeding. Physical examination revealed a 4 cm, exophytic friable mass in the uterine cervix. A cervical biopsy was performed and the initial pathologic diagnosis was endometrioid adenocarcinoma. She underwent a total abdominal hysterectomy, bilateral salpingo-oophorectomy, pelvic lymphadenectomy and omentectomy. The patient is alive with no evidence of disease at 10 months after the surgery.

### Pathology:

**Macroscopic features:** A 4 cm, exophytic, almost circumferential, whitish yellow, friable mass.

**Immunohistochemical studies:** CK7, CAM5.2, EMA, calretinin: (+). Vimentin, CEA, ER and PgR receptors, CD10 (-).

**Diagnosis: Mesonephric adenocarcinoma of the uterine cervix with mesonephric hyperplasia.**

### Comments:

This slide shows three components, mesonephric adenocarcinoma, atypical mesonephric hyperplasia (cystically dilated glandular elements with atypia) and typical mesonephric hyperplasia. Mesonephric adenocarcinoma exhibits varying morphologies; ductal, tubular, papillary and cystic patterns. Spindle cells or heterologous (rhabdomyosarcoma or cartilage) elements were sometimes observed. A lobular or diffuse mesonephric hyperplasia was observed adjacent to mesonephric adenocarcinoma of the uterine cervix in almost all reported cases. The mesonephric adenocarcinoma presented here is considered arising from the mesonephric hyperplasia based on the overall histology, the presence of atypical hyperplasia and immunohistochemical features. Mesonephric

adenocarcinoma may be more common than what is suggested by the previously reported cases owing to their morphologic diversity and potential misclassification as a Mullerian tumors or florid mesonephric hyperplasia. The present tumor was limited in the uterine cervix. Sage I mesonephric adenocarcinoma seems to have a more indolent behavior than their Mullerian counterparts. I hope that members enjoy this typical case of mesonephric adenocarcinoma.

## References:

1. Bague S, Rodriguez IM, Prat J. Malignant mesonephric tumors of the female genital tract: a clinicopathologic study of 9 cases, *Am J Surg Pathol.* 28 (2004) 601-607.
2. Clement PR, Young RH, Keh P et al. Malignant mesonephric neoplasms of the uterine cervix: report of eight cases, including four with a malignant spindle cell component. *Am J Surg Pathol.* 19 (1995):1158-1171.
3. Ferry JA, Scully RE. Mesonephric remnants, hyperplasia, and neoplasia in the uterine cervix: a study of 49 cases, *Am J Surg Pathol.* 14 (1990) 1100-1111.
4. McFarland M, Quick CM, McCluggage WG. Hormone receptor-negative, thyroid transcription factor 1-positive uterine and ovarian adenocarcinomas: report of a series of mesonephric-like adenocarcinoma. *Histopathology.* 68(2016):1013-1020.
5. Mirkovic J, McFarland M, Garcia E, et al. Targeted genomic profiling reveals recurrent KRAS mutation in mesonephric-like adenocarcinomas of the female genital tract. *Am J Surg Pathol.* 42(2017):227-233.

## Case 8

Contributed by Delia Perez-Montiel, MD

---

### Clinical History:

A 75 year old female with history of non Hodgkin lymphoma since 1994 in remission. During follow-up, after 24 years of initial diagnosis of lymphoma, she presented with abdominal discomfort and a toraco-abdominal CT scan showed a pelvic mass, apparently in uterine ligament. Tumor markers were negative.

Resection of abdominal mass and frozen section was performed. During surgery, abdominal cavity was clear of disease.

### Pathology findings:

Grossly a 15x9 cms multinodular soft mass was received in frozen section area. Surface was tan, soft. Internal surface was a multicystic mass with hemorrhagic appearance. Microscopically, the tumor showed extensive hemorrhagic areas, tumor areas shows nests of polygonal large cells with abundant clear cytoplasm, some of them with granular eosinophilic cytoplasm. Border cells were well delimited, nuclei were large and with prominent nucleoli. The nest of tumor was delimited by thin vessels. Necrosis was extensive; however, mitoses were scant. No infiltration to uterine wall or ovary was demonstrated.

Immunohistochemistry stains: HMB45 and Actin were positive in neoplastic cells. CKAE1/AE3, CK7, CK20, EMA, S100 Protein, Calretinin, C-Kit, Melan A and vimentin were Negative.

**Diagnosis: Pcoma.**

### Comment:

Tumors showing perivascular epithelioid cell differentiation (PEComa) is a rare group of mesenchymal tumors with broad histologic features such as nests and/or fascicles of epithelioid cells with clear to granular eosinophilic cytoplasm and/or spindle cell

arrangement around blood vessels with great variation in the proportion of epithelioid and spindle cells. Characteristically, it shows immunohistochemical immunoreactivity to HMB-45 and expression of the other melanoma-associated antigen MART-1 (Melan-A), besides variable coexpression of muscle markers, cytokeratins, and S-100 protein. Some cases show premelanosomes in electron microscopy.

The term PEComa was used by Bonneti et al for the first time in 1992 to describe and unify the concept for tumors that systematically showed melanocytic and smooth muscle differentiation such as angiomyolipoma and the clear cell sugar tumor of the lung, some of the associated to tuberous sclerosis. This concept has been used to group several tumors in the PEComa family including entities such as angiomyolipoma, lymphangiomyoma, and clear cell tumors occurring in the kidney, lung, pancreas, uterus, breast, ligament teres, falciform ligament, eye orbit, soft tissue, urinary bladder, and recently have been described in skin and urethra. The origin of these lesions is thought to be the walls of blood vessels because these cells are intimately related to such structures. Although, the real histologic origin of these neoplasms is still not clear. In the gynecological area, the uterine corpus is the most frequent site of presentation, others sites are broad ligament, ovary, cervix, vagina and vulva. Two distinct molecular groups-classic PEComas with TSC mutations and TFE3-translocation associated PEComas with TFE3 fusions have been described. Recognition of the first group is imperative as these patients may benefit from targeted therapy with mTOR inhibitors. One problematic issue in these tumors is to predict malignant behavior. Some studies have proposed algorithms including: size, larger than 5 cms, significant nuclear atypia (excluding bizarre nuclei), necrosis, lymphovascular invasion and mitosis >1/50 high-power fields. When more than 4 features are present, malignant behavior is expected, but some authors proposed that with only 3 features is enough to call malignant to these lesions. The term "benign" is not recommended because some tumors without worrisome features had presented recurrent disease.

## Selected References:

1. Bennett JA, Braga AC, Pinto A, Van de Vijver K, Cornejo K, Pesci A, Zhang L, Morales-Oyarvide V, Kiyokawa T, Zannoni GF, Carlson J, Slavik T, Tornos C, Antonescu CR, Oliva E. Uterine PEComas: A Morphologic, Immunohistochemical, and Molecular Analysis of 32 Tumors. *Am J Surg Pathol*. 2018 October; 42(10):1370-1383. doi:10.1097/PAS.0000000000001119.

2. Bennett JA, Oliva E. Perivascular epithelioid cell tumors (PEComa) of the gynecologic tract. *Genes Chromosomes Cancer*. 2021 Mar;60(3):168-179. doi: 10.1002/gcc.22908. Epub 2020 Nov 6. PMID: 33099813.
3. Shukla PS, Xia R, Lin LH, Schwartz CJ Gynaecological perivascular epithelioid cell tumour (PEComa): comparative analysis of proposed algorithms for prediction of clinical outcome. *Histopathology*. 2021 Nov;79(5):847-860. doi: 10.1111/his.14434. Epub 2021 Sep 3. PMID: 34157139
4. Wei JJ. Leiomyoma with nuclear atypia: Rare diseases that present a common diagnostic problem. *Semin Diagn Pathol*. 2022 Feb 2:S0740-2570(22)00016-8. doi: 10.1053/j.semdp.2022.01.006.

## Case 9

Contributed by Abbas Agaimy, MD

---

### Clinical history:

A 40-year-old woman without significant clinical history presented with abnormal uterine bleeding. Curetting was performed, followed by total abdominal hysterectomy.

### Macroscopic features:

A 4.9 cm well circumscribed but not encapsulated nodule was seen within the myometrium. The cut-surface was homogeneous whitish to tan. No additional nodules were noted. At the time of surgery, no metastases were detected. The patient was lost to follow-up.

### Histological & immunohistochemical findings:

Histological examination showed a cellular neoplasm composed of uniform plump elongated spindle and fusiform cells arranged predominantly into solid nodules and lobules with prominent dissecting invasive growth pattern through the adjacent myometrium. Variable adenoid, microcystic and pseudorosette-like arrangements were seen as well. In the deeper parts, an admixture of tubular and solid patterns, frequently with sieve-like and retiform arrangements was noted in some slides. Focal areas showed plasmacytoid cytology. In the background, a fibromyxoid pauci-vascular stroma was seen. There was no significant atypia and mitotic activity was low (<5 in 10 hpfs).

Immunohistochemistry (performed either primarily or at second opinion review) revealed strong expression of keratin AE1/AE3, calretinin, estrogen receptor, and progesterone receptor. Other markers (SOX10, SMA, desmin, h-caldesmon, CD99, p63, WT1, CK7, Cyclin D1, EMA, CD56, PAX8 or CD10) were negative.

## Molecular findings

Targeted RNA sequencing (TruSight Panel, Illumina) revealed a GREB1::NCOR2 fusion.

**Diagnosis: Uterine tumor resembling ovarian sex cord tumors (UTROSCT) with GREB1::NCOA2 fusion.**

### Comment:

UTROSCTs are rare primary uterine neoplasms that display striking morphological resemblance to ovarian sex cord tumors, hence their name. Their histology varies greatly and their immunophenotype is highly heterogeneous with polyphenotypic features. Their immunophenotype may recapitulate sex cord elements, epithelial cells, and smooth muscle cells. Their ultrastructure may mimic epithelial and sex cord-like neoplasms. UTROSCT usually lacks true endometrial stromal elements, a feature that in conjunction with their emerging genotypes and phenotypes enables their separation from endometrial stromal neoplasms with variable (focal prominent) sex cord-like differentiation.

Middle-aged women are mainly affected with a mean age of 50 years. Abnormal uterine bleeding and or/ pelvic pain or mass are main presenting features. Hysterectomy with or without bilateral salpingo-oophorectomy was the treatment of most reported cases. The biology of UTROSCT has not been well delineated and most seem to pursue an indolent or benign clinical course. Up to 24% of cases, however, developed extrauterine recurrences and rare cases have metastasized but the full biological potential remains to be defined as some of these aggressive cases might have represented referral bias.

At the molecular level, UTROSCT lacks mutation expected in true sex cord tumors (*FOXL2*, *DICER1*) and also lacks the gene fusions characteristic of true endometrial stromal sarcomas with sex cord differentiation (*JAZF1::BCORL1*, *MEAF6::SUZ12*, *EPC1::SUZ12*, *EPC1::BCOR* and others). Several recently published case series confirmed highly recurrent gene fusions involving *ESR1::NCOA1-3*, *GREB1::NCOA1-3* and other rare fusion variants.

As noted above, true sex cord neoplasms, endometrial stromal sarcoma with sex cord differentiation, Müllerian adenosarcoma with extensive sex cord-like differentiation, Wolffian adnexal tumors and low-grade endometrioid adenocarcinoma with spindle cell-like features represent the major differential diagnostic consideration.

## References:

1. Goebel EA, Hernandez Bonilla S, Dong F, Dickson BC, Hoang LN, Hardisson D, Lacambra MD, Lu FI, Fletcher CDM, Crum CP, Antonescu CR, Nucci MR, Kolin DL. Uterine Tumor Resembling Ovarian Sex Cord Tumor (UTROSCT): A Morphologic and Molecular Study of 26 Cases Confirms Recurrent NCOA1-3 Rearrangement. *Am J Surg Pathol*. 2020 Jan;44(1):30-42.
2. Blake EA, Sheridan TB, Wang KL, Takiuchi T, Kodama M, Sawada K, Matsuo K. Clinical characteristics and outcomes of uterine tumors resembling ovarian sex-cord tumors (UTROSCT): a systematic review of literature. *Eur J Obstet Gynecol Reprod Biol*. 2014 Oct;181:163-70.
- 5.
3. Grither WR, Dickson BC, Fuh KC, Hagemann IS. Detection of a somatic GREB1-NCOA1 gene fusion in a uterine tumor resembling ovarian sex cord tumor (UTROSCT). *Gynecol Oncol Rep*. 2020 Sep 6;34:100636.
4. Sato M, Yano M, Sato S, Aoyagi Y, Aso S, Matsumoto H, Yamamoto I, Nasu K. Uterine tumor resembling ovarian sex-cord tumor (UTROSCT) with sarcomatous features without recurrence after extended radical surgery: A case report. *Medicine (Baltimore)*. 2020 Mar;99(11):e19166.
5. Bennett JA, Lastra RR, Barroeta JE, Parilla M, Galbo F, Wanjari P, Young RH, Krausz T, Oliva E. Uterine Tumor Resembling Ovarian Sex Cord Stromal Tumor (UTROSCT): A Series of 3 Cases With Extensive Rhabdoid Differentiation, Malignant Behavior, and ESR1-NCOA2 Fusions. *Am J Surg Pathol*. 2020 Nov;44(11):1563-1572.
6. Umeda S, Tateno M, Miyagi E, Sakurai K, Tanaka R, Tateishi Y, Tokinaga A, Ohashi K, Furuya M. Uterine tumors resembling ovarian sex cord tumors (UTROSCT) with metastasis: clinicopathological study of two cases. *Int J Clin Exp Pathol*. 2014 Feb 15;7(3):1051-9.
7. Croce S, de Kock L, Boshari T, Hostein I, Velasco V, Foulkes WD, McCluggage WG. Uterine Tumor Resembling Ovarian Sex Cord Tumor (UTROSCT) Commonly Exhibits Positivity With Sex Cord Markers FOXL2 and SF-1 but Lacks FOXL2 and DICER1 Mutations. *Int J Gynecol Pathol*. 2016 Jul;35(4):301-8.
8. Croce S, Lesluyes T, Delespaul L, Bonhomme B, Pérot G, Velasco V, Mayeur L, Rebier F, Ben Rejeb H, Guyon F, McCluggage WG, Floquet A, Querleu D, Chakiba C, Devouassoux-Shisheboran M, Mery E, Arnould L, Averous G, Soubeyran I, Le Guellec S, Chibon F. GREB1-CTNNB1 fusion transcript detected by RNA-sequencing in a uterine tumor resembling ovarian sex cord tumor (UTROSCT): A novel CTNNB1 rearrangement. *Genes Chromosomes Cancer*. 2019 Mar;58(3):155-163.
9. Staats PN, Garcia JJ, Dias-Santagata DC, Kuhlmann G, Stubbs H, McCluggage WG, De Nictolis M, Kommos F, Soslow RA, Iafrate AJ, Oliva E. Uterine tumors resembling ovarian sex cord tumors (UTROSCT) lack the JAZF1-JJAZ1 translocation frequently seen in endometrial stromal tumors. *Am J Surg Pathol*. 2009 Aug;33(8):1206-12.

10. Zamecnik M, Stanik M, Michal M. Smooth muscle/myoid differentiation in uterine tumour resembling ovarian sex-cord tumour (UTROSCT). *Histopathology*. 2009 Nov;55(5):619-20; author reply 620-1.
11. Devereaux KA, Kertowidjojo E, Natale K, Ewalt MD, Soslow RA, Hodgson A. GTF2A1-NCOA2-Associated Uterine Tumor Resembling Ovarian Sex Cord Tumor (UTROSCT) Shows Focal Rhabdoid Morphology and Aggressive Behavior. *Am J Surg Pathol*. 2021 Dec 1;45(12):1725-1728.
12. Dickson BC, Childs TJ, Colgan TJ, Sung YS, Swanson D, Zhang L, Antonescu CR. Uterine Tumor Resembling Ovarian Sex Cord Tumor: A Distinct Entity Characterized by Recurrent NCOA2/3 Gene Fusions. *Am J Surg Pathol*. 2019 Feb;43(2):178-186.
13. Lee CH, Kao YC, Lee WR, Hsiao YW, Lu TP, Chu CY, Lin YJ, Huang HY, Hsieh TH, Liu YR, Liang CW, Chen TW, Yip S, Lum A, Kuo KT, Jeng YM, Yu SC, Chung YC, Lee JC. Clinicopathologic Characterization of GREB1-rearranged Uterine Sarcomas With Variable Sex-Cord Differentiation. *Am J Surg Pathol*. 2019 Jul;43(7):928-942.
14. Tornos C, Silva EG, Ordonez NG, Gershenson DM, Young RH, Scully RE. Endometrioid carcinoma of the ovary with a prominent spindle-cell component, a source of diagnostic confusion. A report of 14 cases. *Am J Surg Pathol*. 1995 Dec;19(12):1343-53.
15. Murray SK, Clement PB, Young RH. Endometrioid carcinomas of the uterine corpus with sex cord-like formations, hyalinization, and other unusual morphologic features: a report of 31 cases of a neoplasm that may be confused with carcinosarcoma and other uterine neoplasms. *Am J Surg Pathol*. 2005 Feb;29(2):157-66.
16. Mohammadizadeh F, Rajabi P, Behnamfar F, Hani M, Bagheri M. Extensive Overgrowth of Sex Cord-Like Differentiation in Uterine Mullerian Adenosarcoma: A Rare and Challenging Entity. *Int J Gynecol Pathol*. 2016 Mar;35(2):153-61.

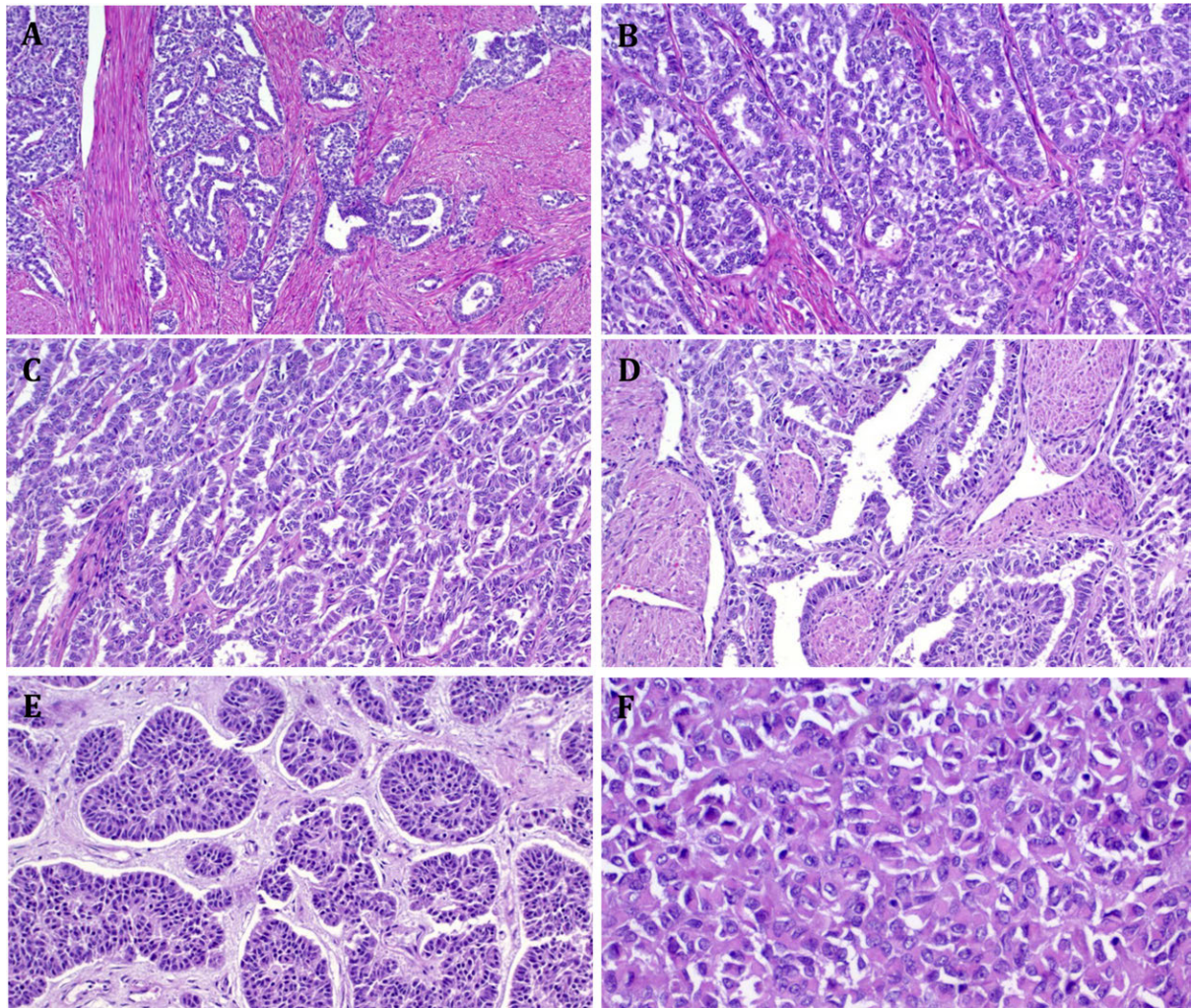


**Figure 1:**

A+B: Solid, tubular and sieve-like growth permeating the myometrium. C: Sex cord like ribbons and trabeculae. D: Retiform sex cord like elements. E: Organoid nesting. F: Solid areas with plasmacytoid/ rhabdoid cytology.

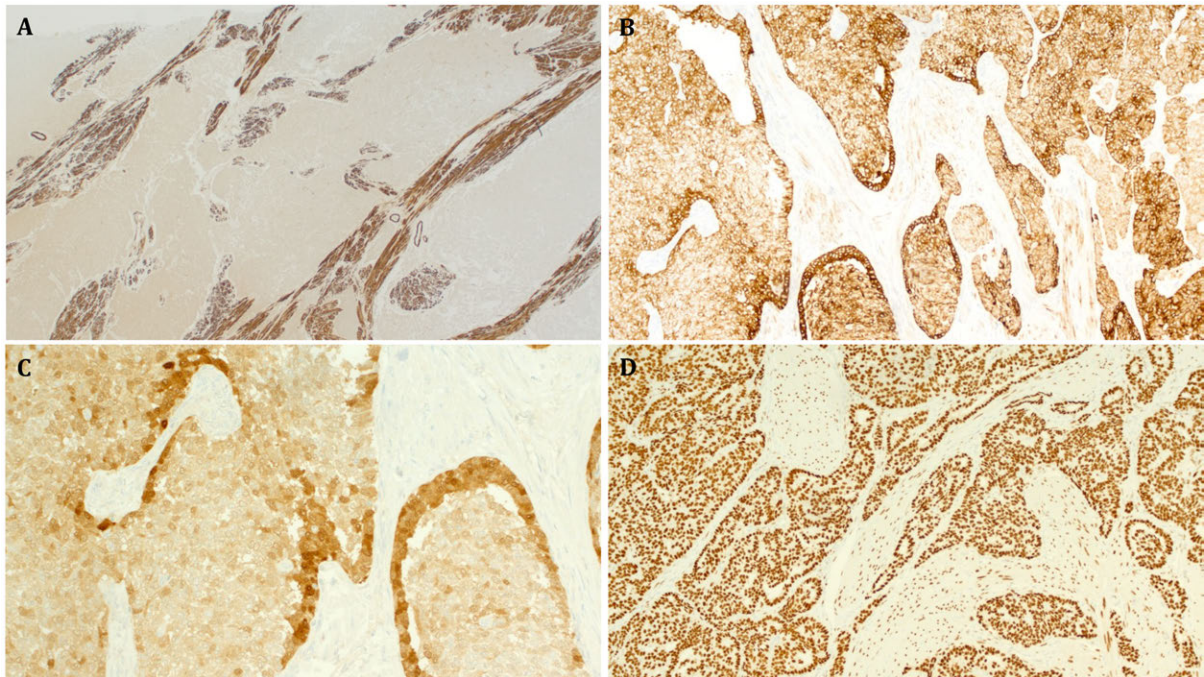


**Figure 2:**

Immunohistochemistry of UTROSCT. A: Desmin highlights extensive invasion into myometrium, the tumor cells are negative. B: Diffuse expression of keratin AE1/AE3. C: Diffuse expression of calretinin (stronger in the glandular elements). D: Homogeneous expression of estrogen receptor.

## Case 10

### Clinical History:

A 42-year-old female patient presented with a well-circumscribed, soft lesion at the vulva, that was completely excised.

### Pathological Findings:

Histologically, a well-circumscribed, multilobulated lesion with variable sized hypocellular fibrous septa is seen. The lobules are composed of variable proportions of mature adipocytes, bland univacuolated and bivacuolated lipoblasts, and cytologically bland, plump spindled tumour cells with short nuclei set in a myxoid stroma with numerous narrow, branching vessels. No increased number of mitoses and no tumour necrosis are present. Immunohistochemically, no nuclear staining for MDM2 and CDK4 is seen, a focal loss of Rb-1 is present, and numerous tumour cells show a weak nuclear expression of PRAME. CD34 stainings highlight the capillary network, but tumour cells are negative.

### Diagnosis: Lipoblastoma-like Tumour of the Vulva

### Comments:

Lipoblastoma-like tumour of the vulva represents a rare mesenchymal neoplasm of the external genital area, that arises predominantly in adult female patients and is seen only rarely in the groin of female and male patients. Although the lesions may recur no metastases or tumour progression has been reported. The well-circumscribed neoplasms are characterized by a multilobular growth and are composed of adipocytes, lipoblasts and undifferentiated, small, spindled tumour cells set in a myxoid stroma with numerous branching vessels. The lack of PLAG1 and HMGA2 expression and the age of affected patients are helpful in the distinction from true lipoblastoma. Although the focal loss of Rb-1 suggests a possible relationship to spindle cell lipoma and lipomatous cellular angiofibroma no evidence of Rb1 regional loss was found by FISH-analysis and genomic copy number analysis by chromosomal microarray showed a normal diploid profile in analysed cases. Myxoid liposarcoma arises in the majority of cases in deep soft tissues of the lower extremities, especially the thigh, and neoplastic cells are characterized by DDIT3 rearrangements.

Mesenchymal neoplasms of the external genital organs comprise the whole spectrum of soft tissue tumours and the group of location specific mesenchymal tumours. The latter group includes fibroepithelial stromal polyp, angiomyofibroblastoma, cellular angiofibroma, deep (“aggressive”) angiomyxoma, praepubertal fibroma of the vulva and lipoblastoma-like tumour of the vulva. Genital leiomyoma tends to be well-circumscribed and is composed relatively frequently of epithelioid tumour cells set in an often myxoid or hyalinised stroma. Atypical smooth-muscle tumours show one the following criteria (infiltrative growth, increased mitoses, nuclear atypia) and malignant smooth muscle tumours three or more of the following criteria (size > 5 cm, infiltrative growth, > mitoses in 10 high power fields, prominently cytological pleomorphism). Alveolar soft part sarcoma of the female genital tract shows a rather indolent clinical behavior in contrast to other anatomical locations.

## References:

1. Droop E, Orosz Z, Michal M, Meleg Z. A lipoblastoma-like tumour of the testicular cord: male counterpart of lipoblastoma-like tumour of the vulva. *Histopathology* 2020; 76: 628-630
2. Lae ME, Pereira PF, Keeney GK, Nascimento AG. Lipoblastoma-like tumour of the vulva: report of three cases of a distinctive mesenchymal neoplasm of adipocytic differentiation. *Histopathology* 2002; 40: 505-509
3. Mirkovic J, Fletcher CDM. Lipoblastoma-like tumor of the vulva: further characterization in 8 new cases. *Am J Surg Pathol* 2015; 39: 1290-1295
4. Schoolmeester JK, Michal M, Steiner P, Michal M, Folpe AL, Sukov WR. Lipoblastoma-like tumor of the vulva: a clinicopathologic, immunohistochemical, fluorescence in situ hybridization and genomic copy number profiling study of seven cases. *Mod Pathol* 2018; 31: 1862-1868
5. Yang S, Huang X, Han S, Chen X, Zhang B. Lipoblastoma-like tumor: expanded clinicopathologic features including male bilateral variant. *Virchows Archiv* in press

# Case 11

**Masaharu Fukunaga, M.D. Shin-yurigaoka General Hospital,  
Kawasaki, Japan**

---

## Clinical history:

A 38-year-old female presented with lower abdominal discomfort. Imaging analyses indicated multiple uterine myomas. A bilateral salpingectomy and myomectomy were laparoscopically performed. The patient is fine and free from disease 36 months after surgery.

## Pathologic findings:

Macroscopically the Fallopian tubes were unremarkable. Histological findings of the right tube included cellular pseudo-stratification, a pronounced papillary arrangement and detachment of the epithelium from the connective tissue, mainly in the fimbria. The changes measured up to 9 mm. Cytological changes included marked nuclear elongation and smudging, eosinophilic cytoplasm and obliteration of cell boundaries and lack of mitotic figures in the epithelial lining. No invasion lesion was noted. These findings mimicked adenocarcinoma in situ of the tube. Immunostaining of p53, WT1 and Ki67 was performed and there were no significant results indicating STIC. Histologically the left tube was normal. The patient has remained asymptomatic after surgery.

**Pathologic diagnosis: Heat artifact simulating tubal intraepithelial carcinoma**

## Comment:

Prophylactic fallopian tube resection has been prevailing because the tubal fimbria is a possible primary site of extra-uterine high grade serous carcinoma in a substantial number of cases. Among pathological changes in tubular resection specimens, serous tubal intraepithelial carcinoma (STIC) is most important for patient management, and heat artifacts simulating tubular neoplasms, including STIC, should be acknowledged in order to avoid histological misdiagnosis.

Heat artifacts from electronic knife usage are not uncommon. The marked papillary pattern of the epithelium was the principal histological characteristic leading to confusion with STIC, likely resulting from the structural characteristics of the tubal fimbria. Heat applied to tissue can produce nuclear elongation, hyperchromatism, smudging of nuclei, eosinophilic cytoplasm, and obliteration of cell boundaries. Awareness of this potential source of diagnostic error leads to its complete avoidance.

# Case 12

Anais Malpica, M.D.

---

## Clinical History:

A 46-year-old woman presented with a 5 month history of abdominal pain. CT scan of abdomen and pelvis showed a 20 cm multicystic, right pelvic mass and mild to moderate ascites. Her serum CA125 was 386 U/mL. Her personal history was unremarkable while her family history showed that her father had skin and prostate cancer in his late 60's. The patient underwent TAHBSO, omentectomy, pelvic and periaortic lymph node sampling and pelvic washings. She also received 6 cycles of adjuvant chemotherapy with Carboplatin and Taxol.

A blood sample of the patient was submitted for hereditary ovarian cancer panel germline testing which included the following genes: *BRCA1*, *BRCA2*, *BRIP1*, *EPCAM*, *MLH1*, *MSH2*, *MSH6*, *PALB2*, *PMS2*, *RAD51C*, and *RAD51D*. No pathogenic mutations were identified in any of the analyzed genes.

## Pathology Findings

**Gross Features:** The right ovary had a 22 cm, multiloculated tumor while the left ovary had a 1.5 cm solid tumor.

**Microscopic Features:** The tumor has marked cytologic atypia, numerous mitoses (>20 mitoses per 10 HPFs) and a transitional cell carcinoma appearance. Other sections show solid areas.

Pelvic washings were negative.

**Immunohistochemical Studies:** The neoplastic cells were positive for keratin 7, WT-1 (x2) (patchy), ER (60%, strong), and PR (20%, strong) while negative or essentially negative for keratin 20, uroplakin, synaptophysin, chromogranin and INSM-1. The tumor was positive for ER (60%, strong), PR (20%, strong). Her-2 neu was 0 while MLH1, PMS2, MSH2 and MSH6 were retained.

**Molecular Analysis:** MDACC MAPP (mutation analysis precision panel) showed the following:

Somatic mutations (SNVs/Indels): ARID1A, CD8A, ROS1, SMARCA2, TOP1 and TP53.

There were no copy number variations (CNVs) or gene fusions.

TMB: 3 mut/Mb

Microsatellite status: Stable (MSS)

**Diagnosis: Right and left ovaries, high grade serous carcinoma with homologous recombination deficiency (HRD) pattern. Right fallopian tube, minute focus of serous tubal intraepithelial carcinoma (STIC).  
Stage: FIGO stage 1 B**

## Discussion:

### 1. Terminology changes:

In 1989, Dr. Silva and coworkers postulated that the presence of a predominant transitional cell carcinoma (TCC) component (>50%) in cases of advanced stage, high grade ovarian carcinoma was associated with a better response to chemotherapy and improved survival. Although initially some investigators disagreed with this proposal, other studies reported similar findings to those of Dr. Silva's. The 2003 WHO classification included TCC under the category of transitional cell tumors and distinguished it from malignant Brenner tumor because of the absence of a benign or atypical proliferative Brenner component, the frequent association with high grade serous carcinoma and its immunohistochemical profile (see below). In 2012, Dr. Soslow and his group included the TCC pattern as one of the histological patterns frequently seen in tumors of patients who had BRCA 1/2 mutations - SET patterns (solid, pseudoendometrioid, transitional). In the 2014 WHO classification, TCC was considered either a variant of high-grade serous carcinoma or high grade endometrioid carcinoma. In the 2020 WHO classification, the term TCC disappeared completely and the term homologous recombination deficiency (HRD) pattern is introduced to designate the previous SET pattern.

Recently, a small study showed that there are proteomic differences between TCC and high-grade serous carcinoma which translated into a higher expression of certain IHC biomarkers (claudin 4 and UCHL1) in TCC; however, no protein was found to serve as a sensitive and specific biomarker for this tumor which led the authors to postulate that high grade serous carcinoma and TCC appear to exist on a continuum.

### 2. SET pattern/ HRD pattern, other considerations

In 2015, Dr. Crum and his group found that the SET and classic patterns of high grade serous carcinoma had an equal distribution in tumors of BRCA positive patients while the

classic pattern predominated over SET in tumors of BRCA negative patients. Interestingly, they also found that younger patients had tumors with a predominance of the SET pattern, no STIC and a better response to chemotherapy and PARP inhibitors while older patients had tumor with a predominance of the classic pattern, STIC and less favorable response to chemotherapy. Subsequently, another study from the same group showed that the SET pattern tends to be seen more frequently in cases with homologous recombination deficiencies and it is indeed associated with a better response to platinum therapy and an improved progression free survival. Of note, HRD in high grade serous carcinoma has been associated with a better prognosis, related to increased sensitivity to current therapies.

**3. IHC Features**

High grade ovarian carcinomas with a transitional carcinoma appearance are typically positive for keratin 7, ER, PAX-8, and WT-1 and negative for keratin 20. Up to 17.6 % of the cases can be positive for thrombomodulin while up to 6% of the cases can be positive for uroplakin III. In addition, p53 immunoexpression tends to be aberrant (overexpressed or null) while p16 tends to be diffuse and strong (63% of cases). They are usually negative for p63 and GATA-3.

**4. STIC and the origin of ovarian/fallopian tube/peritoneal carcinoma**

WHO (2020) recommendations to assign the site of origin

Primary Site	Criteria for Dx
Fallopian Tube	STIC present or mucosal HGSCa present or part or entire length of FT inseparable from tubo-ovarian mass
Ovary	Both FTs separate from ovarian mass and no STIC or mucosal HGSCa in either FT*
Tubo-ovarian	FTs and ovaries not available for complete examination** and pathological findings consistent with extrauterine HGSCa

Peritoneal	<b>Both FTs and ovaries fully examined and no gross or microscopic evidence of STIC or HGSCa in FTs* or ovaries</b>
------------	---

*\*SEE-FIM protocol*

*\*\*Small bx samples or HGSCa developing after previous salpingo-oophorectomy with incomplete tubal examination, or it may apply to postchemotherapy surgical specimens*

STIC has been reported to occur in 40% of advanced or symptomatic high grade serous carcinomas and in 80% of early detected or asymptomatic (risk reducing salpingo-oophorectomy specimens) high grade serous carcinoma. Proteomic analysis and animal models support a dualistic origin for extrauterine high grade serous carcinoma, either from the ovarian surface epithelium or fallopian tube epithelium; however, the role of ovarian stem cells in the genesis of this tumor needs to be studied.

## Bibliography

### Terminology Changes

1. Robey SS, Silva EG, Gershenson DM, et al. Transitional cell carcinoma in high-grade high-stage ovarian carcinoma. An indicator of favorable response to chemotherapy.
2. Cancer. 1989 Mar 1;63(5):839-47.
3. Silva EG, Robey-Cafferty SS, Smith TL, et al. Ovarian carcinomas with transitional cell carcinoma pattern. Am J Clin Pathol 1990; 93: 457-65.
4. Gershenson DM, Silva EG, Mitchell MF, et al. Transitional cell carcinoma of the ovary: a matched control study of advanced-stage patients treated with cisplatin-based chemotherapy. Am J Obstet Gynecol. 1993 Apr;168(4):1178-85.
5. Hollingsworth HC, Steinberg SM, Silverberg SG, et al. Advanced stage transitional cell carcinoma of the ovary. Hum Pathol. 1996 Dec;27(12):1267-72.
6. M.J. Costa, C. Hansen, A. Dickerman, S.A, et al. Clinicopathologic significance of transitional cell carcinoma in nonlocalized ovarian epithelial tumors (stages 2-4). Am J Clin Pathol, 109 (2) (1998), pp. 173-18
7. Kommos F, Kommos S, Schmidt D, et al. Survival benefit for patients with advanced-stage transitional cell carcinomas vs. other subtypes of ovarian carcinoma after chemotherapy with platinum and paclitaxel. Gynecol Oncol. 2005 Apr;97(1):195-9.
8. Guseh SH, Rauh-Hain JA, Tambouret RH, et al. Transitional cell carcinoma of the ovary: a case-control study. Gynecol Oncol. 2014 Mar;132(3):649-53.

9. Logani S, Oliva E, Amin MB, et al. Immunoprofile of ovarian tumors with putative transitional cell (urothelial) differentiation using novel urothelial markers: histogenetic and diagnostic implications. *Am J Surg Pathol*. 2003;27:1434-1441
10. Ali RH, Seidman JD, Luk M, Kalloger S, Gilks CB. Transitional cell carcinoma of the ovary is related to high-grade serous carcinoma and is distinct from malignant Brenner tumor. *Int J Gynecol Pathol*. 2012 Nov;31(6):499-506.
11. Magrill J, Karnezis AN, Tessier-Cloutier B, et al. Tubo-ovarian transitional cell carcinoma and high-grade serous carcinoma show subtly different immunohistochemistry profiles. *Int J Gynecol Pathol*, 2019; 38 (6): 552-561.
12. R.A. Soslow, G. Han, K.J. Park, et al. Morphologic patterns associated with BRCA1 and BRCA2 genotype in ovarian carcinoma. *Mod Pathol*, 25 (2012), pp. 625-636.
13. Tavassoli FA, Devilee P, eds. WHO Classification of Tumours of the Breast and Female Genital Organs. Lyon: International Agency for Research on Cancer; 2003
14. Kurman RJ, Carcangiu ML, Herrington CS, Young RH, eds. WHO Classification of Tumours of Female Reproductive Organs. Lyon: International Agency for Research on Cancer; 2014.
15. WHO Classification of Tumours Editorial Board, eds. WHO Classification of Female Genital Tumours. Lyon: International Agency for Research on Cancer; 2020.
16. Tessier-Cloutier B, Cochrane DR, Karnezis AN, et al. Proteomic analysis of transitional cell carcinoma-like variant of tubo-ovarian high-grade serous carcinoma. *Hum Pathol*. 2020 Jul; 101:40-52.

**SET pattern/ HRD pattern, other considerations**

1. Howitt BE, Hanamornroongruang S, Lin DI, Conner JE, Schulte S, Horowitz N, Crum CP, Meserve EE. Evidence for a dualistic model of high-grade serous carcinoma: BRCA mutation status, histology, and tubal intraepithelial carcinoma. *Am J Surg Pathol*. 2015 Mar;39(3):287-93.
2. Ritterhouse LL, Nowak JA, Strickland KC, et al.. Morphologic correlates of molecular alterations in extrauterine Müllerian carcinomas. *Mod Pathol*. 2016 Aug;29(8):893-903

**STIC and the origin of ovarian/fallopian tube/peritoneal carcinoma**

1. WHO Classification of Tumours Editorial Board, eds. WHO Classification of Female Genital Tumours. Lyon: International Agency for Research on Cancer; 2020.
2. Howitt BE, Hanamornroongruang S, Lin DI, et al. Evidence for a dualistic model of high-grade serous carcinoma: BRCA mutation status, histology, and tubal intraepithelial carcinoma. *Am J Surg Pathol*. 2015 Mar;39(3):287-93.
3. Colvin EK, Howell VM. Why the dual origins of high grade serous ovarian cancer matter. *Nat Commun*. 2020 Mar 5;11(1):1200.

4. Zhang S, Dolgalev I, Zhang T, et al. Both fallopian tube and ovarian surface epithelium are cells-of-origin for high-grade serous ovarian carcinoma. *Nat Commun.* 2019 Nov 26;10(1):5367. doi: 10.1038/s41467-019-13116-2
5. Ottevanger PB. Ovarian cancer stem cells more questions than answers. *Semin Cancer Biol.* 2017 Jun;44:67-71

# Case 14

Masaharu Fukunaga, M.D. Shin-yurigaoka General Hospital,  
Kawasaki, Japan

---

## Clinical history:

A 69-year-old, 4G3P female was admitted because of ascites and an enlarged right ovary. Clinical and image studies indicated a right ovarian cancer, stage IV (lung and peritoneal wall metastases). The patient was treated with simple abdominal hysterectomy, bilateral salpingo-oophorectomy, omentectomy with preoperative chemotherapy. Intraoperative cytologic and histological consultation was performed. Serum alpha-feto protein (AFP) levels were elevated (up to 269ng/ml) after surgery. The patient died of disease 8 months after surgery.

## Pathologic findings

**Cytological findings of the ascites:** It was characterized by papillary or tubular clusters of atypical large cells with round nuclei, prominent nucleoli and abundant PAS-positive clear cytoplasm. The diagnosis of clear cell carcinoma was rendered.

**Macroscopic findings:** The right ovarian tumor measuring 8cm was solid and cystic and invaded the peritoneum.

**Microscopic findings:** Two types of malignant tumor were identified. The first was clear cell carcinoma-like tumor characterized by papillary and glandular proliferation of cuboidal cells with round nuclei, clear cytoplasm and distinguished cell borders. The second tumor was hepatoid carcinoma. It showed trabecular, sinusoidal, or alveolar arrangements of moderately atypical cells. Extensive sampling showed a 4mm high grade serous carcinoma on the surface of the left fallopian tube.

**Immunohistochemical findings:** The ovarian tumor was positive for AFP, Glypican3, CDX2, polyclonal CEA, SALL4 and EMA and negative for ER and PgR. Hepatoid carcinoma was positive for CK7 and CD10.

**Pathologic diagnosis: Somatically derived yolk sac tumor (YST) (malignant ovarian tumor with enteroblastic and hepatoid differentiation and surface high grade serous carcinoma of the left Fallopian tube)**

**Comments:**

This case can be histologically diagnosed as YST, however, clinically and pathologically is not conventional one. There is controversial over its histogenesis, germ cell tumor or somatic malignant tumor in old female cases (1-3). The right ovarian tumor was composed of predominantly enteroblastic component showing tubular and papillary proliferation and tumor cells with sub- and supra nuclear vacuoles and fibrous stroma and of a minor component of hepatoid tumor with a sinusoidal proliferation. Although no other components of YST such as Schiller-Duval bodies, endodermal sinus or microcystic pattern were present, the tumor was histologically compatible with YST. YST generally occur in childhood, adolescent, and early adulthood (median age 16-19 years) and uncommon in individuals aged more than 40 years. A second small peak occurs in postmenopausal patients. The present patient had also small surface high grade serous carcinoma of the left Fallopian tube.

Uncommonly ovarian YSTs occur in older adults, mostly associated with a somatic epithelial neoplasm. The somatic epithelial neoplasm may be of serous, endometrioid, mucinous or clear cell type, and endometrioid and clear cell carcinomas are most common. The YST component is typically a glandular variant. Patients are often with associated with endometriosis. Predominantly or pure glandular YSTs in postmenopausal patients may arise secondarily to total overgrowth of an epithelial neoplasm. The second peak YST in postmenopausal patients may be due to cases of somatically derived YST. Somatically derived YST derives from the epithelial neoplasm through a process that has been referred to as neometaplasia, aberrant differentiation, or retrodifferentiation. Prognosis of patients with this type of tumor is poor.

## References:

1. McNamee T, Damato S, McCluggage WG. Yolk sac tumours of the female genital tract in older adults derive commonly from somatic epithelia neoplasms: somatically derived yolk sac tumours. *Histopathology* 2016; 69:739-751.
2. Nogales FF, Part J, Schuldt M et al. Germ cell tumorous growth patterns originating from clear cell carcinoma of the ovary and endometrium: a comparative immunohistochemical study favouring their origin from somatic stem cells. *Histopathology* 2018; 72:634-647.
3. McCluggage WG. Endometriosis-related pathology: a discussion of selected uncommon benign, premalignant and malignant lesions. *Histopathology* 2020;76:76-92.

# Case 15

## ADSAY

---

### History:

8 years old girl presented with a 14-cm retroperitoneal mass. Resection was performed. The slides that were submitted is from this resection specimen.

### Pathology:

Grossly, the tumor was relatively demarcated and fleshy but showed few areas of necrosis. Microscopically, this was a very cellular, stroma-poor tumor composed of sheet like configuration of round monotonous cells. In some areas, there were vague, ill-defined nest like formations, and in some of the slides there was also barely identifiable small acinar like clustering of cells. But the vast majority of the tumor displayed diffuse sheet like pattern without any specific configuration. The nuclei were round and the chromatin was dense but without any significant clumping. It had some granularity but not quite what is seen in neuroendocrine neoplasia. Monotony created a "small blue cell" appearance, although the cells had fair amount of acidophilic cytoplasm. Nucleoli were conspicuous (not very prominent).

### Diagnosis: Pancreatoblastoma

### Discussion:

Definition and clinical features

Pancreatoblastoma (PBL) is a relatively rare and is typically viewed as a tumor of infants and children that is why it is prone to be under-appreciated and misdiagnosed in adults. It is indeed the most frequent malignant pancreatic neoplasm of childhood (mean age about 4, some cases appear to be congenital), and thus it is the first entity that comes to mind when a malignant cellular neoplasm is encountered in the pancreas of a child. However, there is a second peak that this tumor type is encountered in adults (mean age, about mid-30's) and then the diagnosis is easily missed. Additionally, especially in adults, because it is deep seated and without any specific symptoms PBL often presents as a

large retroperitoneal mass (its pancreatic origin not as evident), or with a large metastatic tumor in the liver. And, if one does not consider this possibility, it can be easily missed. Especially in adults, PBL can be associated with Gardner syndrome (or similar FAP-related tumors, as a result of its beta-catenin/APC pathway association, chr 11p), as well as Beckwith-Wiedemann syndrome. Serum AFP levels may be high in some patients.

## Pathology

As in any of the non-ductal neoplasms including its kindred acinar carcinomas, PBL typically presents as solid, relatively demarcated tumors and since they often show variable patterns and necrosis, radiologically they can show heterogeneity.

As the name implies it is a “blastic” tumor with ability to show multiphenotypic differentiation. Fundamentally it can be described as an epithelial tumor exhibiting acinar differentiation, and lesser degrees of neuroendocrine and occasionally evidence of abortive ductal differentiation. Especially in children, acinar differentiation often predominates to an extent that it may be difficult to distinguish the two. The so-called squamoid corpuscles, which are more like morules seen in other malignancies, which also closely resemble meningothelial whorls are entirely specific and pathognomonic. These are typically vague aggregates of spindled cells, and occasionally they may exhibit frank keratinization but that is a much less common manifestation. These typically show nuclear beta-catenin expression, and in fact, immunohistochemistry for beta-catenin can be extremely helpful in highlighting these morules and arriving at the unequivocal diagnosis of pancreatoblastoma. It is speculated, justifiably that, these morules may be a manifestation of the recently proposed “BROCN” concept (tumors with biotin-rich, optically-clear nuclei) that are associated with b-catenin pathway alterations. According to this proposal, BROCN family of tumors include cribriform-morular thyroid carcinoma, endometrial carcinomas with morules, a distinctive gallbladder tumor recently placed under the designation of intracholecystic tubular non-mucinous neoplasm, pulmonary blastoma (fetal type adenocarcinoma), all of which share these morules (with biotin-rich optically clear nuclei) along with beta-catenin/APC/FAP connection and apparently hormonally driven tumors. This is an interesting concept in terms of etio-pathogenesis but its implication in daily life is not clear.

The typical baseline morphology in pancreatoblastoma is solid, stroma-poor cellular neoplasm forming sheets of relatively monotonous cells. The main tumor cell seen in most

cases closely resembles acinar cell carcinoma (with round nuclei and single nucleolus and often also show acinar differentiation at the immunohistochemical level) but at the same time slightly different than the ordinary acinar carcinoma cells, with less degree of atypia and smaller nucleoli. In fact, the same cell type often appears as a more atypical version of the bland cells that make up solid-pseudopapillary neoplasms. Neuroendocrine differentiation occurs not uncommonly, especially in the adult examples, and has features of classical neuroendocrine cells but often more atypical appearing and forming diffuse areas. Some examples in children can have hypercellular stroma. Occasionally, the stroma even appears neoplastic, and heterologous bone and cartilage formation has been observed.

At the molecular level, PBL is believed to be driven by the APC/beta-catenin pathway (chr 11p), and its association especially with Gardner syndrome in adults confirms this. FGFR2 and IDH2 alterations have been reported.

## Differential diagnosis

Pancreatoblastoma shares many characteristics with the other non-ductal pancreatic tumors (acinar cell, neuroendocrine, solid-pseudopapillary tumors), which distinguish them from ductal neoplasia: They form solid sheets or nested pattern of relatively uniform cells, which translates, at macroscopic level, to relatively round, lobulated, nodular, demarcated tumors that appear fleshy and relatively homogenous except for degenerative and necrotic areas in bigger examples. Histologically, the non-ductal tumors have overlapping features, and in fact, pancreatoblastoma may exhibit virtually all of them; however, there are findings that help us distinguish PBL from other non-ductal neoplasms:

Morules (“squamous corpuscles”) which, if can be identified, are definitively diagnostic of pancreatoblastoma regardless of what else is observed in the tumor. However, morules can be quite subtle. They often appear as small vague zones/clusters of palor amidst a sea of blue. In fact, they may be easier to appreciate in low power sometimes, like detecting subtle germinal centers in a lymph node. They are often composed of more elongated cells with more pale cytoplasm, resembling meningotheelial whorls. Their nuclei often show lesser degree of atypia and finer chromatin, and in some cases/areas an optically clear pseudoinclusions may be seen, but this occurs in the more classical examples. Keratinization that is noted in classical textbooks is actually quite uncommon. Beta-catenin

immunostain often show nuclear expression that highlights these clusters that may not be otherwise readily evident on routine histologic examination.

PBL often shows neuroendocrine differentiation/component (including variable positivity of synaptophysin and chromogranin, which can be extensive and strong), but the tumor typically shows a more diffuse (rather than nested, trabecular) proliferation of cells that are more atypical than a conventional PanNET, and less atypical than a high-grade neuroendocrine carcinoma. Also, there is often acinar cell differentiation along with immunohistochemical expression of acinar marker (trypsin being most reliable - not alpha-1-antitrypsin, but trypsin - followed by chymotrypsin, Bcl10 and lipases) positivity. The fundamental cell of PBL is typically less atypical than an acinar carcinoma cell and nucleoli are not as prominent, but overlaps are common. In contrast, compared to solid-pseudopapillary neoplasm PBL is too atypical and proliferative. Beta-catenin nuclear expression, which is almost invariably diffuse and strong in SPN, is typically confined only to the morules in PBL, although some examples can have diffuse expression. But the cellular atypia, and roundness of the cells should allow recognition of PBL from an SPN. Also, mitotic and proliferative activity (ki67) is invariably very very low (below 2-3% in > 90%) of SPNs whereas PBLs often have substantial proliferative activity. When it is metastasizes to liver PBL can easily be confused with hepatoblastoma. Their overlapping features extend to include elevated AFP and beta-catenin nuclear positive clusters. The presence of acinar differentiation and strong neuroendocrine differentiation may be the only clues to favor PBL which ought to prompt to investigate for a pancreatic primary.

## Treatment and outcome

The behavior of pancreatoblastoma differs in infants versus adults. In childhood, most cases detected before the development of metastases (usually to liver or regional lymph nodes) have been curable by surgery. In patients with control of primary site, metastectomy and even liver transplant becomes a consideration in select cases and may achieve long term survival. In addition, marked responses to preoperative chemotherapy have been achieved. In cases where metastases have occurred, the prognosis has been poor, although newer chemotherapy combinations hold some promise for long term survival in these patients as well. In adults, almost all cases of pancreatoblastoma have been fatal. 5-year survival is about 50%. Many patients initially present with large liver tumors that may be mistaken for a primary because serum AFP levels may also be high.

## References:

1. Reid MD, Bhattarai S, Graham RP, Pehlivanoglu B, Sigel CS, Shi J, Saqi A, Shirazi M, Xue Y, Basturk O, Adsay V. Pancreatoblastoma: Cytologic and histologic analysis of 12 adult cases reveals helpful criteria in their diagnosis and distinction from common mimics. *Cancer Cytopathology*. 127(11):708-719, 2019.
2. Klimstra DS, Wenig BM, Adair CF and Heffess CS. Pancreatoblastoma. A clinicopathologic study and review of the literature. *American Journal of Surgical Pathology* 19: 1371-1389, 1995.

# Case 16

Presented by Ricardo R. Lastra, University of Chicago

---

## Clinical History:

17-year-old male with a 6.6 cm mass in proximal ileum

## Pathology:

*Gross findings:* The mass measured 6.6 x 6.2 x 4.9 cm and was centered in the wall of the ileum. It infiltrated the whole thickness of the wall with involvement of both the serosa and the mucosa in an ulcerated polypoid fashion.

*Microscopic:* Histologic sections demonstrated a cellular epithelioid neoplasm, comprised of loosely cohesive sheets and nests of tumor cells with round to ovoid vesicular nuclei, small nucleoli, and pale eosinophilic to clear cytoplasm. Neither necrosis nor significant nuclear pleomorphism was present. Areas with up to 4 mitotic figures/10HPFs were identified. Resection margins were negative for tumor.

*Metastatic tumor* nodules in omentum, left pericolic gutter, pelvic peritoneum, sigmoid colon, mesentery and liver were also identified.

## Differential diagnosis:

Undifferentiated carcinoma, melanoma, neuroendocrine tumor, epithelioid GIST, malignant gastrointestinal neuroectodermal tumor/clear cell sarcoma-like tumor of the gastrointestinal tract, and desmoplastic small round cell tumor

*Immunohistochemical study:* Diffuse strong positivity for S100 and SOX10, and focal staining for synaptophysin, NSE, PGP-9.5 and EMA. Cytokeratin Cam5.2, AE1/AE3, chromogranin, Melan-A, HMB45, desmin, myogenin, CD45, CD99, FLI-1, CD117, DOG1 are all negative. INI1 and BRG1 are retained.

*Molecular study (FISH):* Positive for *EWSR1* rearrangement but negative for an *EWSR1-ATF1* fusion. However, translocation pattern of *CREB1* were observed in over 80% of tumor cells, indicating *EWSR1-CREB1* fusion. Reverse transcriptase polymerase chain reaction molecular testing confirmed *EWSR1-CREB1* fusion.

## Diagnosis: Malignant gastrointestinal neuroectodermal tumor (GNET) with *EWSR1-CREB1* fusion

### Follow up:

Following induction chemotherapy and radio-embolization of the liver metastasis, cytoreductive surgery with partial liver and sigmoid colon resection, HIPEC with cisplatin and radiation therapy to the whole abdomen were performed. Subsequently, new metastatic tumors were detected in the liver and right diaphragm. He underwent laparotomy with resection of metastatic foci, but the disease continued to progress, and the patient expired 2.5 years after the original diagnosis.

### Comments:

GNET is a rare, malignant neoplasm of the GI tract that was originally proposed as a distinct entity with features resembling clear cell sarcoma of soft parts by Zambrano et al in 2003. To date, 87 cases have been reported. GNET is most often located in the small intestine (67%), but also has been described in the stomach, colon, esophagus, rectum, and even of the oral mucosa (Allanson BM et al, 2018). GNET predominantly affects young adults (2 - 4<sup>th</sup> decade) but can occur at almost any age. It has a slight female predominance. It often metastasizes to liver, peritoneum and regional lymph nodes. It is an aggressive malignant neoplasm with poor prognosis (5-year overall survival of approximately 35%). Currently there are no definitive treatment guidelines.

GNET usually shows a transmural proliferation of epithelioid and some spindled tumor cells arranged in a discohesive nested, pseudoalveolar and pseudopapillary pattern. The cytoplasm of tumor cells ranges from pale eosinophilic to clear. The nuclei are round to ovoid with dispersed chromatin and variably prominent nucleoli. Mitotic activity is variable, but it is often high. Osteoclast-like giant cells may be seen in 35% of cases. A case of oncocytic variant of GNET has also been described (Boland JM, Folpe AL, 2016). GNET shares some morphologic features and *EWSR1* rearrangement with clear cells sarcoma of soft parts, but can be reliably differentiated from the latter by the lack of melanocytic differentiation. GNET is negative for melanocytic markers (Melan-A and HMB45) in contrast to clear cell sarcoma of soft parts. These IHC markers can also be useful to distinguish GNET from primary or metastatic melanoma. In addition, *EWSR1* translocation can rule out melanoma.

GNET also exhibits some histologic features of gastrointestinal neuroendocrine tumors, gastrointestinal stromal tumors, and poorly differentiated carcinomas. Some GNETs may express neuroendocrine markers like synaptophysin and CD56, however chromogranin A and cytokeratins are negative. GNET is also negative for GIST markers (CD117 and DOG1).

Genuine clear cell sarcoma rarely may occur as a primary tumor in the gastrointestinal tract. It shares common molecular genetic abnormalities with GNET, but is distinguished by its morphological and immunohistochemical findings (Green C et al. 2018).

## References:

1. Zambrano E, Reyes-Mugica M, Franchi A, Rosai J. An osteoclast-rich tumor of the gastrointestinal tract with features resembling clear cell sarcoma of soft parts: report of 6 cases of a GIST simulator. *Int J Surg Pathol*. 2003 Apr;11(2):75-81
2. Stockman DL, Miettinen M, Suster S, et al. Malignant gastrointestinal neuroectodermal tumor: clinicopathologic, immunohistochemical, ultrastructural, and molecular analysis of 16 cases with reappraisal of clear cell sarcoma-like tumors of the gastrointestinal tract. *Am J Surg Pathol*. 2012 Jun;36(6):857-868
3. Wang J, Thway K. Clear cell sarcoma-like tumor of the gastrointestinal tract. An evolving entity. *Arch Pathol Lab Med*. 2015 Mar;139(3):407-412
4. Boland JM, Folpe AL. Oncocytic variant of malignant gastrointestinal neuroectodermal tumor: a potential diagnostic pitfall. *Hum Pathol*. 2016 Nov; 57:13-16
5. Libertini M, Thway K, Noujaim J, et al. Clear cell sarcoma-like tumor of the gastrointestinal tract: clinical outcome and pathologic features of a molecularly characterized tertiary center case series. *Anticancer Res*. 2018 Mar;38(3):1479-1483
6. Segawa K, Sugita S, Aoyama T, et al. Detection of specific gene rearrangements by fluorescence in situ hybridization in 16 cases of clear cell sarcoma of soft tissue and 6 cases of clear cell sarcoma-like gastrointestinal tumor. *Diagn Pathol*. 2018 Sep 15;13(1):73
7. Allanson BM et al. Oral malignant gastrointestinal neuroectodermal tumor with junctional component mimicking mucosal melanoma. *Pathology*. 2018 Oct;50(6):648-653
8. Green C et al. Clear cell sarcoma of the gastrointestinal tract and malignant gastrointestinal neuroectodermal tumour: distinct or related entities? A review. *Pathology*. 2018 Aug;50(5):490-498
9. Chang B, Yu L, Guo WW, et al. Malignant gastrointestinal neuroectodermal tumor: clinicopathologic, immunohistochemical, and molecular analysis of 19 cases. *Am J Surg Pathol*. 2020 Apr;44(4):456-466

# Case 17

## ADSAY

---

### History:

This 9 years old boy presented with abdominal discomfort and swelling. His abdominal symptoms and hospitalizations dated back to when he was 7 months old and in the workup at that time, he was diagnosed with tyrosinemia. His parents are second degree relatives. Radiologic examination revealed liver nodularity, some with characteristics of hepatocellular carcinoma. AFP was 125000. Albumin was 3.5 g/dl, ALP 99 (low), bilirubin 0.2 (low), INR 1.03 (high). After detailed work up, the patient underwent liver transplant. The specimen you see is from the explant.

### Pathology:

The underlying liver showed a peculiar form of cirrhosis. The nodularity of the hepatocytes had a more jig-saw puzzle architecture than typical cirrhosis, and the intervening fibrosis was composed of thin bands of more delicate collagen but formed complete bridges. In this backdrop, there were "tumor" nodules that were relatively demarcated and composed of unusual abnormal hepatocytes including with architecture different than the background cirrhotic liver. In one of these, there were also some degree of immature fetal type cellular clusters of the type that are seen more typically in hepatoblastomas. In this particular tumor, glypican and glutamine synthetase showed diffuse but weak labeling distinct from the rest of the liver and the other nodules.

### **Diagnosis: HEPATOCELLULAR DYSPLASIA AND EVOLVING CARCINOMA IN THE BACKGROUND OF TYROSINEMIA-INDUCED CIRRHOSIS IN A CHILD**

### Discussion:

This case illustrates a fascinating aspect of carcinogenesis. Most cancers in children develop because of a genetic abnormality in oncogenic or gatekeeper genes that transform the cell into cancer cells. In contrast, in adulthood, cancers typically develop as

a result of long term exposure to carcinogenetic factor. Whereas, the process in this case is a striking example of another path, which is neither and both: A genetic metabolic disorder leading to over-accumulation of an otherwise normal metabolite which induces cirrhosis, and which in turn also leads to carcinogenesis at early age.

## **Tyrosinemia**

Tyrosinemia is the disease that occurs as a result of genetic alterations that ultimately disrupt the breakdown of the amino acid tyrosine, a building block in most proteins. Typically, these autosomal recessive genes involve the phenylalanine and tyrosine catabolic pathways, and are inherited in an autosomal-recessive pattern. As a result, in addition to problems in protein synthesis, tyrosine and related metabolites (especially succinylacetone) accumulate and cause damages to several organs, but especially the liver.

By far, the most common form of tyrosinemia is type I, which this patient had. Type I tyrosinemia is characterized by the abnormality of FAH gene, which encodes for fumaryl acetate enzyme, defect of which in turn leads to accumulation of succinylacetone. Blood tests that show high levels of succinylacetone is diagnostic. In some parts of eastern rural Turkey which this patient is from, intermarriages among secondary family members still continue, and as a result autosomal recessive diseases like tyrosinemia are prone to occur more common than in the West.

Tyrosinemia type I typically manifests soon after birth by failure to thrive, fever, diarrhea, vomiting, and liver abnormalities. The damage to liver and development of hepatocellular carcinoma are among the most common and significant complications. Treatment with nitisinone, which is an inhibitor of 4-hydroxyphenylpyruvate helps decrease the production of succinyl acetone, combined with strict and patient-specific diet, is often highly successful in preventing the damage. Patients who do not respond to these treatments and still develop liver failure or liver tumors are candidates for liver transplant. This patient developed liver tumors and underwent transplantation.

## **Tyrosinemia and HCC**

Patients with tyrosinemia develop liver disease early on. Hepatocellular dysplasia and carcinoma (HCC) is a very well established and fairly common complication, and develops in young ages.

Dysplasia as a term and an entity is integrated to hepatic tumor classifications. However, its definition, and even its existence has been in question. In the US, the term is rarely employed which is mostly attributed to reproducibility issues and lack of agreed criteria. Another factor is the philosophy that some authors seem to take is that if a hepatocellular nodule is recognizable as neoplastic and does not fulfill the criteria for adenoma, then it is most likely HCC even if it is small. This was also mostly more or less our take on the issue when we were working in the US. However, we have come to appreciate that there may be populational and practice related aspects to this issue. In fact, this case (and other patients of tyrosinemia), illustrates the point that hepatocellular lesions that do not exactly fulfill the criteria for HCC either quantitatively and qualitatively, but that are also abnormal and appear to be early forms of neoplasia (and thus qualify for the diagnosis of "dysplasia") indeed do occur in the liver. In this case, there were multiple demarcated hepatocellular neoplasms that were clearly beyond regenerative nodules as well as beyond being some form of adenoma both by morphology and architecture. At the same time, except for the main lesion, they mostly did not show the atypia and classical characteristics of a hepatocellular carcinoma either. Therefore, they did indeed qualify for the diagnosis of a dysplastic nodule both by morphology and size of the lesion. As such they also lend support to the existence of a definable hepatocellular dysplasia category in certain contexts.

In the main lesion, however, which was available in some but not all of the sections submitted to you, the process was more in keeping with an early hepatocellular carcinoma both by morphology, architecture and immunohistochemistry. This lesion showed small clusters and trabecules that had "small cell change" with high nucleocytoplasmic ratio. These closely resembled the fetal-embryonal patterned clusters seen in hepatoblastomas and as such confirmed that this is HCC. Moreover, this lesion acquired some expression of glypican and glutamine synthetase which was clearly distinct from the background cirrhotic liver as well as from the dysplastic nodules, albeit relatively weak. In summary, we find this case to be fascinating for three reasons: One, that not all cirrhotic patterns are equal, and that some do have different morphologic characteristics. In this child with tyrosinemia the jig-saw puzzle pattern and fine fibrosis were striking. Two, the cancer etiopathogenesis angle, illustrating that a metabolite accumulation can trigger carcinogenetic pathways in childhood. Three, it provides a striking example of "hepatocellular dysplasia" and confirms its existence not only as a concept but also as a morphologically definable and agreeable lesion.

## References:

1. Liu Y, et al. Living-donor liver transplantation for children with tyrosinemia type I. *J Dig Dis*. 2020 Mar;21(3):189-194.
2. Bahador A, et al. Liver Transplant for Children with Hepatocellular Carcinoma and Hereditary Tyrosinemia Type 1. *Exp Clin Transplant*. 2015 Aug;13(4):329-32.

# Case 19

Fátima Carneiro

---

## Clinical History:

Male, 86-year-old, with gastric cancer; a total gastrectomy was performed displaying a polypoid tumor (4.6cm in largest dimension), localized in the esophago-gastric region.

## Pathological Findings

**Macroscopy:** The tumor (4.6x4.2x1.2cm) was excavated, sharply demarcated with raised margins, localized at 1cm from the esophago-gastric junction.

**Histology:** Histopathological examination revealed an invasive adenocarcinoma with tubulo-papillary architecture and solid areas, composed predominantly by neoplastic cells with clear glycogen-rich cytoplasm and irregular hyperchromatic nuclei. In depth, the tumor reached the sub-serosa. Four out of the 33 lymph nodes isolated in the surgical specimen displayed metastases.

**Immunohistochemistry:** The immunohistochemical analysis revealed diffuse nuclear expression of SALL4 and focal expression of glipican-3 and alpha-fetoprotein.

**Diagnosis: Gastric adenocarcinoma with enteroblastic differentiation (GAED)**

## Comments:

Gastric adenocarcinoma with enteroblastic differentiation (GAED) belongs to the group of AFP-producing gastric carcinomas that, besides hepatoid carcinoma, includes well-differentiated papillary or tubular adenocarcinomas with clear cytoplasm (Kim JY *et al*, 2014; Sun W, 2017), and yolk-sac tumor-like carcinoma (Kim JY *et al*, 2014; Sun W *et al*, 2017; Srivastava P *et al*, 2021). A combination of these histological types may be seen in some cases (He F *et al*, 2021).

GAED is a tumor showing tubulo-papillary architecture, composed by columnar neoplastic cells with clear cytoplasm. GAED represents an example of “primitive enterocyte phenotype” cancer because of its morphologic resemblance to early fetal gut

epithelium, and the frequent upregulation of oncofetal proteins such as AFP, glypican 3 (GPC3) and SALL4. Other embryonic stem cell marker genes, including LIN28, and claudin-6 (CLDN6), can also be expressed (Yamazawa S *et al*, 2017; Ushiku T *et al*, 2009; Ushiku T *et al*, 2012). GAED is associated with a very aggressive biological behavior (Yamazawa S *et al*, 2017; Murakami T *et al*, 2016). However, the survival of patients with GAED is better than that of patients with hepatoid carcinoma (Kwon MJ *et al*, 2019). In one series of cases (Murakami T *et al*, 2016), patients with GAED were predominantly male (79 %), and GAED lesions were frequently located in the middle third and lower third of the stomach (79 %). The mean age of patients at diagnosis tended to be older than that of patients with conventional gastric adenocarcinomas. The prevalence of lymphatic involvement and that of venous involvement in GAED (76 and 72 %, respectively) were remarkably higher than those in conventional gastric adenocarcinomas (10-56 %). Furthermore, 31 % of GAED patients had synchronous or metachronous liver metastasis.

Molecular characteristics include frequent *TP53* alterations (mutations, promoter methylation, and LOH of the *TP53* locus) (Akazawa Y *et al*, 2018; Yatagai N *et al*, 2019) and weak association with EBV and MSI. It was demonstrated that HER2 is overexpressed in about 35% of GAEDs. Moreover, HER2-positive intestinal type gastric carcinoma has a higher risk of progression to hepatoid carcinoma and gastric adenocarcinoma with enteroblastic differentiation than HER2-negative gastric carcinoma (Fujimoto M *et al*, 2018). In terms of TCGA molecular classification, GAED constitutes a distinct subset of tumors with chromosomal instability (CIN).

## References:

1. Akazawa Y, Saito T, Hayashi T, *et al*. Next-generation sequencing analysis for gastric adenocarcinoma with enteroblastic differentiation: emphasis on the relationship with hepatoid adenocarcinoma. *Hum Pathol*. 2018;78:79-88.
2. Fujimoto M, Matsuzaki I, Nishino M, *et al*. HER2 is frequently overexpressed in hepatoid adenocarcinoma and gastric carcinoma with enteroblastic differentiation: a comparison of 35 cases to 334 gastric carcinomas of other histological types. *J Clin Pathol*. 2018;71(7):600-607.
3. He F, Fu Y, Sun Q, *et al*. Integrated clinicopathological and immunohistochemical analysis of gastric adenocarcinoma with hepatoid differentiation: an exploration of histogenesis, molecular characteristics, and prognostic markers. *Hum Pathol*. 2021; 115:37-46.
4. Inagawa S, Shimazaki J, Hori M, *et al*. Hepatoid adenocarcinoma of the stomach. *Gastric Cancer*. 2001;4(1):43-52.

5. Kim JY, Park DY, Kim GH, Jeon TY, Lauwers GY. Does clear cell carcinoma of stomach exist? Clinicopathological and prognostic significance of clear cell changes in gastric adenocarcinomas. *Histopathology*. 2014;65(1):90-99.
6. Kwon MJ, Byeon S, Kang SY, Kim KM. Gastric adenocarcinoma with enteroblastic differentiation should be differentiated from hepatoid adenocarcinoma: A study with emphasis on clear cells and clinicopathologic spectrum. *Pathol Res Pract*. 2019;215(9):152525.
7. Murakami T, Yao T, Mitomi H, *et al*. Clinicopathologic and immunohistochemical characteristics of gastric adenocarcinoma with enteroblastic differentiation: a study of 29 cases. *Gastric Cancer*. 2016;19(2):498-507.
8. Srivastava P, Nuzhat Husain N, Shukla S, Pandey A. Pure gastric yolk sac tumor: A case report and review of literature. *Indian Journal of Pathology & Microbiology*, 2021 (online).
9. Sun W, Liu B, Chen J, *et al*. Novel characteristics of alpha-fetoprotein (AFP)-producing gastric cancer. *Oncotarget*. 2017;8(60):101944-101951.
10. Ushiku T, Shinozaki-Ushiku A, Maeda D, Morita S, Fukayama M. Distinct expression pattern of claudin-6, a primitive phenotypic tight junction molecule, in germ cell tumours and visceral carcinomas. *Histopathology*. 2012;61(6):1043-1056.
11. Ushiku T, Uozaki H, Shinozaki A, *et al*. Glypican 3-expressing gastric carcinoma: distinct subgroup unifying hepatoid, clear-cell, and alpha-fetoprotein-producing gastric carcinomas. *Cancer Sci*. 2009;100(4):626-632.
12. Yamazawa S, Ushiku T, Shinozaki-Ushiku A, *et al*. Gastric Cancer with Primitive Enterocyte Phenotype: An Aggressive Subgroup of Intestinal-type Adenocarcinoma. *The American journal of surgical pathology*. 2017;41(7):989-997.
13. Yatagai N, Saito T, Akazawa Y, *et al*. TP53 inactivation and expression of methylation-associated proteins in gastric adenocarcinoma with enteroblastic differentiation. *Virchows Arch*. 2019;474(3):315-324.

# Case 21

## Primary MALToma of liver (L. DiTommaso)

---

### Clinical history:

Man, 71 yrs old. No previous oncological history. A US performed during a check-up for back pain revealed a 2.2 cm lesion in the liver. Imaging (PET; CT; MNR) negative for other lesions. No biopsy performed. Pre-operative diagnosis: cholangiocarcinoma.

### Pathologic findings:

Liver resection 6x5x4 (IV segment); 2.2 cm, whitish lesion with pushing margins. The lesion showed the following immunoprofile: CD20+, CD79+, PAX5+, CD43+, CD3-, CD5-, CD23-, D1 cyclin-, bcl2-, bcl6-; Ki67: 10-10%.

### Diagnosis: MALT lymphoma of the liver

### Discussion:

Primary hepatic lymphoma (PHL) constitutes about 0.4% of all primary extranodal non-Hodgkin lymphoma (NHL) (1). Primary hepatic MALT lymphoma is a very rare, indolent lymphoma, with slightly more than 70 cases reported in the literature. A substantial number of primary hepatic MALT lymphomas were reported to occur in patients with chronic hepatitis B or C, or with primary biliary cirrhosis, suggesting a link between chronic liver inflammation and hepatic MALT lymphomagenesis (2). There are no standard therapeutic protocols or guidelines for the treatment of primary hepatic MALT lymphoma. Surgery, chemotherapy, or radiotherapy alone, or in combination had been commonly used. Most patients, including the present one, were alive and well after a median follow-up time of 2 years (3).

## References:

1. Noronha V et al. Primary non-Hodgkin's lymphoma of the liver. *Crit Rev Oncol Hematol* 2005; 53: 199-207.
2. Dong S, Chen L, Chen Y et al (2017) Primary hepatic extranodal marginal zone B-cell lymphoma of mucosa-associated lymphoid tissue type: a case report and literature review. *Medicine (Baltimore)* 96:e3605. <https://doi.org/10.1097/MD.00000000000006305>
3. Peng Y et al. Lymphoma of the liver: Clinicopathological features of 19 patients. *Exp Mol Pathol*. 2016 Apr;100(2):276-80. doi: 10.1016/j.yexmp.2016.02.001.

## Case 22

### ADSAY

---

#### History:

This 61-year-old male patient presented with abdominal pain and was discovered to have multiple tumors in the liver, largest measuring 8 cm. After a biopsy, the patient underwent a liver transplantation. The specimens you see are from the explant.

#### Pathologic Findings:

Grossly, there were multiple tumors that had targetoid pattern with a band of different colored tumor at the periphery. Microscopically, there was an insidious infiltration composed of individual cells or small irregular clusters in a sclerotic background. The cells were epithelioid and histiocytoid, showing fair amount of cytoplasm with prominent intracytoplasmic vacuoles. In some areas, these vacuoles resembled adipocytes, whereas in others, they gave the impression of glandular differentiation. As such, this infiltrate in the liver closely resembled cholangiocarcinoma. Few of these vacuoles appeared to contain RBCs. The nuclei had washed-off, pale chromatin without any significant clumping. Nuclei were irregular with focal groove formation. In close inspection, an eccentric but relatively small nucleolus was evident in well-preserved cells. Erg and CD31 showed diffuse positivity, confirming the vascular nature of the process.

#### Diagnosis: EPITHELOID HEMANGIOENDOTHELIOMA OF THE LIVER

#### Discussion:

Epithelioid endothelial cell tumors: A spectrum of lesions  
Neoplasms characterized by epithelioid endothelial cells were first recognized by Rosai et al in 1979 in a series of patients reported as *histiocytoid hemangioma*. In this paper, the characteristic cytomorphologic features of epithelioid endothelial cells were established: Fair amount of cytoplasm, round nuclei with pale, fine chromatin, prominent nuclear irregularities including grooves, and single, prominent but relatively small nucleolus.

Later, the spectrum of lesions that are characterized by this cell type was recognized. It is now widely acknowledged that in one end of the spectrum is *angiolymphoid hyperplasia with eosinophilia (ALHE)* which is presumed to be a reactive proliferation. *Epithelioid hemangioma (EH)* is the name given for the presumed neoplastic version of this entity, although some authors use ALHE and EH interchangeably. In this group, the vascular spaces are well-formed and the cells have the hallmark “tombstone” appearance. They have abundant dense cytoplasm, and the intercellular borders are often clefted. Cytoplasmic projections may show thin membranes that fuse with that of the opposing cells and impart a distinctive vacuolated appearance within the vascular space. There is often a myxoid edematous background with or without eosinophils. These (ALHE and/or EH) most commonly occur in the skin.

Those epithelioid (histiocytoid) endothelial cell lesions that are composed of less well-defined vascular spaces, and that exhibit a more cord-like or individual-cell infiltration patterns are classified as *epithelioid hemangioendothelioma (EHE)*. These are more deeply seated than EH, and also occur in visceral organs, in particular the liver and lung. Those that occur in the soft tissue tend to have a myxoid stroma and cord-like infiltrates with only minimal well-formed vessels. Pulmonary EHE has a peculiar infiltration pattern that had at one time led to the misnomer of “intravascular bronchoalveolar tumor”. It may have a coin-lesion appearance with variable degree of myxoid stroma. The cells grow within the alveolar spaces forming wide and often centrally sclerosed projections. The cells of EHE tend to have abundant acidophilic cytoplasm, often with distinct cytoplasmic borders. Because the nuclei show grooves and even inclusions, the cells closely resemble bronchoalveolar tumors. However, in contrast with bronchoalveolar carcinomas they do not line the alveolar walls. By careful inspection, foci of intravascular growth are often identifiable.

While this simplistic approach of subcategorization of EECLs as benign (EH), intermediate/borderline (EHE) and malignant (EA- epithelioid angiosarcoma) is fairly reproducible and applicable to many cases, overlaps are not uncommon and can be problematic. In particular, the distinction of EH from EHE in bone and soft tissue can be an issue because mixed patterns are quite common. This is not as much a problem in the lung or liver where almost all tumors show pattern characteristic of EHE, while well formed, large vascular units characteristic of EH are highly unusual. Thus, most (if not all) pulmonary and hepatic examples are EHE; only a few are angiosarcomas, and EH is practically non-existent in these organs. The problem in these visceral sites instead is

more the distinction of EHE from angiosarcomas. For this, the degree of nuclear atypia, hyperchromasia, the presence of necrosis and mitotic activity, and irregular cleft formation are the key distinguishing features. Clearly, some angiosarcomas arising in these organs have areas otherwise indistinguishable from EHE.

For soft tissue EHE, a grading scheme that utilizes mitotic activity and size of the tumor was proposed and it identifies a high-risk group with significantly worse prognosis.

## **EHE of the liver**

EHE of liver may be seen at any age; however, most occur in young and middle-aged adults with a mean age of 45. It occurs more commonly in females, and an association with oral contraceptives has been suggested but not proven. Some patients present with Budd-Chiari like picture. Multifocality is very common (>70%). They can occur in cirrhotic livers as well, and are commonly misdiagnosed as metastatic carcinoma. Though they are tumors of presumed vascular endothelial cell origin, radiologic findings may not demonstrate significant vascularity. A targetoid pattern can be appreciated both radiologically and grossly. Behavior is variable. However, although it is viewed as a "borderline malignancy", it often follows a highly aggressive clinical course and is fatal in 1 year in some patients. Overall 5-yr survival is estimated to be 50%. Liver transplant is employed and can be highly successful in some cases.

Grossly, EHE is a firm, white to yellow tumor that often has an ill-defined border. The tumor is often multifocal with involvement of both right and left liver lobes.

The cells have the characteristic cytomorphologic features described above in detail. In addition, they show predilection for invading larger vascular structures such as portal and central veins, thereby mimicking the histological appearance of vascular thrombosis. Focal tufted and papillary arrangements are common. Sinusoidal spread of individual tumor cells, which is not uncommon and it closely resembles megakaryocytes, is typically dismissed as extramedullary hematopoiesis.

In the more sclerotic examples, subtle examples are typically dismissed as non-neoplastic fibrosing disorder, especially in small biopsies. More prominent and vessel-forming examples are misdiagnosed as metastasis or cholangiocarcinoma.

Immunohistochemical staining for endothelial markers such as CD34, CD31, ERG, FLI1 and recently developed CAMTA1 is helpful in confirming the diagnosis of EHE and helps in the differential diagnosis with adenocarcinomas and HCC. The utility of YAP1 immunohistochemistry in a subset is under scrutiny. It should be kept in mind that these tumors often express keratins, and therefore the mimicry with adenocarcinoma/cholangiocarcinoma also extends to the immunohistochemistry.

The vast majority of EHE show a *WWTR1-CAMTA1* (*TAZ-CAMTA1*) fusion. In a very small subset, *YAP1-TFE3* fusions are detected. For the latter, there is an impression of more protracted clinical course. It also appears to be more prone to have well-formed vascular channels, although more studies are needed to confirm this impression. In contrast, in epithelioid hemangiomas, *FOSB* alterations are detected, which does not seem to play a role in EHE (so far).

## Follow up

In this patient, the tumors recurred soon after the liver transplantation, and 2.5 years after the transplant the patient is alive but with active and progressive disease and multiple metastases in the bones and possibly also in the mediastinum.

## References:

1. Rosai J, Gold J, Landy R: The histiocytoid hemangiomas. A unifying concept embracing several previously described entities of skin, soft tissue, large vessels, bone, and heart. *Hum Pathol* 10: 707-30, 1979.
2. Tsang WY, Chan JK: The family of epithelioid vascular tumors. *Histol Histopathol* 8: 187-212, 1993.
3. Makhlof HR, Ishak KG, Goodman ZD: Epithelioid hemangioendothelioma of the liver: a clinicopathologic study of 137 cases. *Cancer* 85: 562-82, 1999.
4. Deyrup et al. Epithelioid hemangioendothelioma of soft tissue: a proposal for risk stratification based on 49 cases. *Am J Surg Pathol* 2008 Jun;32(6):924-7.
5. Lerut et al. The place of liver transplantation in the treatment of hepatic epithelioid hemangioendothelioma: report of the European liver transplant registry. *Ann Surgery* 2007 Dec;246(6):949-57.

6. Agostini-Vulaj D et al. Intrasinusoidal Spread of Hepatic Epithelioid Hemangioendothelioma: Implications for the Diagnosis in Minimal Samples. *Am J Surg Pathol*. 2019 Apr;43(4):573-579
7. Rosenbaum et al. Prognostic stratification of clinical and molecular epithelioid hemangioendothelioma subsets. *Modern Pathol*, 2020 April, 33(4): 591-602.
8. Dermawan et al. YAP1-TFE3-fused hemangioendothelioma: a multi-institutional clinicopathologic study of 24 genetically-confirmed cases. *Modern Pathol*, 34: 2211. 2021.
9. Bourgeau et al. Cytologic features of hepatic YAP1-TFE3 rearranged epithelioid hemangioendothelioma. *Diagn Cytopathol*, 2021 Dec;49(12):E447-E452.

## Case 23

### Clinical History:

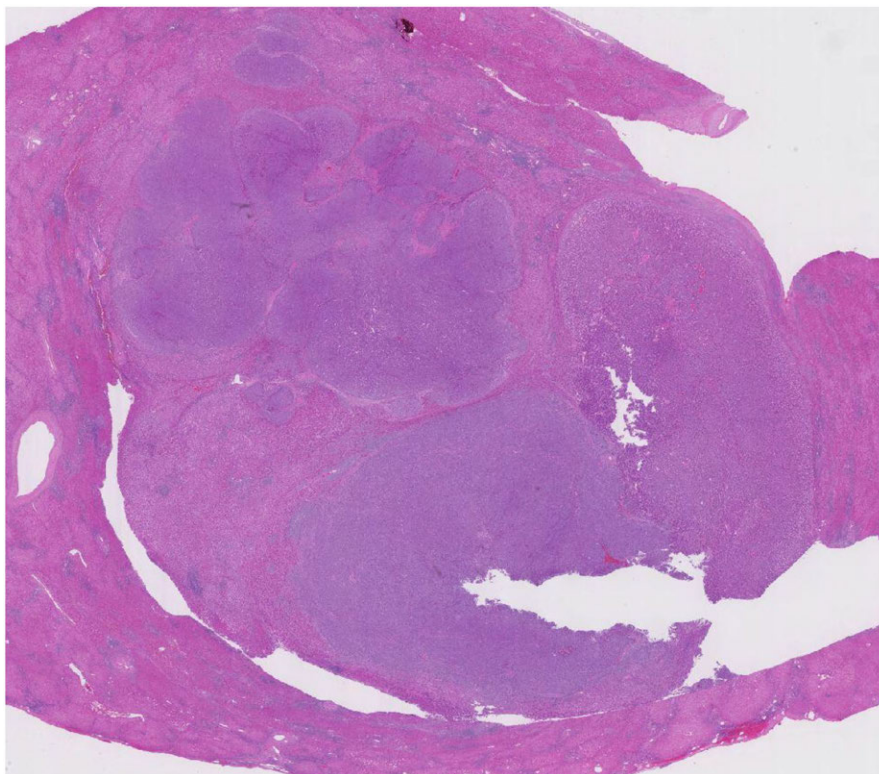
A 67-year-old man with a clinical history of T cell acute lymphoblastic lymphoma, and hepatitis C was found to have a 2.0 cm mass in the left lobe of the liver on routine surveillance imaging

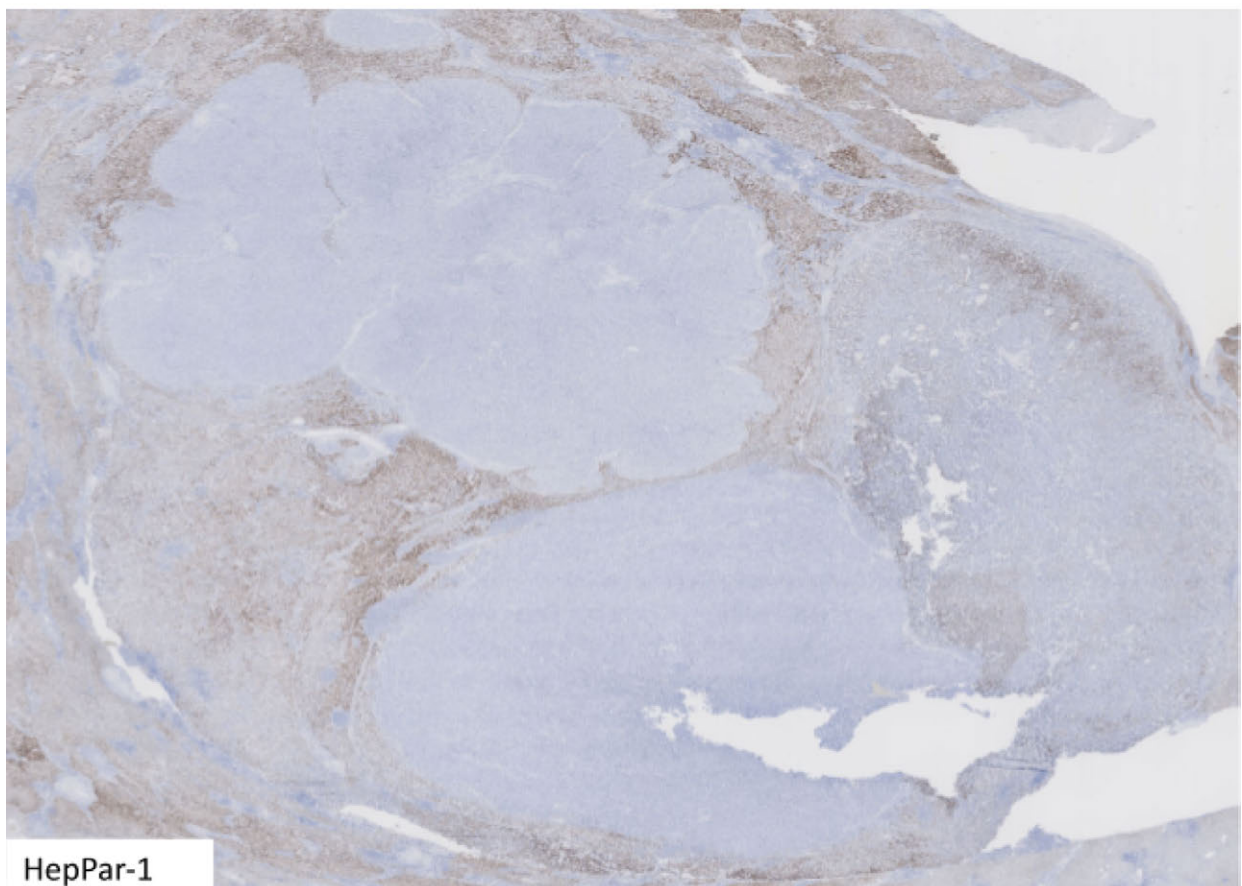
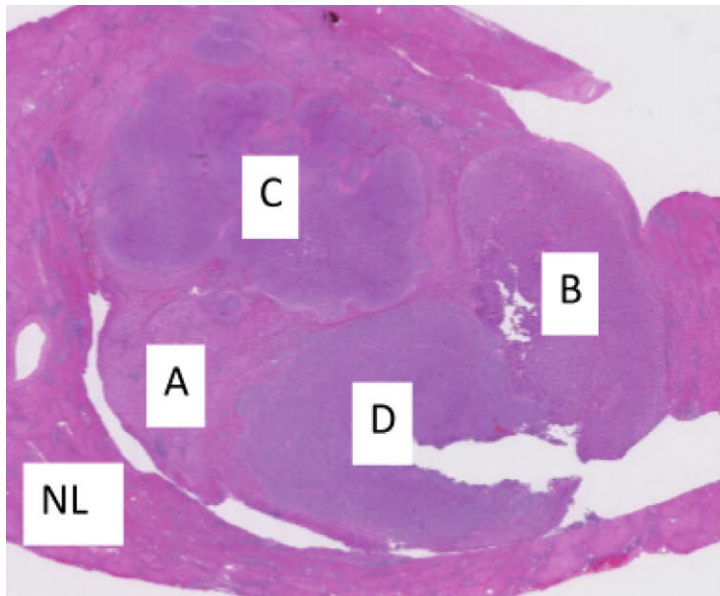
### Macroscopic Features:

A 2.0 cm lesion was identified in the segmentectomy specimen, with grossly uninvolved margins.

### Histological and Immunohistochemical Findings:

Even at low power, four distinct areas are identifiable (labeled A, B, C and D below). At this power, arguably A and B look fairly similar, and C and D look fairly similar, but at higher power, four distinct morphologies are appreciable (see below).





The HepPar-1 immunostain exhibits another interesting phenomenon of preserved staining in the well-differentiated component (sub-nodule A), with attenuated patchy staining in the moderately differentiated component (sub-nodule B), and complete loss of staining in the poorly differentiated component (sub-nodule C), and the sarcomatoid component (sub-nodule D). High power views of the 4 nodules are shown below.

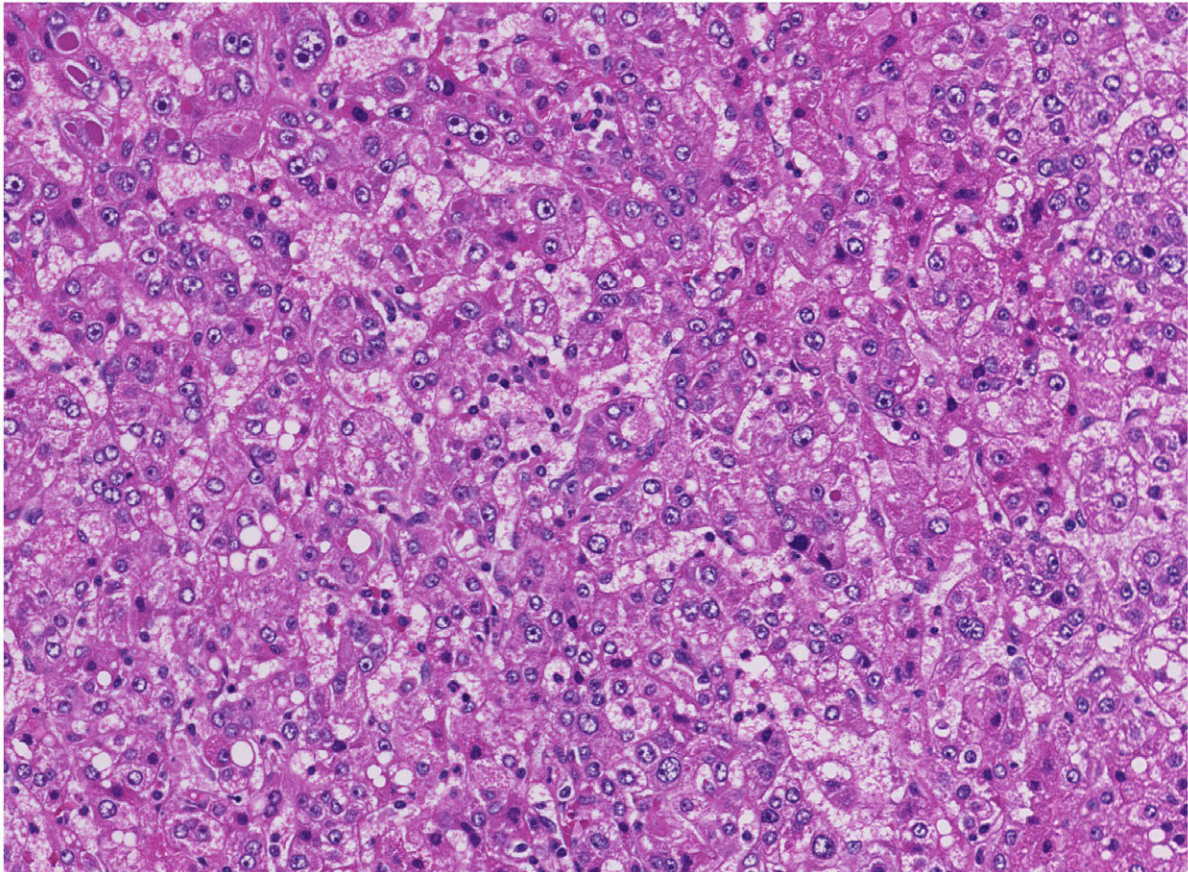


**Figure 1 Sub-nodule A** - Well-differentiated HCC component "hyaline bodies" are appreciable in the upper left hand corner

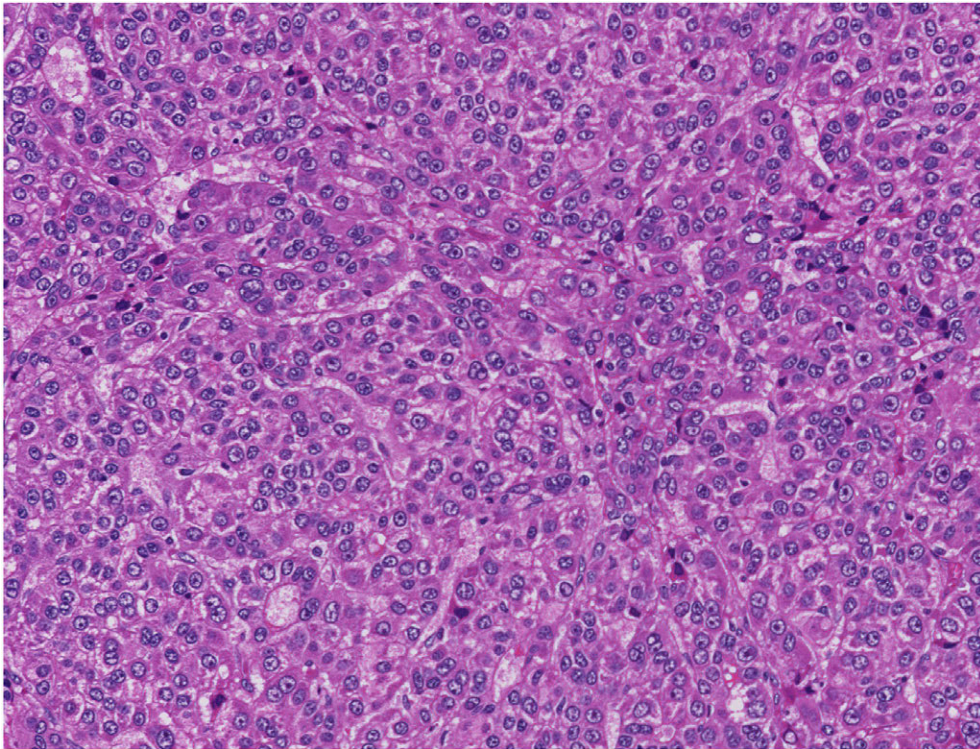


**Figure 2 Sub-nodule B** - Moderately differentiated component - a pseudo-glandular acinus is present in the upper left hand corner

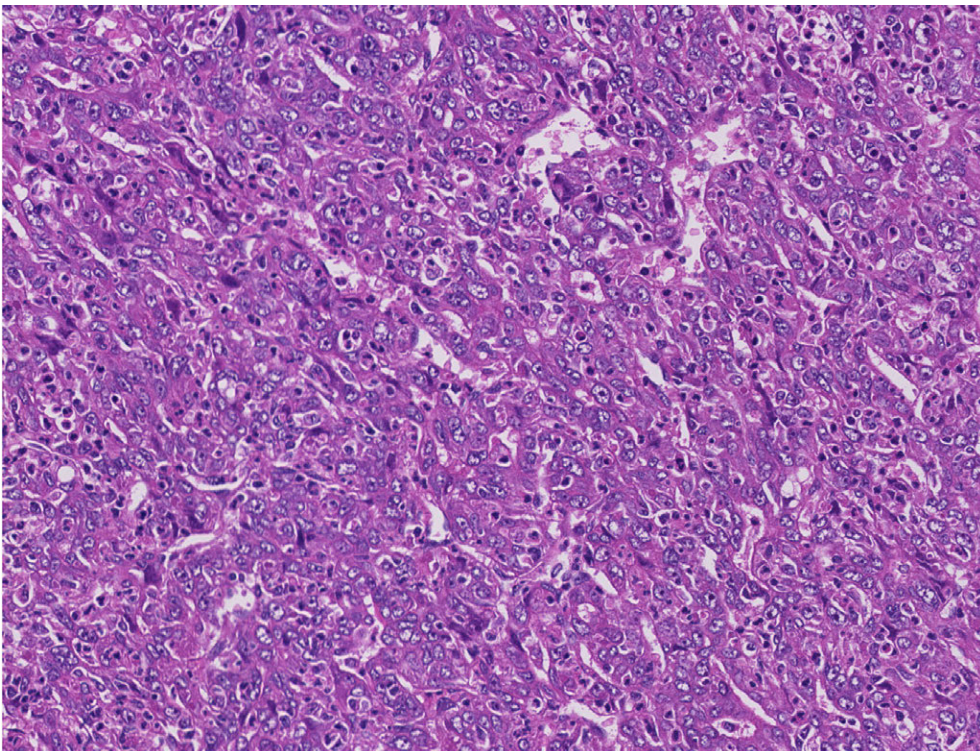


**Figure 3 Sub-nodule C** - poorly differentiated component - rare pseudo-glandular acini are present (top left)

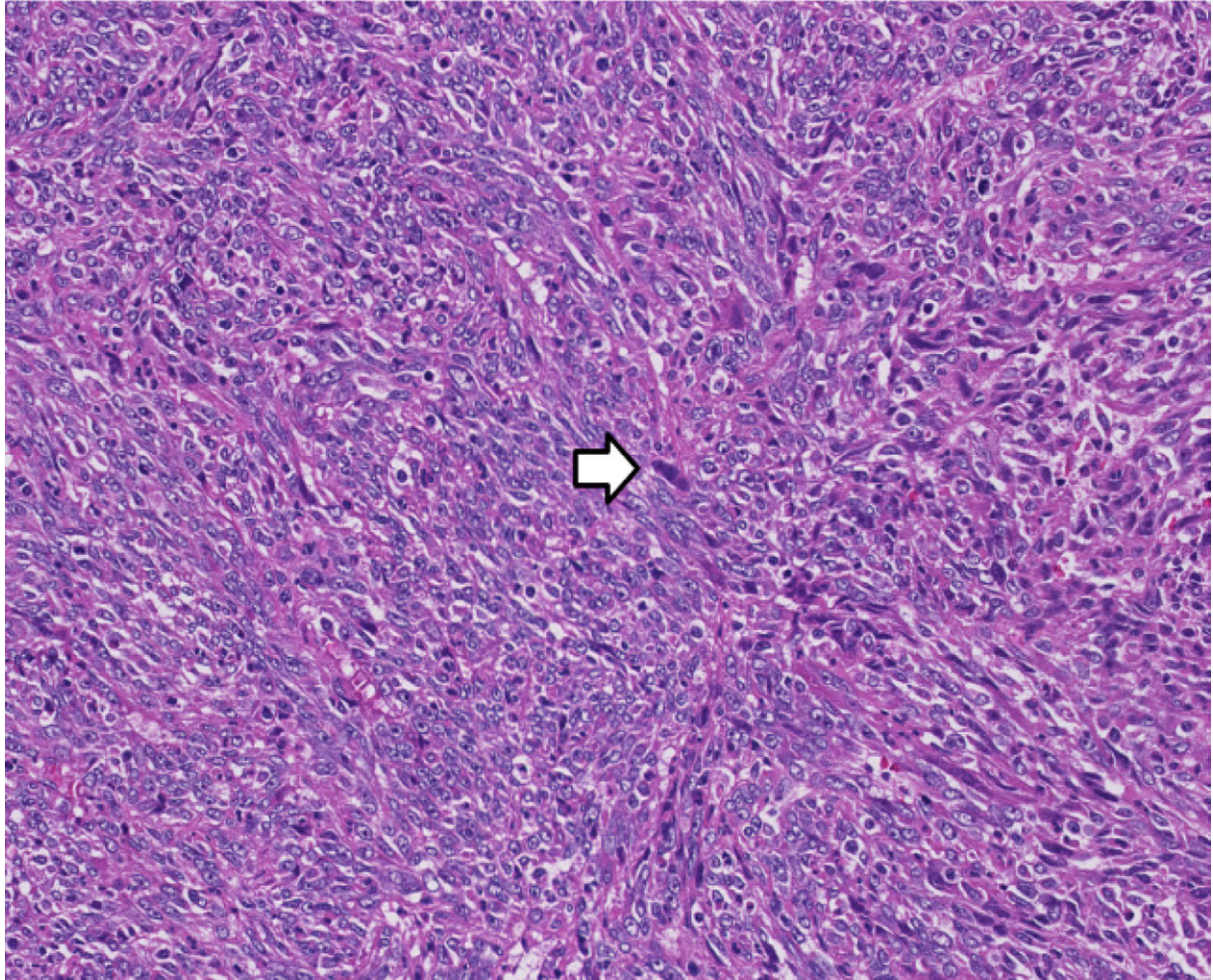


**Figure 4 Sub-nodule D** - Sarcomatoid component - a spindle-cell morphology predominates with occasional large pleomorphic nuclei (arrow)

**Diagnosis: Sarcomatoid hepatocellular carcinoma arising in a background of conventional well to moderately to poorly differentiated hepatocellular carcinoma.**

## Comments:

I thought this case was a useful illustration of sarcomatoid hepatocellular carcinoma arising in a small tumor with a readily appreciable more-differentiated hepatocellular carcinoma components. Despite being only a 2 cm lesion, 4 distinct morphologies are appreciable: well-differentiated HCC (sub-nodule A), moderately differentiated HCC (sub-nodule B), poorly differentiated HCC (sub-nodule C), and sarcomatoid HCC (sub-nodule D). Often a more differentiated hepatocellular carcinoma cannot be identified in sarcomatoid HCC or poorly differentiated HCC, making the diagnosis more challenging. Hepatocellular carcinomas are known to exhibit this "nodule-in-nodule" phenomenon of higher-grade morphologies arising as distinct nodule within larger nodules, but this case represents a remarkable version of this phenomenon, with multiple distinct nodules within the larger 2.0 cm nodule. Unfortunately, this patient passed away two years following this diagnosis, due to T-ALL recurrence.

# Case 24

Fátima Carneiro

---

## Clinical History:

Female, 24-year-old, with a liver mass; the patient was submitted to partial hepatectomy.

## Pathological Findings

**Macroscopy:** In the liver specimen (13.5 cm in largest dimension) a large tumor (12x9x8 cm) was observed with heterogeneous appearance, displaying several cysts (with fluid content), solid areas (yellowish and green) and multifocal necrosis.

**Histology:** The tumor displayed malignant cystic structures and two solid components: a poorly differentiated carcinoma with features of cholangiocarcinoma and a hepatocellular component with enough atypia to be considered as malignant too. Most cystic structures were entirely malignant; a minor component of the cysts was lined by normal biliary epithelium, some by mucinous epithelium.

**Immunohistochemistry:** The neoplastic cells of the cholangiocarcinoma component expressed CK7, CK19, EpCAM and pCEA. In the hepatocellular component there was immunoreactivity for Hep-par1, arginase and glutamine synthetase. The stromal cells below the lining of the cysts were positive for estrogen receptor. Others markers were negative in both components: alpha-fetoprotein, Glypican-3, CD56, HMB45, S100 protein, Melan-A, CD30 and PLAP.

**Diagnosis: Combined hepatocellular-cholangiocarcinoma (cHCC-CCA).**

(The case was seen in consultation by Prof. John Hart and Prof. David Klimstra).

## Comments:

Combined hepatocellular-cholangiocarcinoma (cHCC-CCA) is a primary liver carcinoma (PLC) defined by the unequivocal presence of both hepatocytic and cholangiocytic differentiation within the same tumour; collision tumours are not part of this entity (WHO

2019). cHCC-CCA is a rare tumour, with an incidence that varies among different reports between 0.4 and 14.2% of all Primary Liver Carcinomas (PLCs) (Jarnagin WR *et al*, 2002; Koh KC *et al*; 2005; Brunt E *et al*, 2018). The clinical appearance of cHCC-CCA is similar to that of HCC and iCCA and it is usually silent until advanced states, causing a delay of diagnosis (Cutolo C *et al*, 2022).

Among the risk factors, hepatitis B and hepatitis C virus infections, cirrhosis, and male gender are widely reported (Cutolo C *et al*, 2022).

The **histopathology** of cHCC-CCA is characterized by the coexistence of hepatocytic and cholangiocytic tumour areas. The two components are either close to each other or deeply intermingled, and the transition between them can be either poorly defined or sharp (Brunt E *et al*, 2018). There are no definite data at present to support the inclusion of minimum cut-off amounts of each component for the diagnosis of cHCC-CCA, and this diagnosis is made regardless of the percentage of each component. The biphenotypic differentiation is based on the H&E morphology and can be confirmed by hepatocytic and cholangiocytic immunohistochemical markers. However, immunohistochemistry alone is not sufficient for a diagnosis of cHCC-CCA without supportive histomorphology. Given the substantial intratumour heterogeneity of cHCC-CCA, extensive tumour sampling is highly recommended (sampling all different macroscopic areas with at least 1 block/cm collected at the macroscopic analysis) in order to best cover the various tumour areas throughout the nodule. Distant metastases can show either cHCC-CCA features or an individual component of the original tumour (De Vito C *et al*, 2017).

The **immunohistochemical (IHC)** detection of markers of hepatocytic and cholangiocytic differentiation may help but is neither necessary nor sufficient (Beaufrère A *et al*, 2021). A set of markers is available to confirm a hepatocellular component, including Glypican-3, AFP, HepPar1, and Arginase-1 (Di Tommaso L *et al*, 2007; Sciarra A *et al*, 2020). Arginase-1 performs better in less-differentiated HCC than HepPar1, while AFP is only rarely positive (Beaufrère A *et al*, 2021). Polyclonal carcinoembryonic antigen and CD10 are the most specific IHC markers when a canalicular pattern is observed, but their sensitivity is low (El Jabbour T *et al*, 2019). To confirm a cholangiocytic differentiation, several markers can be used, including CK7 and CK19 (Sciarra A *et al*, 2020). EpCAM positivity is observed in >90% of cholangiocytic differentiation areas and in 10-20% of hepatocellular areas (Sciarra A *et al*, 2020). Finally, if IHC is discordant with the first H&E, it is advised to perform IHC on other slides and to take new tumour samples. Nestin, a marker of bipotent progenitor oval cells may serve as a diagnostic biomarker of cHCC-CCA (Xue R

*et al*, 2019; Sasaki M *et al*, 2022). However, nestin is expressed in a subset of HCC and iCCA, and its value for cHCC-CCA remains to be assessed in large series (Xue R *et al*, 2019).

The **pathogenesis** of cHCC-CCA is not fully elucidated. Plasticity or transdifferentiation of HCC, as demonstrated in several mouse models (Li L *et al*, 2018) and supported by the occurrence of cHCC-CCA after transarterial chemoembolization (TACE), has been proposed (Zen C *et al*, 2011). Liver progenitor/ stem cell origin has also been suggested (Coulouarn C *et al*, 2012).

Several **molecular studies** of cHCC-CCA have supported a common clonal origin of the HCC and CCA components. The variability of the mutation spectrum in different studies probably reflects differences in collective composition. Typical mutations of HCC (e.g. *CTNNB1*) and iCCA (e.g. *KRAS*, *IDH1*) have been found (Cazals-Hatem D *et al*, 2004; Fujimoto A *et al*, 2015; Liu ZH *et al*, 2018; Sasaki M *et al*, 2017). cHCC-CCAs enriched in cells with stem/progenitor morphology are frequently positive for SALL4, fetal-type growth factors, and stem cell signatures (Moeini A *et al*, 2017). It was shown that the most frequently mutated driver genes were *TP53* (49% of the cases), *TERT* promoter (23% of the cases), *AXIN1* (10% of the cases), and *KMT2D* (9% of the cases) (Xue R *et al*, 2019); these mutations may be associated with either HCC or iCCA.

## References:

1. Beaufrère A, Calderaro J, Paradis V. Combined hepatocellular-cholangiocarcinoma: An update. *J Hepatol*. 2021;74(5):1212-1224.
2. Brunt E, Aishima S, Clavien PA, *et al*. cHCC-CCA: Consensus terminology for primary liver carcinomas with both hepatocytic and cholangiocytic differentiation. *Hepatology*. 2018; 68(1):113-126.
3. Cazals-Hatem D, Rebouissou S, Bioulac-Sage P, *et al*. Clinical and molecular analysis of combined hepatocellular-cholangiocarcinomas. *J Hepatol*. 2004; 41(2):292-8
4. Coulouarn C, Cavard C, Rubbia-Brandt L, *et al*. Combined hepatocellular-cholangiocarcinomas exhibit progenitor features and activation of Wnt and TGFβ signaling pathways. *Carcinogenesis*. 2012 Sep;33(9):1791-6.
5. Cutolo C, Dell'Aversana F, Fusco R, *et al*. Combined Hepatocellular-cholangiocarcinoma: What the Multidisciplinary Team Should Know. *Diagnostics (Basel)*. 2022;12(4):890.
6. De Vito C, Sarker D, Ross P, *et al*. Histological heterogeneity in primary and metastatic classic combined hepatocellular-cholangiocarcinoma: a case series. *Virchows Arch*. 2017;471(5):619-629.

7. Di Tommaso L, Franchi G, Park YN, *et al.* Diagnostic value of HSP70, glypican 3, and glutamine synthetase in hepatocellular nodules in cirrhosis. *Hepatology* 2007;45:725-734
8. El Jabbour T, Lagana SM, Lee H. Update on hepatocellular carcinoma: pathologists' review. *World J Gastroenterol* 2019;25:1653-1665.
9. Fujimoto A, Furuta M, Shiraishi Y, *et al.* Whole-genome mutational landscape of liver cancers displaying biliary phenotype reveals hepatitis impact and molecular diversity. *Nat Commun.* 2015;6:6120.
10. Jarnagin WR, Weber S, Tickoo SK, *et al.* Combined hepatocellular and cholangiocarcinoma: Demographic, clinical, and prognostic factors. *Cancer* 2002, 94, 2040-2046.
11. Koh KC, Lee H, Choi MS, *et al.* Clinicopathologic features and prognosis of combined hepatocellular cholangiocarcinoma. *Am. J. Surg.* 2005, 189, 120-125.
12. Li L, Qian M, Chen IH, *et al.* Acquisition of cholangiocarcinoma traits during advanced hepatocellular carcinoma development in mice. *Am J Pathol.* 2018;188(3):656-671.
13. Liu ZH, Lian BF, Dong QZ, *et al.* Whole-exome mutational and transcriptional landscapes of combined hepatocellular cholangiocarcinoma and intrahepatic cholangiocarcinoma reveal molecular diversity. *Biochim Biophys Acta Mol Basis Dis.* 2018;1864(6 Pt B):2360-2368.
14. Moeini A, Sia D, Zhang Z, *et al.* Mixed hepatocellular cholangiocarcinoma tumors: Cholangiolocellular carcinoma is a distinct molecular entity. *J Hepatol.* 2017;66(5):952-961.
15. Sasaki M, Sato Y, Nakanuma Y. Is nestin a diagnostic marker for combined hepatocellular-cholangiocarcinoma? *Histopathology.* 2022;80(5):859-868.
16. Sasaki M, Sato Y, Nakanuma Y. Mutational landscape of combined hepatocellular carcinoma and cholangiocarcinoma, and its clinicopathological significance. *Histopathology.* 2017;70(3):423-434.
17. Sciarra A, Park YN, Sempoux C. Updates in the diagnosis of combined hepatocellular-cholangiocarcinoma. *Hum Pathol* 2020;96:48-55.
18. Xue R, Chen L, Zhang C, Fujita M, Li R, Yan S-M, *et al.* Genomic and transcriptomic profiling of combined hepatocellular and intrahepatic cholangiocarcinoma reveals distinct molecular subtypes. *Cancer Cell* 2019;35 932-947.e8
19. Zen C, Zen Y, Mityr RR, *et al.* Mixed phenotype hepatocellular carcinoma after transarterial chemoembolization and liver transplantation. *Liver Transpl.* 2011; 17(8):943-54.

## Case 25

### Clinical History:

A 38-year-old man with a history of interstitial lung disease and combined variable immunodeficiency (CVID) presented with severe sequelae of portal hypertension, including massive splenomegaly (28.4 cm spleen on imaging), and splenorenal, retroperitoneal, and gastroesophageal varices. Liver function tests were mildly but chronically elevated, which had previously been thought to be due to non-alcoholic fatty liver disease as the patient was obese.

### Macroscopic Features:

The explanted liver showed a vaguely nodular architecture, suggestive of cirrhosis.

### Histological and histochemical Findings:

In the provided representative section, the hepatocyte cords exhibit alternating thinning and thickening, imparting a microscopic nodular appearance. A reticulin stain further confirms the alternating hypertrophic and atrophic cords. A trichrome stain

**Diagnosis: Nodular regenerative hyperplasia arising in combined variable immunodeficiency.**

### Comments:

Nodular regenerative hyperplasia NRH is a hyperplastic pattern of liver injury associated with a variety of underlying conditions including HIV, fatty liver disease, primary biliary cholangitis, and combined variable immunodeficiency, among many other conditions. Regardless of the underlying etiology, the remodeling and hyperplasia of the liver parenchyma is thought to be due to vascular injury.

Essentially, NRH represents a morphologic pattern resulting from vascular injury, secondary to a variety of underlying causes, much like cirrhosis is a morphologic pattern resulting from parenchymal liver injury due to a variety of underlying causes. NRH can present as a solitary nodule and sometimes accounts for a clinical-radiologic impression of a mass lesion, though the majority or entirety of liver parenchyma can be remodeled

into small nodules. Unlike cirrhosis, NRH shows no significant fibrosis. Nonetheless, the liver injury and remodeling can cause severe portal hypertension, and result in the usual sequelae (varices, splenomegaly, ascites, and liver failure). As many as 5% of patients with CVID develop NRH, and three clinical groups have been identified: 1) non-progressive NRH; 2) NRH progressing to portal hypertension and splenomegaly; 3) NRH with an autoimmune-hepatitis (AIH)-like syndrome [1]. Patients in the second group often require intervention such as TIPS placement, spleno-renal shunt, or liver transplantation as in our patient. Data is limited, but CVID patients appear to suffer a more aggressive course of NRH. The patients with NRH and the AIH-like syndrome suffer from portal hypertension complications and seem to be refractory to immunosuppression with regard to AIH-like component [1].

Identifying NRH, whether in the context of CVID or not, can be useful in accounting for the radiologic impression of a mass lesion, as well as for explaining clinical portal hypertension in the absence of significant liver fibrosis. Pathologists and clinicians alike should be aware of non-cirrhotic portal hypertension, and that not every patient with sequelae of portal hypertension exhibits classic cirrhosis.

Following transplant, the patient fully recovered and was able to work full-time again.

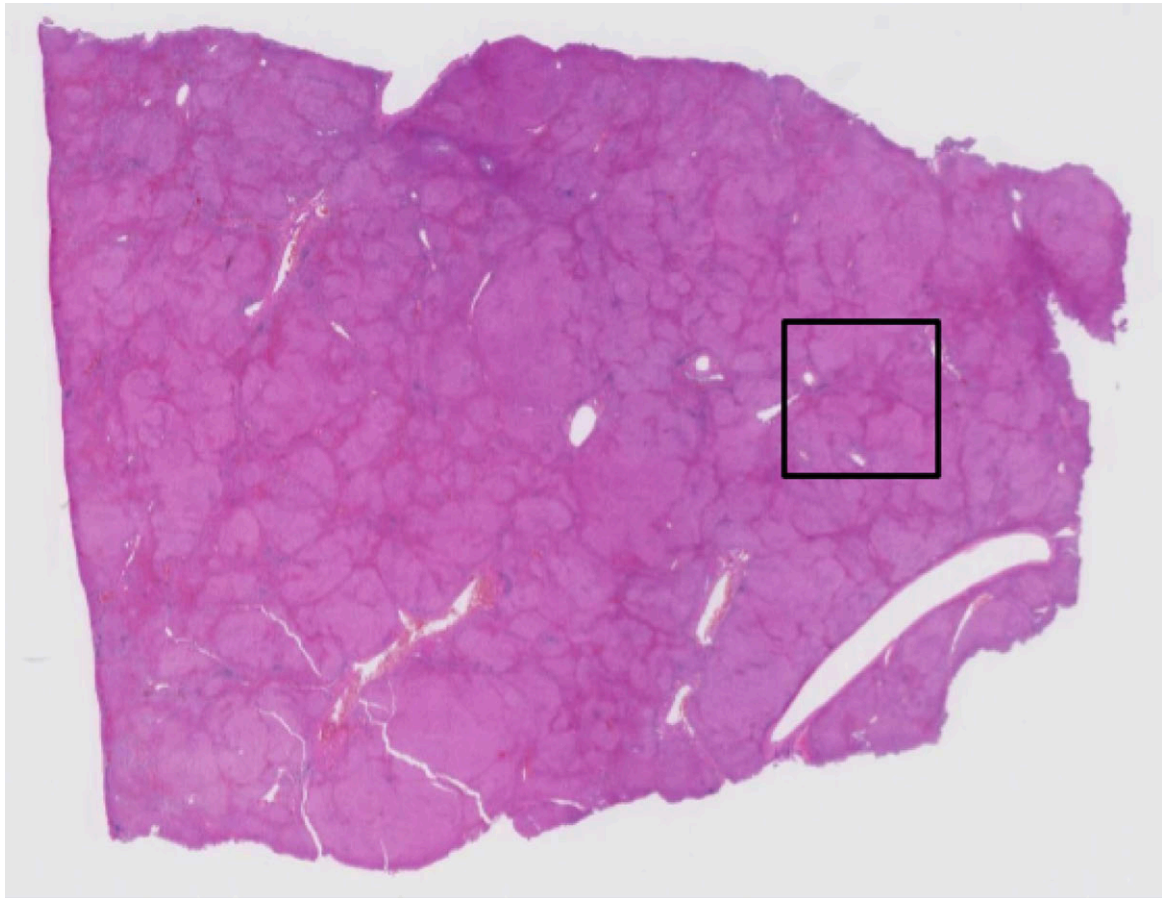
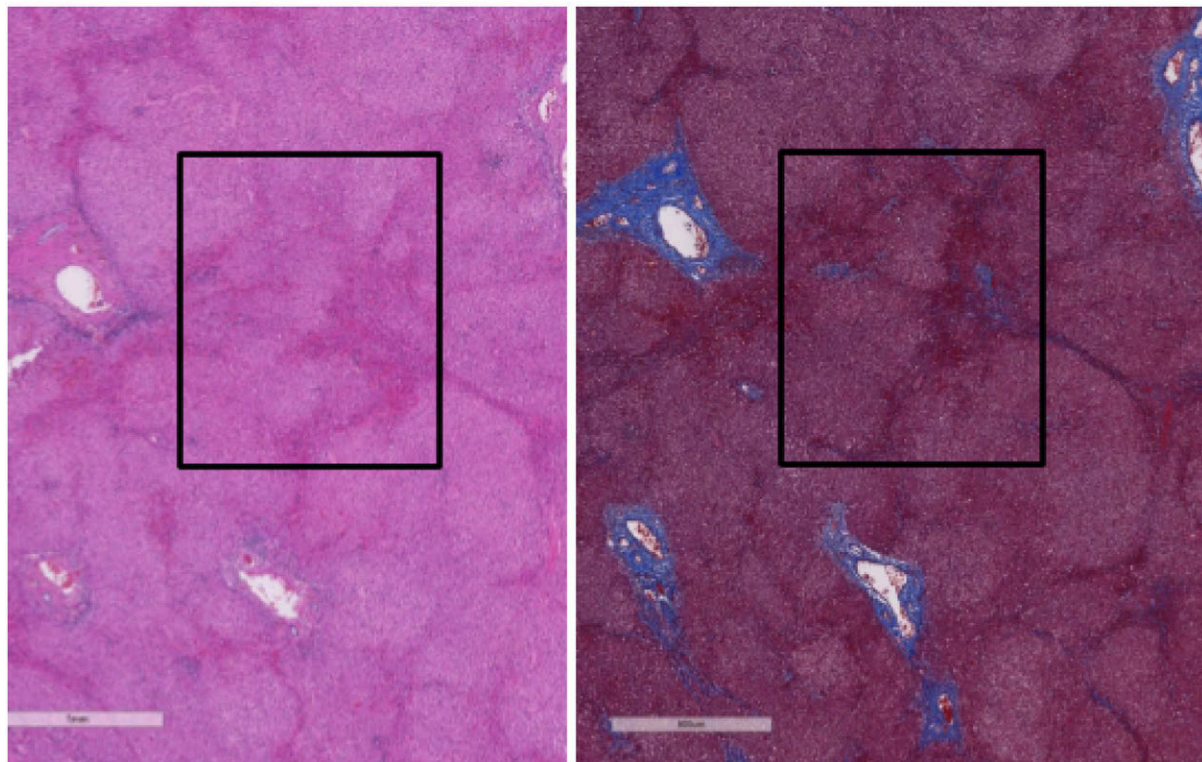
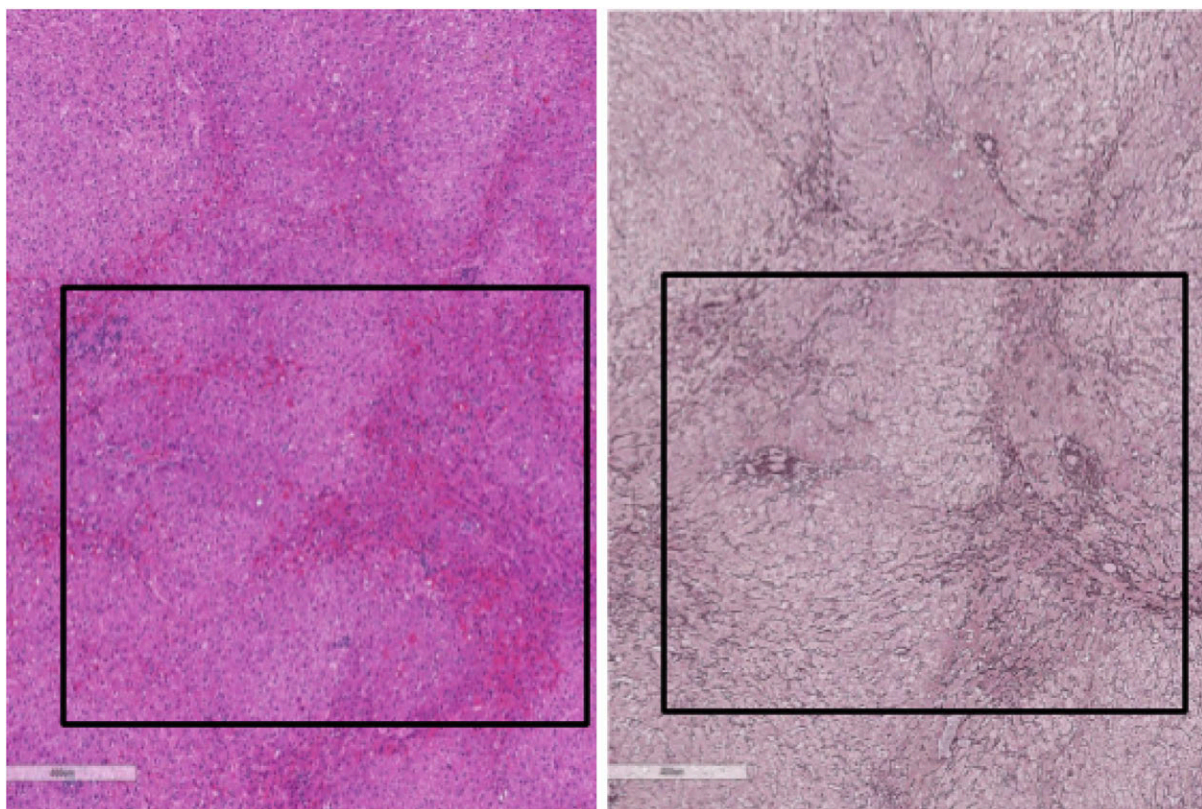


Figure 1H&E



**Figure 2**Left: H&E; Right: Trichrome



**Figure 3** Left: H&E; Right: Reticulin

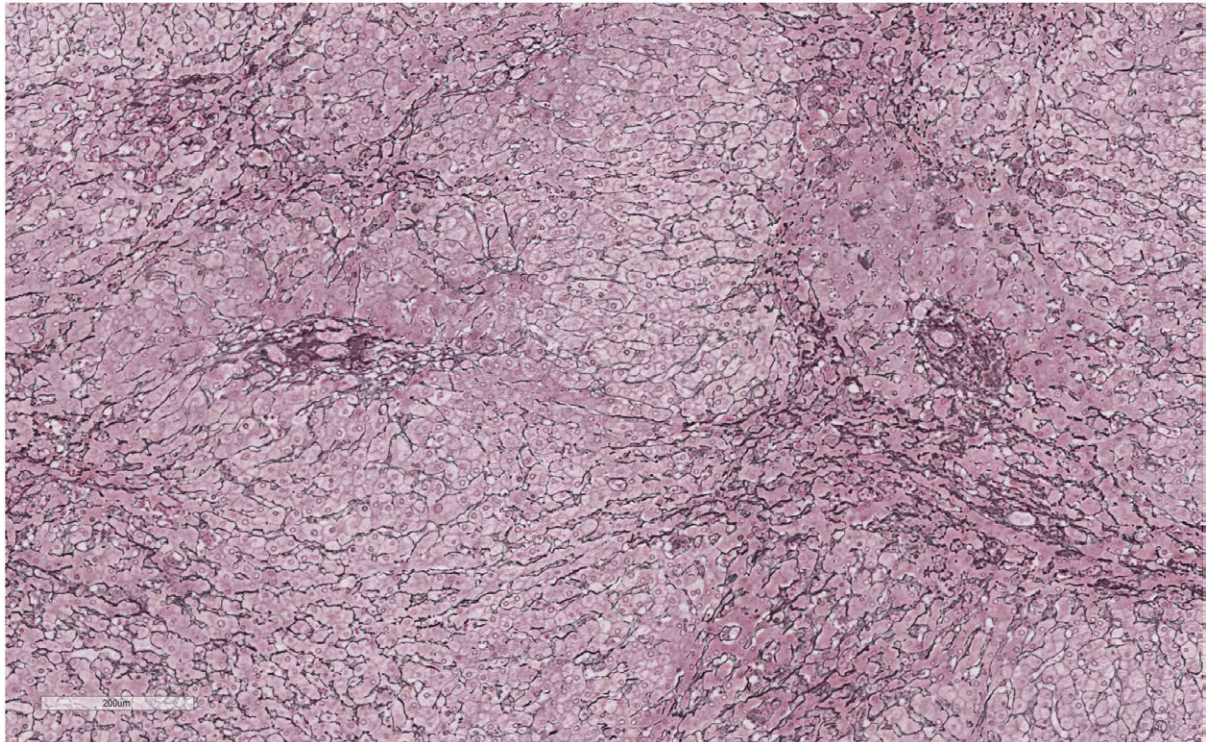


**Figure 4** Reticulin

The above sequence of images highlights the striking low-power nodularity, lack of significant fibrosis, and thickened hypertrophic hepatocyte cords alternating with atrophic hepatocyte cords, which imparts the nodular appearance.

## References:

1. Pecoraro A, Crescenzi L, Varricchi G, Marone G, Spadaro G. Heterogeneity of Liver Disease in Common Variable Immunodeficiency Disorders. *Front Immunol.* 2020 Feb 28;11:338. PMID: 32184784; PMCID: PMC7059194.

## Case 26

### Liver metastases of MANEC (L. DiTommaso)

---

#### Clinical history:

Man, 74 yrs old. History of benign prostatic hyperplasia (TURP performed elsewhere). A US performed during a check-up for acute urine retention revealed 3 lesions in the liver. Imaging (PET; CT; MNR) negative for other lesions. No biopsy performed. Pre-operative diagnosis: cholangiocarcinoma.

#### Pathologic findings:

Liver of 12x7x7 cm (IV and V segments) and gallbladder resection; > 10 lesions, sizing 0.2 to 6 cm; the largest lesion was close to the gallbladder; another lesion (size 3 cm.) was localized in the wall of the gallbladder. All the lesions showed features (synaptophysin+, chromogranin+, Ki67>80%) consistent with a diagnosis of NE carcinoma. The 3 cm-lesion in addition was characterized by a clear-cut adenocarcinomatous component. Both neoplastic components of this mixed NE-ADK were CK7+, CK19+, cdx2+ and TTF1+.

#### Diagnosis. Liver metastases of MANEC.

After the diagnosis the patient underwent prostatic and colorectal biopsy, all with benign findings; CEA, GICA, AFP and PSA negative; the patient died 4 months after the diagnosis; autopsy was not requested.

#### Discussion:

The concept of MANEC was first officially introduced by the World Health Organization classification of tumors of the digestive system in 2010 (1). MANECs constitute a group of tumors characterized by adenocarcinomatous and neuroendocrine differentiation. MANECs most commonly arise in the colon, appendix, rectum or stomach, however a limited number of MANECs have been reported to originate from the bile duct, the pancreas and the gallbladder (2).

## References:

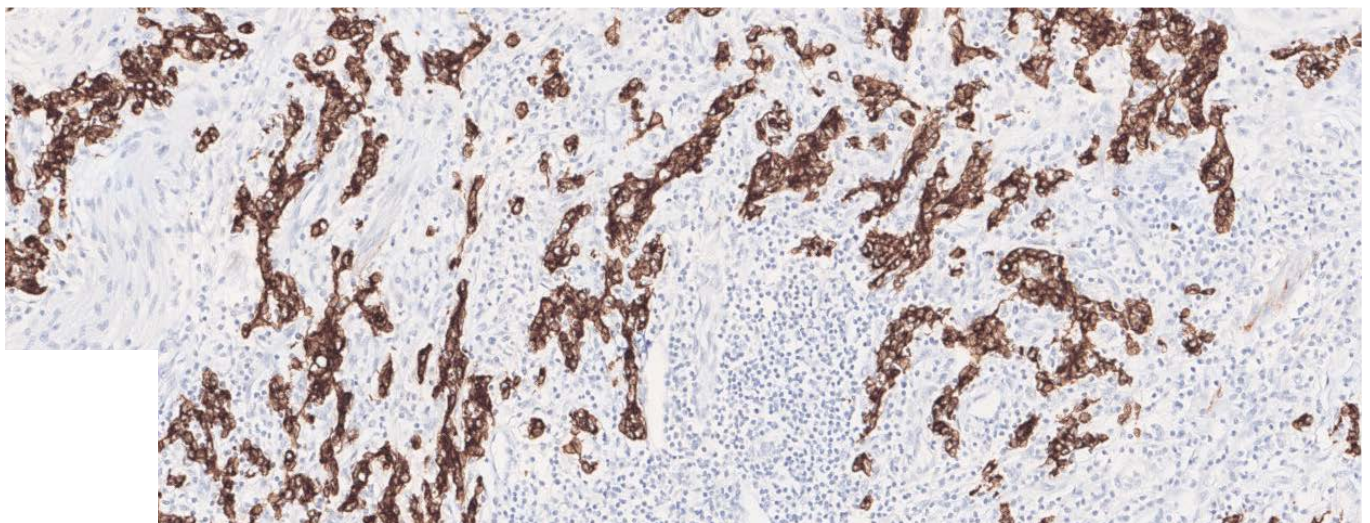
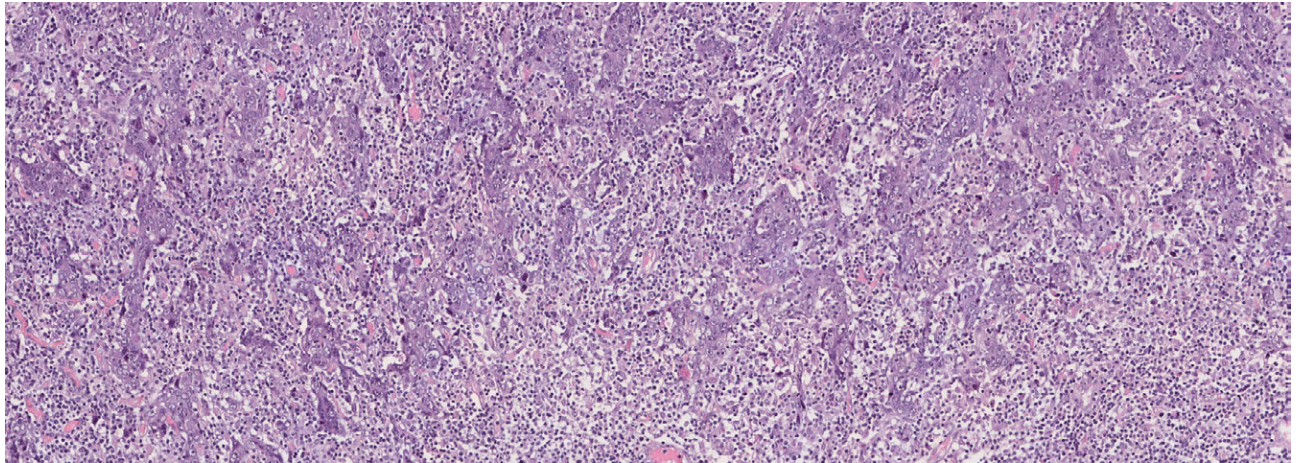
1. Bosman F, et al. WHO Classification of Tumors of the Digestive Tract. 4th Edition. World Health Organization, Geneva. 2010.
2. Acosta AM, et al. Primary biliary mixed adenoneuroendocrine carcinoma (MANEC): A Short Review. Arch Pathol Lab Med 140: 1157-1162, 2016.

# Case 27

Contributed by Irene Gullo, M.D., Ph.D.

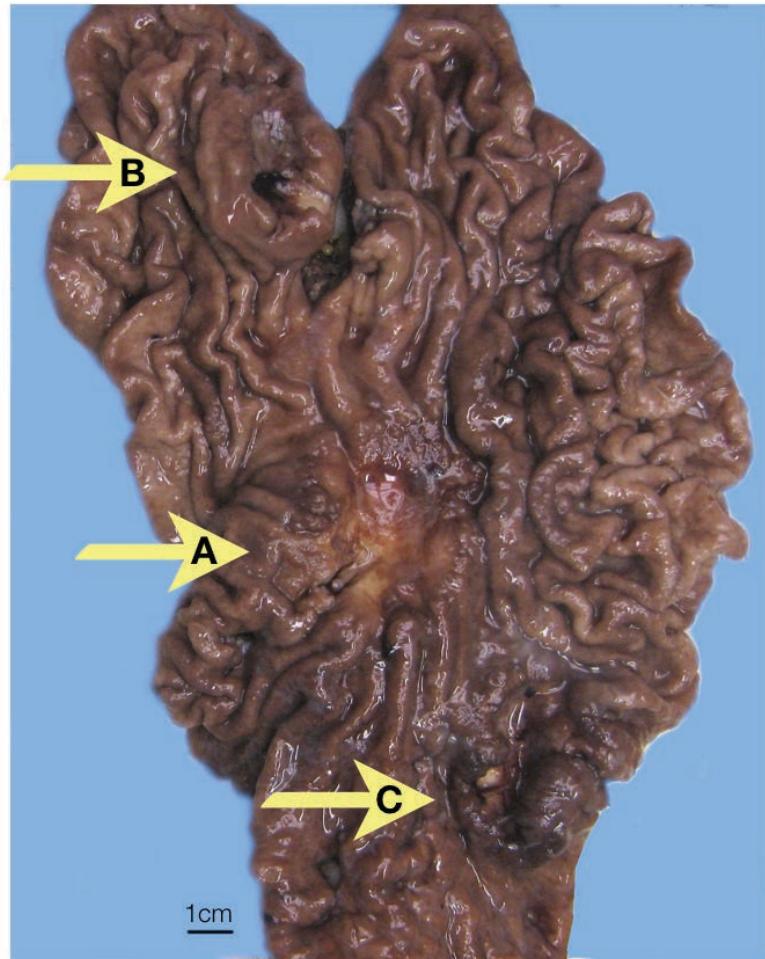
## Clinical history:

77-year-old male with previous history of diffuse large B cell lymphoma of the palatine tonsil, stage I, treated by R-CHOP regimen. He presented with a history of gastrointestinal bleeding due to a gastric ulcerated tumour. He underwent total gastrectomy.



## Gross features:

total gastrectomy specimen showed an ulcerated tumour in the gastric body with 4,5cm (A) and two fungating tumours in the gastric fundus (B) and antrum (C).



## Histopathological findings:

the three tumours showed similar morphologic characteristics. They were composed of irregular sheets, cords and trabeculae of polygonal epithelial cells with pleomorphism and prominent nucleoli, embedded within a prominent lymphoplasmacytic infiltrate, with intraepithelial lymphocytes.

**Diagnosis: gastric cancer with lymphoid stroma.**

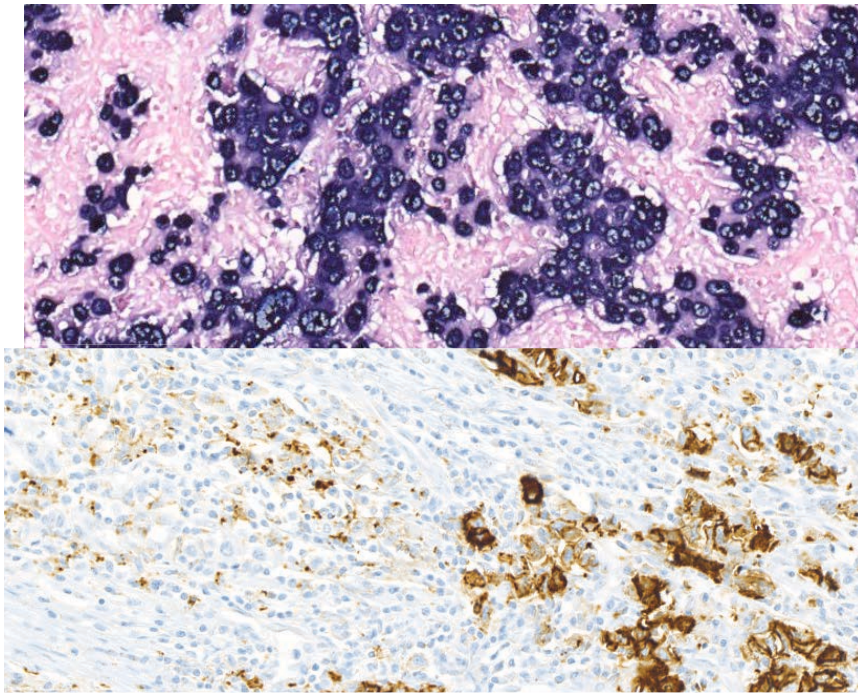
## Comment:

gastric cancer with lymphoid stroma (*alias* medullary carcinoma, lymphoepithelioma-like carcinoma) was first reported by Watanabe *et al* in 1976 and is recognized by the 5th edition of the WHO classification of Digestive Tumours as a rare histological subtype of gastric cancer. The lymphoid infiltrate can be so prominent that immunohistochemical study may be necessary to confirm the epithelial nature of the tumour. As demonstrated by immunohistochemical studies, cytotoxic T lymphocytes constitute the predominant component of the infiltrate, which also contains B lymphocytes, plasma cells, neutrophils and eosinophils.

The tumours are frequently localized in the proximal stomach or gastric stump, they are more common in males and are characterised by a better overall survival. Multiplicity (multiple synchronous or metachronous tumours) is also a characteristic feature, as occurred in our case.

This morphologic subtype is frequently associated to Epstein-Barr virus (EBV) infection (in over 80% of cases). A similar morphology can be observed in gastric cancer with mismatch repair protein deficiency / microsatellite instability. The recognition of these two molecular subtypes is of the utmost importance, since recent clinical trials demonstrated that, in patients with MSI-high and EBV+ gastric cancers, clinical responses to targeted immunotherapy (i.e. Pembrolizumab) are achieved. In the case presented in this seminar, RNA *in situ* hybridisation for EBV (EBER) was positive and immunohistochemistry showed high expression of PD-L1 both in tumour cells and immune cells of the tumour microenvironment. This case stresses the importance of searching for EBV infection, by EBER *in situ* hybridisation and mismatch repair protein deficiency, by immunohistochemistry, in gastric cancers presenting the morphologic features of gastric cancer with lymphoid stroma, for a cost-effective molecular characterisation and selection of patients for targeted immunotherapies.

**Final diagnosis: gastric cancer with lymphoid stroma associated with EBV infection and PD-L1 expression (potentially eligible for targeted immunotherapy).**



## References

1. Watanabe, H., M. Enjoji, and T. Imai. Gastric carcinoma with lymphoid stroma. Its morphologic characteristics and prognostic correlations. *Cancer*, 1976. 38(1): p. 232-43.
2. Yang J, Liu Z, Zeng B, et al. Epstein-Barr virus-associated gastric cancer: A distinct subtype. *Cancer Lett*. 2020;28;495:191-199. doi: 10.1016/j.canlet.2020.09.019.
3. Gullo I, Oliveira P, Athellogou M, et al. New insights into the inflamed tumor immune microenvironment of gastric cancer with lymphoid stroma: from morphology and digital analysis to gene expression. *Gastric Cancer*. 2019;22(1):77-90. doi: 10.1007/s10120-018-0836-8.
4. Gullo I, Carvalho J, Martins D, et al. The Transcriptomic Landscape of Gastric Cancer: Insights into Epstein-Barr Virus Infected and Microsatellite Unstable Tumors. *Int J Mol Sci*. 2018;17;19(7):2079. doi: 10.3390/ijms19072079.
5. Shinozaki-Ushiku A, Kunita A, Fukayama M. Update on Epstein-Barr virus and gastric cancer (review). *Int J Oncol*. 2015;46(4):1421-34. doi: 10.3892/ijo.2015.2856.
6. Kim ST, Cristescu R, Bass AJ, et al. Comprehensive molecular characterization of clinical responses to PD-1 inhibition in metastatic gastric cancer. *Nat Med*. 2018;24(9):1449-1458. doi: 10.1038/s41591-018-0101-z.

## Case 28

### Clinical History:

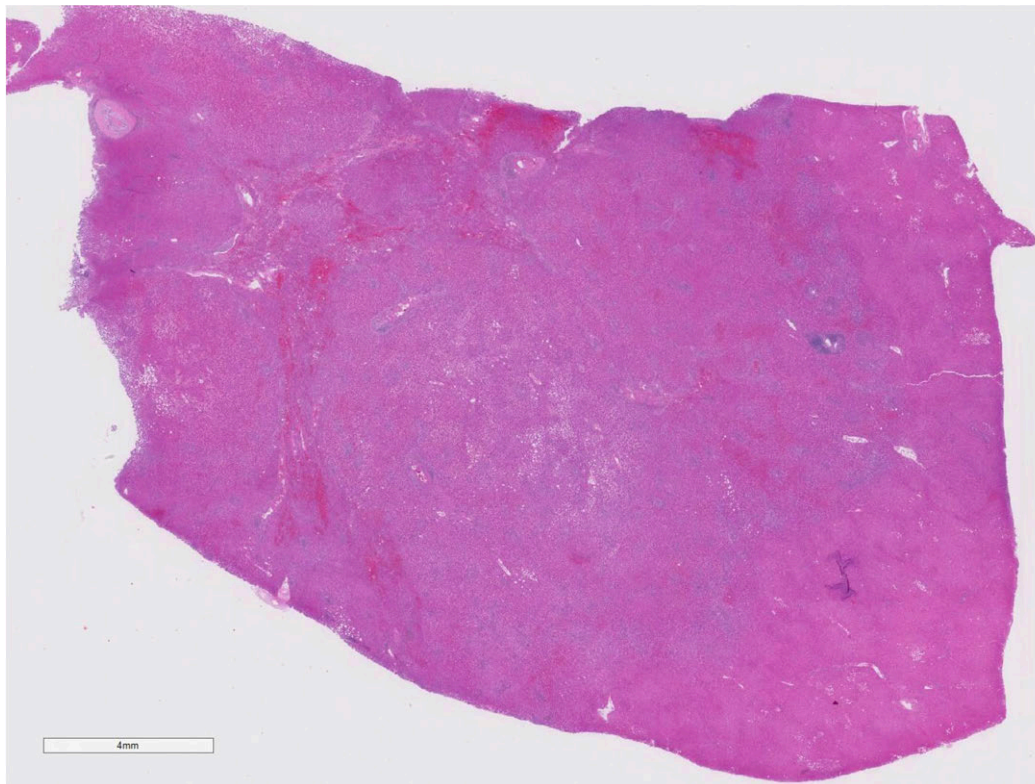
A 41-year-old woman with multiple large liver masses that grew steadily over a 2-year period. Despite conservative management and discontinuation of oral contraceptives for 2 years, transplantation was required due to disease burden. The patient was found to have a PALB2 mutation (a BRCA2 partner gene).

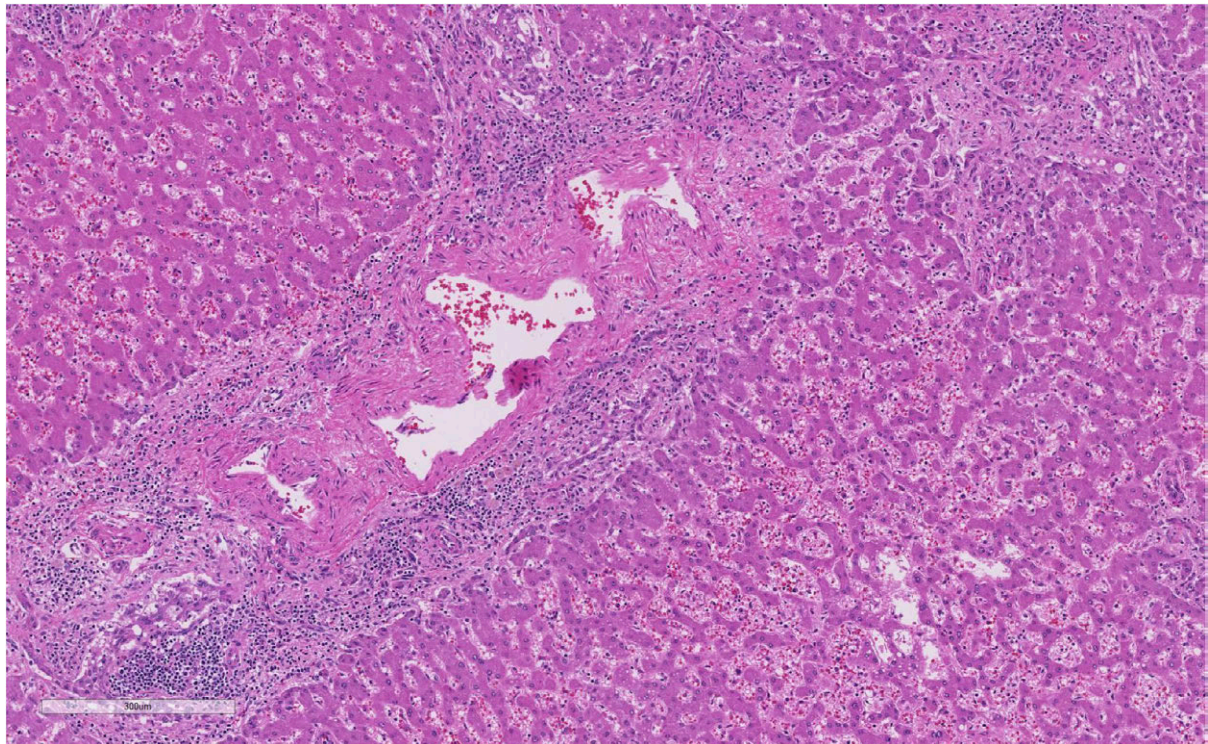
### Macroscopic Features:

Four large dominant circumscribed masses were identified grossly, with the largest measuring 9.2 cm, but innumerable other circumscribed masses were also identified grossly.

### Histological Findings:

At low power, sections of the liver masses appear to show nodular, mildly inflamed benign liver parenchyma.





At higher power, the portal tracts show large irregular arteries, but bile ducts are present (bottom left).

Prominent sinusoidal dilatation is noted (down and right from the portal tract). The background liver showed mild steatosis without evidence of steatohepatitis. Glutamine synthetase immunohistochemistry was strongly and diffusely positive in areas with these abnormal portal tracts (image not shown in handout), while beta-catenin was negative in the nuclei.

**Diagnosis: Hepatocellular adenoma, inflammatory subtype (formerly known as telangiectatic subtype), presenting as adenomatosis, with beta-catenin activation.**

### Comments:

While this case might be somewhat routine for liver pathologists, I thought it would be useful for pathologists in the group who encounter liver lesions in a generalist setting. Also, this represents the extreme end of the spectrum of adenomatosis, wherein the burden of disease required liver transplantation. The inflammatory subtype of hepatocellular adenoma accounts for up to 50% of hepatocellular adenomas and is most

common in women. This sub-type can be challenging and subtle as bile ducts are present in areas of abnormal vessels ("pseudo-portal tracts"). Fibrous septation can be present which can introduce a challenging differential diagnosis of focal nodular hyperplasia - due to this similarity, a subset of focal nodular hyperplasia had been called "telangiectatic focal nodular hyperplasia" but such cases are now known to represent hepatocellular adenoma, inflammatory subtype. Nonetheless, a subset of focal nodular hyperplasia cases can show prominent sinusoidal dilation [1].

Strong diffuse staining for C-reactive protein and/or serum amyloid-associated protein immunohistochemistry is helpful for confirming the diagnosis, with C-reactive protein showing greater sensitivity in this regard. Another subtlety in these neoplasms is the findings of beta-catenin activation in up to 10% of cases. Interestingly, diffuse staining for glutamine synthetase, even without nuclear positivity for beta-catenin is strong evidence of beta-catenin activation [2]. Beta-catenin activation is thought to represent a significant prognostic indicator for progression to hepatocellular carcinoma. The finding of a somatic PALB2 mutation (a BRCA2 partner gene) was a red herring in this case as there is no known association of PALB2 or BRCA2 with hepatocellular adenoma.

## References:

1. Joseph NM et al. Diagnostic utility and limitations of glutamine synthetase and serum amyloid-associated protein immunohistochemistry in the distinction of focal nodular hyperplasia and inflammatory hepatocellular adenoma. *Mod Pathol* 2014;27:62-72.
2. Bioulac-Sage P et al. Hepatocellular adenoma subtype classification using molecular markers and immunohistochemistry. *Hepatology* 2007;46:740-8.

## Case 29

**Michal Michal, Czech Republic**

---

A 38-year-old male had multiple myxoid nodules on the peritoneum of the omentum. The nodules were 0,5 to 3 cm in size. 1 year after the diagnosis the patient seems to be healthy.

**Diagnosis: Reactive nodular fibrous pseudotumor**

### Reference

1. Daum O, Vanecek T, Sima R, Curik R, Zamecnik M, Yamanaka S, Mukensnabl P, Benes Z, Michal M. Reactive nodular fibrous pseudotumors of the gastrointestinal tract. Report of 8 cases. *Int J Surg Pathol* 2004;12:365-374.

## Case 30

Brian Rubin, M.D., Ph.D., Cleveland Clinic, Cleveland, OH, USA

---

### Case History:

57-year-old male with a 7 cm deep-seated mass in the left thigh

### Pathologic Findings:

Grossly the tumor was multinodular, pink and fleshy with large areas of necrosis. Histologically, the lesion was unencapsulated with infiltrative margins. The lesion was characterized by sheets of pleomorphic cells with some extremely large, bizarre cells with multiple nuclei and a large amount of pale pink cytoplasm. There were areas with variable numbers of pleomorphic lipoblasts, with multiple vacuoles that indented and/or scalloped a hyperchromatic nucleus. Mitotic figures including atypical mitotic figures were numerous. There were also extensive areas of necrosis. Immunohistochemical studies revealed the lesional cells to be positive for cytokeratin AE1/AE3 and the cells were negative for cytokeratin Cam5.2, S-100, SOX10, HMB-45, SMA, and desmin. Genetic studies were not performed.

### Diagnosis: Pleomorphic Liposarcoma

### Discussion:

Pleomorphic liposarcoma is a rare sarcoma, accounting for less than 5% of all liposarcomas and less than 1% of all sarcomas. It is slightly more common in males with a peak in the 7<sup>th</sup> decade. It can involve virtually all anatomic sites but has a predilection for the deep soft tissue of the extremities.

Most tumors are large with a median size of 8-10 cm. Their cut surface is white to yellow and they often have areas of hemorrhage and/or necrosis, which can be extensive. Histologically, tumors have infiltrative margins and are characterized by sheets of pleomorphic cells with variable numbers of multivacuolated lipoblasts, which can be very focal. Indeed, strict adherence to criteria for multivacuolated lipoblasts can be helpful in classifying these lesions. Pleomorphic lipoblasts are defined as cells having multiple

vacuoles that indent or scallop a hyperchromatic nucleus. Myxoid stroma can be prominent suggesting a diagnosis of myxofibrosarcoma. Some cases are characterized by less pleomorphic epithelioid cells and are known as the epithelioid variant of pleomorphic liposarcoma. There are no consistent immunohistochemical findings but in general, they are negative for immunohistochemical markers. S-100 highlights can highlight lipoblasts. Keratin can be positive in more epithelioid lesions. MDM2 and CDK4 are not positive, helping to distinguish these lesions from dedifferentiated liposarcoma. Pleomorphic liposarcoma lacks consistent genetic alterations. They have bizarre karyotypes with numerous extra chromosomes and marker chromosomes. *MDM2* and/or *CDK4*.

Pleomorphic liposarcoma is a high grade sarcoma with significant local recurrence and metastatic rates. I grade pleomorphic liposarcoma according to the FNCLCC grading system.

The differential diagnosis is mainly all other pleomorphic neoplasms including pleomorphic variants of carcinoma and melanoma and other pleomorphic sarcomas. Carcinoma and melanoma are excluded by immunohistochemistry for keratins and/or EMA (carcinoma) or S-100 and SOX10 (melanoma). Distinction from other pleomorphic sarcomas is by line of differentiation as other pleomorphic sarcomas will express immunohistochemical markers to help establish their diagnosis. For instance, pleomorphic rhabdomyosarcoma is positive for desmin and myogenin/MyoD1. One potential pitfall is the diagnosis of dedifferentiated liposarcoma with heterologous pleomorphic liposarcomatous differentiation. While the heterologous pleomorphic liposarcomatous component can be identical histologically to conventional pleomorphic liposarcoma, these lesions typically arise in the retroperitoneum and are positive for MDM2/CDK4 by IHC and show *MDM2* gene amplification by fluorescence in-situ hybridization.

## References

1. Oliveira AM, Nascimento AG: Pleomorphic liposarcoma, *Semin Diagn Pathol* 18:274-285, 2001.
2. Miettinen M, Enzinger FM: Epithelioid variant of pleomorphic liposarcoma: a study of 12 cases of a distinctive variant of high-grade liposarcoma, *Mod Pathol* 12:722-728, 1999.
3. Mariño-Enríquez A, Fletcher CD, Dal Cin P, Hornick JL. Dedifferentiated liposarcoma with "homologous" lipoblastic (pleomorphic liposarcoma-like) differentiation: clinicopathologic and molecular analysis of a series suggesting revised diagnostic criteria. *Am J Surg Pathol* 34:1122-31, 2010.

## Case 32

### Clinical History:

A 76-year-old male patient developed an indurated dermo-subcutaneously located neoplasm on his back that was completely excised.

### Pathological Findings:

Histologically, we found a deep dermal, mainly subcutaneously located neoplasm. The partly nodular, partly diffusely infiltrating neoplasm is composed of monomorphic spindle-shaped tumour cells with spindled or wavy nuclei and little cytoplasm. The neoplastic cells are mainly arranged in interweaving cords and fascicles producing a peculiar braided pattern. In transverse sections the tumour cell formations resemble nests, whereas in longitudinal sections they exhibit a plexiform or lamellar-like pattern reminiscent of a neural neoplasm. In the periphery, a diffuse infiltration of the subcutis producing a honeycomb pattern is seen. Immunohistochemically, tumour cells stain positively for CD34, whereas STAT6, S-100 protein, ASMA, desmin, EMA, and Claudin-1 are negative. FISH-analysis showed *COL1A1* rearrangements in 44 out of 50 nuclei counted.

### Diagnosis: Dermatofibrosarcoma protuberans with braided growth pattern

### Comments:

Dermatofibrosarcoma protuberans (DFSP) is a superficial, low-grade, locally aggressive, fibro/myofibroblastic, CD34 positive neoplasm carrying a *COL1A1*-*PDGFB* fusion gene. DFSP usually presents in young to middle aged adult patients, with a slight male predominance. However, a significant number of cases are seen in children (including congenital presentations), and in the elderly. Most of these tumours occur sporadically. A high incidence of DFSP with unique features, such as multicentricity, small size, and occurrence at early age, has been shown in children affected with adenosine deaminase-deficient severe combined immunodeficiency. Although it represents a rare neoplasm (< 1 per 100.000 people per year) DFSP is one of the most common dermal sarcomas. DFSP is characterized by a diffuse infiltration of the dermis and subcutis. The neoplastic cells

grow along the fibrous septa of the subcutaneous tissue and interdigitate with fat lobules, resulting in a typical honeycomb appearance. DFSP is composed of cytologically uniform spindled tumour cells containing plump or elongated wavy nuclei arranged in a predominantly storiform, whorled or cartwheel growth pattern. A braided growth pattern or prominent palisading of tumour cells with formation of Verrocay bodies mimicking a neural neoplasm as well as granular cytoplasmic changes are very rare. Cytological atypia is minimal and mitotic activity is usually low. The collagenous stroma contains small blood vessels. The superficial portion of the neoplasm may be less cellular and thus cause considerable challenges in the differential diagnosis on small, superficial biopsies. Rarely, cases of DFSP present as a subcutaneous mass with infiltration of deep soft tissues. In addition, several rare variants exist that may cause considerable diagnostic problems including pigmented DFSP, DFSP with myoid differentiation, plaque-like DFSP, myxoid DFSP, vascular DFSP, fibrosarcomatous DFSP and DFSP with pleomorphic sarcomatous transformation.

## References:

1. Calonje E, Fletcher CDM. Myoid differentiation in dermatofibrosarcoma protuberans and its fibrosarcomatous variant: clinicopathologic analysis of 5 cases. *J Cutan Pathol* 1996; 23: 30-36.
2. Davis DA, Sanchez RL. Atrophic and plaque-like dermatofibrosarcoma protuberans. *Am J Dermatopathol* 1998; 20: 498-501
3. Kesserwan C, Sokolic R, Cowen EW, Garabedian E, Heselmeyer-Haddad K, Lee CC, Pittaluga S, Ortiz C, Baird K, Lopez-Terrada D, Bridge J, Wayne AS, Candotti F. Multicentric dermatofibrosarcoma protuberans in patients with adenosine deaminase-deficient severe combined immune deficiency. *J Allergy Clin Immunol* 2012; 129: 762-769
4. Kutzner H, Mentzel T, Palmedo G, Hantschke M, Rütten A, Paredes BE, Schärer L, Guillen CS, Requena L. Plaque-like CD34 positive dermal fibroma ("medallion-like dermal dendrocyte hamartoma"): clinicopathologic, immunohistochemical, and molecular analysis of 5 cases emphasizing its distinction from superficial, plaque-like dermatofibrosarcoma protuberans. *Am J Surg Pathol* 2010; 34: 190-201
5. Liang CA, Jambusaria-Pahlajani A, Karia PS, Elenitsas R, Zhang PD, Schmults CD. A systematic review of outcome data for dermatofibrosarcoma protuberans with and without fibrosarcomatous change. *J Am Acad Dermatol* 2014; 71: 781-786
6. Llombart B, Monteagudo C, Sanmartín O, Lopez-Guerrero JA, Serra-Guillen C, Poveda A, Jorda E, Fernandez-Serra A, Pellin A, Guillen C, Llombart-Bosch A. Dermatofibrosarcoma protuberans: a clinicopathological, immunohistochemical, genetic (COL1A1-PDGFB), and therapeutic study of low-grade versus high-grade (fibrosarcomatous) tumors. *J Am Acad Dermatol* 2011; 65: 564-575

7. Mentzel T, Beham A, Katenkamp D, Dei Tos AP, Fletcher CDM. Fibrosarcomatous ("high-grade") dermatofibrosarcoma protuberans: clinicopathologic and immunohistochemical study of a series of 41 cases with emphasis on prognostic significance. *Am J Surg Pathol* 1998; 22: 576-587
8. Mentzel T, Schärer L, Kazakov DV, Michal M. Myxoid dermatofibrosarcoma protuberans: clinicopathologic, immunohistochemical, and molecular analysis of eight cases. *Am J Dermatopathol* 2007; 29: 443-448
9. Sandberg AA, Bridge JA. Updates on the cytogenetics and molecular genetics of bone and soft tissue tumors. Dermatofibrosarcoma protuberans and giant cell fibroblastoma. *Cancer Genet Cytogenet* 2003; 140: 1-12
10. Santos-Briz A, Riveiro-Falkenbach E, Romaan-Curto C, Mir-Bonafe JM, Acquadro F, Mentzel T. Braided pattern in a dermatofibrosarcoma protuberans: a potential mimicker of a neural neoplasm. *Am J Dermatopathol* 2014; 36: 920-924
11. Swaby MG, Evans HL, Fletcher CDM, Prieto VG, Patel KU, Lev DC, Lòpez-Terrada D, Lazar AJ, Wang WL. Dermatofibrosarcoma protuberans with unusual sarcomatous transformation: a series of 4 cases with molecular confirmation. *Am J Dermatopathol* 2011; 33: 354-360
12. Tantcheva-Poor I, Marathovouniotis N, Kutzner H, Mentzel T. Vascular congenital dermatofibrosarcoma protuberans: a new histological variant of dermatofibrosarcoma protuberans. *Am J Dermatopathol* 2012; 34: e46-e49
13. Wei S, Dumas A, Zhang PJ, Cooper K. Palisading and Verocay body-prominent dermatofibrosarcoma protuberans: A case report. *Pathol Res Pract* 2016; 212: 145-147

## Case 33

Michael Michal, M.D., Charles University, Pilsen, Czech Republic

---

### Case history and gross features:

A 56-year-old male presented with a conglomerate of 4 dermal to subcutaneous tumor nodules on his left shin. The tumors elevated the overlying skin and their overall size was 3x2,5x2,5 cm. Enlarged lymph nodes in the left inguinal area sized 4,7x4,4x3 cm were detected at presentation and were later shown to represent metastatic disease (slides submitted to the seminar come the metastasis).

### Histology:

The initial tumor was multinodular and well-circumscribed by mostly a thin fibrous capsule. The neoplasm featured moderately cellular cords and trabeculae of oval to epithelioid cells which had moderate to high nuclear grade and showed 6 mitoses/50 HPF. The background stroma was predominantly sclerotic, occasioning a close resemblance of the whole lesion to sclerosing epithelioid fibrosarcoma. No ossification was present. The metastatic disease showed similar features but higher mitotic activity (10/50 HPF). Immunohistochemically, the tumor was diffusely positive for S100, CD10 and showed a strong and diffuse TFE3 expression. No reactivity was noted with AE1/3, Desmin, SMA, MUC4, EMA, Claudin-1, CD34, Sox-10, HMB-45.

**Diagnosis: Ossifying fibromyxoid tumor (OFMT) with PHF1-TFE3 rearrangement**

### Discussion:

OFMT is a tumor of intermediate malignant potential and most cases follow an indolent clinical course. Criteria identifying the relatively minor subset of cases with a higher risk of malignant behavior have been established (1).

OFMT spans a very wide morphologic spectrum and is often difficult to recognize histologically. Some of the most useful diagnostic features are the presence of ossified areas, thick fibrous capsule at the tumor periphery and S100 expression.

About 80% of OFMT cases harbor rearrangements of the PHF1 gene, most commonly fused to the EP400 gene. A recent study reported a novel PHF1-TFE3 fusion in 5 OFMT cases, 3 of which were classified as malignant, raising the possibility, that this fusion is more commonly associated with malignant behavior. Importantly, all these tumors lacked ossification, had only a thin fibrous capsule at the margin and only 1 case weakly expressed S100 protein. Subsequently, three case reports of very similar tumors were reported, and all were classified as either malignant (n=2) or atypical. All 3 lacked peripheral bone formation and S100 protein expression (3-5).

In our practice, we have encountered 2 OFMTs with an identical fusion, one of which was classified as atypical OFMT and the other as clear-cut malignant (the presented case). Histologically, both cases lacked ossified areas as well as thick fibrous capsule at the periphery and only one was S100 protein positive.

We have also analyzed all other 7 cases of malignant OFMT from our archive to establish, whether this novel fusion is overrepresented among the aggressive subset. However, none of these 7 tumors harbored TFE3 gene break by FISH. Coupled with the published data, our results offer the following 2 conclusions regarding PHF1-TFE3-rearranged OFMTs: 1) PHF1-TFE3 fusion is more commonly associated with aggressive clinicopathologic features; 2) the fusion is relatively rare and most malignant OFMTs harbor other fusion genes.

## References:

1. Folpe AL, Weiss SW. Ossifying fibromyxoid tumor of soft parts: a clinicopathologic study of 70 cases with emphasis on atypical and malignant variants. *Am J Surg Pathol.* 2003;27(4):421-431. doi:10.1097/00000478-200304000-00001
2. Suurmeijer AJH, Song W, Sung YS, et al. Novel recurrent PHF1-TFE3 fusions in ossifying fibromyxoid tumors. *Genes Chromosomes Cancer.* 2019;58(9):643-649. doi:10.1002/gcc.22755
3. Zou C, Ru GQ, Zhao M. A PHF1-TFE3 fusion atypical ossifying fibromyxoid tumor with prominent collagenous rosettes: Case report with a brief review. *Exp Mol Pathol.* 2021 Dec;123:104686. doi: 10.1016/j.yexmp.2021.104686. Epub 2021 Sep 22. PMID: 34560087.

4. Linos K, Kerr DA, Baker M, Wong S, Henderson E, Sumegi J, Bridge JA. Superficial malignant ossifying fibromyxoid tumors harboring the rare and recently described ZC3H7B-BCOR and PHF1-TFE3 fusions. *J Cutan Pathol*. 2020 Oct;47(10):934-945. doi: 10.1111/cup.13728. Epub 2020 Jul 29. PMID: 32352579.
5. Fei F, Prieto Granada CN, Harada S, Siegal GP, Wei S. Round cell tumor with a myxoid matrix harboring a PHF1-TFE3 fusion: Myoepithelial neoplasm or ossifying fibromyxoid tumor? *Pathol Res Pract*. 2021 Sep;225:153578. doi: 10.1016/j.prp.2021.153578. Epub 2021 Aug 4. PMID: 34391181.

# Case 34

Kumarasen Cooper

---

## Clinical History

This 50-year-old male patient presented with a soft tissue mass in the right lateral hip. He had a past history of an injury to his hip 18 months previously, which resulted in a golf-ball size bruise, and grew to be grapefruit in size at presentation. MRI of right hip in March 2016 revealed a well circumscribed 8.5 x 9.0 cm soft tissue subcutaneous mass of the right lateral hip without invasion of the gluteal muscles. The PET/CT scan showed no evidence of metastasis.

## Pathology

The gross examination revealed a superficial tumor within the subcutaneous tissue that appears to be well circumscribed and non-infiltrative tumor. The cut surface showed an overall white tan appearance with focal areas with a hemorrhagic appearance.

Microscopic examination revealed a well circumscribed mesenchymal tumor comprising numerous thin-walled ectatic vessels surrounded by perivascular hyaline material (collagen and fibrin). Sheets of spindled cells and round pleomorphic hyperchromatic cells were present around the angiectatic vasculature. The latter also showed intranuclear cytoplasmic inclusions (pseudoinclusions). A variable population of inflammatory cells were noted (including mast cells).

A battery of immunohistochemical stains were all negative including CD 34 in the spindle cells.

## Diagnosis: Pleomorphic Hyalinizing Angiectatic Tumor (PHAT)

## Discussion

PHAT is an exceedingly rare soft tissue tumor. Since the early description in 1996, fewer than 100 cases have been described in the literature. The seminal publication from Dr Sharon Weiss, likened this tumor to a schwannoma (neurilemoma) with a low-grade biological behavior (local recurrence only). Not surprisingly, PHAT shares the unusual

vasculature, ancient atypia, intranuclear inclusions, the lack of mitoses and an abundance of mast cells with schwannoma. However, the absence of S-100 (diffuse) and encapsulation of schwannoma helps in this distinction. The other main differential diagnosis that may be considered is an undifferentiated pleomorphic sarcoma (UPS) due to similar nuclear pleomorphism and the absence of distinctive features of differentiation. However, UPS has a high mitotic activity and is CD 34 negative.

The majority of PHAT arises in adults (slight female predilection) as slow growing masses ranging in size from 1-20cm (average 5-7cm). PHAT tends to be subcutaneous and in the extremities (especially the lower limbs) and is often clinically mistaken for hematoma or Kaposi sarcoma.

To date there have been no documented cases of metastases and should be graded as tumors of intermediate (borderline) malignancy. Local recurrence has been noted between 33-50% of cases. Hence this tumor is best treated with a complete (or wide) local resection and follow up for recurrence).

The pathophysiology/etiology of PHAT is not known. The theory is that the advancing tumor front engulfs vessels walls resulting in ectatic vessels endothelial damage, plasma leakage and resultant fibrin deposition and hyalinization of vessel walls. The mast cells were thought to contribute to vascular damage due to initiation of vascular permeability. The concept of an early PHAT (potential precursor) characterized by bland spindle cells (some with hemosiderin) with myxoid change and an infiltrative growth pattern into fat and around blood vessels has been proposed. These lesions have been demonstrated to either exist alone or at the periphery of classic PHAT.

## References

1. Smith, Mark; Fisher, Cyril; Weiss, Sharon. Pleomorphic Hyalinizing Angiectatic Tumor of Soft Parts: A Low-grade Neoplasm Resembling Neurilemoma. American Journal of Surgical Pathology. 20(1):21-29, January 1996.
2. Folpe AL, Weiss SW. Pleomorphic hyalinizing angiectatic tumor: analysis of 41 cases supporting evolution from a distinctive precursor lesion. Am J Surg Pathol. 2004 Nov;28(11):1417-25.
3. Marshall-Taylor C, Fanburg-Smith JC. Hemosiderotic fibrohistiocytic lipomatous lesion: ten cases of a previously undescribed fatty lesion of the foot/ankle. Mod Pathol. 2000;13:1192-1199.

4. Elco CP, Marino-Enriquez A, Abraham JA, Dal Cin P, Hornick JL. Hybrid myxoinflammatory fibroblastic sarcoma/hemosiderotic fibro-lipomatous tumor: report of a case providing further evidence for a pathogenetic link. *Am J Surg Pathol* 2010;34:1723-7.
5. Weiss S, Goldblum J, eds. *Enzinger and Weiss soft tissue tumors*, 6th ed. St. Louis: Mosby, Elsevier, 2014

## Case 35

David Suster, M.D., Rutgers University Hospital, Newark, N.J., USA

---

### Clinical History:

A 17-YEAR-OLD young man was seen for insidious onset of buttock pain. Imaging findings showed a large cystic tumor in his left sacrum involving S1-S3. The lesion was locally destructive and showed fluid levels suggestive of aneurysmal bone cyst (ABC). It was first attempted to control the tumor using radiofrequency ablation which failed, and the patient was scheduled for surgery. A preoperative core biopsy showed small fragments of bone matrix associated with numerous large, atypical epithelioid cells with slightly eccentric nuclei, basophilic cytoplasm, and small nucleoli. The biopsy was regarded as atypical and suspicious for malignancy but was felt to be inconclusive. At surgery, the tumor surrounded the nerve roots on the left side of S1, S2 and S3 and the cauda equina. Embolization for hemorrhage control was done prior to surgery causing the lesion to expand into adjacent vertebral levels and poke out of the foramina in front and in back of the bone. The tumor was excised, and the area was bone grafted with internal fixation.

### Histologic Findings:

The resected specimen measured 6 x 6 x 2.5 cm. and showed an extensively hemorrhagic cut surface. Histologic examination showed a proliferation of large epithelioid cells with abundant basophilic cytoplasm and large, hyperchromatic and eccentric nuclei displaying prominent nucleoli, similar to those seen in the preoperative biopsy. In areas the cells adopted a striking plasmacytoid appearance; in other areas the cells were suggestive of atypical epithelial cells. The large cells occupied the intertrabecular spaces and lined microtrabecular aggregates of bone matrix resembling osteoblasts. Some of the atypical cells appeared to be incorporated into the bone trabeculae resembling osteocytes, although they were much larger than normal osteocytes. The stroma contained a sparse fibroblastic spindle cell population and scattered multinucleated osteoclastic giant cells. Some sections demonstrated ABC-like changes, with large vessel-like spaces transitioning with capillary sized vessels. Mitotic activity was noted in the plump osteoblastic cells, but no abnormal mitoses could be identified. Areas of acellular bone matrix consistent with

prior radiofrequency ablation therapy were also seen. Foci containing Gelfoam-like material could also be identified in some sections, consistent with prior embolization procedure. Because of the concern for malignancy, a Ki-67 proliferation marker was done which showed nuclear positivity in only ~2% of the epithelioid cell nuclei.

## **Diagnosis: Epithelioid osteoblastoma with ABC-like changes.**

### **Discussion:**

Osteoblastoma is a rare, bone forming neoplasm that accounts for approximately 1% of all bone tumors.<sup>1,2</sup> They show a predilection for the spine and sacrum, although they can occur in other locations at appendicular sites and in virtually any bone in the body.<sup>2</sup> The prognosis for these tumors is excellent with local recurrence generally being an uncommon event. It has been known for a while that in rare instances the osteoblasts in these tumors can adopt an atypical morphology that can give rise to confusion with a malignancy; some of those tumors have been referred to as atypical osteoblastoma, pseudomalignant osteoblastoma, aggressive osteoblastoma, and epithelioid osteoblastoma.<sup>2,3-7</sup> The current WHO book on bone tumors refers to these tumors as epithelioid osteoblastoma and states that they are not necessarily associated with a more aggressive behavior. The present case is an example of this rare variant of osteoblastoma characterized by a striking epithelioid appearance and associated with ABC-like changes.

The atypical cytologic features of these tumors, with enlarged, hyperchromatic cells with large nuclei and prominent nucleoli, and the occurrence of occasional mitoses can in some instances give rise to confusion with a malignant neoplasm. We recently compiled our experience with 17 cases of epithelioid osteoblastoma (paper submitted for publication).<sup>8</sup> The tumors in our study most commonly arose in the vertebrae and sacrum, followed by mandible and bones of the foot. Our patients' ages ranged from 5 to 33 years, and the tumors ranged in size from 2 to 6.5 cm (mean= 4.1 cm). Imaging studies showed expansile lytic lesions with cortical thickening and a mild rim of sclerosis. Histologically all tumors were characterized by active production of bone with a fibrovascular stroma containing micro trabecular aggregates of bone matrix. The osteoblastic proliferation was atypical and showed enlarged cells with prominent nucleoli and abundant cytoplasm imparting them with a striking epithelioid appearance. In three cases, preoperative core biopsies were done and interpreted as atypical and suspicious for malignancy, or outright diagnosed as high-grade osteosarcoma in one case.

In recent years it has been demonstrated that these lesions have characteristic underlying molecular rearrangements of the *FOS* and *FOSB* genes.<sup>9</sup> It has been claimed that differentiation from osteosarcoma may be possible with the use of immunohistochemical antibodies against *FOS* and *FOSB* although, in practice, tumors may not be amenable to staining due to specialized decalcification procedures required for bone lesions. Molecular studies by FISH and next generation sequencing were attempted in our cases but were unsuccessful, likely due to the decalcification procedure employed in all our cases. We did perform immunohistochemistry for *FOS* and *FOSB* antibodies in 12 cases; the results, however, were variable and difficult to interpret. 4/12 cases showed strong nuclear positivity for *FOS*, and 2/12 cases showed strong and diffuse nuclear positivity for *FOSB*; the remainder of cases showed variable, sometimes overlapping patterns regarded as indeterminate. Proliferative activity was assessed in our cases using antibodies for Ki-67; the Ki-67 proliferation marker showed low nuclear positivity (~2%) in 10 cases and a slight increase (<10%) in two cases. Given that proliferative activity is markedly elevated in osteosarcoma, it was felt that use of Ki-67 antibodies may be of value for the differential diagnosis with malignancy.

The differential diagnosis for these tumors is with conventional high-grade osteosarcoma with areas that contain epithelioid-like cells and less commonly the exceedingly rare osteoblastoma-like variant of osteosarcoma (OLOS).<sup>9-11</sup> The presence of sheets and aggregates of atypical epithelioid osteoblasts seen in the stroma of epithelioid osteoblastoma can potentially be mistaken for conventional osteosarcoma, which can sometimes also show sheets of osteoblast-like malignant cells in the intertrabecular spaces. The absence of marked pleomorphism, abnormal mitotic figures and foci of necrosis are useful features for making this distinction. In cases lacking these features it is necessary to carefully examine the interface of the lesion with the host bone to demonstrate whether there is permeation of the intertrabecular spaces of the host bone by tumor and if there is lack of differentiation at the periphery of the lesion. The presence of overtly malignant features on radiographic studies also will obviously favor the diagnosis of osteosarcoma.

Although epithelioid morphology has been associated in the past with a more aggressive behavior in osteoblastoma, the results of our study confirm that this may not necessarily be the case, thus supporting the current opinion of the WHO that epithelioid morphology should not be equated with aggressive behavior for these tumors. The main importance

of recognizing this morphologic variant of osteoblastoma lies in avoiding a misdiagnosis of malignancy that could result in unnecessary aggressive treatment, particularly when evaluating small core biopsies. Clinical follow up in our patients disclosed no evidence of late recurrences or metastases. The term epithelioid osteoblastoma is preferable in this setting to that of aggressive osteoblastoma to highlight the atypical morphology without suggesting any prognostic implications.

## References:

1. Amary F, Bredella MA, Horvai AE, Mahar AM. Osteoblastoma, in: WHO Classification of Tumours Editorial Board. WHO Classification of Tumors. Soft Tissue and Bone Tumours, 5th Edition, IARC, Lyon, 2020. P. 397-399.
2. Lucas DR, Unni KK, McLeod RA, O'Connor MI, Sim FH. Osteoblastoma: Clinicopathologic study of 306 cases. *Hum Pathol* 1989;23:117-134.
3. Mirra JM, Kendrick RA, Kendrick RE. Pseudomalignant osteoblastoma versus arrested osteosarcoma: a case report. *Cancer* 1976;37:2005-2014.
4. Della Rocca C, Huvos AG. Osteoblastoma: varied histological presentation with a benign clinical course. An analysis of 55 cases. *Am J Surg Pathol* 1996;20:841-850.
5. Dorfman HD, Weiss SW. Borderline osteoblastic tumors: problems in differential diagnosis of aggressive osteoblastoma and low-grade osteosarcoma. *Semin Diagn Pathol* 1984;1:215-234.
6. Angervall L, Persson S, Stenman G, Kindblom LG. Large cell, epithelioid, telangiectatic osteoblastoma: a unique pseudosarcomatous variant of osteoblastoma. *Hum Pathol* 1999;30:1254-1259.
7. Mendes de Oliveira CRGC, Mendonca BB, de Camargo OP, Pinto EM, Nascimento SAB, Latorre MRDO, et al. Classical osteoblastoma, atypical osteoblastoma, and osteosarcoma. A comparative study based on clinical, histological and biological parameters. *Clinics* 2007;62:167-174.
8. Suster D, Mackinnon AC, Jarzembowski J et al. Epithelioid osteoblastoma: Clinicopathologic and immunohistochemical study of 17 cases. (Submitted for publication, 2022).
9. Bertoni F, Bacchini P, Donati D, Martini A, Picci P, Campanacci M. Osteoblastoma-like osteosarcoma: The Rizzoli Institute experience. *Mod Pathol* 1993;6:707-716.
10. Ozger H, Alpan B, Soylemez MS, Ozkan K, Salduz A, Bilgic B, et al. Clinical management of a challenging malignancy, osteoblastoma-like osteosarcoma: a report of four cases and review of the literature. *Ther Clin Risk Manag* 2016;12:1261-1270.
11. Gambarotti M, Dei Tos AP, Vanel D, Picci P, Gilbertoni D, Klein MJ, et al. Osteoblastoma-like osteosarcoma: high-grade or low-grade osteosarcoma? *Histopathology* 2019;74:494-503.

## Case 36

Michael Michal, M.D., Charles University, Pilsen, Czech Republic

---

### Case history and gross features:

A 42-year-old man with a lipomatous tumor in the pectoral area measuring 4,8x3,5x1,4 cm.

### Histology:

Microscopically, the tumor represented a well differentiated lipomatous tumor with a notable adipocytic size variation, patchy single cell fat necrosis, and focal mostly mild adipocytic nuclear atypia. The tumor lacked any spindle cell areas and no ropy collagen bundles were present. Spindled cells were virtually absent. MDM2 IHC as well as FISH were both negative. The tumor cell nuclei show loss of RB1 staining and about 10% of tumor cells expressed p53 protein.

### Diagnosis: Anisometric cell/Dysplastic lipoma

### Discussion:

Anisometric cell/Dysplastic lipoma is a recently characterized tumor first described by Evans in 2016 (1). Two further studies were published since then (2-3), and today almost 80 cases are on record. Based on these reports, the key clinical features of this entity include: 1) a very strong male predominance, 2) a predilection for the posterior neck, upper back and shoulder regions, 3) multifocality in approximately 19% of patients, 4) a rare association with retinoblastoma, and 5) mildly increased risk (currently estimated at around 10%) for local recurrence with simple excision, as compared to a conventional lipoma. To date, all examples have been subcutaneous, though some examples have occurred in locations where tissue planes are somewhat ambiguous (e.g., the lateral/anterior neck and groin regions).

The key histologic features are: 1) notable adipocytic size variation, 2) patchy (typically single cell) fat necrosis, and 3) focal adipocytic nuclear atypia. The atypical adipocytes may be mononucleated or multinucleated. The atypia is generally mild and can be quite

subtle, but in some instances, it is more pronounced and similar to that seen in a conventional atypical lipomatous tumor. Immunohistochemical expression for p53 is always present, but it is limited to a subpopulation of the adipocytes, typically those with the greatest atypia (usually between 5-20% of the nuclei). MDM2 immunoreexpression can be present, but it is almost invariably less prominent than the p53 immunoreexpression, and FISH analysis for MDM2 gene amplification is always negative. Collagen deposition tends to be quite sparse, and ropey collagen bundles have not been encountered. Spindled cells are typically very sparse or absent, they tend to be smaller and more delicate than the spindled cells in spindle cell lipoma, and they consistently have bland nuclei.

## References:

1. Evens H.L Anisometric Cell Lipoma: A Predominantly Subcutaneous Fatty Tumor With Notable Variation in Fat Cell Size But Not More Than Slight Nuclear Enlargement and Atypia. *AJSP: Reviews & Reports*. 2016;21:195-199.
2. Agaimy A. Anisometric cell lipoma: Insight from a case series and review of the literature on adipocytic neoplasms in survivors of retinoblastoma suggest a role for RB1 loss and possible relationship to fat-predominant ("fat-only") spindle cell lipoma. *Ann Diagn Pathol*. 2017;29:52-56.
3. Michal M, Agaimy A, Contreras AL, et al. Dysplastic Lipoma: A Distinctive Atypical Lipomatous Neoplasm With Anisocytosis, Focal Nuclear Atypia, p53 Overexpression, and a Lack of MDM2 Gene Amplification by FISH: A Report of 66 Cases Demonstrating Occasional Multifocality and a Rare Association With Retinoblastoma. *Am J Surg Pathol*. 2018 42 (11), 1530-1540.

## Case 37

Contributed by Franco Fedeli, MD, Malpighi Pathology Academy

---

[www.malpighipathologyacademy.org](http://www.malpighipathologyacademy.org)

### Clinical History:

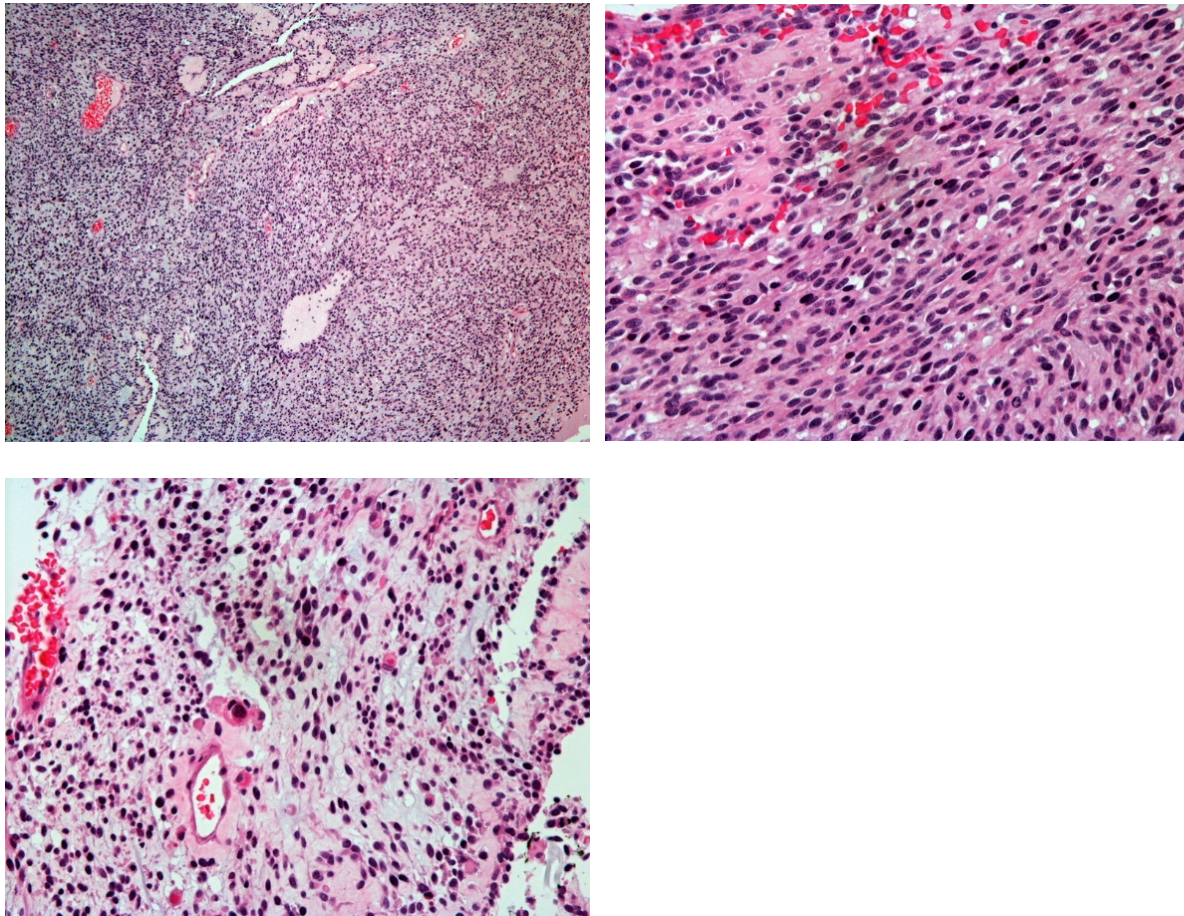
73 years old male with an history of mucinous adenocarcinoma of the colon in 2013. The patient presented with an inguinal mass two years later, which was resected in another institution and relapsed one year later. No follow up was available.

### Macroscopic findings:

The recurred tumor mass was 9.7 x 7.1 x 3.2 cm in size. Macroscopically, the tumor was hard and grayish. No soft and yellowish areas were present at the periphery.

### Histological Findings:

The tumor was composed by a proliferation of undifferentiated small cells. In some areas spindled cells in a fibrous and myxoid stroma were present. No necrosis was seen. The neoplastic cells presented oval to round, slightly hyperchromatic, nuclei. The tumor cell nuclei were larger than those in the endothelial cells of the small capillaries that are supplying blood to the tumor. Focal rhabdomyosarcomatous differentiation with polygonal and strap cells was observed. In this area the neoplastic cells showed abundant deeply eosinophilic cytoplasm. No striated structure was found. No adipocytic component was present.



## Immunohistochemical and Molecular Findings:

Immunohistochemically the tumor cells were positive for Vimentin, focal Muscle Actin (HHF-35), Desmin, CD99, WT1, Caldesmon H, Myogenin and MDM2. Cytokeratin (Cam5.2) and S100 were negative. Fluorescence in situ Hybridization confirmed MDM2 amplification, as did array-based copy number profiling.

## Diagnosis: Dedifferentiated liposarcoma with rhabdomyoblastic differentiation

### Comments:

Dedifferentiated liposarcoma typically presents in middle-aged and older adults with a predilection for occurrence in men (1). The most common site is retroperitoneum, which accounts for approximately half the cases, followed by inguino-scrotal region and thigh. Dedifferentiated liposarcoma is the most heterogeneous of all sarcomas with a wide

variety of histologic patterns including tumors with distinctive patterns, tumors with heterologous and homologous differentiation, and low grade tumors (2). The higher-grade element in most tumors is a grade 2 or spindle cell or pleomorphic sarcoma without a specific line of differentiation. Other patterns include tumors with meningothelial-like whorls, myxoid stroma, tumors resembling solitary fibrous tumor and inflammatory malignant fibrous histiocytoma, inflammatory myofibroblastic tumor-like features and tumors with prominent epithelioid features. Tumors with various forms of heterologous differentiation such as leiomyosarcomatous, rhabdomyosarcomatous, and osteosarcomatous differentiation, as well as tumors with homologous (pleomorphic liposarcomatous) differentiation are well recognized (3). Myogenic differentiation was present in 35% of dedifferentiated liposarcoma while 7% had a rhabdomyoblastic component (4). The tumor with dedifferentiated liposarcoma with rhabdomyoblastic differentiation occurs usually in retroperitoneal location and range from 47 to 72 years (mean age 57.4) in age.

Our patient, of 73 years old, presented an inguinal mass. In our case rhabdomyoblastic cells made up 40% of dedifferentiated area and were scattered or focally distributed, being rounded, band-like or spindled, mostly with abundant eosinophilic cytoplasm. No striated structure was found, and the nuclei were rounded, oval or irregular in shape. Rare rhabdomyoblastic cells were lymphocytoid. By immunohistochemical staining, the rhabdomyoblastic cells were positive for Desmin, Myogenin, SMA and MDM2.

The main challenge in differential diagnosis is distinguishing between a pleomorphic sarcoma infiltrating fat and dedifferentiated liposarcoma.

Dedifferentiated liposarcoma with rhabdomyoblastic differentiation should be distinguished from undifferentiated sarcoma, pleomorphic rhabdomyosarcoma and malignant peripheral nerve sheath tumor with rhabdomyoblastic differentiation (Triton tumor).

Immunohistochemical findings of MDM2 and amplification of MDM2 were helpful when an adipocytic component was absent and a histological diagnosis was difficult.

In a large study, conducted in one institution, patients affected by liposarcoma with a rhabdomyoblastic component of retroperitoneal location died within 8 months.

Rhabdomyoblastic and myogenic differentiation significantly predicted the outcome of retroperitoneal liposarcoma (4).

## References:

1. Weiss SW, Rao VK. Well-differentiated liposarcoma (atypical lipoma) of deep soft tissue of the extremities, retroperitoneum, and miscellaneous sites. A follow-up study of 92 cases with analysis of the incidence of "dedifferentiation". *Am J Surg Pathol.* 1992;16:1051-1058.
2. Dei Tos AP. Dedifferentiated liposarcoma. In: Fletcher CDM, Bridge JA, Hogendoorn PCW, Mertens F, eds. *WHO Classification of Tumours of Soft Tissue and Bone*. Fourth ed. Lyon, France: IARC; 2013:37-38.
3. Suster S, Wong TY, Moran CA. Sarcomas with combined features of liposarcoma and leiomyosarcoma. Study of two cases of an unusual soft-tissue tumor showing dual lineage differentiation. *Am J Surg Pathol.* 1993;17:905-911.
4. Gronchi A, Collini P, Miceli R, et al. Myogenic differentiation and histologic grading are major prognostic determinants in retroperitoneal liposarcoma. *Am J Surg Pathol* 2015;39:383-393.

## Case 38

Michael Michal, M.D., Charles University, Pilsen, Czech Republic

---

### Case history:

A 3-year-old boy presented with a tumor on his upper lip which eventually invaded the orbit.

### Histology:

The tumor had two distinct components. One consisted of a low-grade proliferation of cells with round to oval nuclei having overall bland nuclear features. These cells were growing on a very characteristic background which showed a prominent perivascular and stromal hyalinization (**Fig. 1**). The other area lacked these prominent stromal changes and showed only a spindle cell sarcoma with a fascicular and focally storiform arrangement which was compatible with the diagnosis of infantile fibrosarcoma. Both components showed a relatively diffuse CD34 and S100 co-expression. Next generation sequencing revealed *EML4-NTRK3* fusion.

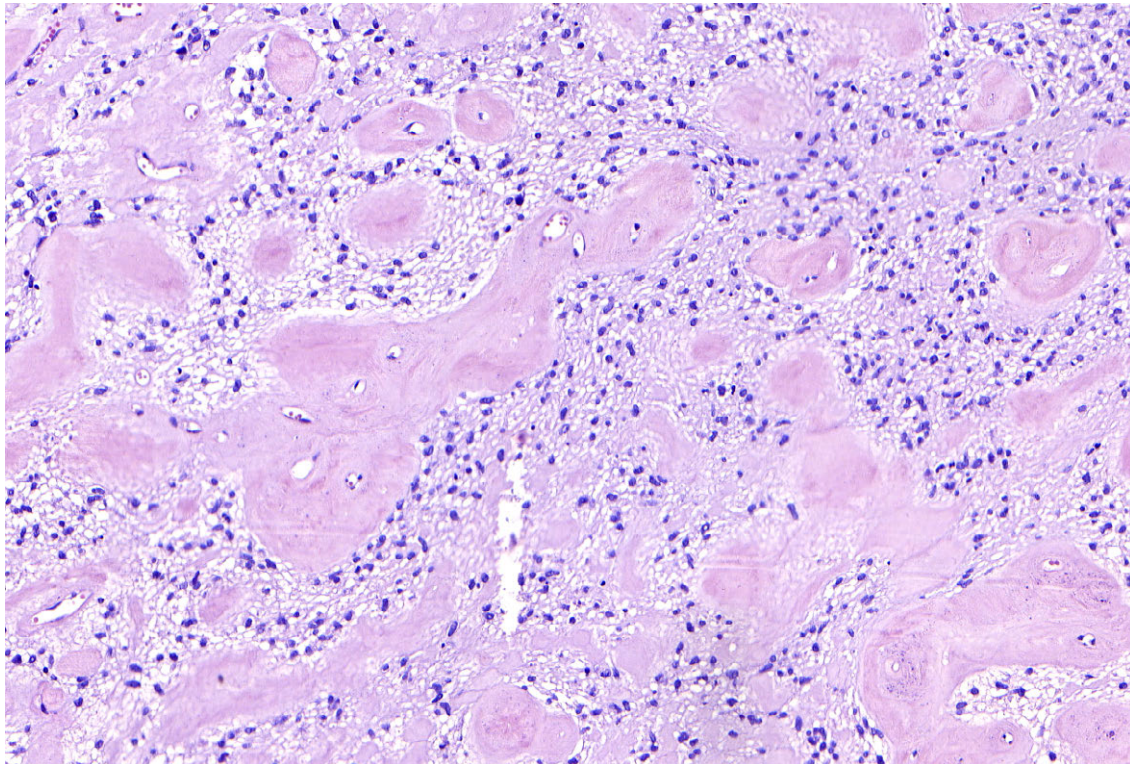


**Figure 1.** The low-grade area not sampled in the attached slides.

## Diagnosis: Infantile fibrosarcoma with EML4-NTRK3 fusion

### Discussion:

Until recently, it has been thought that the ETV6-NTRK3 fusion is the molecular hallmark of the vast majority of infantile fibrosarcomas. However, the wider availability of powerful NGS sequencing tools in recent years has led to the discovery of several other rearrangements in tumors with infantile fibrosarcoma morphology. The EML4-NTRK3 fusion seems to be the second most common fusion gene occurring in these tumors (1). Interestingly, all the other molecular events so far discovered in these neoplasms affected exclusively kinase genes such as NTRK1/2/3, BRAF, MET, or RET genes (2-8), most commonly in the form of gene fusion but a subset of tumors can harbor point mutations in or BRAF genes, as well (8). However, other very significant observations have been made. While infantile fibrosarcoma has been traditionally considered a well-defined entity with a relatively broad morphological spectrum, the recent reports have offered an alternative point of view regarding these tumors. Some reports indicate these tumors may rather represent a morphological subset among a larger group of tumors that could be collectively called “mesenchymal tumors with kinase fusions”. Importantly, although being

more common in infants, these tumors may occur at any age. A beautiful study on this topic has been recently published by Davis et al. While focusing only on mesenchymal tumors with NTRK1/2/3 fusions, the authors have shown that their morphological spectrum is broader than initially reported for infantile fibrosarcoma and although the infantile fibrosarcoma-like morphology is one of the most common appearances, there are many others. These tumors can microscopically look both low and high grade and can show a variety of patterns such as inflammatory myofibroblastic tumor-like or infiltrating fibromatosis-like pattern, others can show nuclear palisading, rhabdoid-like cytomorphology, collagenized areas alternating with primitive myxoid component primitive cells in myxoid background, myoid areas, etc. (2). The recently published lipofibromatosis-like neural tumor seem to fall within this spectrum as well (9). Probably the most characteristic appearance is the one shown in the presented case. It features usually a low-grade proliferation of bland round to oval mesenchymal cells with prominent perivascular and stromal hyalinization. Importantly, neoplasms with this morphology are consistently reactive with CD34 and S100 protein which can be diagnostically useful. In some cases, only the low-grade component is present and such tumors behave in an indolent manner (10-11). Other tumors can also harbor a high-grade component with a fibrosarcomatous appearance and can behave aggressively (11). When taken as a group, there do not seem to be significant differences in clinical behavior between tumors with variant kinase fusions and the classical ETV6-NTRK3-rearranged infantile fibrosarcomas. However, only one study analyzed this in detail and showed this to be true at least when ETV6-NTRK3 and other NTRK-rearranged tumors are compared (2). Nevertheless, more data are needed especially for the non-NTRK rearranged neoplasms. Preliminary observations from the published data indicate, that there might be a good correlation between morphological grading and behavior, i.e. tumors with mild atypia and low mitotic activity seem to behave better than those with high-grade features (5,6, 9-11).

## References:

5. Church AJ, Calicchio ML, Nardi V, et al. Recurrent EML4-NTRK3 fusions in infantile fibrosarcoma and congenital mesoblastic nephroma suggest a revised testing strategy. *Mod Pathol*. 2018;31(3):463-473. doi:10.1038/modpathol.2017.127
6. Davis JL, Lockwood CM, Stohr B, et al. Expanding the Spectrum of Pediatric NTRK-rearranged Mesenchymal Tumors. *Am J Surg Pathol*. 2019;43(4):435-445. doi:10.1097/PAS.0000000000001203

7. Kao YC, Fletcher CDM, Alaggio R, et al. Recurrent BRAF Gene Fusions in a Subset of Pediatric Spindle Cell Sarcomas: Expanding the Genetic Spectrum of Tumors With Overlapping Features With Infantile Fibrosarcoma. *Am J Surg Pathol*. 2018;42(1):28-38. doi:10.1097/PAS.0000000000000938
8. Flucke U, van Noesel MM, Wijnen M, et al. TFG-MET fusion in an infantile spindle cell sarcoma with neural features. *Genes Chromosomes Cancer*. 2017;56(9):663-667. doi:10.1002/gcc.22470
9. Suurmeijer AJ, Dickson BC, Swanson D, et al. The histologic spectrum of soft tissue spindle cell tumors with NTRK3 gene rearrangements. *Genes Chromosomes Cancer*. 2019;58(11):739-746. doi:10.1002/gcc.22767
10. Antonescu CR, Dickson BC, Swanson D, et al. Spindle Cell Tumors With RET Gene Fusions Exhibit a Morphologic Spectrum Akin to Tumors With NTRK Gene Fusions. *Am J Surg Pathol*. 2019;43(10):1384-1391. doi:10.1097/PAS.0000000000001297
11. Davis JL, Vargas SO, Rudzinski ER, et al. Recurrent RET Gene Fusions in Pediatric Spindle Mesenchymal Neoplasms [published online ahead of print, 2020 Jan 28]. *Histopathology*. 2020;10.1111/his.14082. doi:10.1111/his.14082
12. Wegert J, Vokuhl C, Collord G, et al. Recurrent intragenic rearrangements of EGFR and BRAF in soft tissue tumors of infants. *Nat Commun*. 2018;9(1):2378. Published 2018 Jun 18. doi:10.1038/s41467-018-04650-6
13. Agaram NP, Zhang L, Sung YS, et al. Recurrent NTRK1 Gene Fusions Define a Novel Subset of Locally Aggressive Lipofibromatosis-like Neural Tumors. *Am J Surg Pathol*. 2016;40(10):1407-1416. doi:10.1097/PAS.0000000000000675
14. Suurmeijer AJH, Dickson BC, Swanson D, et al. A novel group of spindle cell tumors defined by S100 and CD34 co-expression shows recurrent fusions involving RAF1, BRAF, and NTRK1/2 genes. *Genes Chromosomes Cancer*. 2018;57(12):611-621. doi:10.1002/gcc.22671
15. Michal M, Ptáková N, Martínek P, et al. S100 and CD34 positive spindle cell tumor with prominent perivascular hyalinization and a novel NCOA4-RET fusion. *Genes Chromosomes Cancer*. 2019;58(9):680-685. doi:10.1002/gcc.22758

## Case 39

David Suster, M.D., Rutgers University Hospital, Newark, N.J., USA

---

### Clinical history:

A 70-year-old man with a history of treated chronic myeloid leukemia (CML) was seen for development of left axillary soft tissue mass. A core needle biopsy was performed for the suspicion of myeloid sarcoma. The needle biopsy findings showed a high-grade appearing sarcomatous neoplasm that was interpreted as a high-grade malignant spindle cell tumor consistent with malignant peripheral nerve sheath tumor. A wide excision of the lesion was performed. The specimen consisted of an ellipse of skin with attached underlying portion of the latissimus muscle and multiple small lymph nodes up to 2 cm in greatest diameter in the underlying fat. The tumor measured 6 x 5 x 4 cm and showed a white, glistening and homogeneous cut surface; the tumor reached up to the lateral and deep margins.

### Pathologic findings:

Histologic examination revealed an atypical spindle and pleomorphic cell population involving the superficial dermis and extending deep into the subcutaneous tissue. The tumor cells were embedded in abundant collagenized stroma and contained scattered areas with dense chronic inflammatory infiltrates. A few isolated foci displaying myxoid changes of the stroma were also present in some sections. The tumor cell population consisted of relatively bland appearing spindle fibroblastic cells admixed with larger, pleomorphic, multinucleated or multilobated atypical cells. The atypical cells displayed large vesicular nuclei with prominent eosinophilic nucleoli. In some of the multinucleated cells, the multiple prominent eosinophilic nucleoli closely resembled Reed-Sternberg cells and their variants. Intranuclear vacuolization and intracytoplasmic pseudoinclusions were also present in scattered cells. Despite the marked nuclear pleomorphism, mitoses were extremely rare (~1 per 10 high power fields). Rare abnormal mitoses were also present. There was no evidence of necrosis or hemorrhage. In some areas, entrapped foci of mature fat were seen admixed with the atypical cell population suggestive of an adipocytic malignant neoplasm. Tumor was present at the medial and lateral margins, but the deep margin was free of tumor. The 12 lymph nodes were free of sarcoma but

contained a sinusoidal proliferation of mature and immature granulocytic precursors consistent with involvement by chronic granulocytic leukemia.

## **Immunohistochemical and other findings:**

A large panel of immunohistochemical stains was performed, including S100 protein, CD57, HMB45, CD30, CD68, cytokeratin, actin, desmin, vimentin, MDM2, CD34, bcl-2, and stains for granulocytic precursors including myeloperoxidase, CD33, CD43 and CD117. All stains were negative in the tumor cells, except for vimentin. A FISH test for MDM2 was done for the suspicion of dedifferentiated liposarcoma but was negative. Electron microscopic examination from wet tissue fixed in glutaraldehyde was performed which showed a population of cells with fibroblastic features, including elongated nuclei with irregular nuclear contours, abundant strands of rough endoplasmic reticulum and cisternae filled with granular, homogeneous electron-lucent material. The cell membraned did not contain basal lamina or show any cytoplasmic prolongations or interdigitations, specialized cell junctions, or other type of fibrils. Following the electron microscopic study which helped rule out a malignant peripheral nerve sheath tumor, an additional panel of stains was ordered, which included bcl-1, Factor XIIIa, CD10 and D2-40. The bcl-1 stain showed strong nuclear positivity of the tumor cells. Stains for FXIIIa, CD10 and D2-40 also showed strong and diffuse positivity in the cytoplasm of the tumor cells.

## **Diagnosis: Myxoinflammatory fibroblastic sarcoma.**

## **Discussion:**

Myxoinflammatory fibroblastic sarcoma is a relatively recently described tumor that tends to affect superficial soft tissue, mainly in the distal extremities, but in more recent years more proximal and central forms have also been increasingly identified. These tumors were described simultaneously by three different groups of investigators in the same year,<sup>1-3</sup> and after many permutations in terminology the term "myxoinflammatory fibroblastic sarcoma" (MIFS) was formally adopted by the WHO.<sup>4</sup> The tumors are characterized histologically by a triad of features that includes a fibroblastic and often pleomorphic or atypical spindle cell proliferation, admixed with inflammatory infiltrates, and containing areas with striking myxoid stromal changes. The neoplastic cell population is believed to be a fibroblastic cell that is most often spindled but can also display striking epithelioid morphology, and characteristically harbors scattered larger, atypical

multinucleated cells with prominent inclusion-like or Reed-Sternberg-like nucleoli. Tumors containing abundant myxoid stroma also harbor a distinctive variation of the atypical cells that have been designated as “pseudolipoblastic” cells because of their abundance of multivacuolated cytoplasm. The triad of fibroblastic cells, inflammatory infiltrates and myxoid stroma may not be present in all tumors or may be present in varying proportions, making the diagnosis of this condition quite challenging. It seems like the one feature that is obligatory and commonly seen in all cases is the presence of large, mononuclear or multinucleated atypical cells with prominent inclusion-like or Reed-Sternberg-like nucleoli.

The diagnosis of MIFS can be quite challenging as it can be readily confused for several other soft tissue sarcomas, including myxofibrosarcoma, undifferentiated pleomorphic sarcoma, and dedifferentiated liposarcoma. The closest mimicker of MIFS is dedifferentiated liposarcoma with pleomorphic tumor cells, which can often show myxoid stromal changes and inflammatory elements. The differential diagnosis is aided by the finding of strong nuclear positivity for MDM2 antibodies and positive identification of the *MDM2* gene by FISH. So far, *MDM2* alterations have not been described in MIFS. The location of the lesions is also significant for differential diagnosis as dedifferentiated liposarcoma is generally a tumor of deep soft tissue and is not expected to arise from the dermis or subcutis, particularly in the distal extremities. In the present case, the axillary location and the areas containing entrapped adipose tissue in the deep portion of the lesion lent themselves to the suggestion of dedifferentiated liposarcoma. Distinction of MIFS from myxofibrosarcoma may be more challenging as there are no specific immunohistochemical markers for the latter that can help in the differential diagnosis. In general, myxofibrosarcoma tends to occur in older patients and presents as a large, slow-growing and bulky superficial mass that does not involve the dermis but is confined to the subcutis and superficial soft tissues. Although Reed-Sternberg-like atypical cells can occasionally be encountered in myxofibrosarcoma, they are never as abundant and as noticeable as in MIFS. Undifferentiated pleomorphic sarcoma can also closely resemble MIFS, but unlike MIFS, this tumor tends to occur most often in deep soft tissues and is generally accompanied by tumor cell necrosis and more marked nuclear pleomorphism with abundance of abnormal mitotic figures. A high-grade variant of MIFS has been described by Michal et al<sup>5</sup> that may more closely mimic undifferentiated pleomorphic sarcoma. Identification of transitions with more conventional areas of typical MIFS in a superficial soft tissue tumor, particularly located in the extremities, will favor a diagnosis of high-grade MIFS over undifferentiated pleomorphic sarcoma. Unfortunately, until

recently no sensitive or specific immunohistochemical markers were available for the diagnosis of MIFS.

In recent years, several genetic alterations were identified in MIFS and claimed to serve as distinctive and unique markers for their diagnosis. The most commonly reported has been an unbalanced t(1;10)(p22;q24) translocation that leads to juxtaposition of the *TGFBR3* and *OGA* genes resulting in upregulation of *NPM3* and *FGF8*, the formation of supernumerary ring chromosomes with an amplified region in chromosome 3 leading to overexpression of *VGLL3*, and *BRAF* translocations involving *ROBO1* and *TOM1L2*, as well as *BRAF* amplification.<sup>6-10</sup> These were all proposed as potential molecular markers to facilitate the diagnosis of these tumors. We recently reported our experience with a large series of MIFS (73 cases) that were studied by FISH and/or array CGH and found that these alterations are present in only a small minority of cases.<sup>11</sup> The (1;10) translocation was present in only 3 of 54 cases in our study (5.4%), and *BRAF* alterations were only observed in 4/70 cases (5.7%). The only molecular abnormality that was present in our series with any significance was amplification of *VGLL3* on chromosome 3, which was detected in 8/20 cases (40%). The low reproducibility of the molecular changes, their non-specificity, and the overlap demonstrated with other soft tissue sarcomas calls into question the utility of these markers for a definitive diagnosis of these tumors. In our study we also applied a broad panel of immunohistochemical stains to our cases and found that MIFS appears to have a distinctive immunohistochemical signature characterized by high incidence of positivity for certain markers. The most consistent findings were strong nuclear positivity for bcl-1 observed in 94.5% of our cases. In 89% of cases, >50% of the tumor cells also stained positive for FXIIIa both in the spindle cells and in the large pleomorphic cells. Strong cytoplasmic staining was also observed for CD10 in >80% of the cases, and 56% of cases also stained in their cytoplasm for D2-40. Although none of these markers are specific, the high sensitivity of the combination of bcl-1 and FXIIIa positivity for the diagnosis of these tumors is a feature that we have found helpful for diagnosis, particularly in cases that are located in superficial (subcutaneous) locations, with extensive compromise of the dermis (including superficial dermis), and in which two or more of the triad of histologic findings of MIFS and scattered mono and multinucleated atypical cells with large and prominent nucleoli can be identified. The development of more specific markers for these tumors awaits further study, and for the time being, familiarity with and recognition of the histopathologic features in the appropriate clinical context are the best tools for diagnosing these tumors.

## References:

1. Montgomery EA, Devaney KO, Giordano TJ, Weiss SW. Inflammatory myxohyaline tumor of distal extremities with virocyte or Reed-Sternberg-like cells. A distinctive lesion with features simulating inflammatory conditions, Hodgkin's disease, and various sarcomas. *Mod Pathol*. 1998;11:384-91.
2. Michal M. Inflammatory myxoid tumor of the soft parts with bizarre giant cells. *Pathol Res Pr*. 1998;194:520-33.
3. Meis-Kindblom J, Kindblom L-G. Acral myxoinflammatory fibroblastic sarcoma. A low-grade tumor of the hands and feet. *Am J Surg Pathol*. 1998;22:911-24.
4. WHO Classification of Tumors, 5th Edition: Soft tissue and bone tumors. Edited by the WHO Classification of Tumors Editorial Board, IARC, Lyon, 2020.
5. Michal M, Kazakov DV, Hadravsky L, et al. High-grade myxoinflammatory fibroblastic sarcoma: a report of 23 cases. *Ann Diagn Pathol* 2015; 19:157-163.
6. Antonescu CR, Zhang L, Nielsen GP, et al. Consistent t(1;10) with rearrangements of TGFBR3 and MGEA5 in both myxoinflammatory fibroblastic sarcoma and hemosiderotic fibrolipomatous tumor. *Genes Chromo Cancer*. 2011;50:757-64.
7. Kao YC, Ranucci V, Zhang L et al. Recurrent BRAF gene rearrangements in myxoinflammatory fibroblastic sarcomas but not hemosiderotic fibrolipomatous tumors. *Am J Surg Pathol*. 2017;41:1456-65.
8. Zreik RT, Carter JM, Sukov WR et al. TGFBR3 and MGEA5 rearrangements are much more common in "hybrid" hemosiderotic fibrolipomatous tumors-myxoinflammatory fibroblastic sarcomas than in classical myxoinflammatory fibroblastic sarcomas: a morphological and fluoresce in situ hybridization study. *Hum Pathol* 2016; 53:14-24.
9. Hallor KH, Sciot R, Staaf J et al. Two genetic pathways, t(1;10) and amplification of 3p11-12, in myxoinflammatory fibroblastic sarcoma, hemosiderotic fibrolipomatous tumor, and morphologically similar lesions. *J Pathol*. 2009;217:716-27.
10. Lambert I, Debiec-Rychter M, Guelinks P, et al. Acral myxoinflammatory sarcoma with unique clonal chromosomal changes. *Virchows Arch*. 2001;438:509-12.
11. Suster D, Michal M, Huang H, et al. Myxoinflammatory fibroblastic sarcoma: an immunohistochemical and molecular genetic study of 73 cases. *Mod Pathol* 2020; 33:2520-2533.

## Case 40

Brian Rubin, M.D., Ph.D., Cleveland Clinic, Cleveland, OH, USA

---

### Case History:

40-year-old woman with a 3 cm, superficially located mass involving the vulvovaginal soft tissues.

### Pathologic Findings:

Grossly, was a well demarcated nodule without surrounding tissue and with a white and fibrous cut surface. Histologically, there were alternating zones of cellularity with a collection of benign appearing spindle to epithelioid cells, set in a variably fibrous to myxoid matrix. The spindle cells were admixed with numerous small to medium-sized, thin-walled blood vessels. There was minimal cytological pleomorphism and there was no mitotic activity or necrosis. The tumor cells were positive by estrogen receptor (ER), and variably positive for desmin. Smooth muscle actin and ER was negative.

### Diagnosis: Angiomyofibroblastoma

### Discussion:

Angiomyofibroblastoma is a benign neoplasm that occurs almost exclusively in the superficial vulvovaginal soft tissues. It can rarely occur in the inguinoscrotal region. The tumors are typically small (<5cm), well-circumscribed, tan to pink in color, with a fibrous consistency. Histologically, the lesions are characterized by plump, round to spindle-shaped cells, admixed with numerous thin-walled, capillary-sized vessels. The lesional cells are set in a variably myxoid to collagenous matrix. Occasionally, there is admixed adipose tissue. Typically, there is no mitotic activity. Immunohistochemically, the tumors are positive for ER, PR, and desmin. CD34 and SMA may be positive but are typically negative. No consistent genetic changes have been identified at this time.

The differential diagnosis includes mainly deep (aggressive) angiomyxoma, cellular angiofibroma, and mammary-type myofibroblastoma. Aggressive angiomyxoma is the most important differential since it has recurrent potential. The other neoplasms in the

differential are all uniformly benign. Fortunately, aggressive angiomyxoma is almost always a deep seated neoplasm while angiomyofibroblastoma is almost always superficial. Also, aggressive angiomyxoma is less cellular and tends to have infiltrative margins. I find it difficult to distinguish cellular angiofibroma from spindly cases of angiomyofibroblastoma. The blood vessels of cellular angiofibroma are described as more hyalinized. A lot of emphasis is put on cellular angiofibroma being positive for CD34 and desmin but these can certainly also be positive in angiomyofibroblastoma. Additionally, some have suggested that loss of RB1 can distinguish cellular angiofibroma (lost) from angiomyofibroblastoma (retained). At the end of the day, they are both totally benign so the exercise may be entirely academic. Mammary-type myofibroblastoma is another benign tumor that can rarely occur in the vulvovaginal soft tissues. Mammary-type myofibroblastoma can be positive for desmin but is almost always positive for CD34. It is also characterized by loss of RB1.

## References

1. Fletcher CD, Tsang WY, Fisher C, et al: Angiomyofibroblastoma of the vulva. A benign neoplasm distinct from aggressive angiomyxoma. *Am J Surg Pathol* 16:373-382, 1992.
2. Laskin WB, Fetsch JF, Tavassoli FA: Angiomyofibroblastoma of the female genital tract: analysis of 17 cases including a lipomatous variant, *Hum Pathol* 28: 1046-1055, 1997.

# Case 41

Kumarasen Cooper

---

## Clinical History

Patient is 27-year-old female who presents with incidental splenomegaly comprising 3 splenic masses, characterized on MRI to be likely littoral cell angiomias or SANT, less likely a malignant process. These masses of the spleen were incidental and found when the patient had a CT to evaluate ovarian cysts. She reports no changes in her symptoms, still with a vague pressure in her abdomen 2-3 times per week. Otherwise, she feels well. No fatigue, no weight loss, no fevers, chills, night sweats. Has poor appetite over the past several years with early satiety but stable weight. See abdominal radiological scan.

## Pathology

Spleen weight 858g. Cut surface revealed a 13 X 9cm mass with an irregular border and a heterogeneous cut surface with focal areas of fibrosis. The mass occupies approximately 80% of the splenic parenchyma.

See gross photographs: capsular and cut surface of spleen.

The mass lesion comprises multifocal scattered thin-walled small vessels lined with benign appearing endothelial lining cells. Between these lobules within the splenic parenchyma are tufts of cells with ovoid or spindled morphology, which appear to be intra-vascular.

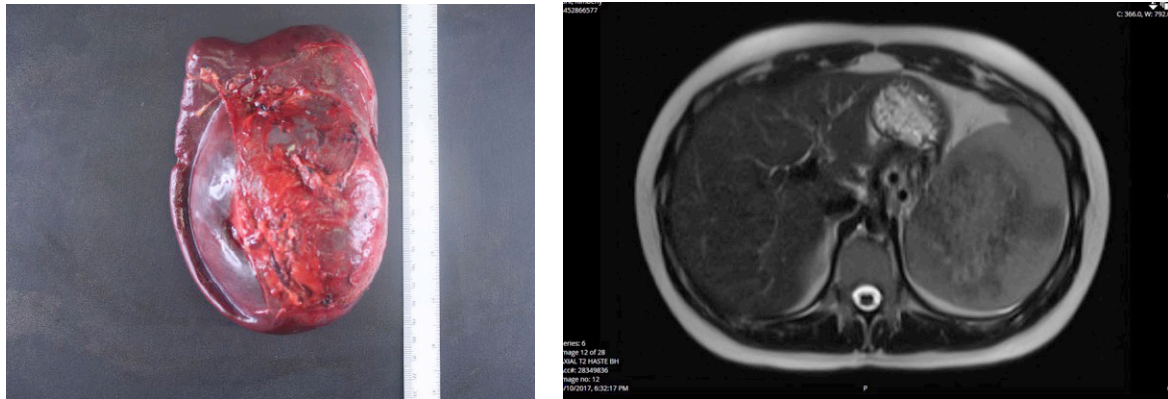
These cells are uniform without atypia or mitotic activity. The tufts of cells are CD 31 and ERG positive (strong and diffuse). Negative for all else!

Gamna-Gandy bodies and hemosiderin deposition are also present in the intervening parenchyma.

**Diagnosis: The mass lesion is a lobular hemangioma with Gamna-Gandy bodies but the tufts of endothelial cells (which appear intravascular) are more complex and was eventually labeled as ATYPICAL ENDOTHELIAL NEOPLASM (see discussion).**

## Discussion

The case was sent to Dr Christopher Fletcher whose comment reads as follows: "The findings do not fit into any presently defined entity. While no overt features of malignancy are identified, the lesion would be best characterized as an ATYPICAL ENDOTHELIAL NEOPLASM, with an uncertain biologic potential. Close surveillance is recommended".



Gross specimen of spleen (surface and cut surface)

MRI radiology showing the heterogeneity of the large splenic masses.

## Case 42

Brian Rubin, M.D., Ph.D., Cleveland Clinic, Cleveland, OH, USA

---

### Case History:

63-year-old woman with a 9 cm, deep seated mass involving the right thigh.

### Pathologic Findings:

Grossly, the lesion was fleshy on cut surface. Histologically, it was highly cellular composed of a proliferation of large cells with abundant eosinophilic cytoplasm, large nuclei with prominent nucleoli, many of them multinucleate, and set in a variably myxoid matrix. There were numerous mitotic figures including atypical mitotic figures. Immunohistochemistry revealed the tumor cells to be positive for HMB45 and negative for S-100, SOX10, keratins, EMA, smooth muscle actin (SMA), Desmin, MyoD1, and myogenin.

### Diagnosis: Malignant PEComa of soft tissue

### Discussion:

PEComas are rare neoplasms occurring predominantly in women. They can arise at any age but have a peak around 45 years of age. They can arise at a wide variety of anatomical sites. Most PEComas are sporadic but they can rarely arise in association with tuberous sclerosis.

Grossly, they are typically well-circumscribed with a fibrous or fleshy cut surface. Tumors range in size from relatively small to very large lesions. Typical PEComas show a nested architecture and composed of epithelioid cells with granular to clear cytoplasm and round nuclei with small nucleoli. Nests of tumor cells are typically invested by small thin-walled blood vessels. PEComas usually show at least focally tumor cells arranged radially around blood vessels. Sclerosing PEComa is composed of cords of epithelioid cells set in a densely collagenous stroma. Typical PEComas lack mitotic activity or necrosis. Some PEComas can have spindle cell morphology with overlapping features of smooth muscle tumors. Malignant PEComas are rare and are characterized by large, pleomorphic,

multinucleate cells with significant mitotic activity including atypical mitotic figures and necrosis. Immunohistochemically, PEComas are positive for HMB-45, MelanA, and MITF and often are positive for muscle markers such as SMA, desmin and caldesmon too. I only require the presence of HMB45 positivity for the diagnosis of PEComa as I find other markers to be positive less consistently. TFE3 is positive in about 15% of cases and is associated with TFE3 gene fusions. Aside from TFE3 gene fusions, PEComas also show genetic alterations in TSC genes. TSC genes regulate mTOR so PEComas with TSC mutations are characterized by activation of the mTOR pathway. mTOR inhibitors are useful therapeutically in this subset.

The differential diagnosis includes mainly epithelioid tumors including carcinoma, melanoma, mesothelioma, and sarcomas with epithelioid cytomorphology.

Immunohistochemistry for keratins and EMA can exclude most cases of carcinoma and mesothelioma. Melanomas typically have positivity for S-100 and SOX10, which are negative in PEComa. Most sarcomas are negative for HMB45 and other melanocytic markers. Spindle cell PEComas can appear to be very similar to smooth muscle tumors, especially when they are located in the uterus. However, typical smooth muscle tumors are negative for melanocytic markers.

## References:

1. Bonetti F, Pea M, Martignoni G, et al: PEC and sugar, *Am J Surg Pathol* 16:307-308, 1992.
2. Bonetti F, Pea M, Marignoni G, et al: Clear cell ("sugar") tumor of the lung is a lesion strictly related to angiomyolipoma—the concept of a family of lesions characterized by the presence of the perivascular epithelioid cells (PEC), *Pathology* 26:230-236, 1994.
3. Folpe AL, Mentzel T, Lehr HA, et al: Perivascular epithelioid cell neoplasm of soft tissue and gynecologic origin. A clinicopathologic study of 26 cases and review of the literature, *Am J Surg Pathol* 29:1558-1575, 2005.
4. Folpe AL, Kwiatkowski DJ: Perivascular epithelioid cell neoplasms: pathology and pathogenesis, *Hum Pathol* 41:1-15, 2010.
5. Agaram NP, Sung YS, Zhang L, Chen CL, Chen HW, Singer S, Dickson MA, Berger MF, Antonescu CR. Dichotomy of Genetic Abnormalities in PEComas With Therapeutic Implications, *Am J Surg Pathol* 39:813-25, 2015.

## Case 43

**David Suster, M.D., Rutgers University Hospital, Newark, N.J., USA**

---

### Clinical history:

A 75-year-old woman with no significant past medical history was seen for shortness of breath and chest pain. CT scans revealed a large anterior mediastinal mass displacing the large vessels and compressing the innominate vein. A transsternal resection of the mass was undertaken, including an attached wedge resection of left lung, 4 mediastinal lymph nodes, and a portion of the innominate vein. The resected specimen contained a firm tumor mass 7.5 x 6.7 x 5.0 cm surrounded by adipose tissue. Cut section showed a fleshy, lobulated mass with areas of hemorrhage and cystic degeneration. There was a partial fibrous capsule surrounding the lesion but focal infiltration of fat by tumor could be seen grossly.

### Pathologic findings:

Histological examination showed a tumor composed of sheets of oval to spindle cells separated into lobules by bands of fibrous tissue imparting the lesion with a nodular configuration. The tumor cells showed large, oval to spindled nuclei with dense chromatin pattern surrounded by an ample rim of eosinophilic to amphophilic cytoplasm. Some of the cell nuclei showed prominent nucleoli. In a few areas, the cells adopted a more round, epithelioid appearance and showed well-defined cell membranes with sharp cell borders. Scattered mitoses could be seen and some of the nuclei were enlarged and showed a mild degree of nuclear pleomorphism. A scant number of scattered small lymphocytes were present in the stroma. Abortive small cystic structures resembling atrophic glandular spaces could be identified focally in association with the tumor cells. Structures resembling neural rosettes were also present focally in some areas. A few tumor implants were present in the surrounding adipose tissue, separate from the main tumor mass, as well as a focus of infiltration of lung parenchyma. Two foci of vascular invasion were also noted.

## Immunohistochemical findings:

Immunohistochemical stains showed strong nuclear positivity of the tumor cells for p40 and p63, and cytoplasmic staining for cytokeratin AE1/AE3. The tumor cells also showed cytoplasmic staining for bcl-2. MIB1 stains showed a mild increase in proliferative activity (15-20% nuclear positivity). Stains for vimentin, SMA, desmin, S100, MDM2, EMA, CD99, chromogranin, synaptophysin, OCT4 and SALL4 were negative. PAX8 showed focal nuclear positivity in about 30% of the tumor cells. Stains for CD5 and CD117 were also positive in a number of the tumor cells.

**Diagnosis: Atypical thymoma, spindle cell type (WHO B3 thymoma, spindle cell variant).**

## Discussion:

Atypical thymoma is a term introduced by Suster and Moran<sup>1</sup> to designate a primary thymic epithelial neoplasm that retains some of the organotypical features of the thymus, such as lobulation, encapsulation and admixture of thymic epithelial cells with immature T lymphocytes, but also displays a moderate degree of cytologic atypia and mitotic activity. As such, these tumors were felt to represent an intermediate stage of differentiation or malignant progression between conventional thymoma and thymic carcinoma. These tumors are currently included under the category of "atypical type A thymoma" in the WHO classification, although it is mentioned by the WHO that "... spindle cells can occur focally in an otherwise typical B3 thymoma. Whether a pure spindle cell subtype of type B3 thymoma exists is unclear, and distinction from atypical type A thymoma is difficult".<sup>2</sup>

We recently published our experience with a series of 120 thymomas that displayed cytologic atypia.<sup>3</sup> 32 cases in that study were characterized by a predominant population of oval to spindle cells, which would represent the equivalent of what the WHO currently terms "atypical type A thymoma".<sup>2</sup> The tumors are characterized by a dense proliferation of oval to spindle cells with little intervening stroma and scant numbers of immature T-lymphocytes. Areas of transition with preexisting spindle cell thymoma (WHO type A) are frequently found, but the cell population shows increased cytologic atypia, with dense nuclear chromatin pattern, prominence of nucleoli, and scattered mitotic activity. In our

study, mitotic activity ranged from 0-12 (average: 2.5 mitoses per 10 high power fields). An interesting finding was cytoplasmic positivity for bcl-2 in the spindle cells in 50% of cases, as well as an increase in the proliferation labeling index (average: 11.6% nuclear positivity). In a previous study we showed that bcl-2 was a marker for spindle cell thymoma observed in 90% of WHO type A thymoma and 89% of type AB thymoma, whereas all of type B thymomas were negative for this marker.<sup>4</sup> In a related article we advocated for the close kinship of WHO type A and type AB due to the similarly high expression rate for this marker in the tumor cells.<sup>4</sup> Another interesting finding in our study was positivity for CD5 and CD117 in the spindle tumor cells in 25% and 14% of cases, respectively.<sup>3</sup>

Atypical thymoma, also known as type B3 thymoma in the WHO classification, is a controversial entity that has been claimed to pose difficulties for distinguishing it from squamous cell carcinoma of the thymus. It was thought initially that staining of the tumor cells for CD5 and CD117 would be helpful for separating the two, but the demonstration of CD5/CD117 positivity in a significant number of atypical thymoma cases (WHO B3) limits considerably the utility of these markers for differential diagnosis.<sup>3</sup> An added controversy is presented by the current WHO definition of the spindle cell tumors with atypia as "atypical type A thymoma", implying that they merely represent a variant of type A thymoma, a tumor with a considerably more indolent behavior than type B3 thymoma. The high rate of recurrence and metastases in the cases we studied, as well as the frequent transformation or progression to thymic carcinoma, argue otherwise.<sup>3</sup> We have recently argued that "atypical type A thymoma" in the WHO classification would be better reclassified as a spindle cell variant of type B3 thymoma due to its more aggressive clinical behavior, presentation at more advanced stages, and increase in cytologic atypia, mitoses, and proliferative activity.<sup>6</sup>

Irrespective of the terminology assigned to these tumors, the fact is that they represent biologically a more advanced step in the process of malignant transformation of thymic epithelial neoplasms. Even though these tumors can retain many of the features of thymic differentiation, such as lobular growth pattern separated by fibrous connective tissue bands, dilated perivascular spaces, and a sprinkling of immature T lymphocytes, their increase in cytologic atypia, nuclear hyperchromasia, prominence of nucleoli and increase in mitotic activity betray their more aggressive potential. Minute and focal areas of coagulative necrosis and foci of vascular invasion can also be features observed in these tumors. Frequent transitions between these tumors and preexisting areas of more conventional spindle cell thymoma speak to their close kinship and supports a gradual

process of enhanced malignant transformation for the atypical variants.<sup>6</sup> In our study, 5 cases showed transitions with higher-grade areas showing features of poorly-differentiated non-keratinizing squamous cell carcinoma, spindle cell carcinoma, basaloid carcinoma and anaplastic carcinoma.<sup>3</sup>

The importance of recognizing this spindle cell variant of WHO type B3 thymoma lies in acknowledging its enhanced potential for aggressive behavior over that of conventional type A thymoma. Thymic epithelial neoplasms composed of sheets of spindle or oval cells with increased cytologic atypia, scattered mitotic figures, prominent nucleoli, and increased proliferation indexes should be regarded as potentially aggressive tumors requiring appropriate management to prevent recurrences or metastases.

## References:

1. Suster S, Moran CA. Thymoma, atypical thymoma and thymic carcinoma. A novel conceptual approach to the classification of neoplasms of thymic epithelium. *Am J Clin Pathol* 1999;111: 826-833.
2. WHO Classification of Tumors, 5th. Edition: Thoracic Tumors, WHO Classification of Tumors Editorial Board, IARC, Lyon, 2021.
3. Suster D, Mackinnon AC, DiStasio M, et al. Atypical thymomas with squamoid and spindle cell features: Clinicopathologic, immunohistochemical and molecular genetic study of 120 cases with long-term follow up. *Mod Pathol*, Feb. 2022, DOI: 10.1038/s41379-022-01013-x.
4. Suster D, Pihan G, Mackinnon CA, et al. Distinctive expression patterns of beta-catenin, E-cadherin, PAX8, bcl-2, EMA and MIB1 in thymomas: an immunohistochemical study of 126 cases. *Mod Pathol* 2021; 34:1831-1838.
5. Suster D, Mackinnon AC, Pihan G et al. Lymphocyte-rich spindle cell thymoma: Clinicopathologic, immunohistochemical, ultrastructural and molecular genetic study of 80 cases. *Am J Surg Pathol* Jan 2022; DOI: 10.1097/PAS.0000000000001855.
6. Suster S. The WHO 2021 thymoma classification: A work in progress. *J Cancer Metastasis Treat* 2022; DOI: 10.20517/2394-4722.2021.203.

## Case 44

Contributed by Abbas Agaimy, MD

---

### Clinical history:

A 65-year-old woman with significant smoking history (40 py) presented with a 7.5 cm lung mass in the left lower lobe (Fig. 1). She underwent left lower lobectomy and systemic lymph node dissection followed by adjuvant radiotherapy. She presented 23 months later with an extensively invasive mass involving the renal pelvis and extending into the inferior vena cava, for which she received a radical nephrectomy with lymph node dissection. The histopathological assessment performed at another center was interpreted as anaplastic urothelial carcinoma with multiple involved lymph nodes (slides were not available for review). Thereafter, multiple metastases were detected by imaging in the liver, peritoneum and in the inguinal, iliac, inter-aortocaval, para-aortic and mesenteric lymph nodes. Under palliative treatment, the patient died of progressive disease, 34 months from initial diagnosis.

### Macroscopic features:

The resection specimen (see illustration) revealed a 5.8 cm well circumscribed non-infiltrative mass with homogeneous tan to whitish soft cut-surface.

### Histological & immunohistochemical findings:

Histology showed undifferentiated small round cell malignancy composed of monotonous epithelioid and round cells arranged into diffuse sheets and compact nests within sparse stroma with variable endobronchial/bronchocentric growth, mucoid/myxoid stromal changes and focal reticular-myxoid pattern (Fig. 2A). The myxoid areas displayed monomorphic small rounded or epithelioid to spindle cells with variable reticular and chordoid patterns (Fig. 1B). Solid areas were composed of tightly packed small to medium-sized monotonous epithelioid or spindle cells with a few scattered rhabdoid or plasmacytoid-looking elements (Fig. 1C). These solid areas revealed occasionally larger nuclei with vesicular chromatin and prominent centrally located nuclei. The neoplastic

cells revealed brisk mitotic activity and areas of confluent necrosis. Abrupt squamous differentiation and keratinization were absent.

Extensive immunohistochemistry performed in different centers showed expression of pankeratin (focal), CD56, CD30, PLAP and NUT, while being negative for CK20, CK7, TTF1, BerEp4, EMA, MUC4, SOX10, synaptophysin, chromogranin, CD117, CD99, LCA, MelanA, GATA3, WT1, CD31, CD34, CK5/14, ERG, CD68, S100, ALK, CD20, CD43, CDX2, OCT3/4, Glypican 3, CD117,  $\beta$ -HCG, SALL4, AFP, Granzyme-B, CD3 and perforin. PLAP and p63 showed similar distribution of expression in 40% of the neoplastic cells with abrupt transition between positive and negative components (Fig. 1D, E). The monoclonal NUT antibody was diffusely positive with distinctive punctate nuclear expression (Fig. 1F). The SWI/SNF proteins (SMARCB1/INI1, SMARCA4, SMARCA2 and ARID1A) were retained.

## Molecular findings

Next generation sequencing analysis revealed a *ZNF532-NUTM1* fusion where exon 6 of *ZNF532* (transcript variant 19, RefSeq NR\_148459) was fused to exon 5 of *NUTM1* (transcript variant 1, RefSeq NM\_001284292) (Fig. 4A). The fusion gene is predicted to encode roughly half of *ZNF532*, inclusive of four of its eleven zinc fingers, and most of *NUT*, including all of its known domains.

## Diagnosis: Pulmonary NUT carcinoma harboring a rare *ZNF532::NUTM1* fusion

### Comment:

*NUT Midline Carcinoma Family Member 1 (NUTM1, AKA: NUT)* rearrangements define a rare highly aggressive malignancy with predominant occurrence in the midline structures (mainly mediastinum and sinonasal cavities) of children, adolescent and young adults, but may occur at any site and in any age group. Due to its frequently non-descript undifferentiated morphology, diagnosis of NUT carcinoma largely relies on a high suspicion index in the appropriate context (undifferentiated or unclassified high-grade malignancy in younger patients in typical locations) aided by the use of either NUT immunohistochemistry or genetic testing. To date, the only context-independent morphological hint to diagnosis is the presence of abrupt squamous differentiation in a background of undifferentiated malignancy. However, this feature is limited to 33% to

40% of cases. With increasing use of the former adjunct tools, NUT carcinoma became increasingly recognized. The consequences of enhanced case detection are recognition of non-midline locations and expansion of the immunophenotype with recognition of keratin-poor and p63-negative cases: Increasing identification of novel fusion partners enables deeper insights into the pathobiology of *NUTM1*-rearranged neoplasia.

The *bromodomain containing 4 (BRD4)* mapped to 19p13.12 represents the most frequently encountered fusion partner (detected in 70% of cases) leading to formation of the BRD4-NUT chimeric protein. Less frequently, *bromodomain containing 3 (BRD3)* (mapped to 9q34.2), another member of the bromodomain family, and *Nuclear Receptor Binding SET Domain Protein 3 (NSD3)* mapped to 8p11.23) are identified as variant fusion partners. However, the list of novel fusion partners in *NUTM1*-rearranged neoplasia has been rapidly increasing to include *MGA*, *CIC14*, *MXD4*, *MXD1*, *BCORL1*<sup>2</sup>, *ZNF532*, *ZNF592*, and *AXTN1*. While *BRD4*, *BRD3*, *NSD3*, *ZNF532* and *ZNF592* represent fusion partners in NUT carcinoma, the other genes listed above have been detected as fusion partners in neoplasms of probably mesenchymal or unknown histogenetic origin.

Involvement of the ZNF family members in *NUTM1*-rearranged neoplasms is rare. To date, only 5 such cases have been described. The reported *ZNF*-rearranged NUT carcinomas affected five females aged 18 to 65 years (median, 52). Two tumors each originated in the lung and the bones (pelvis and mandible) and one in the parotid. They were characterized by non-descript undifferentiated epithelioid and round cell morphology with occasional minor rhabdoid cell component. Squamous differentiation had been reported in single case. All tumors expressed the NUT protein diffusely and they tended to be keratin-poor. Three patients died of metastatic disease at 1, 13 and 34 months after diagnosis and two were alive without disease at 8 and 42 months. Among the fusions detected, *ZNF532* was the most frequent partner involved (n=4) while *ZNF592* was involved in only one case. Both patients with a lung tumor harbored the *ZNF532-NUTM1* fusion variant.

Current data is consistent with the notion that the *ZNF-NUTM1* variants likely act in a homologous way as BRD-NUT fusions in NUT carcinoma and that they might hence be treatable by BET inhibitors similar to their classical *BRD*-rearranged counterparts. The current case represented a true diagnostic challenge due to aberrant immunophenotype which in conjunction with the undifferentiated morphology of the tumor was the cause of this confusion. The initial assessment suggested poorly differentiated neuroendocrine

carcinoma due to CD56 expression, but lack of other more specific neuroendocrine markers precluded this diagnosis. Detection of CD30 expression was misinterpreted as suggestive of a hematological malignancy, which was then ruled out by a hematopathology referral assessment. The issue became further complicated by the prominent expression of PLAP and CD30, which together was interpreted as suggestive of a germ cell origin. However, lack of more sensitive and reliable germ cell marker expression such as SALL4 and Oct3/4 justified seeking further opinion, which revealed expression of p63 and NUT and enabled a diagnosis of NUT carcinoma.

Several reports have documented frequent elevation of elevated  $\alpha$ -fetoprotein (AFP) in the serum of patients with NUT carcinomas (reviewed in ref <sup>32</sup>). To our knowledge, however, there exist no detailed data on germ cell marker expression in NUT carcinoma. Review of the previous six cases with an elevated serum AFP revealed no expression of the germ cell markers tested. Agaimy et al tested a subcohort of 8 genetically characterized NUT carcinomas and found focal expression of SALL4 in three cases (two associated with variable AFP expression), but none expressed CD30, PLAP or OCT3/4. Two additional unpublished cases harboring same ZNF532::NUTM1 fusion (Agaimy & French) were negative for germ cell markers, hence arguing against possible association of this fusion variant with germ cell phenotype.

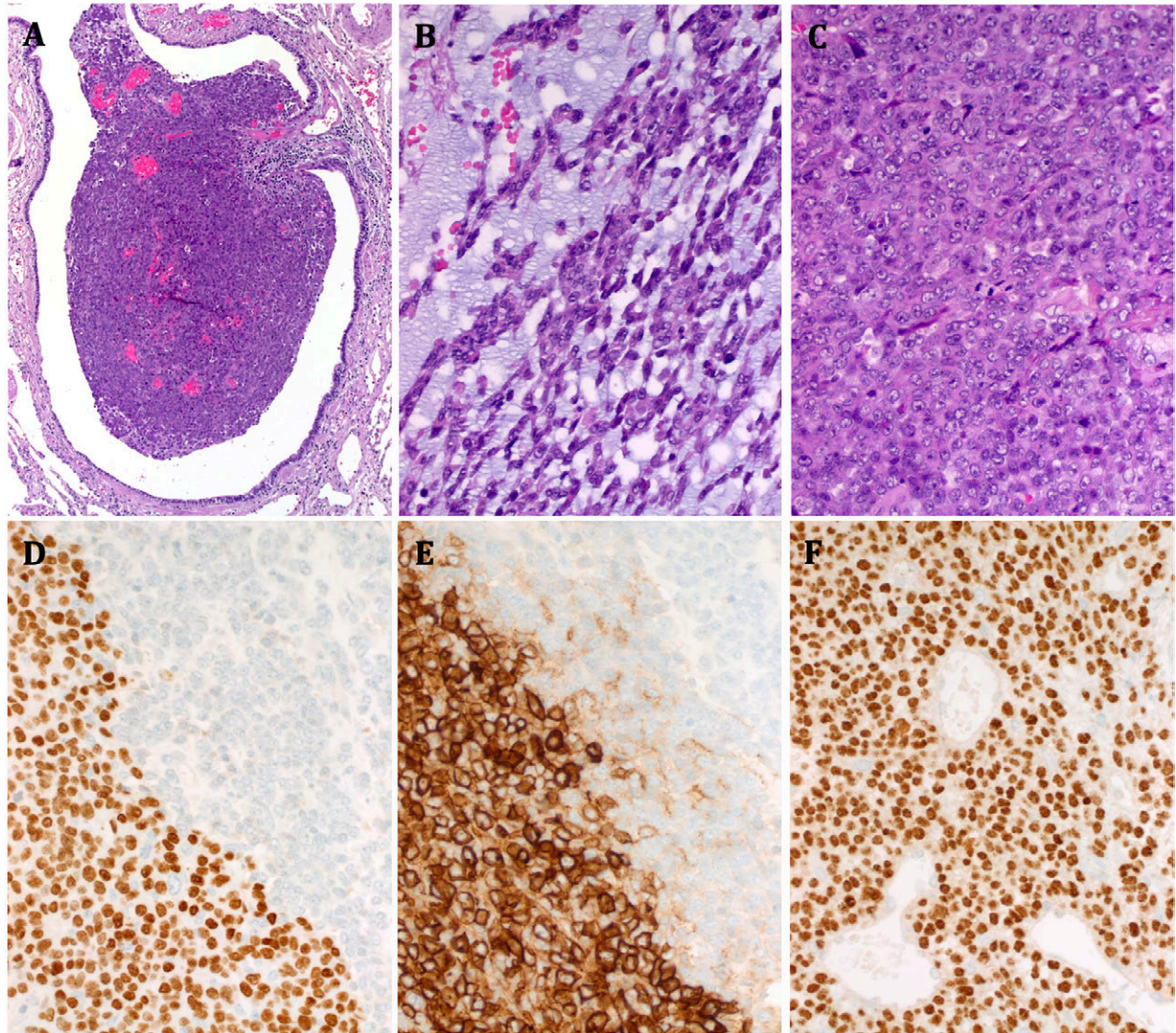


**FIGURE 1:** Representative examples of the histological features of the ZNF532-NUTM1 rearranged NUT carcinoma. A: Prominent endobronchial growth. B: Large tumor areas contained a prominent myxoid stroma (D) with epithelioid and spindled cells in chordoid morphology reminiscent of primary pulmonary myxoid sarcoma or myoepithelial neoplasms. C: Solid areas with monotonous epithelioid morphology. Immunohistochemistry showed abrupt transition between positive and negative areas for p63 (D) and PLAP (E): F: Homogeneous nuclear expression of the NUT antibody.

## References

1. Kubonishi I, Takehara N, Iwata J, et al. Novel t(15;19)(q15;p13) chromosome abnormality in a thymic carcinoma. *Cancer Res.* 1991;51:3327-3328.
2. French CA, Kutok JL, Faquin WC et al. Midline carcinoma of children and young adults with NUT rearrangement. *J Clin Oncol.* 2004;22:4135-4139.
3. French C. NUT midline carcinoma. *Nat Rev Cancer.* 2014;14:149-150.
4. Stelow EB, French CA. Carcinomas of the upper aerodigestive tract with rearrangement of the nuclear protein of the testis (NUT) gene (NUT midline carcinomas). *Adv Anat Pathol.* 2009;16:92-6.
5. French CA. The importance of diagnosing NUT midline carcinoma. *Head Neck Pathol* 2013;7:11-16.
6. Chau NG, Ma C, Danga K, Al-Sayegh H, Nardi V, Barrette R, Lathan CS, DuBois SG, Haddad RI, Shapiro GI, Sallan SE, Dhar A, Nelson JJ, French CA. An Anatomical Site and Genetic-Based Prognostic Model for Patients With Nuclear Protein in Testis (NUT) Midline Carcinoma: Analysis of 124 Patients. *JNCI Cancer Spectr* 2019;4:pkz094.
7. Agaimy A, Fonseca I, Martins C, Thway K, Barrette R, Harrington KJ, Hartmann A, French CA, Fisher C. NUT Carcinoma of the Salivary Glands: Clinicopathologic and Molecular Analysis of 3 Cases and a Survey of NUT Expression in Salivary Gland Carcinomas. *Am J Surg Pathol.* 2018;42:877-884.
8. Dickson BC, Sung YS, Rosenblum MK, Reuter VE, Harb M, Wunder JS, Swanson D, Antonescu CR. NUTM1 Gene Fusions Characterize a Subset of Undifferentiated Soft Tissue and Visceral Tumors. *Am J Surg Pathol.* 2018;42:636-645.
9. Stevens TM, Morlote D, Xiu J, Swensen J, Brandwein-Weber M, Miettinen MM, Gatalica Z, Bridge JA. NUTM1-rearranged neoplasia: a multi-institution experience yields novel fusion partners and expands the histologic spectrum. *Mod Pathol.* 2019;32:764-773.
10. Le Loarer F, Pissaloux D, Watson S, Godfraind C, Galmiche-Rolland L, Silva K, Mayeur L, Italiano A, Michot A, Pierron G, Vasiljevic A, Ranchère-Vince D, Coindre JM, Tirode F. Clinicopathologic Features of CIC-NUTM1 Sarcomas, a New Molecular Variant of the Family of CIC-Fused Sarcomas. *Am J Surg Pathol.* 2019;43:268-276.
11. Van Treeck BJ, Thangaiah JJ, Torres-Mora J, Stevens TM, Rothermundt C, Fassan M, Loupakis F, Diebold J, Hornick JL, Halling KC, Folpe AL. NUTM1-rearranged colorectal sarcoma: a clinicopathologically and genetically distinctive malignant neoplasm with a poor prognosis. *Mod Pathol.* 2021 Mar 13. doi: 10.1038/s41379-021-00792-z.
12. Shiota H, Elya JE, Alekseyenko AA, Chou PM, Gorman SA, Barbash O, Becht K, Danga K, Kuroda MI, Nardi V, French CA. "Z4" Complex Member Fusions in NUT Carcinoma: Implications for a Novel Oncogenic Mechanism. *Mol Cancer Res* 2018;16:1826-1833.

13. Chien YW, Hsieh TH, Chu PY, Hsieh SM, Liu ML, Lee JC, Liu YR, Ku JW, Kao YC. Primary malignant epithelioid and rhabdoid tumor of bone harboring ZNF532-NUTM1 fusion: the expanding NUT cancer family. *Genes Chromosomes Cancer* 2019;58:809-814.
14. Alekseyenko AA, Walsh EM, Zee BM, Pakozdi T, Hsi P, Lemieux ME, Dal Cin P, Ince TA, Kharchenko PV, Kuroda MI, French CA. Ectopic protein interactions within BRD4-chromatin complexes drive oncogenic megadomain formation in NUT midline carcinoma. *Proc Natl Acad Sci U S A* 2017;114:E4184-E4192.
15. Agaimy A, Haller F, Renner A, Niedermeyer J, Hartmann A, French CA. Misleading Germ Cell Phenotype in Pulmonary NUT Carcinoma Harboring the ZNF532-NUTM1 Fusion. *Am J Surg Pathol.* 2022;46:281-288.
16. Chen M, Zhao S, Liang Z, Wang W, Zhou P, Jiang L. NUT carcinoma of the parotid gland: report of two cases, one with a rare ZNF532-NUTM1 fusion. *Virchows Arch.* 2022;480:887-897.

# Case 45

Anais Malpica, M.D.

---

## Clinical History:

A 54 year-old woman presented with a 2 week history of epigastric pain. She was status-post cholecystectomy, appendectomy and hysterectomy and had a strong family history of malignancies. Her mother had colon cancer and uterine adenocarcinoma, her father had colon and prostate carcinomas, her sister had basal cell carcinoma, two maternal aunts had gynecological cancers, one maternal uncle had gastric cancer and her maternal grandmother had ovarian carcinoma. The patient underwent imaging studies and a 9 cm tumor was found in the upper abdomen (arising in the gastrohepatic ligament and extending to the abdominal wall and gastric serosa). A biopsy was obtained and the patient was treated with three cycles of neoadjuvant chemotherapy followed by surgery. Residual disease was confined to area mentioned above.

## Pathology Findings

### Gross Features

A 9.8 cm tumor was attached to a 4.7 cm portion of abdominal wall, an 8.0 cm portion of gastric serosa and a 10 x 9 x 3.7 cm portion of liver (left lateral hepatectomy). The tumor was well circumscribed, soft, pink-tan and hemorrhagic with areas of necrosis.

### Microscopic Features

The tumor is mostly composed of epithelioid cells with a few areas where the cells became spindle-shaped. The cytoplasm is eosinophilic and the atypia is severe. Macronucleoli and intranuclear inclusions are seen. Mitotic figures, including atypical forms, are unevenly distributed (up to 7 mitoses per 10 HPFs). There are foamy cells, inflammation and foci of necrosis. There is a variety of patterns: papillary, adenomatoid, solid, and tubular.

### Immunohistochemical Features

The tumor cells were positive for pankeratin, keratin 7, calretinin, keratin 5/6, thrombomodulin, and WT-1 while negative for Ber-EP4, MOC-31, B72.3, PAX-8, ER, PR,

CEA, glypican, and villin. BAP-1 expression was retained and the expression of MSH2 and MSH6 was lost. PDL1 (clone 22 C3) showed a TPS=10%.

### **Molecular Findings**

Somatic mutations (SNVs/Indels) > 5 genes (*ACVR2A*, *ADGRA2*, *ANKRD11*, *ARAF*, *CARD11*, *DIS3*, *GLI1*, *MET*, *NF2*, *SMARCB1*, *WT1*)

Copy Number variations (CNVs): Amplification of *DNAJB* and *RAC1*

Gene fusions: none

TMB: 7 mut/Mb

MSI: Stable (MSS)

Also, a germline variant, *MSH2* c.1861C>T p.R612 was detected in the tumor and in the germline peripheral blood sample.

### **Genetic Testing**

Pathogenic mutation in *MSH2* consistent with Lynch syndrome.

## **Diagnosis: Localized malignant mesothelioma of the peritoneum**

## **Discussion**

Localized malignant mesothelioma is an uncommon tumor characterized by the presence of a serosal/subserosal mass, lacking diffuse serosal spread, but with the histological features of the more common diffuse malignant mesothelioma. This tumor can occur in the peritoneum of women of a wide age range (mean: 57 years; median: 54 years). Most patients present with abdominal pain, but a rare case can be incidentally found. An elevated CA125 (up 1,202 U/mL) or ascites are not typical, but they can be seen. Recently, we studied a cohort of 18 women with localized mesothelioma of the peritoneum and we found that one third of them had a personal history of cancer -breast, ovarian or endometrial. In all these patients, the localized mesothelioma had been diagnosed after the other malignancies. Also, all of our patients with available family history had malignancies in their relatives, mostly in their first or second-degree relatives. The association of localized mesothelioma and a family history of malignancies had not been reported before. Of note, the tumors in these families have been described in the following tumor predisposition syndromes: *BAP1*, Lynch, hereditary breast and ovarian cancer and Li-Fraumeni. **Due to the retrospective nature of our study, only two cases that underwent NGS were found to have germline variants, *MSH6* and *MSH2*,**

**respectively, with the latter being confirmed as Lynch syndrome on germline testing.**

Interestingly, the patient with *MSH6* mutation had also *CDKN2A* mutation as well as multiple family members with melanoma; therefore, it is likely that this patient had a melanoma-dominant syndrome due to the *CDKN2A* mutation rather than Lynch syndrome. About 30% of patients with localized mesothelioma of the peritoneum have reported indirect or direct exposure to asbestos. Also, a history of abdominopelvic surgery, inflammatory conditions, or endometriosis is common.

In women, tumors range in size from 0.9 cm to 28 cm and are usually epithelioid -less frequently biphasic. Adenomatoid areas are uncommon and the degree of cytologic atypia and mitotic activity is variable. In our study, we found a prominent inflammatory infiltrate in 94.4% of our cases. This feature, which had not been underscored before, could have potential therapeutic implications. From the immunohistochemical standpoint, the usual mesothelioma profile is seen; these are a few caveats: 1) tumors with clear cells are usually calretinin negative, 2) PAX-8 can be patchy positive, 3) inhibin can be focally positive, 4) loss of BAP-1 may not be seen. The experience with homozygous deletion of *CDKN2A* by FISH and localized malignant mesothelioma is limited, but we found no homozygous deletion of *CDKN2A* by FISH in a single case tested, which interestingly had a *CDKN2A* pathogenic mutation by NGS.

The molecular landscape of localized malignant mesothelioma of the peritoneum is yet to be defined. One case has been reported with *CHECK2* nonsense mutation while we found two cases with a variety of pathogenic mutations. One case had *CDKN2A*, *MSH6*, *PRKAR1A*, *SMARCA4*, *SUFU*, *NF2*, and *TP53* while the other had *ACVR2A*, *ADGRA2*, *ANKRD11*, *ARAF*, *CARD11*, *DIS3*, *GLI1*, *MET*, *NF2*, *SMARCB1*, and *WT1* and copy number variations in *DNJB1* and *RAC1*. Some of the mutations listed above have been described in diffuse malignant mesothelioma.

In our experience, there are several confounding factors that can lead to misdiagnosis in cases of localized mesothelioma, for example: a previous history of malignancy, a solid pattern or individual cells in a limited tissue sample, the predominance of clear cells with numerous blood lakes, a spindle cell component, marked inflammation and an adenomatoid pattern. Being mindful of the occurrence of localized malignant peritoneal mesothelioma in patients with previous malignancies and the heterogeneous appearance of this disease will allow for the judicious use of ancillary testing to make the correct diagnosis. It is also important to exert caution when making the diagnosis of adenomatoid tumor of the peritoneum as this tumor is extremely rare in this location; therefore, malignant mesothelioma with an adenomatoid/microcystic pattern needs to be excluded through a combination of clinical findings and ancillary testing including loss of BAP-1

immunohistochemistry and *CDKN2A* homozygous deletion by FISH. Of note, some cases of malignant mesothelioma will not show the loss of BAP-1 by immunohistochemistry or the *CDKN2A* homozygous deletion by FISH. Adenomatoid tumors show an intact expression of BAP-1 and a robust membranous staining for L1 cell adhesion molecule (L1CAM) by immunohistochemistry.

The recurrence rate of localized malignant peritoneal mesothelioma in women has ranged from 29 % to 53%, and although no definitive conclusion can be drawn regarding prognostic factors, small size, low grade cytology and low mitotic index appear to be associated with an indolent behavior.

## References

1. Allen TC, Cagle PT, Churg AM, et al. Localized malignant mesothelioma. *Am J Surg Pathol.* 2005;29(7):866-873.
2. Attanoos RL, Churg A, Galateau-Salle F, Gibbs AR, Roggli VL. Malignant Mesothelioma and Its Non-Asbestos Causes. *Arch Pathol Lab Med.* 2018;142(6):753-760.
3. Baker PM, Clement PB, Young RH. Malignant peritoneal mesothelioma in women: a study of 75 cases with emphasis on their morphologic spectrum and differential diagnosis. *Am J Clin Pathol.* 2005;123(5):724-737.
4. Clement PB, Young RH, Scully RE. Malignant mesotheliomas presenting as ovarian masses. A report of nine cases, including two primary ovarian mesotheliomas. *Am J Surg Pathol.* 1996;20(9):1067-1080.
5. Goldblum J, Hart WR. Localized and diffuse mesotheliomas of the genital tract and peritoneum in women. A clinicopathologic study of nineteen true mesothelial neoplasms, other than adenomatoid tumors, multicystic mesotheliomas, and localized fibrous tumors. *Am J Surg Pathol.* 1995;19(10):1124-1137.
6. Marchevsky AM, Khoo A, Walts AE, et al. Localized malignant mesothelioma, an unusual and poorly characterized neoplasm of serosal origin: best current evidence from the literature and the International Mesothelioma Panel. *Mod Pathol.* 2020;33(2):281-296.
7. Kobayashi Shimizu S, Okamura T, Koyama K, Seura H, Nishida N. A Case of Localized Malignant Peritoneal Mesothelioma With Lung Cancer Detected by 18F-FDG PET/CT. *Clin Nucl Med.* 2020;45(10):795-797.
8. Maeda S, Hosone M, Katayama H, et al. Deciduoid mesothelioma in the pelvic cavity. *Pathol Int.* 2004;54(1):67-72.
9. Notue YA, Mbessoh UI, Nganwa G, et al. Sarcomatoid malignant peritoneal mesothelioma presenting as a localized mesenteric tumor with no previous asbestos exposure. *J Surg Case Rep.* 2020;2020(10):rjaa419.

10. Phillips-Yelland J, Payton D, Land R, Kaur A. Incidental fallopian tube mesothelioma diagnosed at time of elective bilateral salpingectomy for sterilisation: A case report. *Gynecol Oncol Rep.* 2017;22:1-3.
11. Vimercati L, Cavone D, Delfino MC, et al. Primary Ovarian Mesothelioma: A Case Series with Electron Microscopy Examination and Review of the Literature. *Cancers (Basel).* 2021;13(9).
12. Marubayashi S, Ohdan H, Asahara T, et al. Malignant mesothelioma originating in the hepatic falciform ligament: report of a case. *Surg Today.* 1998;28(9):929-931.
13. Kohama T, Sakamoto T, Okino T. Parahiatal Hernia Sac Tumor of Localized Malignant Peritoneal Mesothelioma. *Ann Thorac Surg.* 2021;112(1):e57-e60.
14. Xu T, Hu J, Zhang X, Cao J, Chen Y. A Case of Localized Malignant Peritoneal Mesothelioma Evaluated by 18F-FDG PET/CT. *Clin Nucl Med.* 2020;45(11):890-891.
15. Asim Q, Vaidyanathan G, Ikram B, Moza K. Papillary Mesothelioma of peritoneum involving fallopian tube: A challenging case. *J of Solid Tumors.* 2016;7(1):20-22.
16. Malpica A, Euscher ED, Marques-Piubelli ML, et al. Malignant Mesothelioma of the Peritoneum in Women: A Clinicopathologic Study of 164 Cases. *Am J Surg Pathol.* 2021;45(1):45-58.
17. Crotty TB, Myers JL, Katzenstein AL, Tazelaar HD, Swensen SJ, Churg A. Localized malignant mesothelioma. A clinicopathologic and flow cytometric study. *Am J Surg Pathol.* 1994;18(4):357-363.
18. Husain AN, Colby TV, Ordonez NG, et al. Guidelines for Pathologic Diagnosis of Malignant Mesothelioma 2017 Update of the Consensus Statement From the International Mesothelioma Interest Group. *Arch Pathol Lab Med.* 2018;142(1):89-108.
19. Churg A, Le Stang N, Dacic S, et al. Solid papillary mesothelial tumor. *Mod Pathol.* 2022;35(1):69-76.
20. Hung YP, Dong F, Dubuc AM, Dal Cin P, Bueno R, Chirieac LR. Molecular characterization of localized pleural mesothelioma. *Mod Pathol.* 2020;33(2):271-280.
21. Attanoos RL, Gibbs AR. Primary malignant gonadal mesotheliomas and asbestos. *Histopathology.* 2000;37(2):150-159.
22. Farioli A, Ottone M, Morganti AG, et al. Radiation-induced mesothelioma among long-term solid cancer survivors: a longitudinal analysis of SEER database. *Cancer Med.* 2016;5(5):950-959.
23. Butnor KJ, Pavlisko EN, Sporn TA, Roggli VL. Malignant Mesothelioma in Individuals With Nonmesothelial Neoplasms. *Arch Pathol Lab Med.* 2018;142(6):730-734.
24. Carbone M, Yang H, Pass HI, Krausz T, Testa JR, Gaudino G. BAP1 and cancer. *Nat Rev Cancer.* 2013;13(3):153-159.
25. Wadt KA, Aoude LG, Johansson P, et al. A recurrent germline BAP1 mutation and extension of the BAP1 tumor predisposition spectrum to include basal cell carcinoma. *Clin Genet.* 2015;88(3):267-272.

26. Karamurzin Y, Zeng Z, Stadler ZK, et al. Unusual DNA mismatch repair-deficient tumors in Lynch syndrome: a report of new cases and review of the literature. *Hum Pathol.* 2012;43(10):1677-1687.
27. Shih AR, Kradin RL. Malignant mesothelioma in Lynch syndrome: A report of two cases and a review of the literature. *Am J Ind Med.* 2019;62(5):448-452.
28. Panou V, Gadiraju M, Wolin A, et al. Frequency of Germline Mutations in Cancer Susceptibility Genes in Malignant Mesothelioma. *J Clin Oncol.* 2018;36(28):2863-2871.
29. Ceelen WP, Van Dalen T, Van Bockstal M, Libbrecht L, Sijmons RH. Malignant peritoneal mesothelioma in a patient with Li-Fraumeni syndrome. *J Clin Oncol.* 2011;29(17):e503-505.
30. Leachman SA, Lucero OM, Sampson JE, et al. Identification, genetic testing, and management of hereditary melanoma. *Cancer Metastasis Rev.* 2017;36(1):77-90.
31. Vogl M, Rosenmayr A, Bohanes T, et al. Biomarkers for Malignant Pleural Mesothelioma-A Novel View on Inflammation. *Cancers (Basel).* 2021;13(4).
32. Hayashi H, Kawata T, Shimokawa I. Malignant peritoneal mesothelioma, clear cell variant, in a female and its differentiation from clear cell carcinoma. *Pathol Res Pract.* 2017;213(5):580-584.
33. Karpathiou G, Hiroshima K, Peoc'h M. Adenomatoid Tumor: A Review of Pathology With Focus on Unusual Presentations and Sites, Histogenesis, Differential Diagnosis, and Molecular and Clinical Aspects With a Historic Overview of Its Description. *Adv Anat Pathol.* 2020;27(6):394-407.
34. Erber R, Warth A, Muley T, Hartmann A, Herpel E, Agaimy A. BAP1 Loss is a Useful Adjunct to Distinguish Malignant Mesothelioma Including the Adenomatoid-like Variant From Benign Adenomatoid Tumors. *Appl Immunohistochem Mol Morphol.* 2020;28(1):67-73.
35. Mori D, Kido S, Hiraki M, et al. Peritoneal adenomatoid (microcystic) mesothelioma. *Pathol Int.* 2020;70(11):876-880.
36. Goode B, Joseph NM, Stevers M, et al. Adenomatoid tumors of the male and female genital tract are defined by TRAF7 mutations that drive aberrant NF- $\kappa$ B pathway activation. *Mod Pathol.* 2018;31(4):660-673.
37. Malpica A, Euscher ED, Marques-Piubelli ML, et al. Localized Malignant Peritoneal Mesothelioma (LMPeM) In Women: A Clinicopathologic Study of 18 Cases. *Am J Surg Pathol* submitted

# Case 46

Cesar A. Moran, MD, M D Anderson Cancer Center

---

## Clinical History:

54-year-old man presented with symptoms of cough, chest pain and dyspnea. Diagnostic imaging shows the presence of a large anterior mediastinal mass.

## Diagnosis: High Grade Thymic Carcinoma

## Discussion:

Credit for the first original description of squamous cell carcinomas of the thymus is due to Dr. Shimosato who described a series of 8 cases of these tumors originating in the thymus. Prior to that description, important publications such as the AFIP fascicles had failed to provide more insights into this particular tumor. Also, important to highlight is the fact that in some publication the term "malignant thymoma" has been used as a synonym with thymic carcinoma, which is of course incorrect as "invasive thymoma" and "thymic carcinoma," represent two different pathological entities.

In general terms thymic carcinomas are unusual neoplasms with only a few large series of cases presented up to now. Also, in general terms, these tumors have traditionally been grouped as "low" and "high" grade carcinomas. Essentially, the low-grade carcinomas are the basaloid carcinoma and the Low-grade mucoepidermoid carcinomas, while everything else may represent a high-grade carcinoma. Although histologically, the diagnosis of thymic carcinoma may not represent a diagnostic challenge, the challenge rests in ascribing site of origin for the carcinoma. There is nothing specific about thymic carcinoma and the histological features may be seen in other carcinomas from other sites including lung. Therefore, the diagnosis of thymic carcinoma becomes a true clinical-radiological-pathological correlation.

The immunohistochemical features of these tumors are also non-specific as the majority of thymic carcinoma will show squamous differentiation, thus p40, keratin 5/6, and p63 will show positive staining. Other immunohistochemical stains that have been reported as positive in some thymic carcinomas include GLUT-1 and CD117, but yet, those stains are also seen positive in other non-thymic carcinomas.

## Differential Diagnosis

Often the most important differential diagnosis is separating thymic carcinoma from Atypical thymoma (WHO B3). In such cases, the use of strict criteria such as marked cytological atypia, and loss of organotypical features will favor thymic carcinoma. Because thymomas and thymic carcinoma share similar immunohistochemical features, it is complicated the separation of these tumors by means of immunohistochemical markers. However, as stated earlier some reports have stated that the use of GLUT1 and CD117 may help in separating those two tumors.

The second most important consideration is an extension of a carcinoma from the lung into the mediastinum or a metastasis from an extra thoracic organ to the mediastinum. In those cases, the clinical information and diagnostic imaging will aid in the proper interpretation.

## Clinical Follow-up

The importance in separating thymoma from thymic carcinoma is not only in the treatment of choice but also in the post surgical treatment and follow up. In cases of encapsulated or minimally invasive thymoma, the treatment of choice is surgery alone and the clinical outcome for those patients is good.

On the other hand, the treatment of thymic carcinoma not only may require surgical resection of the tumor but also additional medical treatment that often involves chemotherapy.

The clinical follow up that has been reported for thymic carcinomas is somewhat variable with reports of 56% survival at 1 year and 33% survival at 5-years. while other have estimated a 76% survival at 3-years and 67% at 5-years.

At this point, it is important to highlight that the most important predictor of clinical outcome is the stage of the tumor at the time of diagnosis. Unfortunately, until recently the staging system used was the one that Masaoka proposed for thymoma. This is represents a failure in recognizing the thymoma and thymic carcinoma are two different pathological entities. More recently, the same mistake was proposed by including the TNM system for thymic epithelial neoplasms that not only is incorrect from the anatomical aspect but also from the pathological approach. What has been observed in large series of cases in which the tumors have been staged is that regardless of anatomical location, lymph node involvement in thymic carcinoma portends a worse prognosis.

## Selected References

1. Moran CA, Suster S. Thymic carcinoma: current concepts and histological features. *Hematol Oncol Clin N Am* 2008; 22:393-407.
2. Suster S, Rosai J. Thymic carcinoma: a clinicopathologic study of 60 cases. *Cancer* 1991; 67:1025-1032.
3. Weissferdt A, Moran CA. thymic carcinoma, Part 1. A clinicopathologic and Immunohistochemical study of 65 cases. *Am J Clin Pathol* 2012; 138:103-114.
4. Moran CA, Walsh G, Suster S, Kaiser L. Thymoma II: a clinicopathologic correlation of 250 cases with a proposed staging system with emphasis on pathologic assessment. *Am J Clin Pathol* 2012; 137:451-461.
5. Weissferdt A, Moran CA. Thymic carcinoma, part 2: a clinicopathologic correlation of 33 cases with a proposed staging system. *Am J Clin Pathol* 2012; 138:115-121.

## Case 47

Contributed by Abbas Agaimy, MD

---

### Clinical history:

A 76-year-old man was diagnosed with a paraaortic intrathoracic mass initially thought to represent lung cancer (see imaging). Pleural effusion cytology failed to demonstrate any malignant cells. Surgical resection was performed. He underwent surgical resection of multifocal chest wall recurrences 16 months later.

### Macroscopic features:

The resection specimen (see illustration) revealed a 5.8 cm well circumscribed non-infiltrative mass with homogeneous tan to whitish soft cut-surface.

### Histological & immunohistochemical findings:

Histological examination revealed medium-sized to large epithelioid cells with copious cytoplasm disposed into diffuse sheets, macrotrabeculae and nests with prominent cytoplasmic vacuoles frequently resulting into double-barrel phenomena and cytoplasmic bridging with variable resemblance to adenomatoid tumors. Mild to moderate atypia and mitoses were present. IHC showed consistent expression of vimentin, pankeratin, CK5, calretinin, HMBE, WT1 and podoplanin (representative images shown in the figure composite). Complete loss of BAP1 was evident in the neoplastic cells. Retrospective assessment of pleural cytology was negative for tumor cells. No other manifestations were detected at time of release from hospital.

**Diagnosis: Localized malignant epithelioid mesothelioma, microcystic-adenomatoid-like variant, BAP1-deficient.**

### Comment:

Malignant mesothelioma is notorious for being difficult to distinguish from a variety of reactive and benign mesothelial lesions/neoplasms on one side and from aggressive

primary or metastatic malignancies (mainly adenocarcinomas) on the other side. The difficulty in distinguishing malignant mesothelioma from reactive mesothelial hyperplasia and benign adenomatoid tumors is mainly a reflection of the lack of cytological features of malignancy in many cases of MM making infiltrative destructive growth the sole reliable feature of malignancy in many cases. On the other hand, the presence of unequivocal infiltrative growth in most of benign adenomatoid tumors makes distinction from malignant mesothelioma on the basis of infiltrative growth alone of limited reliability, particularly in limited or less well-oriented biopsies. This issue is further complicated by the inoperable nature of the vast majority of malignant mesothelioma, which makes limited biopsy material often the only available tissue for firm diagnosis before initiation of palliative systemic therapy. Compensational issues related to occupational asbestos exposure as the major etiological factor in malignant mesothelioma cases is another point complicating diagnosis of malignant mesothelioma and underlining the need for solid diagnosis in individual cases.

Malignant mesothelioma may rarely present as a localized mass as in this case and thus represents a potential source of confusion regarding both histogenetic line and dignity of the lesion. Prominent bland-looking adenomatoid features have been reported in malignant mesothelioma from all sites and may represent a diagnostic challenge due to their often bland looking histology.

The BRCA1-associated protein-1 (BAP1), a member of nuclear deubiquitinating enzymes, is encoded by the *bap1* gene mapping to chromosomal region 3p21.1. It functions as a tumor suppressor via binding to the Breast/Ovarian Cancer Susceptibility Gene product (BRCA1) RING finger domain. Loss of BAP1 (due to gene mutations, homozygous deletions or epigenetic silencing) is reported in a variety of sporadic and inherited neoplasms including uveal melanoma, malignant mesothelioma, cholangiocarcinoma, renal cell carcinoma, breast carcinoma and others. Loss of BAP1 in malignant mesothelioma was associated with increased survival. Several studies have investigated the value of BAP1 loss in distinguishing malignant mesothelioma from benign mesothelial proliferations, A subset of mesothelioma is known to harbor inactivating BAP1 mutations which is illustrated by loss of BAP1 IHC. This is highly useful in effusions and on limited biopsy as loss of this tumor suppressor is limited to malignant mesothelial proliferations and it has not been reported in reactive and benign lesions such as adenomatoid tumors. However, retained expression does not help in this distinction. Up to 50% of mesotheliomas are BAP1-lost with this being seen across all subtypes. However, there is

evidence that BAP1-lost cases tend to show epithelioid morphology and bland-looking histology with or without adenomatoid features.

BAP1 inactivation may be either due to acquired (somatic) mutations or an indication of germline mutations (the latter has been referred to as "BAPomas" or BAP1 tumor syndrome. The spectrum of the hereditary BAP1-related diseases includes melanocytic tumors, malignant mesothelioma, uveal melanoma, cholangiocellular carcinoma, clear cell renal cell carcinoma, breast cancer and many other rare conditions. It has been shown that patients with germline BAP1 defects and asbestos exposure develop mesotheliomas some 10 yrs earlier than control individuals. The current patient had no history of asbestos exposure.

In the current case, I was initially unwilling to comment on possible heredity of the condition as the patient was 76 yo at time of diagnosis. However, surprisingly, at the post-operative MDT meeting, the patient was known to have underwent a tumor nephrectomy at age 28, but details of the histology was not available. Thus, this is likely a genetic disorder with unusual very long latency between his renal tumor (which was likely a ccRCC) and the current mesothelioma. In addition, the possibility of a germline BAP1 defect would better explain this remarkably unusual presentation of malignant mesothelioma. I am not sure whether this variant was overrepresented among previous series on localized malignant mesotheliomas or not.

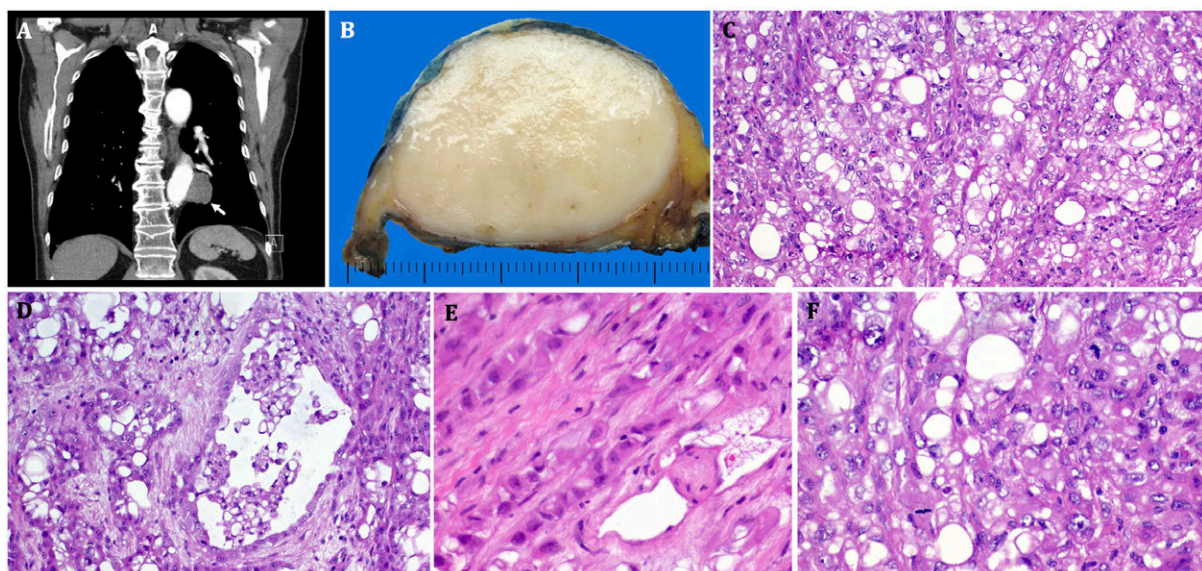


**Figure 1:**

A: Imaging (CT) and B: gross of the tumor (white arrow). C: Microcystic adenomatoid and sieve-like growth. D: focal intracystic glomeruloid papillary foci. E: Focal Indian file growth

pattern. F: Mergence of adenomatoid bland foci with area with higher atypia and brisk mitotic activity.

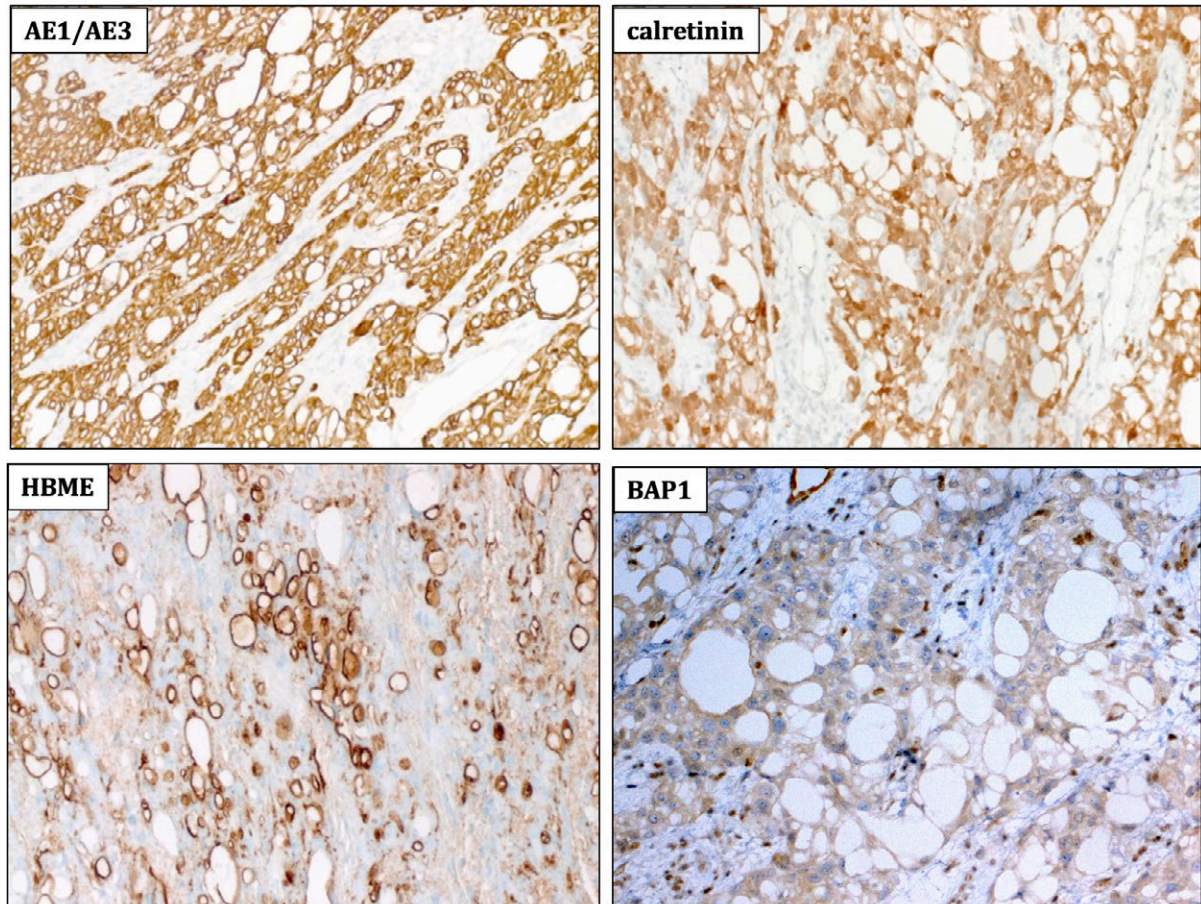


**Figure 2:**

Representative immunostains of the tumor.

## References

1. Weissferdt A, Kalhor N, Suster S. Malignant mesothelioma with prominent adenomatoid features: a clinicopathologic and immunohistochemical study of 10 cases. *Annals of diagnostic pathology*. 2011;15(1):25-9.
2. Carbone M, Ferris LK, Baumann F, Napolitano A, Lum CA, Flores EG, Gaudino G, Powers A, Bryant-Greenwood P, Krausz T, Hyjek E, Tate R, Friedberg J, Weigel T, Pass HI, Yang H. BAP1 cancer syndrome: malignant mesothelioma, uveal and cutaneous melanoma, and MBAITs. *J Transl Med*. 2012 Aug 30;10:179.
3. McGregor SM, Dunning R, Hyjek E, Vigneswaran W, Husain AN, Krausz T. BAP1 facilitates diagnostic objectivity, classification, and prognostication in malignant pleural mesothelioma. *Hum Pathol*. 2015 Nov;46(11):1670-8.

4. Betti M, Aspesi A, Biasi A, Casalone E, Ferrante D, Ogliara P, et al. CDKN2A and BAP1 germline mutations predispose to melanoma and mesothelioma. *Cancer Lett.* 2016;378(2):120-30.
5. Erber R, Warth A, Muley T, Hartmann A, Herpel E, Agaimy A. BAP1 Loss is a Useful Adjunct to Distinguish Malignant Mesothelioma Including the Adenomatoid-like Variant From Benign Adenomatoid Tumors. *Appl Immunohistochem Mol Morphol.* 2019 Jan 11. doi: 10.1097/PAI.0000000000000700. [Epub ahead of print].
6. Dacic S. Pleural mesothelioma classification-update and challenges. *Mod Pathol.* 2022 Jan;35(Suppl 1):51-56.
7. Terra SBSP, Roden AC, Aubry MC, Yi ESJ, Boland JM. Utility of Immunohistochemistry for MUC4 and GATA3 to Aid in the Distinction of Pleural Sarcomatoid Mesothelioma From Pulmonary Sarcomatoid Carcinoma. *Arch Pathol Lab Med.* 2021 Feb 1;145(2):208-213.
8. Allen TC, Cagle PT, Churg AM, Colby TV, Gibbs AR, Hammar SP, Corson JM, Grimes MM, Ordonez NG, Roggli V, Travis WD, Wick MR. Localized malignant mesothelioma. *Am J Surg Pathol.* 2005 Jul;29(7):866-73.
9. Mann S, Khawar S, Moran C, Kalhor N. Revisiting localized malignant mesothelioma. *Ann Diagn Pathol.* 2019 Apr;39:74-77.

## Case 48

Alberto M. Marchevsky, M.D. Cedars-Sinai Medical Center, Los Angeles, CA, USA

---

### Clinical History:

The patient was a 36 y.o. woman who presented with progressive shortness of breath and pneumothorax. Chest X ray showed some hyperinflation and mild reticulation suspicious for interstitial lung disease. Chest CT showed mild interlobular septal thickening and multiple thin walled cysts of variable size distributed throughout the parenchyma of both lungs. She underwent a wedge biopsy of the left lung. The condition worsened over a 2-year period and she underwent a left single lung transplant. She did well for approximately 2 years but developed right lung herniation that required pneumonectomy. She developed postoperative complications and died with bronchopneumonia, chronic rejection of the left lung allograft, chronic renal insufficiency and disseminated intravascular coagulation (DIC).

### Pathologic Findings:

The wedge biopsies showed multiple thin-walled cysts in a peribronchiolar distribution (Fig 1). They resemble centriacinar emphysema but the peribronchiolar spaces and the alveoli were thickened in some areas. The patchy areas of thickening showed proliferation of spindle cells with eosinophilic cytoplasm admixed with vascular spaces (Fig 2). The spindle cells had a smaller cytoplasm than normal smooth muscle cells, lacked desmin immunoreactivity and exhibited cytoplasmic immunoreactivity for HMB-45 (Fig 3). The cells lining vascular spaces exhibited D2-40 immunoreactivity, characteristic for lymphatics (1-3).

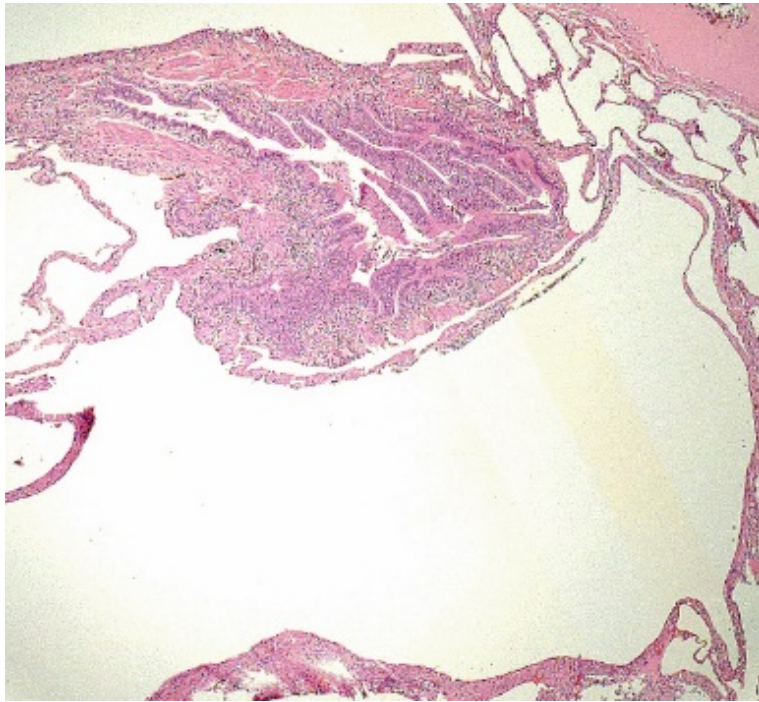


**Figure 1:** Cyst at low power

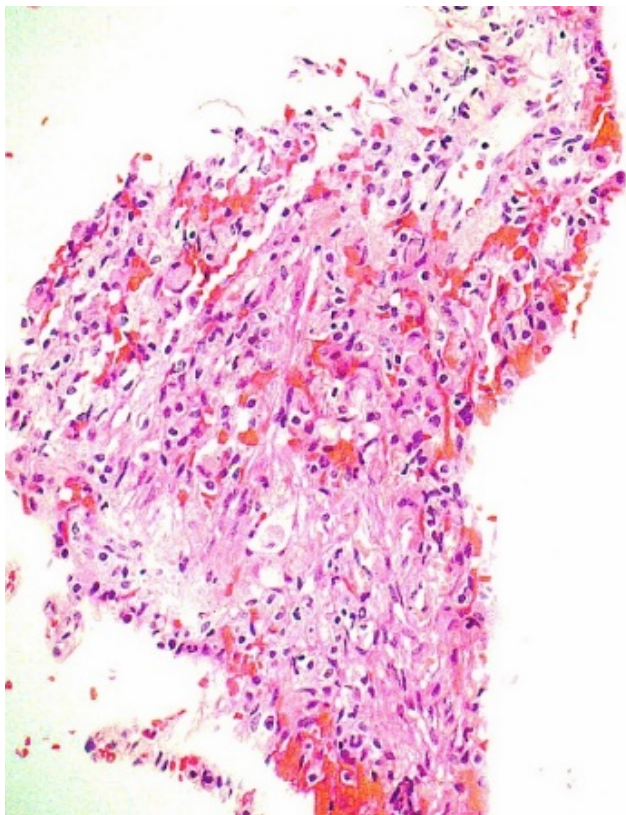


**Figure 2:** Spindle cells and vascular spaces

## Diagnosis: Lung with lymphangioleiomatosis (LAM)

### Discussion:

LAM is a rare disease that involves mostly childbearing age women, with an incidence of up to 8 cases per million women. LAM has been described in only rare men with tuberous sclerosis (TS) and children. It occurs sporadically or in association with tuberous sclerosis in women with autosomal germline mutations of the tuberous sclerosis complex genes TSC1 or TSC2. Approximately 20-50% of women with TS exhibit cystic lung changes suspicious for pulmonary involvement.

LAM patients can have isolated lung disease, such as our case, or exhibit pulmonary and extrapulmonary lesions such as perivascular epithelioid cell tumors (PEComas) of the kidney,

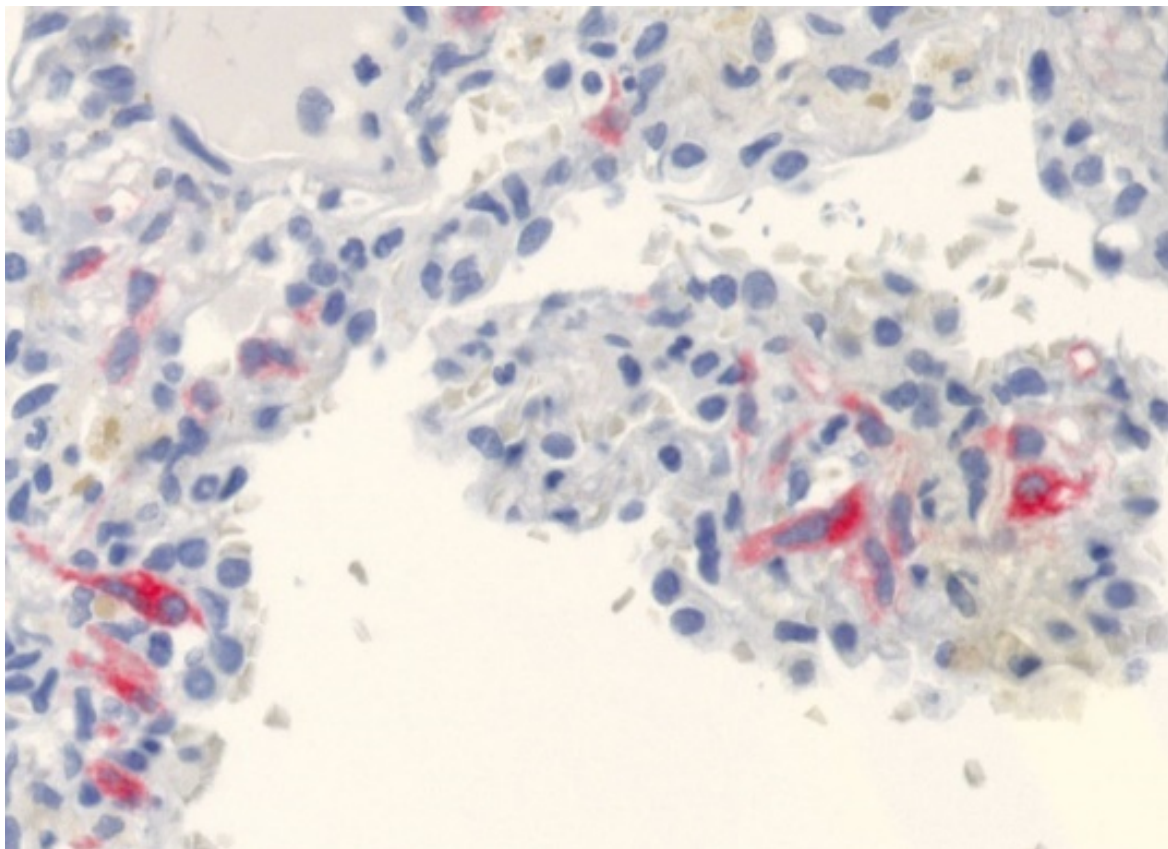


**Figure 3:** HMB-45 immunoreactivity

Rhabdomyomas of the heart, subependymal giant cell astrocytoma of the brain and/or facial angiofibromas. All these lesions are now included within the spectrum of PEComas, mesenchymal tumors composed of cells that exhibit co-expression of myogenic and melanocytic markers, such as HMB-45, Melan A, MITF, smooth muscle actin and, less frequently, desmin.

Various guidelines have been proposed for the diagnosis of LAM. The European Respiratory Society (2011) guidelines classify patients into definite LAM in the presence of characteristic high-resolution chest CT scan (HRCT) findings, a lung biopsy showing LAM and any one of the following: renal angiomyolipoma, thoracic or abdominal chylous effusion, lymphangiomyoma of lymph node, and/or TS. Patients with characteristic HRCT findings and either renal angiomyolipoma or thoracic or abdominal chylous effusion are diagnosed as probable LAM while those with only HRCT findings are classified as possible LAM. The American Thoracic Society and the Japanese Respiratory Society published guidelines in 2016 that use, in addition to the features listed above, the presence of an elevated serum VEGF-D level > 800 pg/ml, and demonstration of clusters of the characteristic cells on cytological examination of effusions or lymph nodes, as additional criteria that can be considered for the diagnosis of definitive LAM.

LAM can be easily overlooked in lung biopsies and diagnosed as emphysema if small clusters or nests of the neoplastic cells are not suspected and confirmed with the presence of immunostains. In more advanced cases, the LAM cells infiltrate into the walls of distal airways and vessels leading to airway obstruction, air trapping, bullae formation with pneumothorax, hemoptysis and hemosiderosis. LAM cells are also associated with lymphatic proliferation and/or obstruction, resulting in chylothorax. In addition to HMB-45, Melan-A, MITF, actin, and/or desmin, LAM cells can exhibit immunoreactivity for estrogen and/or progesterone receptors. The pathologic differential diagnosis includes Langerhans granulomatosis, benign metastasizing leiomyoma, emphysema, diffuse pulmonary lymphangiomatosis and diffuse pulmonary meningotheliomatosis.

Inactivation of TSC1 or TSC2 induces activation of the mammalian target of rapamycin complex (mTOR), resulting in proliferation of LAM cells. The disease can therefore be controlled in some patients with the use of mTOR inhibitors such as rapamycin (sirolimus) or its analog everolimus. Recent studies have also shown good responses to immunotherapy, combining anti-PD1 with anti-CTLA4 antibodies. Patients with progressive

LAM, such as our patients, are treated with lung transplantation, with good long-term results.

## References:

1. Kurosaki T, Otani S, Miyoshi K, Okazaki M, Sugimoto S, Suno M, Yamane M, Kobayashi M, Oto T, Toyooka S. Favorable survival even with high disease-specific complication rates in lymphangioleiomyomatosis after lung transplantation-long-term follow-up of a Japanese center. *Clin Respir J* 2019.
2. Liu HJ, Krymskaya VP, Henske EP. a for Lymphangioleiomyomatosis and Tuberous Sclerosis: Progress and Future Directions. *Chest* 2019.
3. Martignoni G, Pea M, Reghellin D, Gobbo S, Zamboni G, Chilosi M, Bonetti F. Molecular pathology of lymphangioleiomyomatosis and other perivascular epithelioid cell tumors. *Arch Pathol Lab Med* 2010; 134, 33-40.

# Case 49

Kumarasen Cooper

---

## Clinical History

Adult male with lung "tumor". Patient resides in Botswana.

## Pathology

Microscopy: The cyst wall which appears in fragments in your slide comprise a diagnostic eosinophilic laminated wall with parts of the wall demonstrating a germinal layer. Some slides may show a protoscolices which on high power show refractile hooklets. Some slides show lung tissue with secondary granulomatous and chronic inflammation (and calcium).

**Diagnosis: Hydatid cyst of the lung (*Echinococcus granulosus*) (Helminth, cestode).**

## Discussion

The diagnosis is not difficult if you have encountered this characteristic laminated wall (cuticle) before.

This is a parasitic tapeworm with animals acting as the definitive host (commonly dogs and sheep in Southern Africa) with ingestion of contaminated water and food. The swallowed eggs hatch in the small intestine and produce minute hooked embryos that burrow through the bowel and is transported to various organs such as the liver, lung, brain, eyes and bone.

The organisms produce a hydatid unilocular larval cyst (your slide) with an inner germinal layer that produces brood capsules which via an asexual budding process produces new larval tapeworms (protoscolices).

The cysts can achieve a large size from 2-30 cm with a thick wall and contain clear fluid (neutral pH, sodium chloride, proteins, glucose, ions, lipids and polysaccharides). Needless to say, the fluid is antigenic and surgical removal is hazardous since rupture in the OR can result in anaphylactic shock.

## Reference:

1. Kradin R.L. Diagnostic Pathology of Infectious Disease. Elsevier; 2010. Pages 284, 369 and 422.

## Case 50

**Alberto M. Marchevsky, M.D. Cedars-Sinai Medical Center, Los Angeles, CA, USA**

---

### Clinical History:

The patient is a 51-year-old woman, nonsmoker with a past medical history of papillary thyroid carcinoma that was treated with partial thyroidectomy 3 years ago. She developed right hip pain. A chest X-ray was performed during her workup and showed an ill-defined density in the retrocardiac left lower lung zone. Chest CT showed a 3 cm spiculated mass suspicious for malignancy. PET-CT showed that the mass had an SUV of 21.7. She underwent mediastinoscopy and wedge biopsy of the mass. Frozen section showed an invasive adenocarcinoma. She underwent a left lower lobe completion lobectomy under the same anesthesia. Segmental and hilar lymph nodes showed metastatic tumor, so the lesion was staged as pT1b, pN1, pathologic stage IIA. The patient was subsequently treated with 4 cycles of cisplatin + pemetrexed chemotherapy. Post-operative radiation therapy was not recommended. The possibility of treatment with an ALK inhibitor was considered, but no clinical trial was available at the time of diagnosis.

### Pathologic Findings:

The lung shows a typical adenocarcinoma with micropapillary and acinar growth features. The micropapillary component involved approximately 60% of the tumor, so the lesion was classified as invasive adenocarcinoma, micropapillary predominant according to current WHO guidelines. We analyzed the tumor with our current panel for invasive pulmonary adenocarcinomas that includes molecular studies with next generation sequencing (NGS), mutation burden, FISH for EML4-Alk, MET and ROS1 and immunohistochemistry for PD-L1. The tumor showed EML4-Alk fusion in 44.9% of tumor cells examined, low mutation burden (1 mut/Mb) and no clinically significant mutations or gene rearrangements.

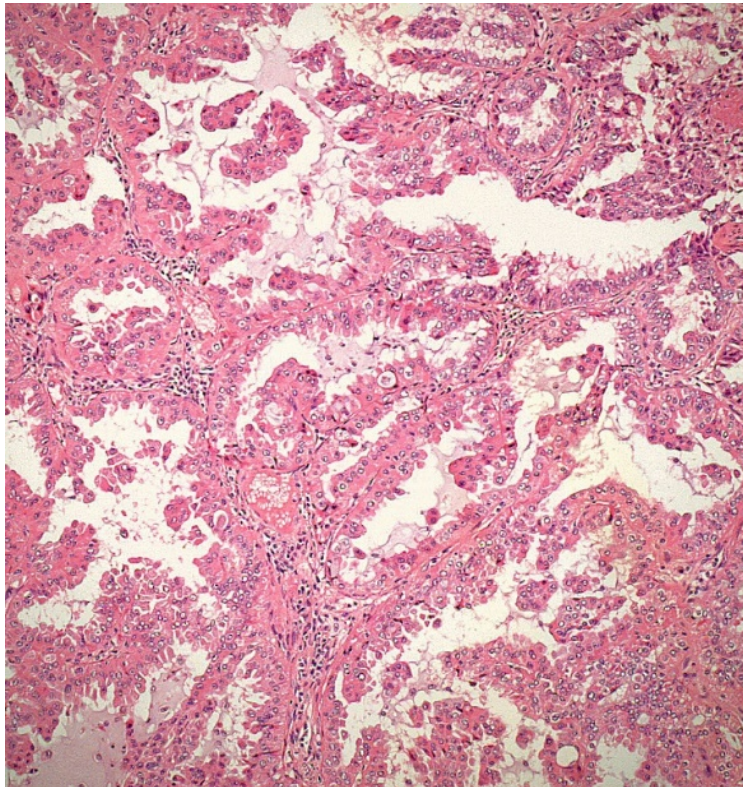


**Figure 1:** Adenocarcinoma, micropapillary predominant

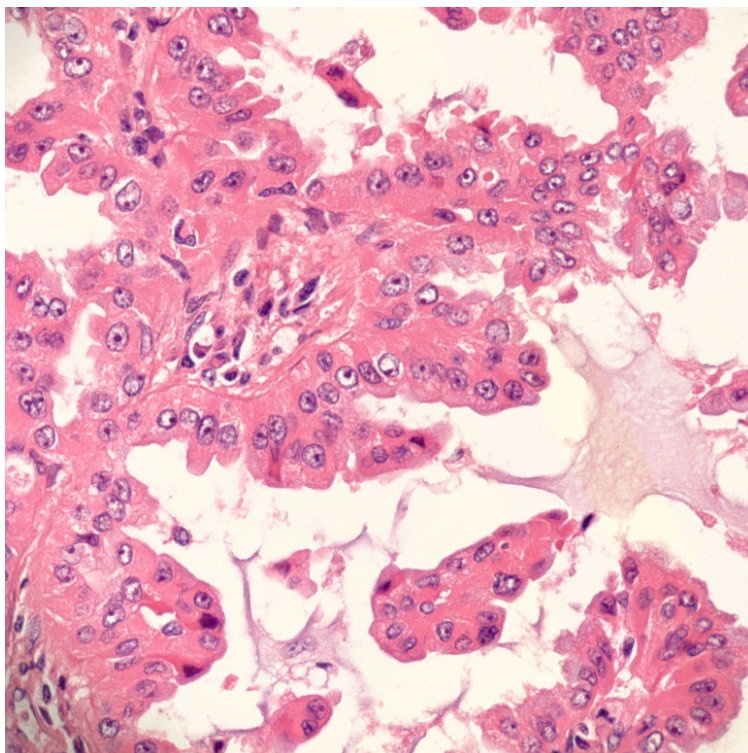


**Figure 2:** Micropapillary features

## Diagnosis: Lung with invasive adenocarcinoma, micropapillary predominant

### Discussion:

The tumor was classified as adenocarcinoma, micropapillary predominant using current methods of comprehensive histologic assessment recommended by WHO (1, 2). However, as it will be discussed, the methodology is prone to interobserver variability and uses cutoffs that are arbitrary and poorly reproducible amongst pathologists. Identification of a micropapillary growth pattern is important, as it has been associated with poor prognosis in multiple retrospective observational studies (1-3). It is unclear whether the tumor must show micropapillary features as the predominant growth feature, or whether any proportion of micropapillary growth pattern is sufficient to estimate that the patient is more likely to have a poor prognosis. There is also no consensus as to whether the presence of micropapillary growth features should be reported at the time of frozen section; some experts have suggested that patients with this type of tumor should be treated with lobectomy rather than sublobar resections.

The current state of the art for the pathologic examination of lung adenocarcinomas includes testing with molecular and other methods that can detect abnormalities that could be used for targeted therapy. The College of American Pathologists in conjunction with the International Association for the Study of Lung Cancer and the Association for Molecular Pathology updated their guidelines in 2018 and recommend testing for EGFR and BRAF mutations, and ROS1 and ALK rearrangements. Molecular testing is generally recommended for advanced lung cancer, although the CAP/IASLC guideline does not indicate which stage is already advanced. In general, there is controversy amongst pathologists and oncologists whether to study all invasive lung adenocarcinomas, a practice that is preferred in our hospital, with molecular testing.

Variable rates of EGFR, KRAS and BRAF mutations have been reported in micropapillary lung adenocarcinomas. In some studies, they have been shown to harbor EGFR mutations more frequently than in other variants of adenocarcinoma but our tumor did not show this change (4). EML4-Alk translocation, as seen in this case, is also variable and has been

reported in up to approximately 10% of micropapillary adenocarcinomas of the lung. The incidence of PD-L1 expression is also quite variable and is frequently associated with KRAS mutations and infrequent in tumors that exhibit EGFR mutations.

## References:

1. Monroig-Bosque PDC, Morales-Rosado JA, Roden AC, Churg A, Barrios R, Cagle P, Ge Y, Allen TC, Smith ML, Larsen BT, Sholl LM, Beasley MB, Borczuk A, Raparia K, Ayala A, Tazelaar HD, Miller R, Kalhor N, Moran CA, Ro JY. Micropapillary adenocarcinoma of lung: Morphological criteria and diagnostic reproducibility among pulmonary pathologists. *Ann Diagn Pathol* 2019; 41, 43-50.
2. Wright J, Churg A, Kitaichi M, Yang HM, Hyde D, Yi E. Reproducibility of visual estimation of lung adenocarcinoma subtype proportions. *Mod Pathol* 2019; 32, 1587-1592.
3. Pyo JS, Kim JH. Clinicopathological Significance of Micropapillary Pattern in Lung Adenocarcinoma. *Pathol Oncol Res* 2018; 24, 547-555.
4. Cai YR, Dong YJ, Wu HB, Liu ZC, Zhou LJ, Su D, Chen XJ, Zhang L, Zhao YL. Micropapillary: A component more likely to harbour heterogeneous EGFR mutations in lung adenocarcinomas. *Sci Rep* 2016; 6, 23755.

# Case 51

Cesar A. Moran, MD, M D Anderson Cancer Center

---

## Clinical History

63-year-old man presents with shortness of breath, loss weight, chest pain, cough, and general malaise. Diagnosis imaging revealed the presence of thickening and nodularity of the right pleura.

## Diagnosis: Malignant Mesothelioma, Sarcomatoid Type

## Discussion

In general terms, mesotheliomas are uncommon neoplasm that may be seen in approximately 1 in 100 thousand individuals. The association with asbestos exposure is important and the latency period varies from 20 to 40 years. The tumor is more common in adults although series of mesotheliomas in children have been presented in the literature. Although adequate tissue sample is important for diagnosis, also important for proper interpretation is the diagnostic imaging, as the great majority of mesothelioma will show diffuse pleural thickening. Only a small percentage of cases will present with a pleural-based tumor.

Histologically, the tumor has been separated into epithelioid, sarcomatoid and mixed. However, it is worth mentioning that a wide array of growth patterns have been described in those categories. In today's practice the use of histochemical stains such as PAS, D-PAS, and mucicarmine are rarely performed and have been substituted for the use of immunohistochemical stains. In that regard, over the years a wide number of immunohistochemical stains have been employed in the separation of epithelioid mesothelioma and adenocarcinoma. However, currently the use of "positive" mesothelioma markers such as calretinin and keratin 5/6 has made a change in the immunohistochemical approach. Currently, the use of calretinin, keratin 5/6, and D2-40 are common stains in the arsenal to evaluate mesotheliomas. Although those stains are highly important in the assessment of mesothelioma, when the histology is that of Sarcomatoid mesothelioma, the positive staining of those markers is variable. Other stain

that has also been reported positive with variable results in sarcomatoid mesothelioma is GATA3. However, often, the only positive stain in sarcomatoid mesothelioma is a Pan Keratin, which although important is not conclusive. The use of carcinomatous epitopes such as TTF-1, CD15, CEA, B72.3, etc is indicated in the evaluation of possible mesotheliomas.

More recently the use of BAP1 and p16 FISH have been used with some success in the evaluation of difficult cases of mesothelioma. However, we have also noticed that the use of p16 is more reliable in terms of identifying the homozygous deletion; however, if the tumor does not show the homozygous deletion, it does not rule out the diagnosis, as there is a variable percentage of these tumors that may not show the homozygous deletion. Highly important to mention is the fact that different laboratories use different cut offs for the interpretation of positive homozygous deletion (2%, 5%, 10%, >10%). Therefore, it is important to check with your laboratory what their cut off is for such interpretation. On the other hand, the use of BAP1 as a sole aid in the interpretation of mesothelioma may prove risky, as we have seen numerous cases of BAP1 retained in overtly invasive mesotheliomas, while we have seen loss of BAP1 in completely benign pleuritis.

## Differential Diagnosis

The first and most important step is the separation from atypical mesothelial hyperplasia. In that regard, the use of landmarks such as skeletal muscle and adipose tissue will be of aid, as an important feature of mesotheliomas is the infiltration of those areas. Once that is established, and then it will depend on the type to formulate a differential diagnosis. In epithelioid mesotheliomas, the most important differential diagnosis is with Adenocarcinoma, while in the case of sarcomatoid mesothelioma will be with a benign fibrous pleurisy and with other type of true mesenchymal neoplasm.

## Clinical Follow-up

In the past, the use of extra-pleural pneumonectomy was a surgical option for patients with mesothelioma. However, it is not as common today. Currently, neo-adjuvant chemotherapy followed by decortication may be an alternative. The survival of these patients has improved over the years.

## Selected References

1. Cagle, P.T. and A. Churg, Differential diagnosis of benign and malignant mesothelial proliferations on pleural biopsies. *Arch Pathol Lab Med*, 2005. 129(11): p. 1421-7.
2. Arrossi, A.V., et al., Histologic assessment and prognostic factors of malignant pleural mesothelioma treated with extrapleural pneumonectomy. *Am J Clin Pathol*, 2008. 130(5): p. 754-64.
3. Moran, C.A., M.R. Wick, and S. Suster, The role of immunohistochemistry in the diagnosis of malignant mesothelioma. *Semin Diagn Pathol*, 2000. 17(3): p. 178-83.
4. Mann, S., et al., Revisiting localized malignant mesothelioma. *Ann Diagn Pathol*, 2019. 39: p. 74-77.
5. Zaleski M, Kalhor N, Fujimoto J, Wistuba I, Moran CA. Sarcomatoid mesothelioma: a CDKN2A molecular analysis of 53 cases with immunohistochemical correlation with BAP1. *Pathology - Research and Practice* 2020; 216(12): PMID 33176261
6. Oramas DM, Zaleski M, Moran CA. Sarcomatoid Mesothelioma: A clinicopathological and immunohistochemical study of 64 cases. *Int J Surg Pathol* 2021; 29:820-825.

## Case 52

**P. E. Wakely, Jr., M.D., Department of Pathology, The Ohio State University, Wexner Medical Center, James Cancer Hospital, Columbus, OH. USA**

---

### History:

A 58-year old woman presented with abdominal discomfort, bloating, and history of a 70 pound weight loss over the past year. A severe episode of abdominal pain led her to the emergency room at an outside community hospital. CT scan showed a 20 cm. pelvic mass thought to be ovarian extending into abdomen, a 3.5 cm right hepatic lobe/diaphragm mass, moderate ascites, normal pancreas, and normal chest. The diaphragmatic mass was thought to represent a serosal implant. Serum levels for CA125 were 293.9, CEA 109 (normal <5), HE4 79 (normal <140), and CA19-9 14.7 (normal). After transfer to Wexner Medical Center, bilateral salpingo-oophorectomy, appendectomy, and resection of the diaphragmatic mass were performed. The patient is alive with no evidence of disease four years later.

### Pathology:

The left ovary was a distorted 1,898 grams and 18.5 cm structure containing a pink-tan mass with innumerable locules containing viscous, gelatinous material. Pathologic diagnosis of the ovarian mass was mucinous cystadenoma. The separate diaphragmatic mass consisted of an 18.7 gram, 6.0 cm. aggregate of gray-pink, solid, soft and rubbery tissue. Microscopic examination showed a highly cellular solid neoplasm composed of innumerable rosettes. Rosettes contained coarse fibrillar material surrounded by uniform nuclei. Both perivascular pseudorosettes and true ependymal rosettes were seen. The former consisted of cells circumferentially arranged around blood vessels with zones of fibrillar eosinophilic stroma, while the latter had columnar cells radially placed around a central lumen. Cell nuclei were rounded, oval, and elongated with coarse, granular chromatin, and occasional small nucleoli. Mitoses were rare. No teratomatous elements were found. Immunoprofile: positive stains with bcl-2, GFAP, and scattered staining for MNF116, CAM5.2, CK AE1/AE3, chromogranin, and EMA. Negative stains: inhibin,

HMB45, SOX10, TLE-1, CD10, synaptophysin, Olig2, CD34, CD117, STAT-6, smooth muscle actin and S-100. Conventional cytogenetic analysis showed normal chromosomes.

## **Diagnosis: PRIMARY PERITONEAL EPENDYMOMA.**

### **Discussion:**

Extra-axial ependymomas (EAE) are rare. A germ cell origin, displaced ependymal rests, and monodermal teratomatous proliferation are proposed theories for their origin. Reported anatomic sites include the ovary, broad ligament, sacrococcygeal region, lung and mediastinum. For unknown reason(s) these neoplasms occur primarily in women regardless of location, and most frequent in the 2nd to 4th decade of life.

Most cases occur in the ovary, para-ovarian tissues, and pelvis with thoracic cases arising almost exclusively in the posterior mediastinum. Most EAEs behave in an indolent manner, but regional nodal and distant metastases have been described. Most reports describe tumors with solid, trabecular, cystic, or papillary architecture. Both true ependymal rosettes and perivascular pseudorosettes are present. Their immunophenotype largely mimics their CNS counterparts being positive for GFAP, WT1, and cytokeratin AE1/AE3. However, Idowu et al. found an immunophenotypic difference between CNS and EAE cases with the latter preferentially expressing 34bE12, CK18, CAM 5.2, CK7, ER, and PR, but CNS cases found to more frequently express CD99.

### **References:**

1. Verdun TP, Owen DA. Primary peritoneal ependymoma. *Pathol Res Pract.* 2015; 211:268-70.
2. Kleinman GM, Young RH, Scully RE. Ependymoma of the ovary: report of three cases. *Hum Pathol* 1984; 15:632-638.
3. Whittemore DE, Grondahl RE, Wong K. Primary extraneural myxopapillary ependymoma of the broad ligament. *Arch. Pathol. Lab Med* 2005;129:1338-1342.
4. Wilson RW, Moran CA. Primary ependymoma of the mediastinum: a clinicopathologic study of three cases, *Ann Diagn Pathol* 1998; 2: 293-300.
5. Idowu MO, Rosenblum MK, Wei XJ et al. Ependymomas of the central nervous system and extra-axial ependymomas are morphologically and immunohistochemically

distinct - a comparative study with assessment of ovarian carcinomas for expression of glial fibrillary acidic protein. *Am J Surg Pathol* 2008; 32: 710-718.

6. Bell DA, Woodruff JM, Scully RE. Ependymoma of the broad ligament. A report of two cases. *Am J Surg Pathol* 1984;8:203-9.
7. Ye WB, Zhou JP, Xu YQ, et al. Primary mediastinal ependymoma: A case report and literature review. *Medicine (Baltimore)*. 2019; 98:e17686.

## Case 53

Cesar A. Moran, MD, M D Anderson Cancer Center

---

### Clinical history

63-year-old woman is found during a routine chest film to have a mass in the right upper lobe. The mass appears to be peripheral and subpleural. The patient does not have any history of malignancy anywhere else. Right upper lobectomy is performed showing a 2.5 cm intrapulmonary mass.

**Diagnosis: Mucin-rich, so-called Colloid Carcinoma of the lung.**

### Discussion

Primary non-small cell carcinomas of the lung are the most common malignant tumors worldwide in both genders. Although the most common histologies are adenocarcinoma (conventional histology) and squamous cell carcinomas, the existence of mucin-rich adenocarcinomas of the lung has been known for sometime.

Although initially, there was some controversy about "Colloid-Carcinoma," it has now been fully determined that it does represent an unusual form of adenocarcinoma.

Therefore, designations such as borderline mucinous tumor, mucinous tumor, mucinous cystadenomas, should not be used as they likely represent the same entity. The tumor characteristically shows extensive mucin production with only focal areas in which one can observe the presence of mucinous epithelium lining the alveolar wall. In some cases, the extensive areas of mucin may show the presence of malignant cell floating in the sea of mucin. The use of mucicarmine stain may help in easily identifying the mucinous alveolar lining in cases in which it may be rather subtle.

The use of immunohistochemical stains may often show variable staining and to some extent somewhat non-specific. For instance, colloid carcinoma may show positive staining for CDX-2 and negative staining for TTF-1. However, keratin 7 appears to be consistently positive in these tumors while keratin 20 is generally negative.

## Differential Diagnosis

Because of the mucinous rich qualities of this tumor, any tumor of extra-pulmonary origin rich in mucin should be considered in the differential diagnosis. We have observed metastasis from colorectal, breast, and bladder mucinous carcinomas to the lung that on histology can easily be interpreted as primary colloid carcinoma of the lung. Therefore, clinical information is crucial with the appropriate immunohistochemical stains.

## Clinical Follow-up

The treatment of choice for any non-small cell carcinoma that is T1 (<3 cm) N0 and M0 is surgery alone. For these tumors the follow up reported has been generally good. However, for tumors that are T2 or more, the use of additional medical treatment may be necessary.

## Selected References

1. Moran CA, Hochholzer L, Fishback N, Travis WD, Koss MN: Mucinous (so-called colloid) carcinoma of the lung. *Mod Pathol* 1992; 5:634-638.
2. Moran CA: Mucin-rich tumors of the lung. *Advances in Anatomic Pathology* 1995; 2:299-305.
3. Zenali M, Weissferdt A, Solis LM, Tang X, Mehran R, Wistuba I, Moran CA, Kalhor N. Update on Clinicopathological, immunohistochemical and molecular profile of colloid carcinoma of the lung. *Hum Pathol* 2015; 46(6):836-842.

## Case 54

**Alberto M. Marchevsky, M.D. Cedars-Sinai Medical Center, Los Angeles, CA, USA**

---

### Clinical History:

The patient is a 83-year old man, with a cigarette smoking history of 100 pack-year. He quit smoking 8 years ago but developed chronic cough, dyspnea and other findings consistent with chronic obstructive lung disease (COPD). Other past medical history included hypertension, coronary artery disease with a myocardial infarct treated with coronary bypass surgery (CABG) and a cerebrovascular accident. He presented with cough and weakness. Chest X ray showed emphysema and multiple small lung nodules. Chest CT showed multiple bronchiectasis and multiple micronodular and nodular densities, changes suspicious for mycobacteria avium complex infection (MAC) and an ill-defined right lung base density suspicious for pneumonia. He underwent bronchoscopy and transbronchial biopsy that showed high grade dysplasia of the bronchial epithelium. A CT-guided needle core biopsy of one of the larger right upper lobe nodules was performed.

### Pathologic Findings:

The needle biopsy showed a poorly differentiated non-small cell carcinoma (fig 1). The tumor cells exhibited nuclear immunoreactivity for p40 (fig 2) and cytoplasmic immunoreactivity for desmoglein-3. Immunostains for TTF-1 and Napsin A were negative. The lesion was classified as nonkeratinizing squamous cell carcinoma on the basis of the immunophenotype. Next generation sequencing (NGS) of the lesion showed no actionable mutations. FISH tests for EML4-Alk, ROS1 and MET were negative. Immunostains for PD-L1 (FDA approved test using 22C3 antibody) showed strong membrane immunoreactivity in >95% tumor cells (fig 3).

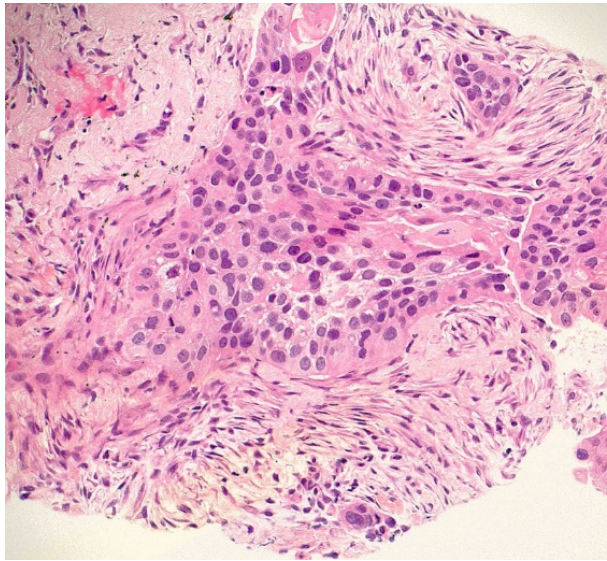


**Figure 1:** Non-keratinizing squamous cell carcinoma

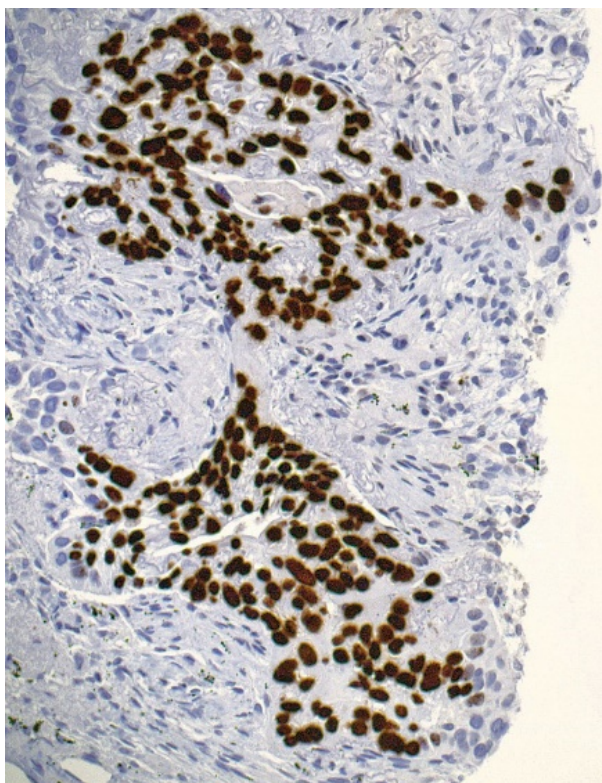


**Figure 2:** p40 nuclear immunoreactivity

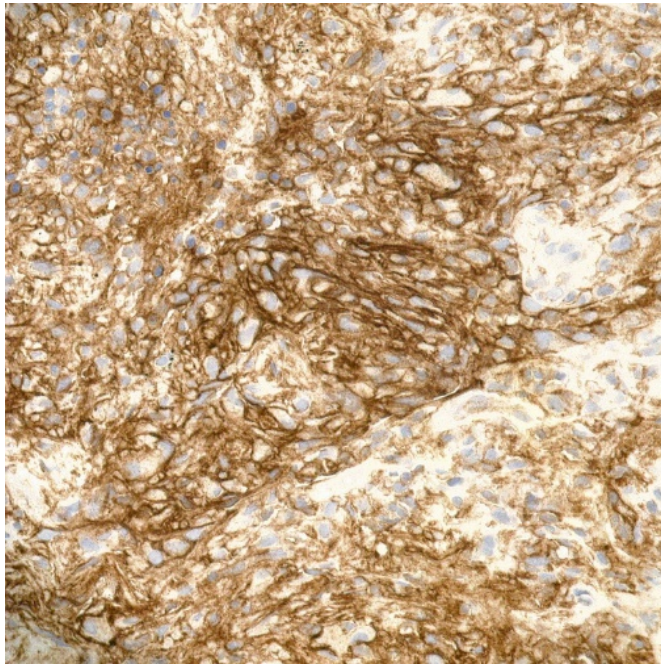


**Figure 3:** High expression of PD-L1

## Diagnosis: Squamous cell carcinoma of the lung

### Discussion:

No glass slides of this case are being provided as the lesion is very common and raises no diagnostic problems. The case will be used to discuss current concepts about PD-L1 testing in patients with non-small cell carcinomas of the lung (1-5).

The immune system is regulated through a number of receptor-ligand interactions designed to protect the host from exogenous antigens and prevent autoimmune reactions (2). One of the most important systems to prevent autoimmune reactions is the interaction of PD-1 expressed on cytotoxic T lymphocytes and PD-L1 on antigen presenting cells. Once this checkpoint system is activated, cells expressing PD-L1 become "invisible" to the immune system. Cancer cells can also express PD-L1 on their cell surface, activating the PD-1/PD-L1 cascade and allowing for tumor progression without interference from the immune system. Various checkpoint inhibitor drugs such as Pembrolizumab, Nivolumab and others have been developed to inhibit the PD1-PD-L1 cascade. Several clinical trials have shown that these drugs are as effective or more effective than chemotherapy for the treatment of non-small cell carcinomas of the lung and other neoplasms. Tumors that express membranous immunoreactivity for the 22C3 antibody using the Dako testing platform on 50% or greater number of neoplastic cells,

such as our patient, are classified as high-expressors and are eligible for Pembrolizumab therapy (Fig 4). The table shown in the next page summarizes some details about the PD-L1 assays being used for non-small cell lung cancer testing (2).

Summary of PD-L1 assays approved for non-small cell lung cancer testing

Performance	Clone	PD-L1 assay			
		22C3	28-8	SP263	SP142
Developer	Dako	Dako	Dako	Ventana	Ventana
Host species	Mouse monoclonal	Rabbit monoclonal	Rabbit monoclonal	Rabbit monoclonal	Rabbit monoclonal
Epitope location	Extracellular domain	Extracellular domain	Cytoplasmic domain	Cytoplasmic domain	Cytoplasmic domain
Platform	Link 48 autostainer	Link 48 autostainer	Benchmark ultra	Benchmark ultra	Benchmark ultra
Detection kit	Envision FLEX	Envision FLEX	Optiview	Optiview	Optiview
Amplification	No	No	No	No	Yes
Interpretation	Scoring	TC	TC	TC	TC and IC
Staining pattern for positivity	Membranous	Membranous	Membranous ± cytoplasmic	Membranous ± cytoplasmic	Membranous=cytoplasmic
Minimum TC number	100	100	100	100	50 with associated stroma
Cut-off (mandatory)	≥ 50% (≥ 2nd line), ≥ 1% (1st line)	All comer	All comer	All comer	All comer
Cut-off (proven survival benefit)		≥ 1%, ≥ 5%, ≥ 10%	≥ 25% (for durvalumab) <sup>a</sup> , ≥ 10% (for nivolumab) <sup>b</sup>	TC ≥ 5% or IC ≥ 5%	TC ≥ 5% or IC ≥ 5%
Pharma	Immune checkpoint inhibitor	Pembrolizumab	Nivolumab	Durvalumab Nivolumab <sup>b</sup>	Atezolizumab
FDA approval	Companion	Complementary	Complementary	Complementary	Complementary

PD-L1, programmed death-ligand 1; TC, tumor cell; IC, immune cell; FDA, Food and Drug Administration.

<sup>a</sup>Applied only in Korea;

<sup>b</sup>Approved by Conformite Europeenne (CE) and Korea Food and Drug Administration.

## References:

1. Chang S, Park HK, Choi YL, Jang SJ. Interobserver Reproducibility of PD-L1 Biomarker in Non-small Cell Lung Cancer: A Multi-Institutional Study by 27 Pathologists. *J Pathol Transl Med* 2019; 53, 347-353.
2. Kim H, Chung JH. PD-L1 Testing in Non-small Cell Lung Cancer: Past, Present, and Future. *J Pathol Transl Med* 2019; 53, 199-206.
3. Liu HJ, Krymskaya VP, Henske EP. Immunotherapy for Lymphangioleiomyomatosis and Tuberous Sclerosis: Progress and Future Directions. *Chest* 2019.
4. Mok TSK, Wu YL, Kudaba I, Kowalski DM, Cho BC, Turna HZ, Castro G, Jr., Srimuninnimit V, Laktionov KK, Bondarenko I, Kubota K, Lubiniecki GM, Zhang J, Kush D, Lopes G, Investigators K-. Pembrolizumab versus chemotherapy for previously untreated, PD-L1-expressing, locally advanced or metastatic non-small-cell lung cancer (KEYNOTE-042): a randomised, open-label, controlled, phase 3 trial. *Lancet* 2019; 393, 1819-1830.
5. Williams GH, Nicholson AG, Snead DRJ, Thunnissen E, Lantuejoul S, Cane P, Kerr KM, Loddo M, Scott MLJ, Scorer PW, Barker C. Inter-observer Reliability of Programmed Cell Death Ligand-1 Scoring Using the VENTANA PD-L1 (SP263) Assay in Non-Small Cell Lung Cancer. *J Thorac Oncol* 2019.

## Case 55

### Ira J Bleiweiss, MD - Silicone Migration to Lung

---

#### Brief clinical history:

A 73 year old female presented with an incidental 1.4 cm spiculated lung nodule found during a work-up for long-standing back pain. She also complained of a new non-productive cough for two months.

Short summary of case:

A 73 year old female presented with an incidental 1.4 cm spiculated lung nodule found during work-up for long-standing back pain. She also complained of a new non-productive cough for two months.

Past medical history included: Allergic rhinitis, anemia, arthritis, fibromyalgia, gastroesophageal reflux disease (GERD), hypothyroidism, irritable bowel syndrome (IBS), lumbar pain, and morbid obesity.

Past surgical history included: bilateral carpal tunnel release (1991), cholecystectomy (remote),

multiple back surgeries (2007-2017), bilateral total hip replacement (2016), breast augmentation s/p 5x replacements (1970s - present) with silicone implants, gastric bypass surgery (2002), left knee replacement (2005).

Social History: dental hygienist, retired, no known asbestos or TB exposure, significant mold exposure (2010), former 8 pack-year smoker, no illicit drug use.

Two years previously she presented to a plastic surgeon for evaluation of bilateral axillary lymphadenopathy. As noted above she had had bilateral breast augmentation with silicone implants in the 1970's which initially ruptured and subsequently required 4 replacements with the last replacement performed in 1980's. Bilateral MRI (4 years previous) demonstrated multiple bilateral axillary lymph nodes, with the largest in the left axilla measuring 5 cm. The lymph node was surgically excised in 2012 and showed reactive changes with foreign body reaction to refractile foreign material (silicone adenopathy). Bilateral axillary adenopathy persisted, and bilateral excision in 2017 again

showed silicone adenopathy. As noted above a CT performed for spinal stenosis revealed a lung lesion which was later evaluated by dedicated CT. She was largely asymptomatic except for a new non-productive cough of 2 months duration. Chest CT showed a 1.4 cm somewhat spiculated nodule with irregular borders in the left lower lobe. Multiple scattered ground glass and solid pulmonary nodules were seen bilaterally measuring up to 0.4 cm. Additional scattered calcified granulomas were also noted. PET/CT revealed that the 1.4 cm spiculated nodule had minimal FDG avidity. The findings were concerning for an indolent malignancy, and a wedge resection of lung was performed along with sampling of mediastinal lymph nodes. Both the lymph nodes and the lung wedge resection show numerous foreign body giant cells, many of which contain refractile, non-polarizable material, consistent with silicone. The foreign body reaction is extensive in the pulmonary parenchyma with a lymphovascular distribution as well as being peribronchial and perivascular and forming larger nodules with alveolar involvement.

### **Diagnosis: Chronic Pulmonary Silicone Embolism Syndrome (Silicone migration to lung) with mediastinal and axillary silicone adenopathy, secondary to breast implants**

#### **Discussion:**

Silicone gel-containing breast implants have been in use for many years now, both in the setting of elective breast augmentation and in reconstruction after mastectomy (malignancy or prophylaxis). What is silicone and why is it used? Silicone (polydimethylsiloxane) PDMS is the most commonly used silicon-based polymer (aka silicones). It is inert, optically clear, non-toxic, non-flammable and was originally thought to be well-tolerated by tissues with little local and no systemic inflammatory response. When silicone was first used it was believed to be inert and biostable. Silicones were reported to be resistant to extreme temperatures, acid, and alkali. Silicones did not appear to deteriorate with time and did not stick to tissues. It was reported to have most of the chemical and physical qualities defined for an ideal synthetic soft tissue: not physically modified by soft tissue; chemically inert; not inducing inflammation or foreign body reaction; noncarcinogenic; not provoking allergy or hypersensitivity; capable of resisting mechanical strains; capable of fabrication in the form desired; and capable of sterilization. However, with time and experience evidence documented that silicone does not fulfill many of these characteristics.

The story of silicone and breast augmentation (1) is not limited to implants, however, and begins with the now illicit practice of direct silicone injection. This began in Japan after World War II and was quickly introduced in the US, initially in California, Nevada, and Texas. Reports of complications quickly emerged, including granulomatous hepatitis, local skin changes, silicone migration, and fatal ARDS. Chastre et al (2) reported a series of 13 transsexual male to female patients: All had latent or acute pneumonitis, and bronchio-alveolar lavage fluids all demonstrated presence of silicone in alveolar macrophages.

Silicone was not alone. In 1895 Vincent Czerny, a physician in Heidelberg, Germany attempted to remedy a lumpectomy defect by implanting a lipoma from her flank. Over the next four decades, other materials were utilized include glass balls, ivory balls, ground rubber, ox cartilage, wool, rubber, and polyethylene chips.

In 1962 Thomas Cronin, a Texas surgeon, postulated that a transfusion bag felt remarkably like a breast, and he solicited the help of Dow Chemical company (at that time, a large silicone manufacturer with hundreds of biomedical products) in order to create a silicone sac. They eventually created the first silicone implant which was experimentally implanted into dogs with apparent success.

In the 1970's there were reports of high failure rates, silicone leakage, contractures, the later potential association with autoimmune disorders, and increased cancer risk. In 1992 the FDA banned silicone breast implants, but the ban was rescinded in 2006 due to major studies showing the lack of a direct connection to systemic disease, at the same time requiring manufacturers to closely monitor implanted patients for 10 years with documentation.

In 2011 the FDA recognized ~60 cases of Breast implant associated anaplastic large cell lymphoma (BIA-ALCL) worldwide and in 2019 rising concerns for BIA-ALCL (457 US cases as of Sept 30, 2018), silicone implant incompatibility syndrome (SIIS), autoimmune syndrome induced by adjuvants such as vaccines, silicone, infection, etc. (ASIA) resulted in an FDA hearing. No products were banned as a result; however, better future research, reporting systems, and patient pamphlets were recommended.

Leakage from intact silicone gel implants is extremely common (3). The material is identifiable in capsules (often removed for contracture) as refractile non-polarizable material in histiocytes and/or foreign body giant cells. Migration can cause adenopathy usually in the axilla which has a fairly distinctive microscopic appearance. As might be expected, these findings are particularly extensive when associated with implant rupture. A chronic pulmonary silicone embolism syndrome has been described (4-6). Gopinath et al (6) first reported silicone breast implant leakage in a 41 year old woman which resulted

in chronic progressive dyspnea. Chest imaging showed widespread ground glass opacity involving all lobes with subpleural (aka peripheral) distribution. Singh, et al (7) indirectly assessed whether such patients had pulmonary disease serious enough to require lung transplant but found no association by retrospectively reviewing 1518 lung transplant patients, 578 of which were female. Only 10 of these patients had a history of breast augmentation, and none had histologic evidence of silicone embolism in their explanted lungs after a median of 29.5 years duration between breast augmentation and lung transplant. Thus, this may be an under-recognized condition, being relatively asymptomatic.

Life-threatening systemic complications as a result of silicone have also been described (8-11). Schmid (8) described cases of acute silicone embolism syndrome between 1965 and 2004. Lyapichev, et al (9) updated the search from 2004 to 2015 with data on 64 total patients: 28 female, 5 male (body-builders), and 31 male to female transgender individuals. The symptomatology included hypoxemia (92%), dyspnea (88%), fever (70%), alveolar hemorrhage (64%), cough (52%), and neurologic symptoms (33%). All of the cases followed, by days or even months, direct injections of silicone in breasts, buttocks, or arms. Direct injections of silicone gel are generally illegal, but a black market exists and the practice persists with occasionally fatal results (11). Other injectable materials also exist, for example polyacrylamide gel (12).

## Selected References:

1. Champaneria MC, Wong WW, Hill ME, et al. The evolution of breast reconstruction: a historical perspective. *World J Surg.* 2012;36:730-42.
2. Chastre J, Brun P, Soler P, et al. Acute and latent pneumonitis after subcutaneous injections of silicone in transsexual men. *Am Rev Respir Dis.* 1987;135:236-40.
3. Kappel RM, Boer LL, Dijkman H. Gel bleed and rupture of silicone breast implants investigated by light, electron microscopy, and energy disperse X-ray analysis of internal organs and nervous tissue. *Clinical Medical Reviews and Case Reports.* 2016;3(1).
4. Arora A, Inaty H, Mukhopadhyay S, et al. Chronic Pulmonary Silicone Embolism Related to Saline Breast Implants. *Annals ATS.* 2016;13:139-140.
5. Bois MC, Hu X, Roden AC, et al. Increasing pulmonary infiltrates in a 72-year-old woman with metastatic breast cancer. *Chest.* 2014;146:208-211.
6. Gopinath PP, Ali A, Tornout FV, et al. Chronic silicone embolism syndrome due to PIP breast implant leakage - a new entity?. *Histopathology.* 2015;66:904-905.
7. Singh J, Inaty H, Muhopadhyay S, et al. *Hindawi: Pulmonary Medicine.* 2018:1-5.

8. Schmid A, Tzur A, Leshko L et al. Silicone Embolism Syndrome: A Case Report, A Review of the Literature, and Comparison with Fat Embolism Syndrome. *Chest*. 2005;127:2276-2281.
9. Lyapichev K, China FM, Poveda J, et al. Pulmonary Empty Spaces: Silicone Embolism - A Decade of Increased Incidence and Its Histological Diagnosis. *Case Reports in Pathology*. 2016:1-5.
10. Chung KY, Kim SH, Kwon IL, et al. Clinicopathologic Review of Pulmonary Silicone Embolism with Special Emphasis on the Resultant Histologic Diversity in the Lung - A Review of Five Cases. *Yonsei Medical Journal*. 2002;43:152-159.
11. Price EA, Schueler H, Perper JA. Massive Systemic Silicone Embolism: A Case Report and Review of Literature. *Am J Forensic Med Pathol*. 2006;27:97-102.
12. Unukovych U, Khrapach V, Wickman M, et al. Polyacrylamide gel injections for breast augmentation: management of complications in 106 patients, a multicenter study. *World J Surg* 2012;36:695-701.

# Case 56

Fredrik Petersson

---

## Clinical History and Gross Features:

A 79-year-old man with hypertension and hyperlipidemia had noticed a painless, enlarging mass over the right parotid region for the past 2 weeks. On clinical examination, a 2.5 cm soft, well-delineated mass in the parotid region was noted. A FNA biopsy was performed followed by a CT-scan which showed a heterogeneously enhancing, fairly well circumscribed mass in the superficial lobe of the right parotid gland measuring 2.5 cm. A superficial parotidectomy was performed. Grossly, the tumor appeared as a well-circumscribed, yellowish, soft mass measuring 2.0 cm in maximum dimension.

## Cyto- and Histopathology:

FNA-smears contained cohesive and individual cells with ovoid to elongated nuclei with no atypia intimately admixed with eosinophilic myxoid stroma. In addition, numerous atypical cells with enlarged, pleomorphic nuclei, and also frequent multinucleated atypical cells were identified. The combination of the three above mentioned features raised an initial suspicion of a malignant tumor (carcinoma or carcinosarcoma) ex PA. However, on close review of the FNA specimen, no mitotic figures or necrosis was identified. Very focally, vague fat-like vacuoles were seen intermingling with the spindle cells in the stromal component. Moreover, the morphological features of the myxoid stromal component lacked the characteristic fibrillary appearance with frayed edges that typify the stromal component in a PA.

Histopathological examination of the resected specimen revealed lobules of mature adipose tissue and spindle cells with several atypical mononuclear cells with large, irregular, hyperchromatic nuclei and also multinucleated floret cells. Several lipoblasts were identified. No atypical mitotic figures, necrosis or areas of prominent vascularity were noted. In addition to a collagenous stroma with focal "ropey" structure, the stroma displayed a variable, but frequently prominent myxoid component with a distinct paucity of adipocytes. Neoplastic cells did not infiltrate the surrounding salivary gland parenchyma, but in areas where the tumor was bordered by striated muscle, neoplastic

cells were seen infiltrating deep into the muscle with tumor cells surrounding isolated striated muscle cells.

## Immunohistochemistry and molecular genetics:

Immunohistochemistry on the cell block showed that the ovoid/spindled cells as well as the large atypical cells strongly and diffusely expressed CD34 while SMA, S100-protein and cytokeratins (AE1/3 and CAM5.2) were negative. The Ki-67 proliferation index was low (< 2%). Selected blocks from the resected specimen were immunostained with anti CD34 which revealed strong and diffuse expression. IHC for Rb-protein was done which showed no expression in the lesional cells (with good internal control). FISH for mdm2 revealed no amplification.

## Diagnosis: Primary salivary gland pleomorphic lipoma with myxoid change

### Comments:

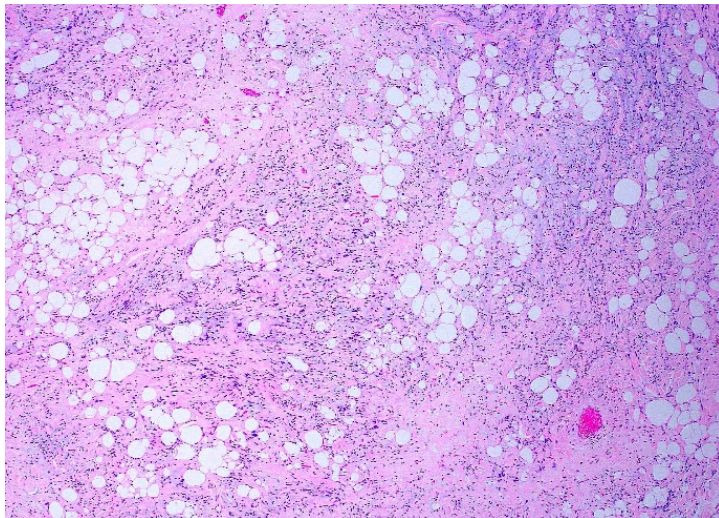
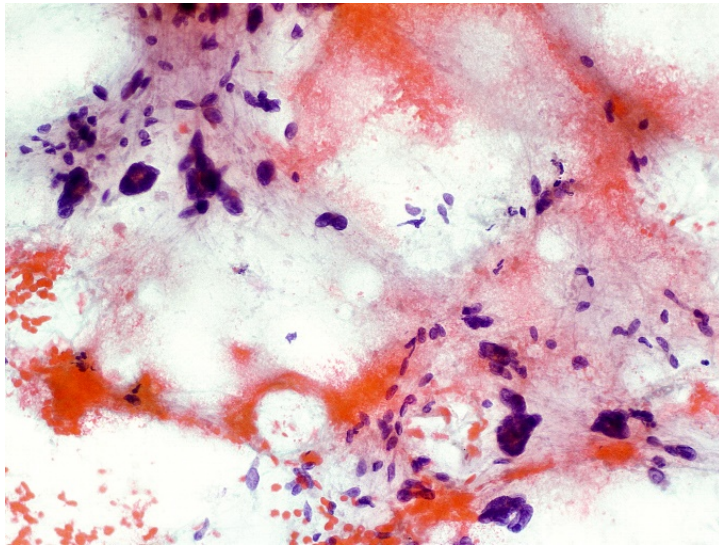
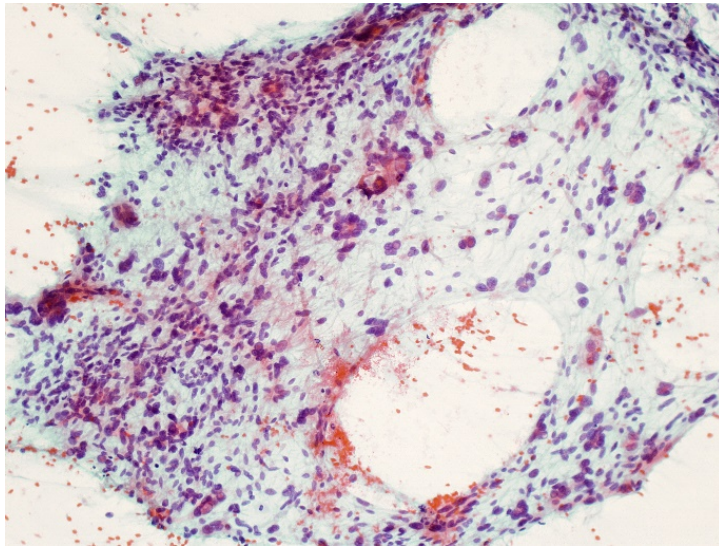
Bona-fide lipogenic tumors can, albeit extremely rarely, arise in the salivary glands and are indistinguishable from their soft tissue counterparts. These include lipoma and its variants as well as atypical lipomatous tumor/well differentiated liposarcoma (1). Pleomorphic lipoma (PL) is a benign adipocytic neoplasm, first described by Shmookler and Enzinger in 1981 and is closely related to spindle cell lipoma (SPCL). Most investigators perceive PL and SPCL to represent two ends of a morphological spectrum and it is not uncommon to see both features of PL and SPCL within one and the same tumor (2). This similarity is further supported by the genetic finding of loss of retinoblastoma (Rb) expression secondary to chromosome 13q deletion, in both tumors, which thus reinforces their close pathobiologic relationship. On a similar note, cellular angiofibromas, most mammary-type myofibroblastomas also belong to this group of tumors with 13q deletion. In addition to the presence of spindle cells, PL is typified by floret-like giant cells. Moreover, both PL and SPCL frequently display areas of myxoid change which may on occasion be so prominent that the lipomatous nature of the tumor is obscured, so called "fat-free SPCL" (3). In these instances, the tumors may show a pseudolymphomatous appearance. Both PL and SPCL usually arises in subcutaneous tissue of the head and neck region, shoulder and back of men older than 45 years, but these tumors have been described in a wide variety of anatomical sites and over a broad

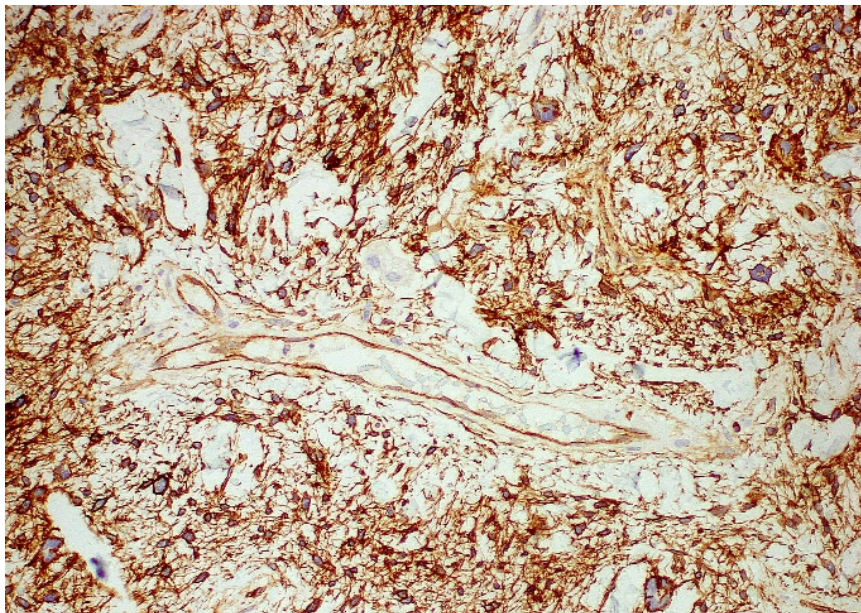
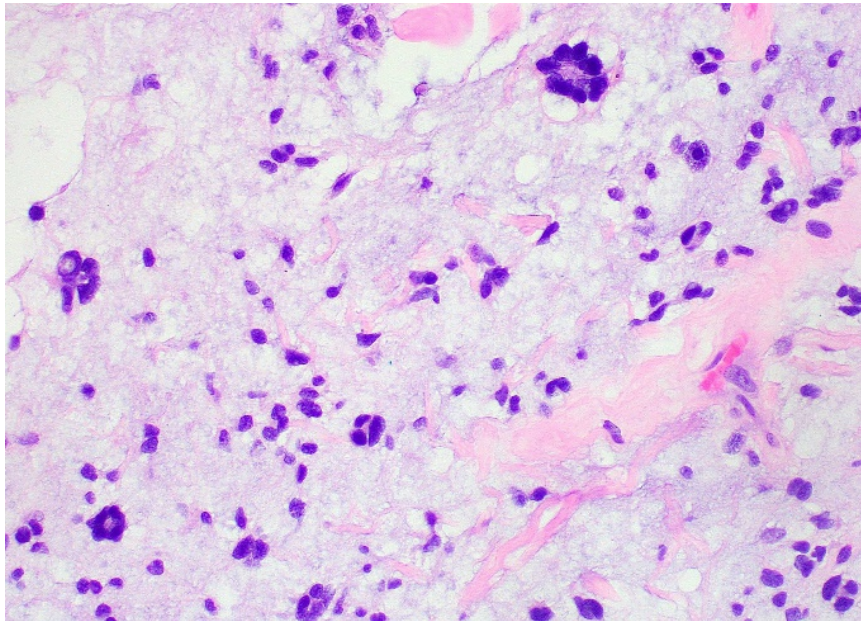
age spectrum. Primary PL and SPC of the major salivary glands are extremely rare with only a handful of cases described in the English literature (4-7).

Tumors of the salivary glands containing fat give rise to a broad morphologic spectrum depending on the intratumoral cellular constituents, which can range from minor scattered adipocytic elements within an otherwise typical salivary gland tumor to predominantly lipogenic salivary gland tumors and pure lipomatous mesenchymal lesions. Salivary gland tumors eg. pleomorphic adenoma, basal cell adenoma and myoepithelioma are known to contain areas of stromal lipometaplasia. The adipocytic component may range from 20 to 90% of the tumor but unequivocal areas of typical pleomorphic/basal cell adenoma and myoepithelioma are usually present with adequate sampling. Sialolipoma is a rare tumor that is composed of normal salivary gland elements admixed with a variable but distinct adipocytic component.

In the initial workup of the FNA of the actual case, the spindle cells, which were present in myxoid material, were interpreted as possible myoepithelial cells closely admixed with metachromatic matrix suggesting a pleomorphic adenoma. In addition, the presence of atypical cells with enlarged, pleomorphic nuclei raised the possibility of a malignant tumor arising on a background of pleomorphic adenoma, e.g., a carcinoma or carcinosarcoma ex PA. However, other features of malignancy that one should look out for in this context; mitotic figures including atypical forms and necrosis (especially when such a degree of nuclear pleomorphism is encountered) were absent. On careful scrutiny of the myxoid matrix, it lacked the fibrillary appearance with frayed edges seen in metachromatic stroma typical of pleomorphic adenoma and plasmacytoid myoepithelial cells were not identified. The absent expression of epithelial and myoepithelial markers also argued strongly against the possibility of a component of pleomorphic adenoma. The appearance of the "floret" type giant cells and focal presence of adipocytes with positive expression of CD34 marker suggested the diagnosis of a pleomorphic lipoma. The presence of "floret" cells was once considered pathognomonic of pleomorphic lipoma but it is now known that these cells can occasionally be seen in both SCL and well differentiated liposarcoma. In addition, in contrast to classic text book wisdom, bona fide lipoblasts are not uncommonly encountered in SCL/PL (and may be numerous) (8).

## Figures





FNA revealed cohesive and individual cells with ovoid to elongated nuclei with no atypia admixed with atypical cells with enlarged, pleomorphic nuclei, and also frequent multinucleated atypical cells. On histopathological examination, a fat containing tumor admixed with spindle cells, collagen, areas of myxoid change and multinucleated giant (foret) cells. Tumor cells were strongly positive for CD34.

## References

1. Agaimy A. Fat-containing salivary gland tumors: a review. *Head Neck Pathol.* 2013;7 Suppl 1:S90-96.
2. Chen BJ, Marino-Enriquez A, Fletcher CD, et al. Loss of retinoblastoma protein expression in spindle cell/pleomorphic lipomas and cytogenetically related tumors: an immunohistochemical study with diagnostic implications. *Am J Surg Pathol.* 2012;36:1119-1128.
3. Billings SD, Folpe AL. Diagnostically challenging spindle cell lipomas: a report of 34 "low-fat" and "fat-free" variants. *Am J Dermatopathol.* 2007;29:437-442.
4. Thirumala S, Desai M, Kannan V. Diagnostic pitfalls in fine needle aspiration cytology of pleomorphic lipoma. A case report. *Acta Cytol.* 2000;44:653-656.
5. Dundas KE, Wong MP, Suen KC. Two unusual benign lesions of the neck masquerading as malignancy on fine-needle aspiration cytology. *Diagn Cytopathol.* 1995;12:272-278; discussion 278-279.
6. Graham CT, Roberts AH, Padel AF. Pleomorphic lipoma of the parotid gland. *J Laryngol Otol.* 1998;112:202-203.
7. Rosenthal LS, Garzon S, Setty S, et al. Left-sided facial mass. Spindle cell lipoma of the parotid gland. *Arch Pathol Lab Med.* 2006;130:875-876.
8. Michal M, Kazakov DV, Hadravsky L, et al. Lipoblasts in spindle cell and pleomorphic lipomas: a close scrutiny. *Hum Pathol.* 2017;65:140-146.

## Case 57

Contributed by: Vania Nosé, MD, PhD - Massachusetts General Hospital, Harvard Medical School, Boston, MA, USA

---

### Clinical History:

This 54 y.o. female comes for consultation about treatment of her large, symptomatic, right thyroid nodule with FNA cytology showing a follicular neoplasm with positive NRAS mutation. Thyroseq suggest an 80% risk of associated thyroid malignancy.

Symptoms: The patient complains of hoarseness, but denies dyspnea, dysphagia, or neck discomfort.

Complications: No hyperthyroidism, hypothyroidism, airway obstruction

FH: There are no known family members with thyroid malignancy. Her mother had thyroidectomy, unknown reason

XRT: The patient has not received any previous head or neck radiation exposure

Meds: The patient does not take any thyroid medications

Imaging: Neck ultrasound two months prior surgery showed a 3.8 cm right thyroid, mostly solid, solitary nodule

FNA: Right thyroid nodule cytology was suspicious for follicular neoplasm, repeat NRAS positive

### Considerations on the findings on this patient:

*NRAS* mutation in a thyroid nodule can mean several disease processes, most of which cannot be decided on cytology alone, requiring full evaluation of the capsule of the nodule. While the data is new, clearly most *NRAS* tumors behave in a non-invasive fashion. Recent reclassification of some thyroid malignancies such as the encapsulated follicular variant of papillary thyroid carcinoma as a benign entity now called: Non-Invasive Follicular Tumor with Papillary nuclear features (NIFTP) has made explaining this to patients somewhat more challenging. This classification is new and thus the molecular profile and behavior is not very well established. This is confusing to patients sometimes. When a thyroid nodule is *NRAS* mutated, the hence of more aggressive malignancy is around 20%, some of these tumors are follicular carcinomas (around 10%), some are follicular variant PTC with an infiltrative pattern (around 10%) and many (around 80%,

thought the literature on this is new and thus sparse) are now considered a benign behaving encapsulated tumor- NIFTP- a newly classified tumor that was previously called encapsulated follicular variant papillary thyroid cancer.

Given the patient's symptoms, size of the nodule, *NRAS*, and concern for malignancy, a total thyroidectomy was recommended.

## Pathological Findings:

On gross examination, the 30.0 grams' thyroid showed a 3.1 cm well-circumscribed nodule involving the mid and lower right lobe. The remaining parenchyma is red-brown, and homogenous.

## Final Diagnosis:

Non-invasive follicular thyroid tumor with papillary-like nuclear features (NIFTP), well-circumscribed, non-invasive, 3.1 cm, occupying mid and lower right lobe.

No definitive lymphovascular invasion identified.

No definitive perineural invasion identified.

The lesion approaches the inked tissue edges.

The tumor has diverse areas with small solid components present within the follicular component.

Mitosis up to 2/10 HPF.

Immunohistochemistry performed at MGH reveals the following profile:

POSITIVE: HBME1

NEGATIVE: BRAF

PTEN is maintained, not lost

P53

Ki67 proliferative index is 6%.

**Diagnosis: Non-invasive follicular thyroid tumor with papillary-like nuclear features (NIFTP), well-circumscribed, non-invasive, 3.1 cm, occupying most of the right lobe.**

## Discussion:

The follicular variant of PTC was broadly recognized in the mid-1970s as a tumor composed of neoplastic follicles rather than papillae, but with follicular cells showing nuclear features characteristic of PTC. Two main subtypes are known to occur: infiltrative (or nonencapsulated) and encapsulated.

Encapsulated FVPTC (EFVPTC) is a challenging and controversial diagnosis in thyroid gland pathology. EFVPTC has increased in incidence by an estimated 2- to 3-fold over the past 2 to 3 decades and makes up 10% to 20% of all thyroid cancers currently diagnosed. However, more recent studies over have demonstrated that FVPTC overall, and particularly EFVPTC, has an indolent behavior and is genetically distinct from infiltrative tumor.

An international group of expert pathologists and clinicians reexamined the entity currently known as EFVPTC through a review of a set of cases with long follow-up to establish standardized diagnostic criteria and to identify terminology that would appropriately address the biological and clinical characteristics of this lesion. The study evaluated cases of EFVPTC to establish consensus diagnostic criteria and develop new nomenclature. Among 109 patients with noninvasive EFVPTC, most of whom were treated with lobectomy only and none with radioiodine, all were alive with no evidence of disease at a median follow-up of 13 years. The consensus from this work group is that thyroid tumors currently diagnosed as noninvasive EFVPTC have a very low risk of adverse outcome and should be termed "noninvasive follicular thyroid neoplasms with papillary-like nuclear features" (NIFTP). For decades, classification of thyroid nodules remained strictly binary, that is, benign or malignant. However, the progress in understanding of oncogenesis has established that cancer develops through multiple morphological steps driven by progressive accumulation of genetic alterations. Progression from benign disease to overt invasive cancer through distinct stages of dysplasia and carcinoma in situ is well defined for colorectal, breast, cervical, and many other common cancer types. Such progression is driven by accumulation of specific mutations and other genetic alterations.

The consensus from this work group is that thyroid tumors currently diagnosed as noninvasive EFVPTC have a very low risk of adverse outcome and should be termed "noninvasive follicular thyroid neoplasms with papillary-like nuclear features" (NIFTP). The new proposed terminology, NIFTP, reflects key histopathologic features of this lesion, i.e., lack of invasion, follicular growth pattern, and nuclear features of PTC. Molecular

analysis demonstrating that most of these lesions are driven by clonal genetic alterations and are therefore neoplasms rather than hyperplastic proliferations.

In the thyroid gland, a NIFTP represents such a tumor, driven by well-characterized oncogenes, that occupies an intermediate position between true benign lesions and invasive cancer. Indeed, when EFVPTCs, that is, tumors with NIFTP morphology, are removed at more advanced, invasive stage, they are true cancers associated with 12% risk of tumor recurrence and 2% risk of tumor-related mortality. For that reason, NIFTP cannot be considered benign and these tumors have to be surgically excised to evaluate the tumor capsule for invasion. However, when surgically removed, these lesions have extremely low risk of recurrence, estimated to be less than 1% in 15 years based on more than 400 reported cases. Therefore, when molecular testing is positive for genetic alterations characteristic of NIFTP, such as RAS or PAX8-PPARG, this result cannot be considered false positive. Instead, it provides an accurate prediction of an oncogene-driven premalignant tumor, NIFTP, or a low-risk cancer, both of which, following the 2015 American Thyroid Association Management Guidelines, can be removed by limited surgery, that is, thyroid lobectomy. The removal is needed to evaluate for tumor invasion and prevent possible progression of NIFTP to invasive EFVPTC.

According to the WHO "Endocrine and Neuroendocrine Tumour" 5th edition, 2022, the definition of NIFTP is: Non-invasive follicular thyroid neoplasm with papillary-like nuclear features (NIFTP) is a non-invasive encapsulated/well demarcated follicular cell derived tumour with a follicular growth pattern and nuclei resembling papillary thyroid carcinoma (PTC) that has an extremely low malignant potential.

### **Consensus Diagnostic Criteria for the Encapsulated Follicular Variant of Papillary Thyroid Carcinoma (EFVPTC):**

#### *1. Major Features: Encapsulation or clear demarcation*

Follicular growth pattern

Nuclear features of papillary thyroid carcinoma (PTC) : Enlargement, crowding/overlapping, elongation, irregular contours, grooves, pseudoinclusion, chromatin clearing

#### *2. Minor Features:*

Dark colloid

Irregularly shaped follicles

Intratumoral fibrosis

"Sprinkling" sign

Follicles cleft from stroma

Multinucleated giant cells within follicles

*3. Features Not Seen/Exclusion Criteria:*

Psammoma bodies

Infiltrative border

Tumor necrosis

High mitotic activity

Cell/morphologic characteristics of other variants of PTC

**Diagnostic Criteria for NIFTP (updated according to the 5<sup>th</sup> ed 2022 WHO):**

---

1. Encapsulation or clear demarcation

---

2. Follicular growth pattern with all of the following: <1% true papillae; No psammoma bodies; <30% solid/trabecular/insular growth pattern

---

3. Nuclear features of papillary carcinoma (nuclear score of 2-3)

---

4. No vascular or capsular invasion

---

5. No tumour necrosis

---

6. Low mitotic count (<3 mitosis / 2mm<sup>2</sup>)

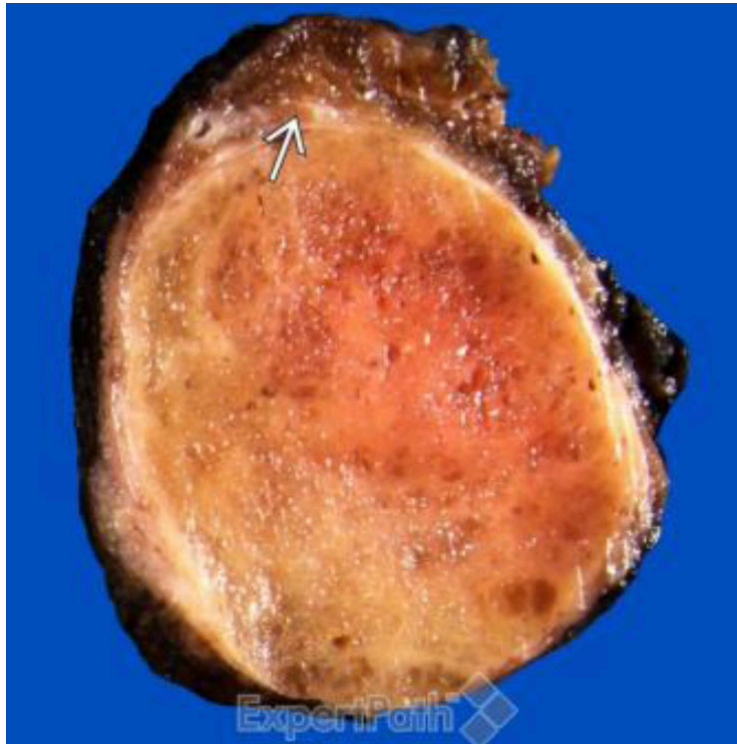
---

7. Lack of cytoarchitectural features of papillary carcinoma variants other than follicular variant (tall cell features, cribriform-morular variant, solid variant, etc).

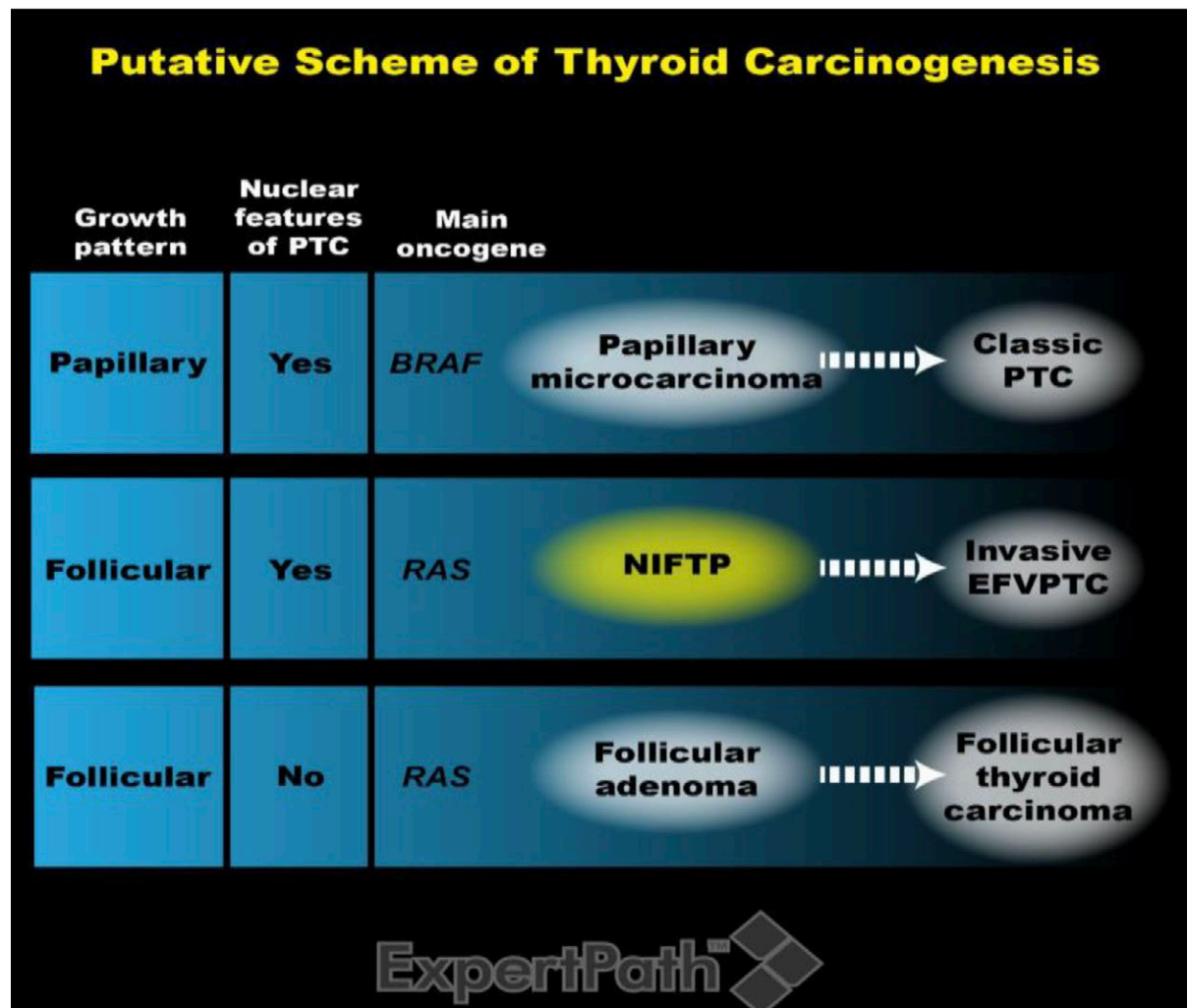
---

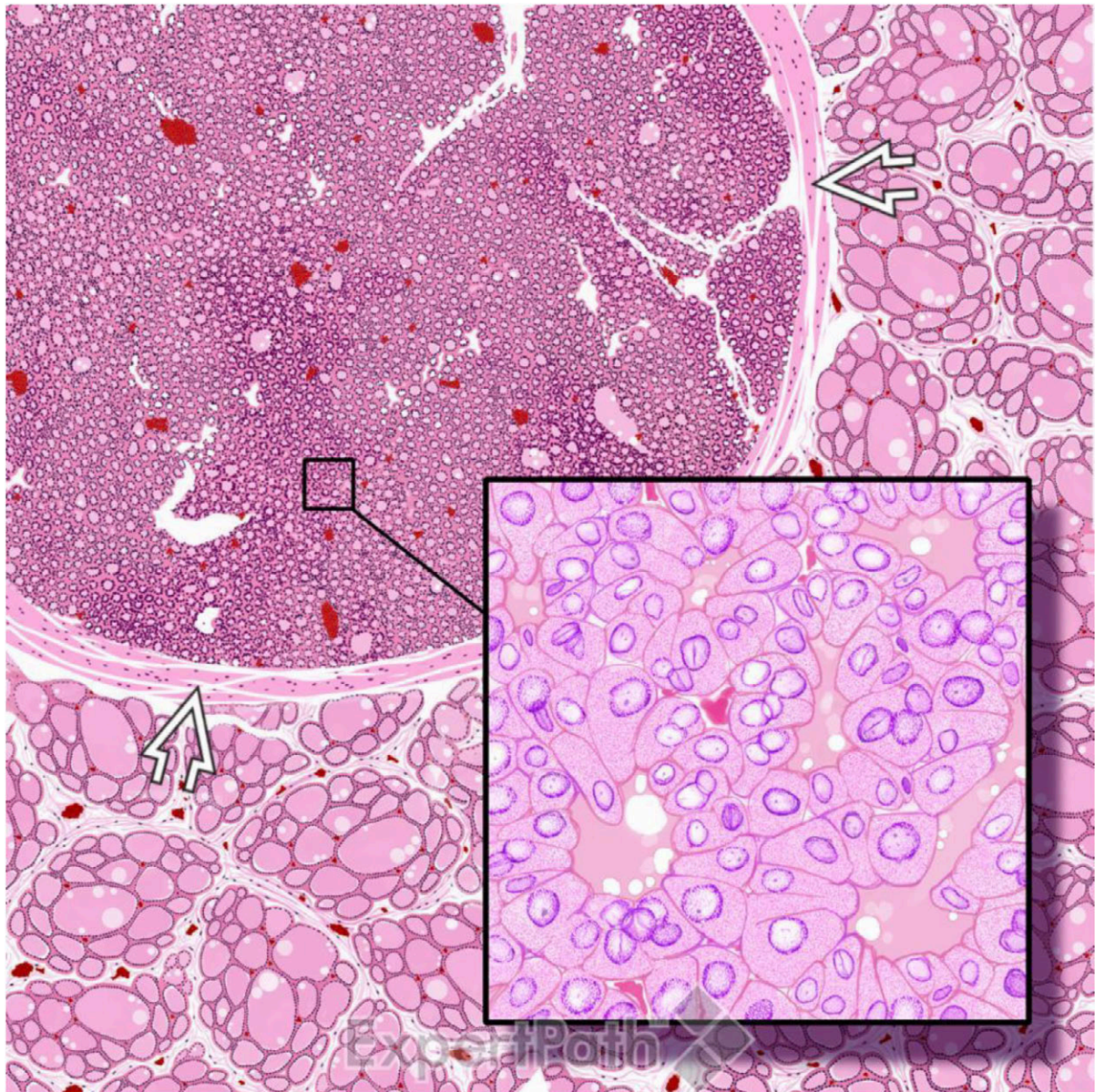
**Diagnostic molecular pathology**

BRAF p.V600E mutation detected by immunostaining or genotyping excludes the diagnosis

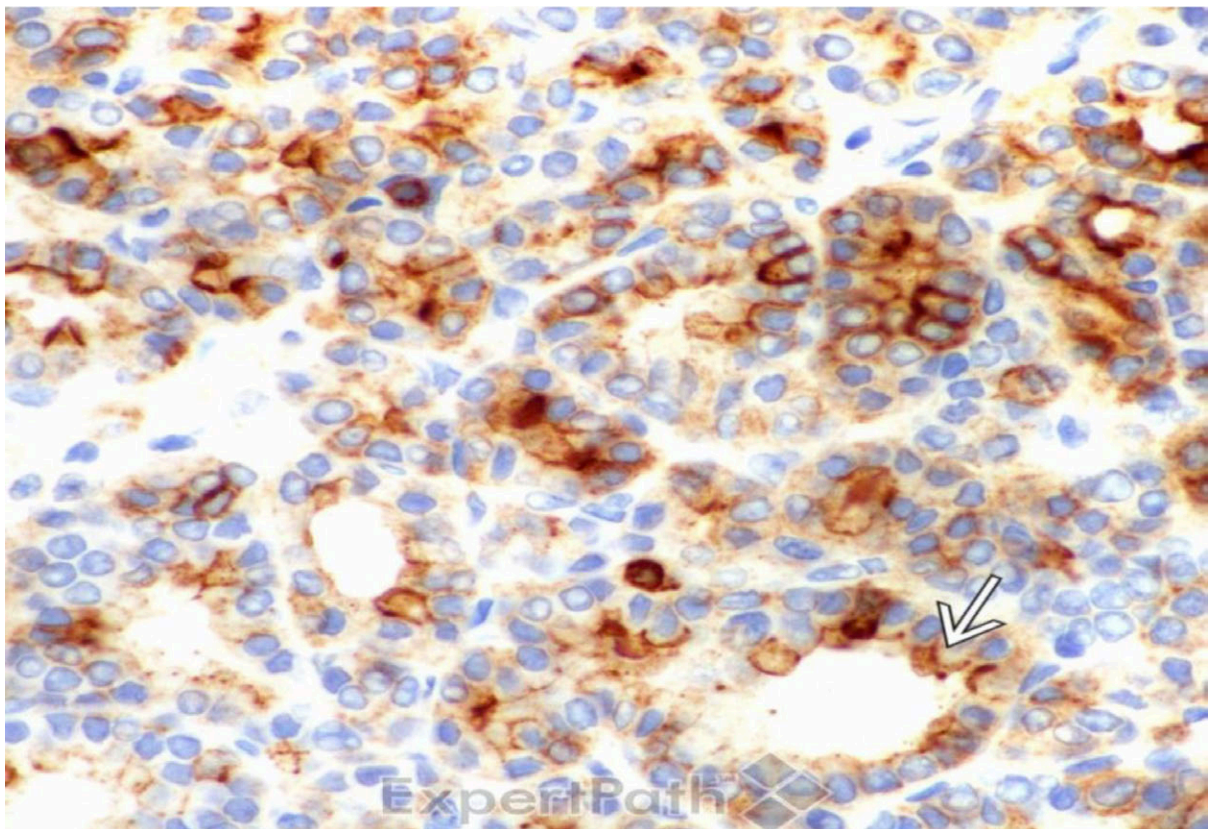
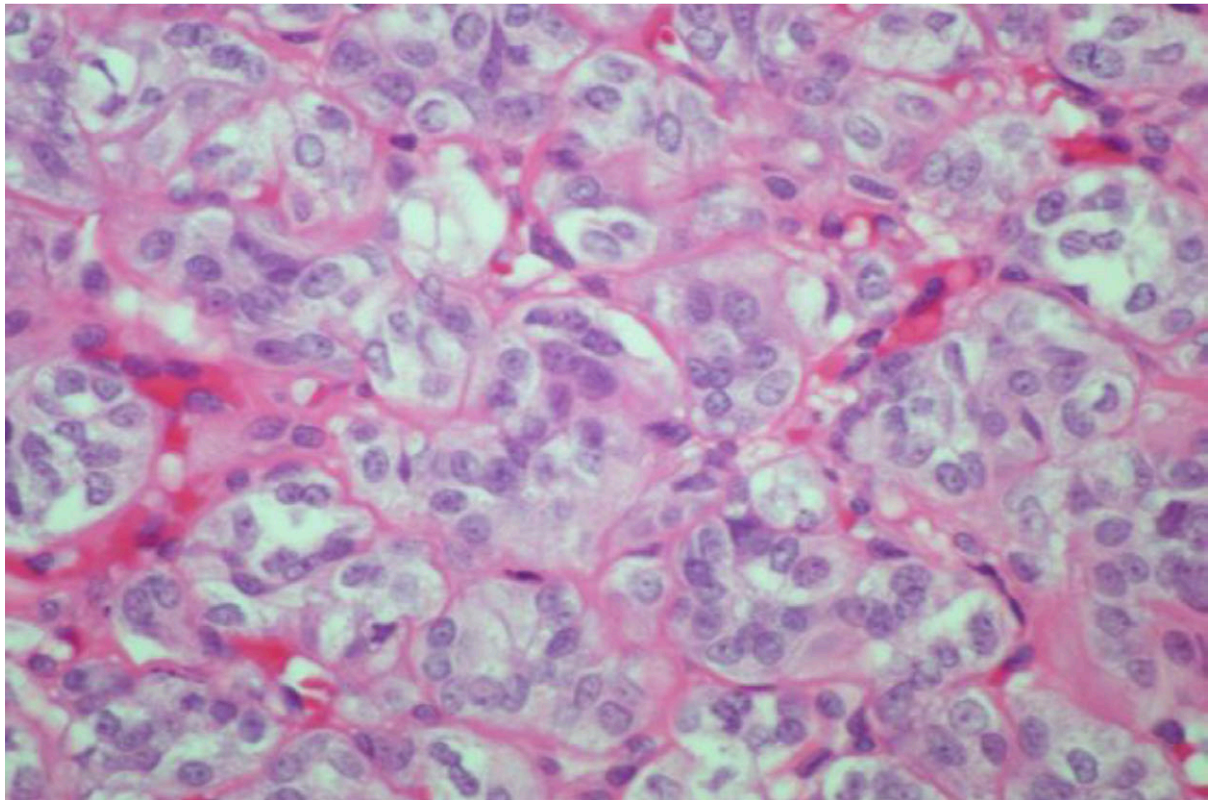


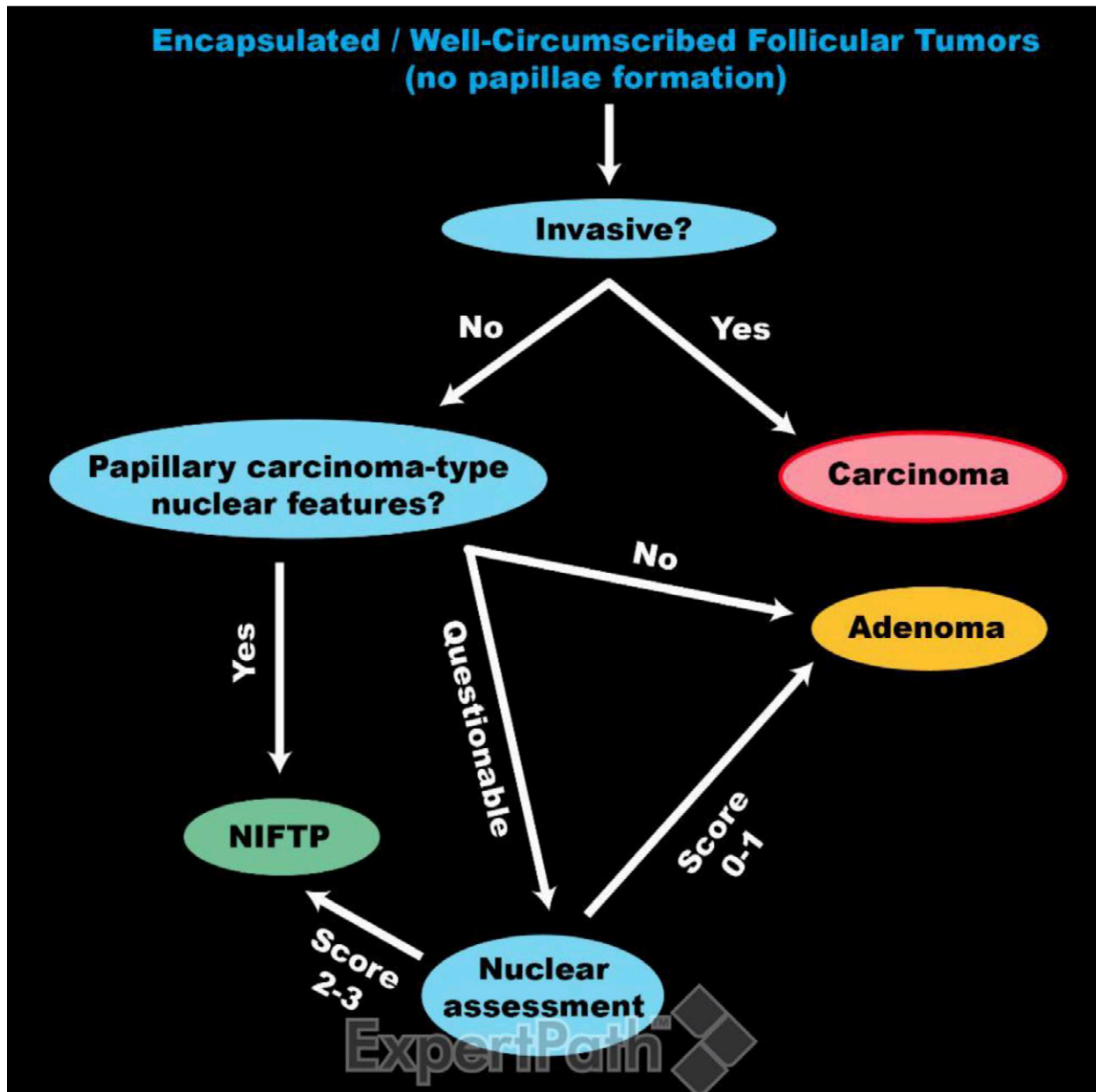
The gross characteristic features of NIFTP is a well-circumscribed or encapsulated nodule, which is lighter than the adjacent thyroid parenchyma, and compresses the red-brown adjacent thyroid parenchyma (white solid arrow) - from "Diagnostic Pathology: Endocrine".





Well-circumscription, well-demarkation, or encapsulated follicular-patterned neoplasm (white open arrow), with no capsular invasion are some of the criteria for the diagnosis of NIFTP. Nuclear features of papillary thyroid carcinoma (inset) must be present. No papillae should be seen - from "Diagnostic Pathology: Endocrine".





This diagnostic algorithm for the evaluation of encapsulated follicular-patterned neoplasms uses the evaluation of the capsular invasion and papillary carcinoma-type nuclear features differentiating NIFTP from follicular adenoma and carcinoma. – from “Diagnostic Pathology: Endocrine”.

## References:

1. Nikiforov YE, Seethala RR, Tallini G, Baloch ZW, Basolo F, Thompson LD,
2. Barletta JA, Wenig BM, Al Ghuzlan A, Kakudo K, Giordano TJ, Alves VA, Khanafshar E, Asa SL, El-Naggar AK, Gooding WE, Hodak SP, Lloyd RV, Maytal G, Mete O, Nikiforova MN, Nosé V, Papotti M, Poller DN, Sadow PM, Tischler AS, Tuttle RM, Wall KB, LiVolsi VA, Randolph GW, Ghossein RA. Nomenclature Revision for Encapsulated Follicular Variant of Papillary Thyroid Carcinoma: A Paradigm Shift to Reduce Overtreatment of Indolent Tumors. *JAMA Oncol.* 2016 Aug 1;2(8):1023-9.
3. Nikiforov YE. Ramifications of New Terminology for Encapsulated Follicular
4. Variant of Papillary Thyroid Carcinoma-Reply. *JAMA Oncol.* 2016 Aug 1;2(8):1098-9.
5. Richard C, Debreuve-Theresette A, Patey M, et al. Long-term progression of non-invasive follicular thyroid neoplasm with papillary-like nuclear features: A single-center retrospective study of the French Marne-Ardenne thyroid cancer registry. *Ann Endocrinol (Paris).* 2020 Feb;81(1):34-38
6. Nosé, V: *Diagnostic Pathology: Endocrine*; 2nd edition; 2018, Elsevier Inc; non-invasive follicular thyroid neoplasm with papillary-like nuclear features: 92-100.
7. Xu B, Ghossein RA. Noninvasive Follicular Thyroid Neoplasm with Papillary-Like Nuclear Features (NIFTP): An Update. *Head Neck Pathol.* 2020 Jun;14(2):303-310.
8. WHO "Endocrine and Neuroendocrine Tumours", IARC, WHO, 5th edition, 2022

## Case 58

Contributed by Manuel Sobrinho-Simões - University Hospital of São João & Ipatimup, Porto, Portugal

---

### Clinical history

67-year-old man with rapid enlarging mass of the left side of the thyroid. FNA of the large nodule of the left lobe - Follicular tumour (Bethesda IV). The patient was submitted to left lobectomy and isthmectomy.

### Macroscopy

A 36-gram "hemithyroidectomy" was received in our Institute (Institute of Molecular Pathology and Immunology of the University of Porto - Ipatimup). The surgical specimen included a 4.5x4.5x3.3cm left lobe almost totally occupied by a partially encapsulated, heterogeneous, predominantly whitish nodule measuring 4.4x4.0x3.3cm and isthmus measuring 1.6x1.8x0.5cm. (Courtesy of Prof. Catarina Eloy, director of Ipatimup Diagnostics).

### Histologically

The tumour had a very heterogeneous appearance displaying predominant solid/trabecular/insular growth patterns amongst areas exhibiting follicular architecture (microfollicles and medium sized follicles). Most of nuclei of the neoplastic cells had nuclear features of the follicular-cell type but there were also PTC-like nuclei in foci of follicular-patterned areas of the tumour, usually in areas looking like follicular subtype of PTC with interstitial fibrosis. In the center of several areas of solid growth pattern there were incipient papillary structures without PTC-like nuclei (The nuclei of these papillae were follicular-cell type nuclei). Throughout the tumour, namely in solid/trabecular/insular areas, there was relatively high mitotic activity and, focally, prominent neoplastic necrosis, acquiring a peritheliomatous appearance (necrosis and/or fibrosis).

The tumour border was demarcated by an expansive growth appearance. Overall, the tumour was circumscribed and partially encapsulated. There were signs of capsular

invasion and prominent signs of vascular invasion in the capsule and beyond the capsule, involving large blood vessels.

## Immunohistochemistry

The tumour cells were diffusely positive for TTF1, PAX8, and several low weight cytokeratins. Thyroglobulin immunoreactivity varied a lot from area to area, focally displaying a dot-like appearance. Calcitonin, synaptophysin, and chromogranin were negative. Immunostaining for p53 was wild type. Ki-67 proliferation index was around 20%.

## Molecular results

The study was performed in four areas displaying different aspects of the tumour, obtaining DNA from thick sections of two paraffin blocks under histological control. No mutations were detected in TERTp, BRAF V600E, NRAS, HRAS, KRAS or p53 (Ex. 5 to 11).

## Diagnosis

Poorly differentiated thyroid carcinoma (Turin approach) with prominent signs of capsular and vascular invasion.

**Treatment and follow-up** (Limited by the source of data).

January 2018 - Total thyroidectomy and I<sup>131</sup> (150mCi)

March 2020 - Lung metastases - I<sup>131</sup> (200mCi)

February 2021 - I<sup>131</sup> (200mCi) due to structural recurrence (bone metastases)

May 2021 - Surgical removal of metastases in the 4<sup>th</sup> and 5<sup>th</sup> left ribs

April 2022 - The patient is "alive with distant metastases" (no further information).

## Comments

This case (#58) was selected together with Case #60 in order to stress a couple of practical points in the broad field of follicular cell-derived tumours.

Before starting the discussion about making a diagnosis of poorly differentiated thyroid carcinoma it is crucial to find clear cut signs of invasion, this is particularly important whenever one is dealing with foci of high-grade features (see below).

The first point regards the growing importance of macroscopy, architecture and invasiveness of thyroid tumours for Diagnosis, Prognosis and Therapy selection, regardless of the nuclear features of the neoplastic cells. I think the only three other major criteria are Staging, Surgery and Therapy responsiveness.

The second point regards the need to balance the present pressure towards finding molecular data in (almost) every thyroid tumour, frequently regardless of the context. Besides the challenge of finding possible targetable therapies whenever I<sup>131</sup> radiotherapy is not efficient (Volante et al, 2021), the issue of searching for molecular data with prognostic significance will be dealt in connection with Case #60. Finally, this case provides clinico-pathological features helpful to understand the diagnostic and classification problems linked with poorly differentiated thyroid carcinomas.

In the new classification of thyroid neoplasms (Baloch ZW et al, 2022), follicular cell-derived tumours are divided into benign, low risk and malignant neoplasms. Within malignant neoplasms, "The Turin consensus criteria (Volante M et al, 2007) - endorsed by the 2017 WHO classification, as well as the current WHO classification of tumours of endocrine organs - clarified the histologic criteria to diagnose a poorly differentiated thyroid carcinoma and validated its prognosis intermediate between well and undifferentiated (anaplastic) carcinomas". The new WHO classification recognises two groups of high-grade non-anaplastic follicular-cell derived carcinomas that have intermediate prognostic risk that corresponds to Poorly differentiated thyroid carcinoma (PDTC) and Differentiated high-grade thyroid carcinoma (DHGTC) (Baloch ZW et al, 2022).

The differences between PDTC and DHGTC are found at histologic examination (Table 1). (Baloch ZW et al, 2022).

**Table 1.** Diagnostic criteria for high-grade follicular cell-derived thyroid carcinomas

	PDTC (Turin criteria)	DHGTC
<b>Growth pattern</b> <b>Nuclear cytology</b> <b>Other features: tumor necrosis, mitosis and convoluted nuclei</b>  <b>Anaplastic features</b>	<b>Required: solid/trabecular/insular</b> <b>Required: no features of PTC</b> <b>Minimum requirement: one of the following three features:</b> <b>Mitotic count <math>\geq 3/2</math> mm<sup>2</sup></b> <b>Tumor necrosis</b> <b>Convoluted nuclei</b> <b>Absent</b>	<b>Papillary, follicular, solid*</b> <b>Any</b> <b>Minimum requirement: one of the following two features:</b> <b>Mitotic count <math>\geq 5/2</math> mm<sup>2</sup></b> <b>Tumor necrosis</b> <b>Absent</b>

PDTC, poorly differentiated thyroid carcinoma; DHGTC, differentiated high-grade thyroid carcinoma

\* Tumors with solid growth and PTC nuclear features are classified as high-grade differentiated thyroid carcinoma

At variance with most PDTC, the present case was (partially) encapsulated and focally extended beyond the thyroid and exhibited capsular and gross vascular invasion. We did not observe small dark nuclei with a convoluted “raisin-like” appearance reminiscent of PTC-nuclei (Carcangiu ML et al, 1984). This finding is not any more considered as a valuable feature for diagnostic prognosis in contrast to invasiveness, necrosis and proliferation activity. In the present case, we observed foci of differentiated carcinoma that corresponds to Follicular subtype of PTC.

A last point to stress that we did not find any of the more frequent pathogenic mutations of thyroid carcinomas, despite searching for their presence in four different areas of PDTC (Namely, we did not detect any RAS mutation nor TERTp mutation).

It would be very interesting to compare the primary tumour with bone metastases that were surgically removed three years after the initial diagnosis. This comparison could provide useful information regarding molecular alteration(s) that would be therapeutically targetable. Unfortunately, we were not (yet?) allowed to study the metastases.

## References

1. Carcangiu ML et al. Poorly differentiated ("insular") thyroid carcinoma. A reinterpretation of Langhans' "wuchernde Struma" . *Am J Surg Pathol*. 1984 8:655-68, 1984
2. Volante M et al. Poorly differentiated thyroid carcinoma: the Turin proposal for the use of uniform diagnostic criteria and an algorithmic diagnostic approach. *Am J Surg Pathol* 31:1256-64, 2007
3. Rivera M et al. Histopathologic characterization of radioactive iodine-refractory fluorodeoxyglucose-positron emission tomography-positive thyroid carcinoma. *Cancer* 113:48-56, 2008
4. Wong KS et al. Papillary thyroid carcinoma with high-grade features versus poorly differentiated thyroid carcinoma: An analysis of clinicopathologic and molecular features and outcome. *Thyroid* 31:933-40, 2021
5. Volante M et al. Molecular pathology of well-differentiated pulmonary and thymic neuroendocrine tumors: What do pathologists need to know? *Endocr Pathol* 32:154-68, 2021
6. Baloch ZW et al. Overview of the 2022 WHO classification of thyroid neoplasms. *Endocr Pathol* 33: 27-63, 2022

## Case 59

Contributed by: Vania Nosé, MD, PhD - Massachusetts General Hospital, Harvard Medical School, Boston, MA, USA

---

### Clinical History

A 42-year-old female music teacher presented to her primary care provider after experiencing progressive throat tightness over the preceding year. She also noticed an anterior neck mass and bilateral cervical lymph nodes, which have been gradually enlarging. The patient had been otherwise a healthy non-smoker and social drinker. Family history included benign thyroid nodules in her mother and an unknown type of skin cancer in her father.

Cervical sonography and computer tomography both revealed a 5.4 x 5.1 x 4.3 cm mass replacing the entire right thyroid lobe with extension into the isthmus. Also noted was bilateral central neck adenopathy and right lateral neck adenopathy. Fine needle aspiration was positive for papillary thyroid carcinoma. The patient consented to total thyroidectomy with bilateral central neck dissection and right lateral neck dissection.

### Histopathology

An 86-gram total thyroid was received at the Surgical Pathology processing area at the Massachusetts General Hospital, including a 6.6 x 5.3 x 3.8 cm nodular right lobe, a 3.7 x 1.8 x 1.1 cm left lobe, a 1.8 x 1.1 x 0.9 cm isthmus, and adherent skeletal muscle on the anterior aspect of the right lobe. Upon sectioning, the right lobe was essentially replaced by a 6.6 x 5.2 x 3.1 cm tan-white multilobulated mass with a central stellate fibrotic scar. The left lobe and isthmus displayed brown-red thyroid parenchyma without gross lesion. Also received were separate cervical dissection specimens that contained numerous enlarged lymph nodes measuring up to 2.8 cm in size.

Microscopically, the right lobe mass showed a large central area of hyalinization, which gave rise to radiating bands of fibrosis that extended into the cellular peripheral zone, where a lobulated growth pattern was seen with ramifying fibrotic septa separating tumor cells into irregular islands (**Figure 1**). Tumor border was not clearly demarcated due to the presence of numerous satellite nodules in the adjacent non-neoplastic thyroid parenchyma (**Figure 2**). Extensive angiolymphatic invasion (**Figure 3**) and extrathyroidal

extension into the strap skeletal muscle were noted. On high magnification, the tumor cell islands were composed of solid growth of oncocytic cells with nuclear grooves and clearing, focal formation of follicles and scant colloid production (**Figure 4**).

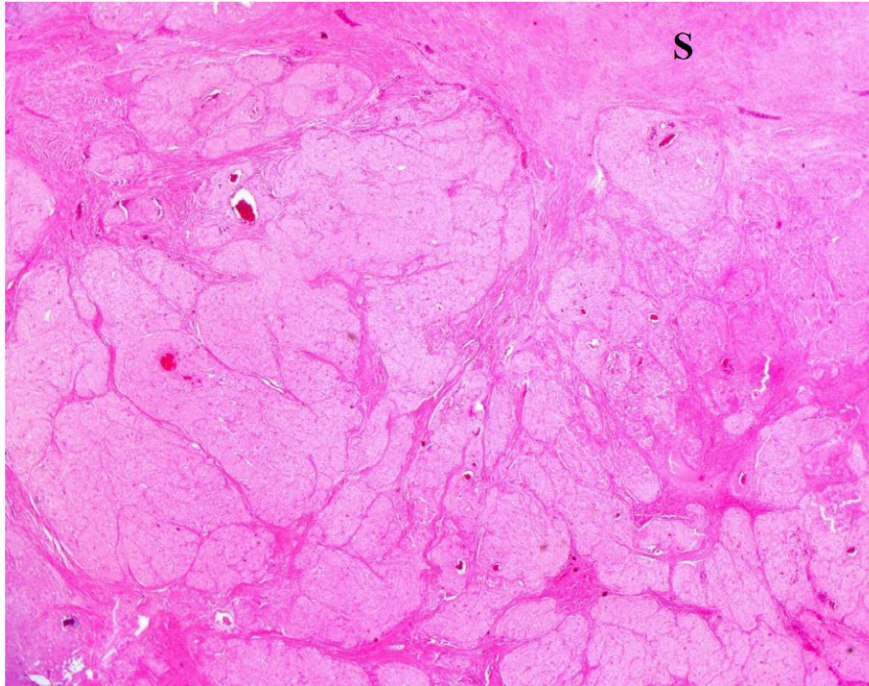


**Figure 1:** The tumor displayed a lobulated pattern with a central fibrotic scar (S) and radiating fibrotic bands that divided tumor cells into geographic islands.

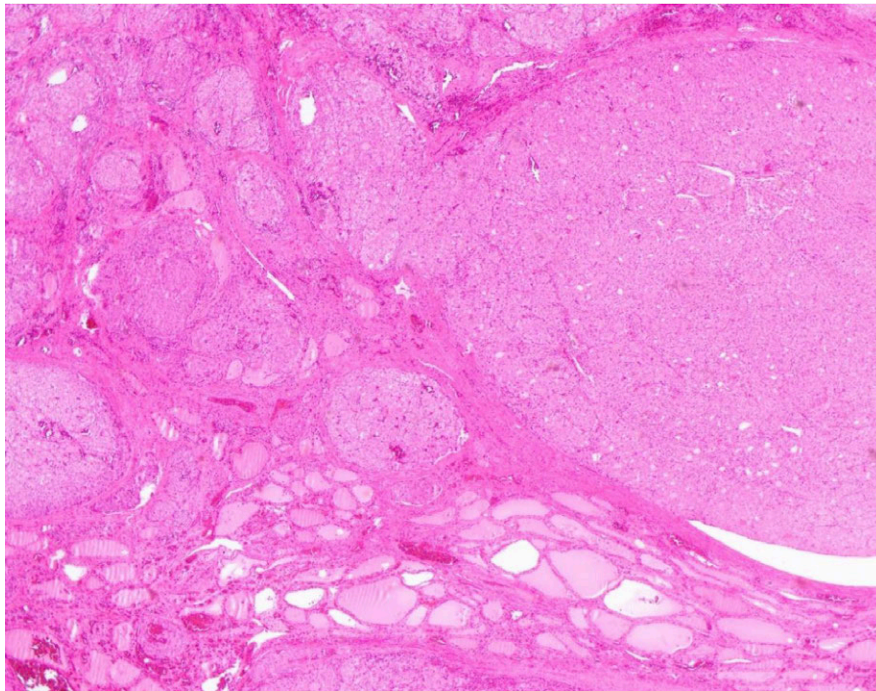


**Figure 2:** Tumor interface with the adjacent thyroid parenchyma was straddled by multiple satellite nodules.

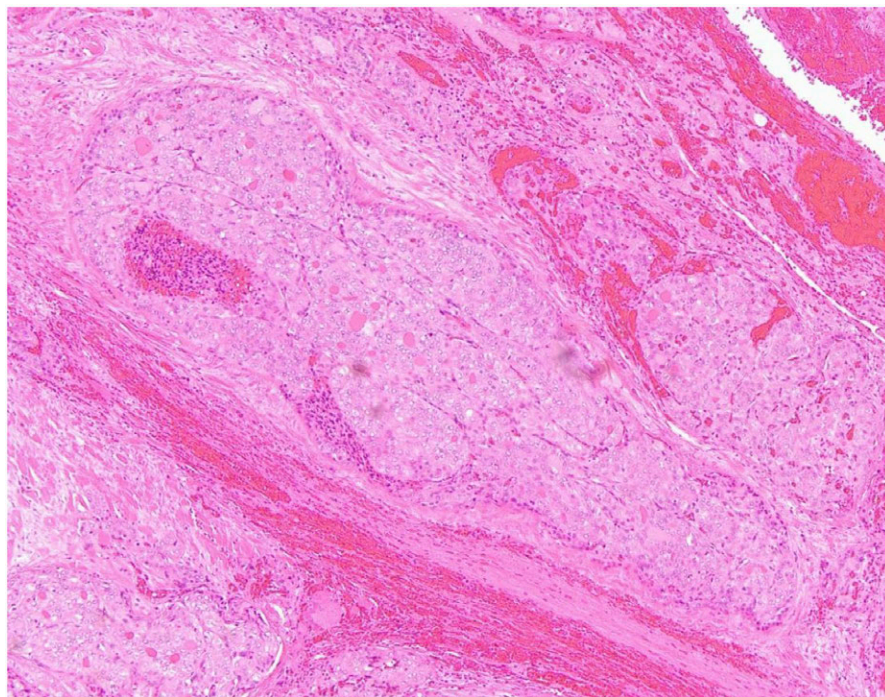


**Figure 3:** Extensive lymphovascular invasion was present.

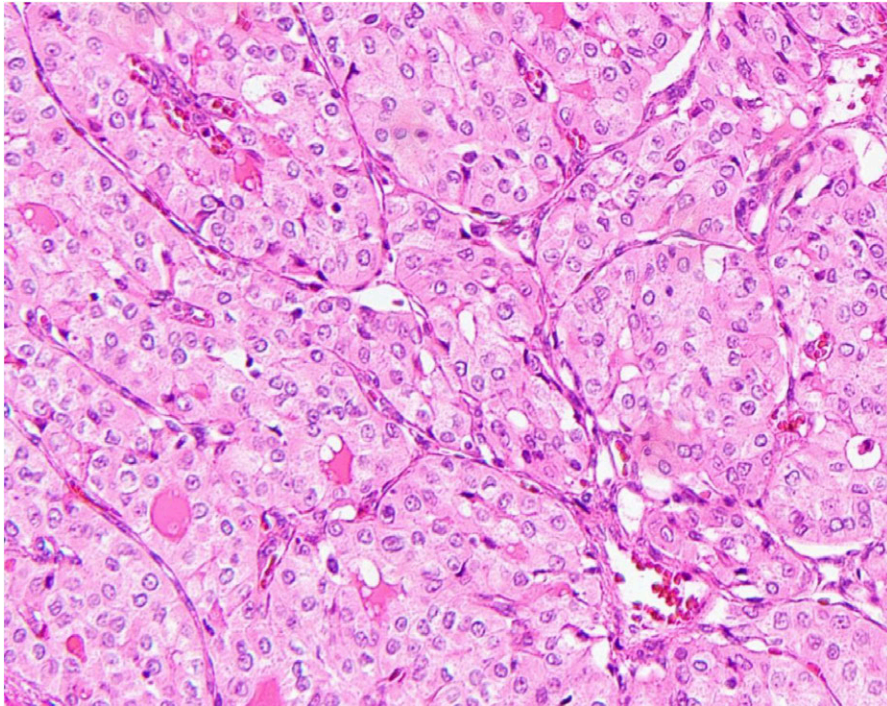


**Figure 4:** The tumor was composed of solid nests of oncocytic cells with PTC nuclear features and scant colloid production.

## Immunohistochemistry

By immunohistochemistry, the tumor cells were diffusely positive for HBME-1 (Figure 5), focally positive for thyroglobulin, and negative for calcitonin, synaptophysin, and chromogranin. Staining for p53 was wild-type. Ki67 proliferation index was around 4% with scattered mitotic figures (1-2 per 10 high-power fields). Immunohistochemistry for *BRAF* V600E mutation using the mutation-specific BRAF (VE1) antibody was negative, indicating the absence of *BRAF* V600E mutation (Figure 6).

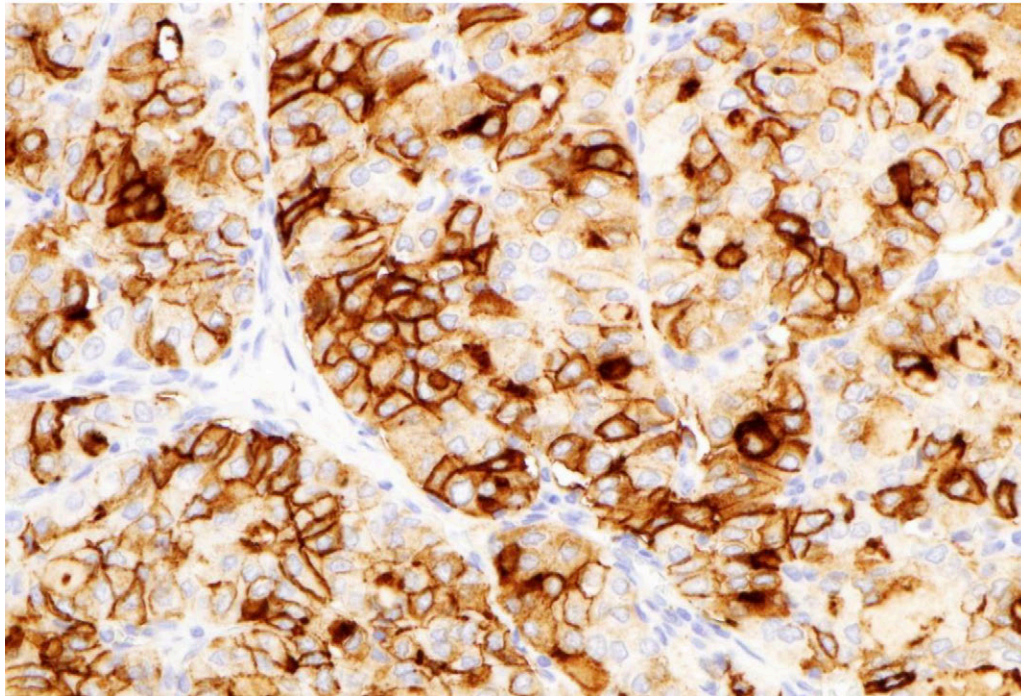


**Figure 5:** HBME-1 immunohistochemistry showed strong membranous staining.

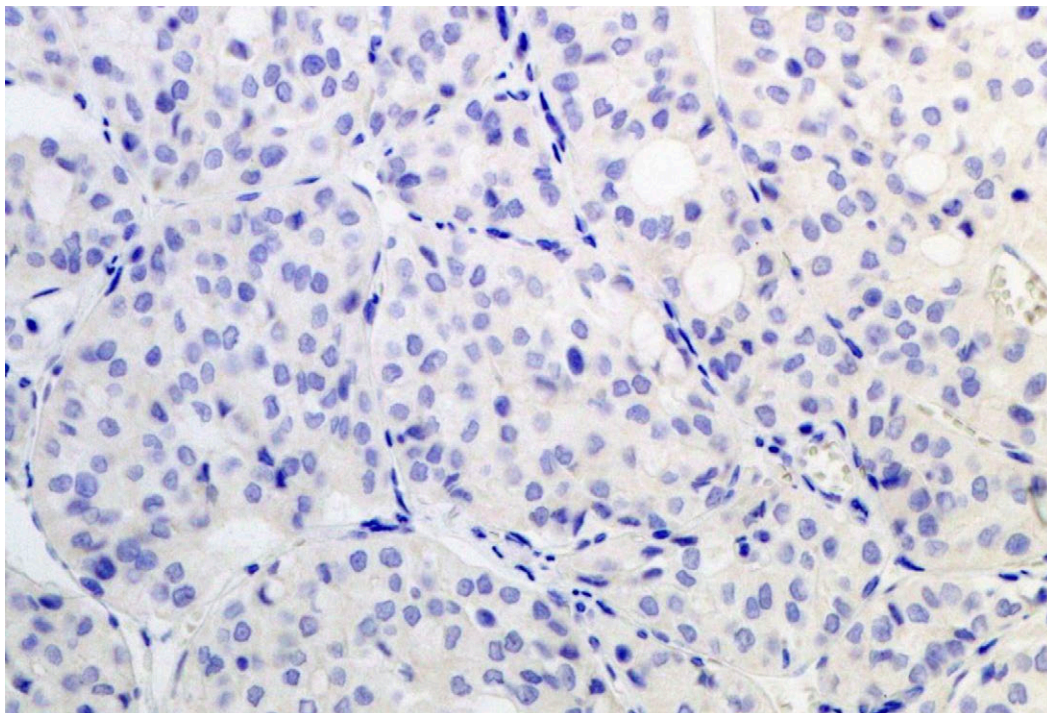


**Figure 6:** Immunolabeling specific for BRAF V600E mutant was negative.

## Genetic Profiling

Tumor-derived total nucleic acid was subjected to Anchored Multiplex PCR (AMP) followed by next generation sequencing (NGS)-based targeted fusion transcript detection, which revealed a *SQSTM1-NTRK3* fusion involving the *SQSTM1* exon 6 and the *NTRK3* exon 14 [1]. Concurrent NGS mutation profiling that covered hotspot variants in over 90 genes including *AKT1*, *APC*, *BRAF*, *CTNNB1*, *EGFR*, *HRAS*, *IDH1*, *KIT*, *KRAS*, *MEK1*, *NRAS*, *NOTCH1*, *NRAS*, *PIK3CA*, *PTEN*, *TERT* and *TP53* was negative.

## Discussion

Papillary thyroid carcinoma (PTC) is the most common type of thyroid malignancy, accounting for 80-90% of thyroid cancer cases. The genetic makeup of PTC encompasses a spectrum of nucleic acid alternations that are accompanied by distinct histomorphologic correlations. On one end of the spectrum are the classic type and the tall cell variant, both of which are highly associated with the *BRAF* V600E mutation (80% and >90%, respectively). On the other end of the spectrum is the follicular variant, which overlaps with the follicular thyroid neoplasms by carrying frequent *RAS* mutations (45%, mostly *NRAS*, followed by *HRAS* and *KRAS*), the *PAX8-PPARG* rearrangement (up to 30%), *EIF1AX* mutations (5%) and non-V600E *BRAF* mutations (mostly K601E). Most PTCs encountered in daily practice may show mixed patterns, and molecular analysis is needed to determine the underlying genetic alternations. Activating mutations in the *TERT* promoter region occur in 5-15% of PTCs of various subtypes and have been associated with worse clinical prognosis.

Two special PTC patient populations are the pediatric cases and those with prior radiation exposure, both of which are frequently associated with rearrangements of receptor tyrosine kinase-encoding genes, such as *RET* and *NTRK* [2-7]. Around 60-80% of PTCs that developed in the post-Chernobyl reactor accident victims harbored *RET-PTC* rearrangements, most commonly *RET-PTC3*, followed by *RET-PTC1*, *RET-PTC2*, and rarely *RET-PTC5*, *RET-PTC6*, *RET-PTC7*, *RET-PTC9*, *RET-AFAP1L2* and *RET-PPFIBP2* [2, 6, 7]. PTCs carrying the *RET-PTC3* fusion predominantly (68%) show the solid variant morphology, whereas tumors carrying the *RET-PTC1* fusion are mostly of the classic type (46%) or the follicular variant (33%) with rare diffuse sclerosing variant (8%) [6]. *RET-PTC* rearrangements, mostly *RET-PTC1*, have also been identified in 26-65% of sporadic (non-radiation-related) pediatric PTCs [2, 7]. *NTRK* rearrangements are much less common,

occurring in 3-15% of post-Chernobyl PTCs and 2-26% of sporadic pediatric PTCs [4-6]. The *ETV6-NTRK3* fusion accounts for the majority of *NTRK*-rearranged PTCs, reported in a total of 25 cases (15 follicular variant, 8 classical type, 2 solid variant) [5]. There have been rare reports of PTCs harboring *TPR-NTRK1* (two cases, one solid variant [7] and one follicular variant [4]), *TPM3-NTRK1* (one case [6]) and *SQSTM1-NTRK3* (one case, classical type [3]) fusions. *RET* and *NTRK* rearrangements have both been associated with more aggressive tumor behavior [4, 6].

The current literature is scarce on *NTRK*-rearranged PTCs due to their overall rarity. One recent study has provided a detailed description of PTCs carrying the *ETV6-NTRK3* fusion, including an infiltrative and nodular appearance, central scar-like fibrosis, extensive lymphovascular invasion and lymph node metastases in most cases [4]. It is noteworthy that these histologic features were also seen in the current index case, which harbors a *SQSTM1-NTRK3* fusion. However, based on the published photographs [4], there seemed to be more abundant colloid production compared to the current case. The only previously published PTC case with *SQSTM1-NTRK3* fusion was reportedly of the classic type; however, neither further morphologic specifications nor photographs were provided [3].

Overactivity the mitogen activated protein kinase (MAPK) signaling cascade is cardinal to the oncogenesis of thyroid cancers. Therapeutic agents have been developed to target various components of the pathway [8]. All the *RET-PTC*, *ETV6-NTRK3*, and *SQSTM1-NTRK3* rearrangements have been shown to increase MAPK signaling [3, 7]. Aberrant upregulation can also result from activating mutations in important pathway mediators such as RAS and BRAF. Moreover, *ALK* translocations, found in 2% of PTCs, can also activate the RAS proteins [9, 10]. Targeted kinase inhibitors approved by the Food and Drug Administration (FDA) for the treatment of advanced/refractory thyroid cancers include cabozantinib (RET inhibitor, approved for medullary thyroid carcinoma), Dabrafenib (BRAF V600E variant inhibitor, for BRAF V600E-positive anaplastic thyroid carcinoma), lenvatinib (RET inhibitor, for differentiated thyroid carcinomas), larotrectinib (NTRK inhibitor, for *NTRK*-rearranged solid tumors), sorafenib (RET and BRAF inhibitor, for differentiated thyroid carcinomas), and vandetanib (RET inhibitor, for medullary thyroid carcinoma). Additional agents are under varying stages of development [8].

## Summary:

**Definition:** Kinase fusion-related thyroid carcinomas (KFTC) include histologically diverse group of thyroid malignancies driven by oncogenic kinase gene rearrangements. *RET* is most commonly rearranged kinase gene (~ 50% of KFTC), followed by *NTRK* (~ 30%), *BRAF* (~ 10%), *ALK* (~ 5%), *MET*, *ROS1*, and *FGFR* (< 5%)

**Microscopic characteristics:** Multilobulated/multinodular growth and prominent intratumoral fibrosis are seen in most cases; extensive lymphovascular invasion; wide histologic spectrum has been reported, including papillary thyroid carcinoma (most common), poorly differentiated thyroid carcinoma, anaplastic thyroid carcinoma, primary thyroid secretory carcinoma, and medullary thyroid carcinoma. No morphologic findings are specific to KFTC, and initial screening with BRAF V600E-specific immunostain is advisable given that kinase fusions are mutually exclusive with BRAF V600E mutation

**Molecular correlation:** Several unusual morphologic findings have been proposed to guide selective molecular testing based on their frequent presence in KFTC (algorithm): Lobulated/multinodular growth; prominent intratumoral fibrosis; mixed architectural patterns (papillary, follicular, solid); extensive lymphovascular invasion; glomeruloid structures; BRAF-negative by immunohistochemistry.

### Immunohistochemistry:

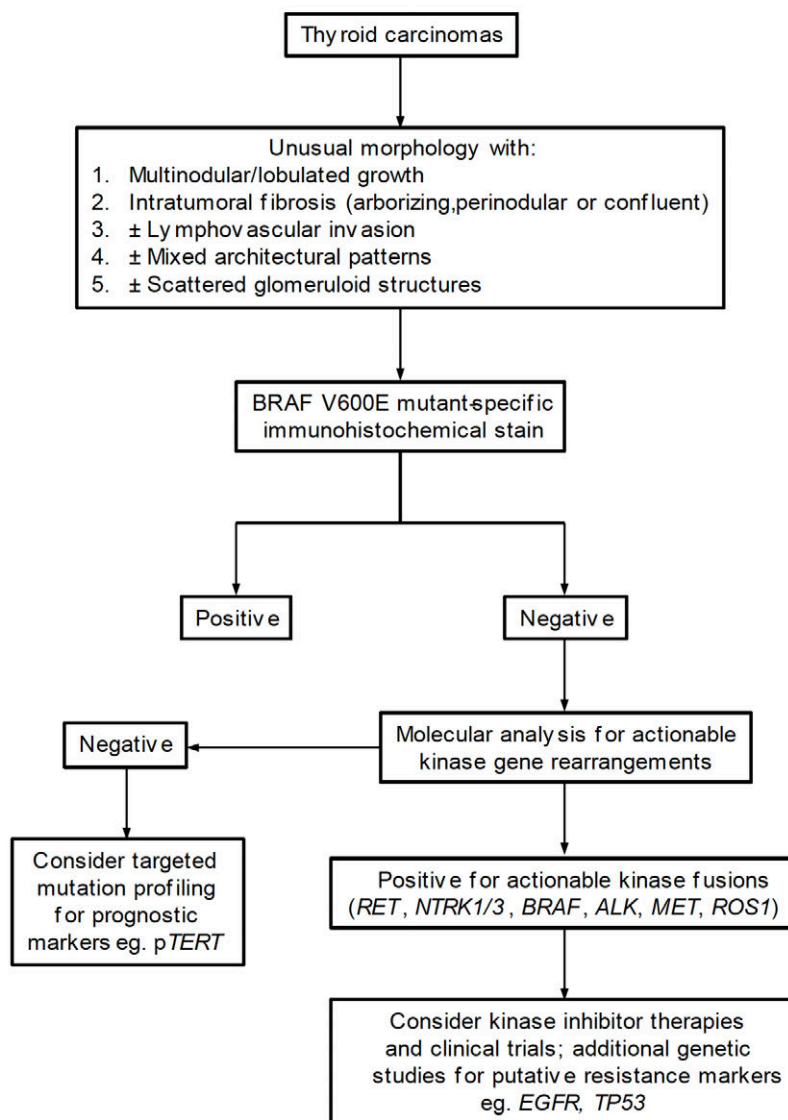
NTRK-rearranged thyroid carcinomas: Pan-TRK immunohistochemistry has reported sensitivity of 58-82% and specificity of 100%. Sensitivity appears to be higher in NTRK1- (96-100%) and NTRK2- (100%) rearranged cases compared to NTRK3- rearranged cases (50-79%)

ALK-rearranged thyroid carcinomas: ALK immunohistochemical stain has reported sensitivity of 100% and specificity of 75-100%

### Molecular Testing:

FISH is conventional standard method with limited multiplexing capability. Next-generation sequencing provides comprehensive approach for identifying therapeutic targets with high throughput advantage.

### Algorithmic Approach for Selective Molecular Testing



## References

1. Z. Zheng, M. Liebers, B. Zhelyazkova, Y. Cao, D. Panditi, K. D. Lynch, et al., "Anchored multiplex PCR for targeted next-generation sequencing," *Nat Med*, vol. 20, pp. 1479-84, Dec 2014.
2. Y. E. Nikiforov, J. M. Rowland, K. E. Bove, H. Monforte-Munoz, and J. A. Fagin, "Distinct pattern of ret oncogene rearrangements in morphological variants of radiation-induced and sporadic thyroid papillary carcinomas in children," *Cancer Res*, vol. 57, pp. 1690-4, May 1 1997.
3. K. Iyama, M. Matsuse, N. Mitsutake, T. Rogounovitch, V. Saenko, K. Suzuki, et al., "Identification of Three Novel Fusion Oncogenes, SQSTM1/NTRK3, AFAP1L2/RET, and

- PPFIBP2/RET, in Thyroid Cancers of Young Patients in Fukushima," *Thyroid*, vol. 27, pp. 811-818, Jun 2017.
4. M. L. Prasad, M. Vyas, M. J. Horne, R. K. Virk, R. Morotti, Z. Liu, et al., "NTRK fusion oncogenes in pediatric papillary thyroid carcinoma in northeast United States," *Cancer*, vol. 122, pp. 1097-107, Apr 1 2016.
  5. R. J. Leeman-Neill, L. M. Kelly, P. Liu, A. V. Brenner, M. P. Little, T. I. Bogdanova, et al., "ETV6-NTRK3 is a common chromosomal rearrangement in radiation-associated thyroid cancer," *Cancer*, vol. 120, pp. 799-807, Mar 15 2014.
  6. H. M. Rabes, E. P. Demidchik, J. D. Sidorow, E. Lengfelder, C. Beimfohr, D. Hoelzel, et al., "Pattern of radiation-induced RET and NTRK1 rearrangements in 191 post-chernobyl papillary thyroid carcinomas: biological, phenotypic, and clinical implications," *Clin Cancer Res*, vol. 6, pp. 1093-103, Mar 2000.
  7. J. C. Ricarte-Filho, S. Li, M. E. Garcia-Rendueles, C. Montero-Conde, F. Voza, J. A. Knauf, et al., "Identification of kinase fusion oncogenes in post-Chernobyl radiation-induced thyroid cancers," *J Clin Invest*, vol. 123, pp. 4935-44, Nov 2013.
  8. M. E. Cabanillas, M. Ryder, and C. Jimenez, "Targeted Therapy for Advanced Thyroid Cancer: Kinase Inhibitors and Beyond," *Endocr Rev*, vol. 40, pp. 1573-1604, Dec 1 2019.
  9. A. Chou, S. Fraser, C. W. Toon, A. Clarkson, L. Sioson, M. Farzin, et al., "A detailed clinicopathologic study of ALK-translocated papillary thyroid carcinoma," *Am J Surg Pathol*, vol. 39, pp. 652-9, May 2015.
  10. G. Hrustanovic and T. G. Bivona, "RAS-MAPK in ALK targeted therapy resistance," *Cell Cycle*, vol. 14, pp. 3661-2, 2015.
  11. Chu YH et al: Clinicopathologic and molecular characterization of NTRKrearranged thyroid carcinoma (NRTC). *Mod Pathol*. 33(11):2186-97, 2020
  12. Chu YH et al: Clinicopathologic features of kinase fusion-related thyroid carcinomas: an integrative analysis with molecular characterization. *Mod Pathol*. 33(12):2458-72, 2020

# Case 60

Contributed by Manuel Sobrinho-Simões - University Hospital of São João & Ipatimup, Porto, Portugal

---

(The case was sent to us for a second opinion during the follow-up)

## Clinical history

48-year-old woman submitted to total thyroidectomy after FNA of large nodule of the right lobe - Suspicious of papillary carcinoma (Bethesda V). The right lobe was almost totally occupied by a well circumscribed, 3.6 cm tumour. No molecular study had been performed.

## Macroscopy

The thyroid weighed 20g. The right lobe was occupied by a well-circumscribed nodule, partially encapsulated, solid and whitish, measuring 3.6x2.2x2.0 cm. The remaining parenchyma was brownish and homogenous.

## Histologically

The tumour looks like a typical a predominantly follicular subtype (Substituting "variant" by "subtype") of papillary thyroid carcinoma. Despite the frank predominance of follicular growth pattern there were dispersed minute foci with papillary architecture, as well as neoplastic infoldings resembling incipient papillae.

The tumour was circumscribed and partially encapsulated (thin or very thin capsule). In several foci, the submitted slides displayed equivocal signs of capsular or vascular invasion. There were no foci displaying so-called high-grade features (No necrosis and rare mitoses).

We did not observe unequivocal signs of capsular or vascular invasion. Since the proposed diagnosis had been "Encapsulated, predominantly follicular subtype of PTC with capsular and vascular invasion" we asked for as many as possible recuts, searching for signs of invasion by immunohistochemistry.

## Immunohistochemistry

We did not observe any hint of capsular or vascular invasion using CD31, D2-40 and CD-34. The ki-67 proliferation index was very low. (No problem if it was greater...).

Immunohistochemistry for BRAF V600E mutation (VE1) was negative.

## Molecular results

No mutations were detected in TERTp, BRAF V600E, NRAS, HRAS, KRAS or p53 (Ex. 5 to 11).

**Diagnosis: Non-invasive, encapsulated, predominantly follicular subtype of papillary thyroid carcinoma (See comments below)**

## Treatment and follow-up

October 2017 - After the diagnosis of Encapsulated predominantly follicular subtype of PTC with capsular and vascular invasion, the patient was treated with I<sup>131</sup> (150mCi).

During the follow-up no problems were detected and in October 2021 the patient was OK (Cervical echography without alterations and frenation of thyroglobulin under control).

## Comments

We selected this particularly innocent case in order to discuss a number of points, now that we are preparing the publication of the 5th ed of the WHO Endocrine Tumours, using the updated frame and a couple of novelties advanced by Baloch et al (2022).

Cases like this one, as well as oncocytic tumours, isolated or multiple, and cases similar to case #57 presented by Vania Nosé which were classified as NIFTP, altogether such cases correspond to (fairly) well circumscribed tumours that encompass the large majority of thyroid neoplasms sent to us for a second opinion.

Before addressing the most interesting issues related to the diagnosis of benign and/or (extremely) low malignant tumours, I guess it is necessary to stress two "previous" points: a) The handout of case #57 (NIFTP) made by Vania Nosé is very well written and covers in depth many aspects of the diagnosis of well differentiated follicular patterned thyroid tumours. Please use her handout as an Introduction to NIFTP and similar neoplasms

(Personally, I think the name is not adequate and, hopefully, it will be possible to progress towards a better approach and a clearer nomenclature in the future).

b) We realize that the submitted diagnosis of Invasive EV(S) PTC in Case #60 had already led to overtreatment of the patient (I131 - 150mCi). I am specifically mentioning this aspect, regardless of the concrete situation which was not adequately treated, because many authors are discussing the advantages of "Thyroidectomy without radioiodine in patients with low-risk thyroid cancer" (Leboulleux S et al, 2022). This point deserves to be considered in the future whenever making a diagnosis of low-risk thyroid cancer.

[A parenthesis regarding the limitations radioiodine of therapy. Incidentally, this is particularly important in cases that were previously diagnosed as papillary microcarcinoma. The new classification of PTC (WHO, 2022) requires subtyping of papillary microcarcinomas similar to their counterparts that exceed 1.0 cm and recommends designating as histopathologic subtypes of PTC rather than a papillary microcarcinoma (Baloch et al, 2022).

I fully agree with this reclassification and it is good to "kill" the papillary microcarcinoma but it does not solve the huge problem of millions of incidentally found (very) small neoplasms. I (and many other authors) go on thinking that the Porto Proposal made 20 years ago, by Juan Rosai and three old/very good friends, makes sense regarding the need to identify "papillary microtumours" in the appropriate context (Rosai J et al, 2003). Unfortunately, this suggestion was not adopted by WHO despite the excellent study entitled "Thyroid Papillary Microtumor: Validation of the (Updated) Porto Proposal Assessing Sex Hormone Receptor Expression and Mutational BRAF Gene Status" made by the group of José Manuel Cameselle-Teijeiro (Aliyev et al, 2020)]

Besides the problem of separating adenoma from NIFTP, as well as the problem of uncertain malignant tumours (see Case #57), the diagnostic difficulties in our Consultancy Practice in benign /low malignancy tumours in neoplasms raising the diagnosis of PTC for architectural reasons, together with nuclear features, stem from the following:

The amount of papillae allowing the classification of NIFTP (<1% papillae? more?)

The putative meaning of BRAF V600E mutations in predominantly follicular patterned tumours (Namely in molecular terms because IHC still raises some difficulties).

More rarely (despite progressively more frequent), the putative meaning of TERT promoter mutation alone or together with other mutations. Our group was not particularly impressed by the putative prognostic meaning of BRAF mutations (Soares P et al, 2003; Trovisco V et al, 2004; Melo M et al, 2017).

In this concrete case, there were dispersed minute foci of papillary structures in a tumour whose nuclei were typical PTC nuclei (score 3). Since it was a well

circumscribed/encapsulated tumour without signs of capsular or vascular (venous) invasion, and wild type BRAF V600E, one might be inclined to classify the tumour as NIFTP, provided the papillae were rare. I did not follow this classification because I think the criterion of 1% threshold is too fragile, namely if one finds many minute “true” papillae throughout the tumour. It is also known that if one finds BRAF-V600E mutation, we usually find some (few) papillary structures and question the diagnosis of NIFTP.

I would follow a similar approach in well-circumscribed cases in which the molecular study discloses the presence of a TERT promoter mutation. In our experience, this type of finding is rare since they tend to coexist with advanced carcinomas. In well circumscribed tumours, TERTp mutation are more frequent in the follicular “side” than in the papillary “side”, sometimes together RAS mutation, but, per se, I would not jump to a diagnosis of carcinoma, unless there are unequivocal signs of capsular or, more importantly, vascular (venous) invasion. In other words, I think we can not make a diagnosis of malignancy based upon only in molecular findings. Since our group has been particularly involved in the demonstration of the prognostic value of TERT promoter mutations in thyroid carcinomas (Melo M et al, 2017) it is important to stress that we have shown the presence of TERT promoter mutations in thyroid adenomas associated to previous radiation (Boaventura P et al, 2017). This finding fits with a couple of consultancy cases of “Follicular adenomas” with TERTp and RAS mutation recently proposed with the diagnosis of malignancy.

We, as the large majority of thyroid tumour pathologists, feel the need to follow the separation of follicular carcinomas from papillary carcinomas upon morphology, architecture and invasiveness, rather than upon nuclear features. Molecular features may help in the aforementioned separation whenever it is possible to use the presence/absence of mutations as a distinctive characteristic in the appropriate context. The existence of a group of thyroid carcinomas without RAS and BRAF mutations encompasses very interesting cases and deserves a special interest in etiopathogenesis (e.g. DICER1 mutation and oncocytic tumours at large).

In this particular setting (case #60) we did not observe RAS, BRAF, TERT promoter and p53 mutations and concluded: Not invasive, encapsulated, predominantly follicular subtype of PTC. I am convinced this subtype of tumours, provided there is not any signs of invasion, will turn into Follicular Adenoma (As well as the NIFTPs in the future).

## References

1. Soares P et al. BRAF mutations and RET/PTC rearrangements are alternative events in the etiopathogenesis of PTC. *Oncogene* 22: 4578-80, 2003
2. Rosai J et al. Renaming papillary microcarcinoma of the thyroid gland: the Porto proposal. *Int J Surg Pathol.* 11:249-51, 2003
3. Trovisco V et al. BRAF mutations are associated with some histological types of papillary thyroid carcinoma. *J Pathol.* 202:247-51, 2004
4. Boaventura P et al. TERT promoter mutations: A genetic signature of benign and malignant tumours occurring the context of tinea capitis irradiation. *Eur J Endocrinol* 176:49, 2017
5. Melo M et al. TERT, BRAF, and NRAS in Primary Thyroid Cancer and Metastatic Disease. *J Clin Endocrinol Metab.* 102:1898-1907, 2017
6. Aliyev E et al. Thyroid Papillary Microtumor: Validation of the (Updated) Porto Proposal Assessing Sex Hormone Receptor Expression and Mutational BRAF Gene Status. *Am J Surg Pathol.* 44:1161-1172, 2020
7. Leboulleux S et al. Thyroidectomy without Radioiodine in Patients with Low-Risk Thyroid Cancer. *N Engl J Med.* 386:923-932, 2022
8. Baloch ZW et al. Overview of the 2022 WHO Classification of Thyroid Neoplasms. *Endocr Pathol.* 33:27-63, 2022

## Case 61

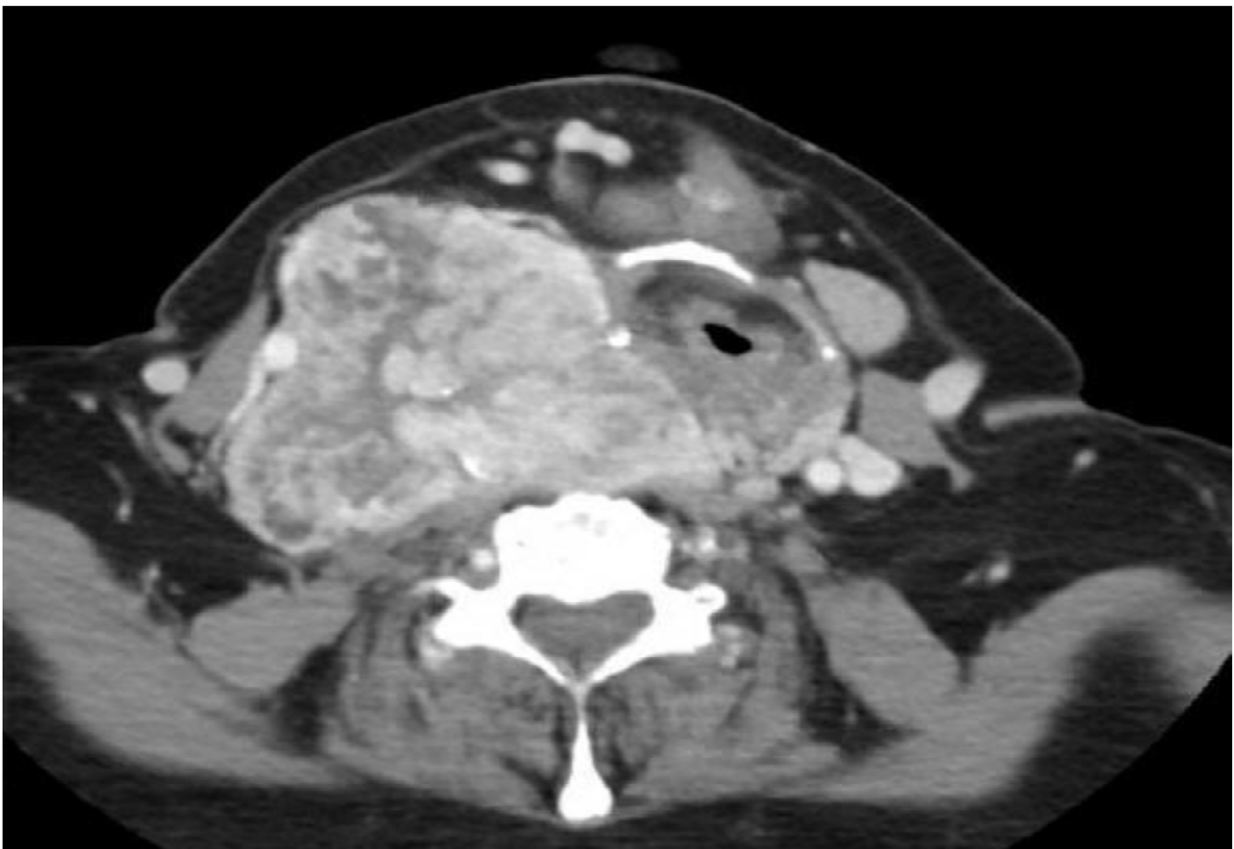
Contributed by: Vania Nosé, MD, PhD - Massachusetts General Hospital, Harvard Medical School, Boston, MA, USA

---

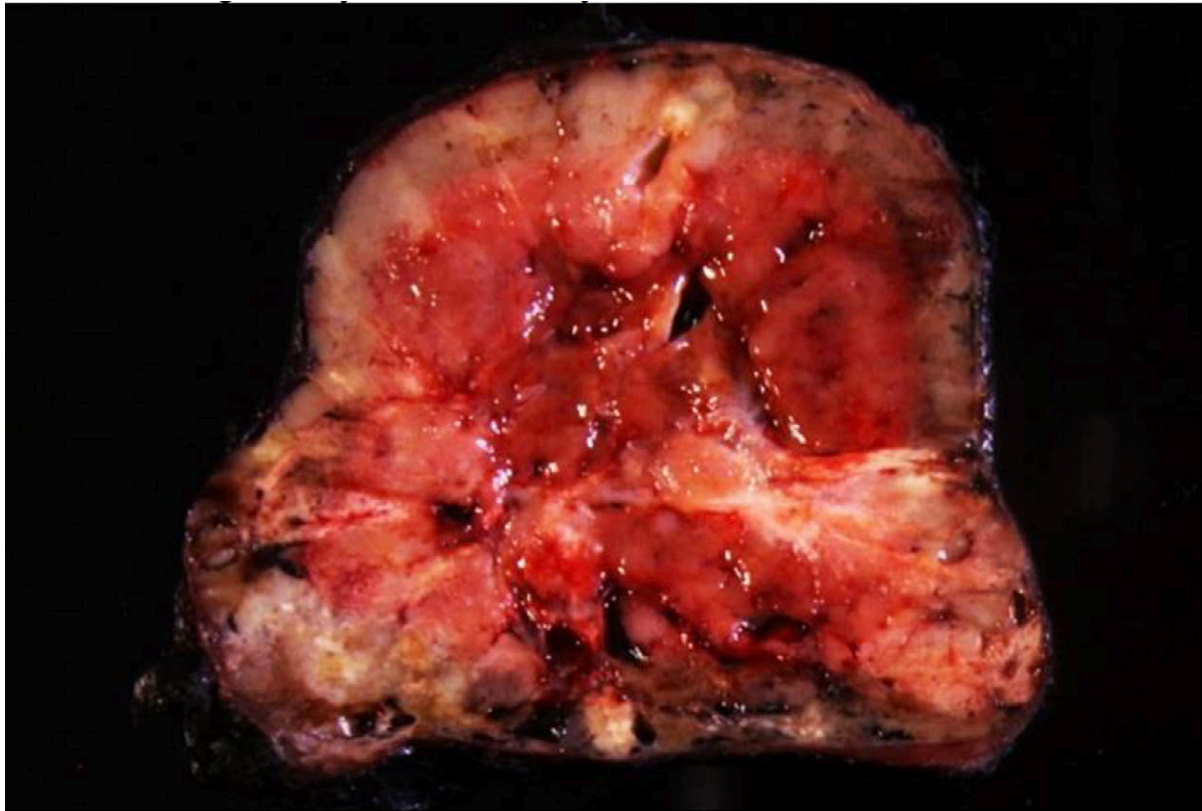
### Clinical History:

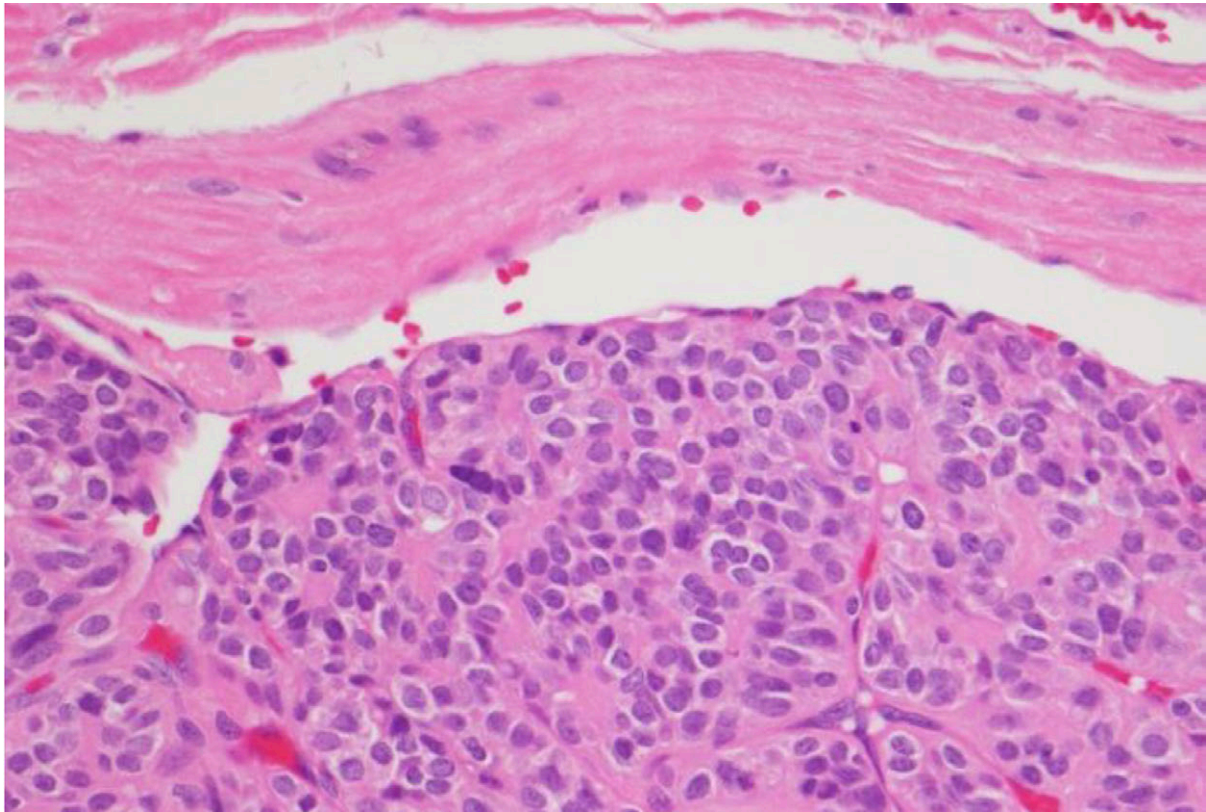
75-year-old woman with slowly enlarging thyroid followed for several years, with a large goiter on the right side she also has HPT with a calcium of 10.9 and PTH of 93 with a possible parathyroid adenoma adjacent to the left that is the smaller side thyroid. CT scan and ultrasound shows a right lobe which is mass of 9 cm going from the parotid to just below the clavicle. She has several small nodules in the left lobe as well. FNA were done in several occasions, benign.

### Neck US and CT:



**Right thyroidectomy:**





## Final Diagnosis:

RIGHT LOBE THYROID (223 grams): Follicular thyroid carcinoma, angioinvasive, composed by architecturally distinct nodules with follicular pattern, solid pattern, and sinusoidal pattern with fibrosis, cystic changes and focal calcifications, occupying most of the right thyroid lobe (8.0 cm). Mitosis up to 2/50 HPF. No necrosis is seen.

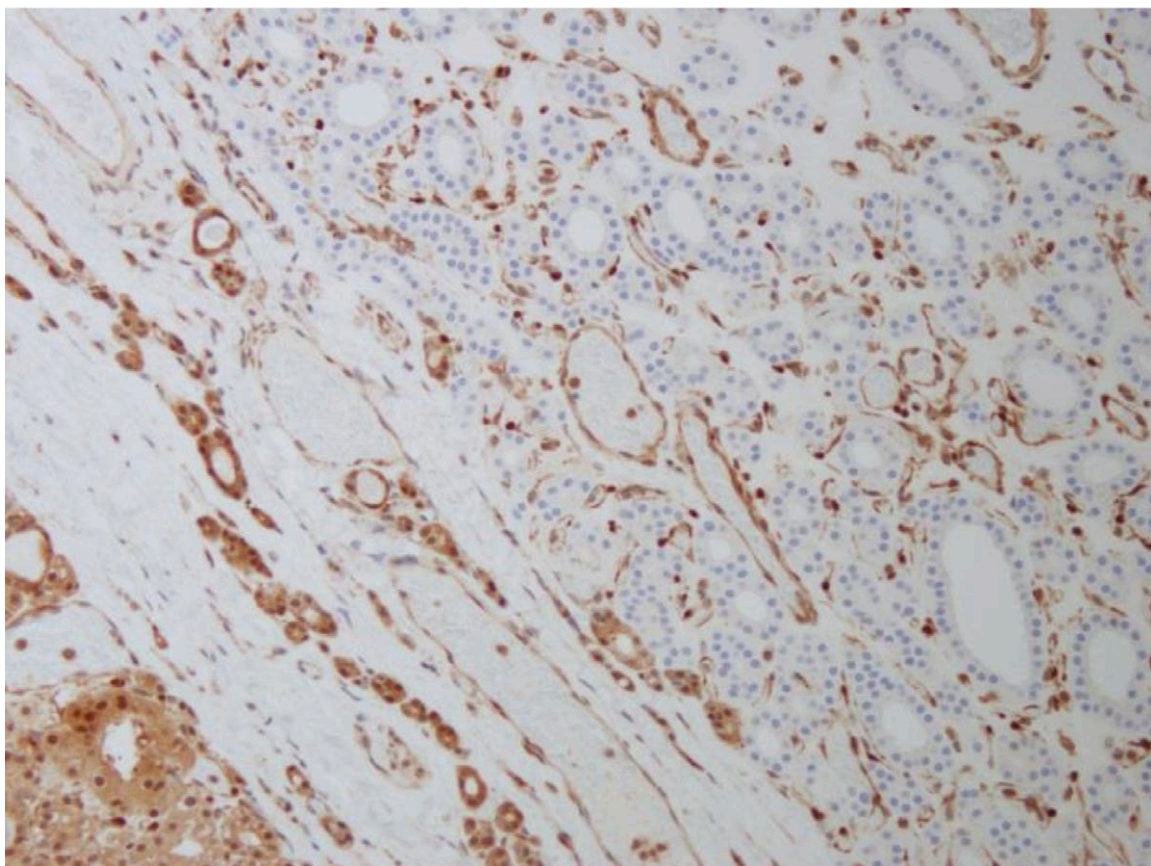
Immunohistochemistry performed at MGH reveals the following profile in the lesional cells: POSITIVE: PTEN (lost in follicular cells) NEGATIVE: p53 (wild type) HBME1  
Immunohistochemistry performed for BRAFV600E mutation using the mutation-specific BRAF (VE1) antibody is NEGATIVE in tumor cells, consistent with an absence of BRAFV600E mutation in this tumor. Ki67 proliferative index is focally up to 6.5%. No parathyroid and no lymph nodes present.

**Note:** This large tumor nodule occupying most of the 223 g right lobe which, is well circumscribed and encapsulated, is composed by coalescents nodules with distinct architectural patterns with different morphology in different sections of the lesion. The

different areas of this tumor showed areas with solid component, areas with follicular component, areas with more sinusoidal trabecular component with the cystic changes, fibrosis, as well as areas with hemorrhage, fibrosis, and calcification.

RIGHT PARATHYROID, EXCISION: Enlarged (380 mg) parathyroid with a central nodular hypercellular with mixed oncocytic and clear cell change and an apparent normocellular rim. The findings, in context, would support a diagnosis of parathyroid adenoma. Clinical and serologic correlation are needed.

THYROID, LEFT LOBECTOMY (7.2 g): Diffuse nodular hyperplastic and adenomatous changes with focal oncocytic change. Scar with foreign body giant cell reaction infiltrating skeletal muscle consistent with prior surgical site.



PTEN loss by immunohistochemistry. Endothelial cells and adjacent thyroid with preserved PTEN immunoreexpression. Patient suggested to get *PTEN* mutation analysis and was found to have germ line mutation of *PTEN* gene.

## PTEN Hamartoma Tumor Syndrome (PHTS)

PTEN hamartoma tumor syndrome (PHTS) is the molecular diagnostic term describing patients with diverse syndromes. It is an autosomal dominant disorder caused by a germline mutation in *PTEN* (*phosphatase and tensin homolog, deleted on chromosome 10*). PTEN Hamartoma Tumor Syndrome includes Cowden syndrome (CS), Bannayan-Riley Ruvalcaba syndrome (BRRS), Proteus syndrome (PS), and Proteus-like syndrome. First described in 1963 (named after the family in which it was described). CS is the most common syndrome and characterized by the development of multiple hamartomas and with a high risk for benign and malignant tumors of the thyroid, breast, and endometrium. Affected individuals usually have macrocephaly, trichilemmomas, and papillomatous papules, and present by the late 20s. BRRS is a congenital disorder characterized by macrocephaly, intestinal hamartomatous polyposis, lipomas, and pigmented macules of the glans penis. PS is a complex, highly variable disorder involving congenital malformations and hamartomatous overgrowth of multiple tissues, as well as connective tissue nevi, epidermal nevi, and hyperostoses. Proteus-like syndrome is undefined but refers to individuals with significant clinical features of PS who do not meet the diagnostic criteria for PS.

### Etiology:

The diagnosis of PHTS is made only when a *PTEN* pathogenic variant is identified. When accrued from tertiary referral centers, up to 85% of individuals who meet the diagnostic criteria for CS and 65% of individuals with a clinical diagnosis of BRRS have a detectable *PTEN* pathogenic variant. However, in prospective accrual series, from both academic and community clinical settings, approximately 25% of individuals who meet the clinical diagnostic criteria for CS have a germline *PTEN* pathogenic variant. Preliminary data also suggest that up to 50% of individuals with a Proteus-like syndrome and up to 20% of individuals who meet the clinical diagnostic criteria of Proteus syndrome have an identifiable *PTEN* pathogenic variant.

## Epidemiology:

Although CS has a reported incidence of 1 in 200,000, it is likely that it is actual more common and that cases are overlooked because of the complex clinical criteria for CS, the fact that many of the manifestations of CS are common in the general population, and the finding that only about half of the patients with CS have a known family history. However, a diagnosis of CS is important because it confers a significant risk for cancer. Once a diagnosis of CS is made, there are screening and genetic counseling guidelines outlined by the NCCN. Thus, recognition of CS is important so that cancer screening and genetic counseling can be initiated.

## Genetic susceptibility:

Germline mutations in *PTEN* were first described in patients with CS in 1997. *PTEN* is a tumor suppressor gene that maps to 10q23.3 and encodes a 403 amino acid dual-specificity (lipid and protein) phosphatase. While most cases are inherited in a family for generations, following an autosomal dominant pattern, at least 10% and perhaps as many as 44% of cases are due to a new (de novo) mutation. Approximately 85% of patients with CS harbor intragenic mutations of *PTEN* or mutations in the promoter region. Germline pathogenic *PTEN* mutations cause PHTS, but rarely, other genes can be involved: *PIK3CA*, *AKT1*, *SDHx*, *KLLN* and *SEC23B*. 8% of CS/CS-like and BRRS so-called *PTEN*-wild-type patients, other gene alterations were reported with *MUTYH*, *RET*, *TSC2*, *BRCA1*, *BRCA2*, *ERCC2*, and *HRAS*.

## Clinical features:

Clinical presentations can vary dramatically from patient to patient, even among those in the same family. Features of this condition that may assist in diagnosis prior to cancer development can be subtle and difficult to recognize. Clinical criteria for CS based on guidelines put forth by the International Cowden Consortium have been delineated by the National Comprehensive Cancer Network (NCCN) and include pathognomonic, major, and minor criteria.

Adult Lhermitte-Duclos disease (LDD), autism spectrum disorder with macrocephaly, and 2 biopsy-proven trichilemmomas are all pathognomonic for CS.

The major criteria include breast cancer, mucocutaneous lesions (trichilemmomas, multiple palmo-plantar keratoses, multifocal or extensive oral mucosal papillomatosis,

multiple cutaneous facial papules, and macular pigmentation of the glans penis), endometrial cancer, nonmedullary thyroid cancer, macrocephaly, and multiple gastrointestinal hamartomas or ganglioneuromas.

The minor criteria include mental retardation, autism spectrum disorder, fibrocystic disease of the breast, other thyroid lesions (adenomas and nodular hyperplasia), lipomas, fibromas, renal cell carcinoma, and uterine fibroids.

CS is a multiple hamartoma syndrome with a high risk for benign and malignant tumors of the thyroid, breast, and endometrium. Affected individuals usually have macrocephaly, trichilemmomas, and papillomatous papules, and present by the late 20s. The lifetime risk of developing breast cancer is 85%. Moreover, the average age at diagnosis is between 38 and 46 years, younger than patients with sporadic breast cancer. The lifetime risk for thyroid cancer

(usually follicular, rarely papillary, but never medullary thyroid cancer) is approximately 35%. The risk for endometrial cancer, although not well defined, may approach 28%.

Although breast, endometrial, and thyroid malignancies are the most frequent cancers in CS patients, patients with CS also appear to be at increased risk for developing renal cell carcinoma, melanoma, and glial tumors.

BRRS is characterized by macrocephaly, intestinal hamartomatous polyposis, lipomas, and pigmented macules of the glans penis.

PS is a disorder involving malformations and hamartomatous overgrowth of multiple tissues, as well as connective tissue nevi, epidermal nevi, and hyperostoses.

Proteus-like syndrome is undefined but refers to individuals with significant clinical features of PS who do not meet the diagnostic criteria for PS.

## Thyroid Findings:

The thyroid disease in PHTS is part of the so-called “syndromic familial follicular cell-derived thyroid tumors”.

Thyroid pathologic findings in patients with PHTS that normally affect the follicular cells include multinodular thyroid disease, multiple adenomatous nodules (MAN), follicular adenoma, follicular carcinoma, and less frequently papillary carcinoma. Follicular carcinoma is an important feature in CS and BRRS. Per the diagnostic criteria for CS, follicular carcinoma is a major criterion, and multinodular thyroid disease, adenomatous nodules, and follicular adenomas are minor criteria, with a frequency of 50% to 67%.

In an important study evaluating thyroidectomy specimens from patients with CS and BRRS, Laury et al found that multiple adenomatous nodules were the most common

finding (present in 75%), followed by papillary thyroid carcinoma (PTC; 60%), lymphocytic thyroiditis (55%), C-cell hyperplasia (55%), follicular carcinomas (45%), follicular adenomas (25%), and nodular hyperplasia (25%).

Multiple adenomatous nodules are characteristic findings in these syndromes, and present grossly as multiple firm yellow-tan well-circumscribed nodules. These nodules are multicentric, bilateral, well-circumscribed unencapsulated features like follicular adenomas. These tumors are more frequently multicentric. Most carcinomas arise in a background of MAN. Although cancer risk in BRRS was expected to be like the general population, Laury et al found 4 cases of follicular thyroid carcinoma (67%), showing that this type of carcinoma was more frequent in the pediatric population; we believe that these patients should follow the same management guidelines as CS.

Immunohistochemistry for PTEN shows loss of staining of the follicular cells.

Medullary thyroid carcinoma (MTC) is not considered part of the spectrum of PHTS, however, earlier studies, including two studies by us, have identified C-cell hyperplasia (CCH) in individuals affected with this syndrome.

Careful phenotyping gives further support for the suggestion that BRRS and CS are actually one condition, presenting at different stages. The constellation of histologic findings in thyroidectomy specimens from CS is unusual, but are non-specific for CS. There were no morphologic differences between the thyroid findings in CS and BRRS. Also, there was no correlation between specific *PTEN* germline mutations and pathologic findings.

## References:

1. Nosé V, Gill A, Teijeiro JMC, Perren A, Erickson L.. Overview of the 2022 WHO Classification of Familial Endocrine Tumor Syndromes Endocr Pathol Mar13, 2022. Online ahead of print
2. Yehia L and Eng C (2020) PTEN hamartoma tumour syndrome: what happens when there is no PTEN germline mutation? Hum Mol Genet 29:R150-R157
3. Guilmette J, Nosé V. Hereditary and familial thyroid tumors. Histopathology. 2018;72(1):70-81.
4. Nosé V. Genodermatosis Affecting the Skin and Mucosa of the Head and Neck: Clinicopathologic, Genetic, and Molecular Aspect--PTEN-Hamartoma Tumor Syndrome/Cowden Syndrome. Head Neck Pathol. 2016 Jun;10(2):131-8.
5. Nosé V. Familial thyroid cancer: a review. Mod Pathol. 2011 Apr;24 Suppl 2:S19-33.

6. Laury AR, Bongiovanni M, Tille JC, Kozakewich H, Nosé V. Thyroid pathology in PTEN hamartoma tumor syndrome: characteristic findings of a distinct entity. *Thyroid*. 2011 Feb;21(2):135-44.
7. J Dotto and V Nosé. Familial Thyroid Carcinoma A diagnostic algorithm. *Adv Anat Pathol* 2008;15:332-349.
8. Harach HR, et al. Thyroid pathologic findings in patients with Cowden disease. *Am Diagn Pathol* 1999, 3:331-339.
9. Robert Pilarski. Cowden Syndrome: A critical review of the literature; *J Genet Counsel*, 2009 18:13.

## Case 62

Contributed by Elisabete Rios - University Hospital of São João

---

### Clinical history

82-year-old, female, with a solid nodule (EU-TIRADS-4) in the right lobe of thyroid and multiple right cervical lymph nodes, the largest measuring 5cm, detected on routine surveillance after a cardiac surgery for symptomatic severe aortic stenosis. The patient was submitted to total thyroidectomy with lymph node dissection.

### Macroscopy

The thyroid weighted 20gr and included a 4.7x2.6x1.7cm right lobe, a 4.5x3.1x1.9cm left lobe and a *central compartment lymph node* dissection attached to the isthmus, from which 14 lymph nodes were isolated. The external surface was focally lacerated in the upper right lobe. On cut surface, a poorly circumscribed whitish solid nodule measuring 1.5x0.9x0.7cm with some calcifications was identified in the upper right lobe (figure 1). Additionally, it was received a right cervical lymph node dissection, from which 13 lymph nodes were isolated, the largest one measuring 5x4.5x4.2cm, displaying tan solid/cystic and necrotic features on cut surface (figure 2). Some muscle tissue exhibiting whitish infracentimetric solid areas was identified in the lymph node dissection specimen.

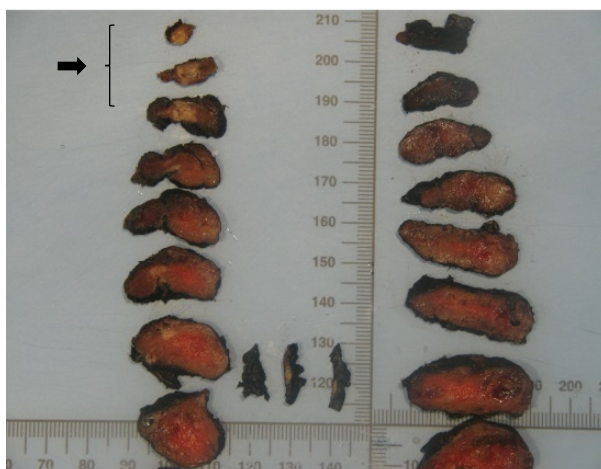


Figure 1. Total



Figure 2. Largest right cervical lymph node.

## Microscopy

The thyroid nodule displayed predominant follicular growth pattern and, focally, papillary architecture in the setting of extensive sclerotic stroma with dystrophic and occasional psammomatous calcifications. The neoplastic cells had nuclear features of PTC, and focally (around 10%) exhibited tall cell features. The tumor infiltrated the thyroid parenchyma invading also the perithyroidal soft tissue, including the muscle tissue. There was *lymphatic* and *venous* invasion. Lymph node metastases were identified in 2 of the 14 lymph nodes isolated from the central compartment and in 9 of the 13 lymph nodes isolated from the right cervical lymph node dissection. Metastatic tumor displayed several growth patterns, including papillary, cystic, follicular and trabecular growth patterns and were composed *predominantly* or, even entirely, by tall cells disclosing abundant 'oncocytoïd' eosinophilic cytoplasm. *Extranodal extension* was observed in the *largest metastatic lymph node*. The resection margin was less than 1mm and the tumor was staged as pT3bN1b (AJCC 8<sup>th</sup> edition).

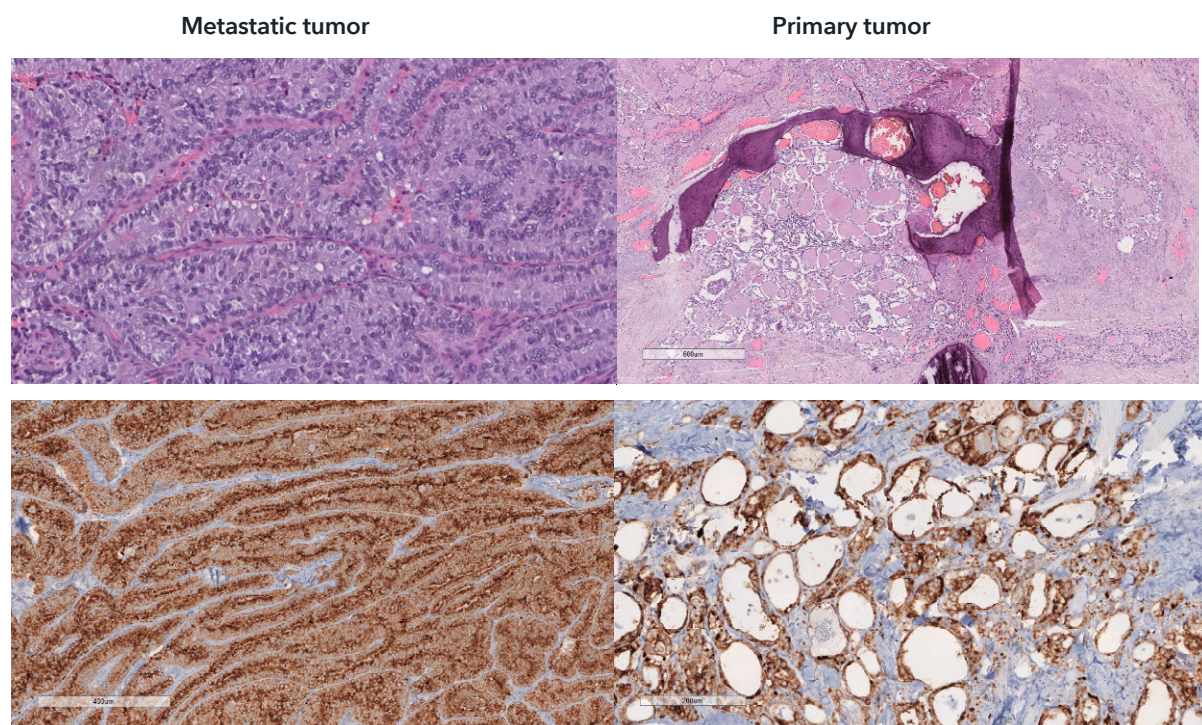


Figure 3. Histological features and IHC of BRAFV600E protein of both primary and metastatic tumors.

## Immunohistochemistry

The tumor cells were diffusely positive for TTF-1, thyroglobulin, PAX8 and BRAF V600E (VE1 clone).

## Molecular results

The study was performed in the tumor, obtaining DNA from thick sections (10 µm) of one paraffin block under histological control. No mutations were detected in *TERT*, *BRAF V600E*, *NRAS*, *HRAS*, *KRAS* or *p53*.

## Diagnosis

For practical purposes, our diagnosis was tall cell papillary thyroid carcinoma, taking in consideration also the metastases. Based only in the primary tumor some would rather prefer to classify it as papillary thyroid carcinoma with focal tall-cell change.

## Treatment and follow-up

After the diagnosis the patient was treated with I<sup>131</sup> (150mCi).  
During the follow-up no progression of disease were detected.

## Comments

This case (#62) was selected in order to stress some practical points regarding both the tall cell papillary thyroid carcinoma (TC-PTC), a subtype of PTC, and the papillary thyroid carcinoma with focal tall-cell change (PTC-TC), included in the spectrum of classical papillary thyroid cancer (PTC). Both are composed of cells that are 'tall', i.e. they are 2-3 times taller than wide, but in TC-PTC the tall cells comprise ≥30% of the tumor, while in PTC-TC the tall cells comprise <30% of the tumor. Compared to classical PTC, both tall-cell groups (especially those exceeding 10% tall-cell features) had higher rates of "aggressive" features, i.e. vascular invasion, gross extension to extrathyroidal tissues and spread to the lymph nodes in the neck. Additional features of TC-PTC include complex papillary formation with trabecular architecture ('tram track' pattern), older age, and the common occurrence of BRAF V600E mutations (approximately 80% of cases). Dedifferentiation of TC-PTC to spindle squamous variant of anaplastic thyroid carcinoma has been described.

According to current guidelines, patients with TC-PTC are considered at least intermediate-risk and are managed more aggressively in terms of surgery and adjuvant radioactive iodine (RAI) administration. Furthermore, it is known that TC-PTC represents a significant fraction of radioiodine refractory thyroid carcinomas.

Bongers PJ et al. (2019) emphasizes that papillary thyroid carcinomas with focal tall cell change are as aggressive as tall cell subtypes and should not be considered as low-risk disease, advocating that patients with a tall-cell proportion >10% should be also targeted for more aggressive therapy and closer monitoring.

Taking together all the above, it is important to recognize correctly TC-PTC. Unfortunately, its diagnosis is rather inconsistent among pathologists (even at the expert level) and discrepancies are probably due to the subjective nature of the interpretation of morphologic criteria, their frequently nonuniform distribution within the tumor and the lack of immunohistochemical or molecular markers for TC-PTC.

This case is consistent with the expected clinical, morphological and immunohistochemical characteristics of the TC-PTC; however, there was a notorious morphological discrepancy between the primary tumor (exhibiting focal tall cell changes) and the metastatic tumor (with tall cell features comprising at least 30% or more of the tumor), reinforcing the WHO recommendation that tall cell changes, even focal, should be documented.

The evaluation of surgically resected TC-PTC or PTC-TC by immunohistochemistry for BRAF mutation has diagnostic, prognostic and therapeutic implications. In this particular setting (case #62) the tumor cells were strongly positive for BRAF V600E by immunohistochemistry, but no mutation was found by Sanger sequencing. We think that this is due to false-negative genotyping rather than false-positive staining. Compared with wild-type PTCs, BRAF-mutated PTCs are associated with higher risk for recurrence, lymph node metastasis, extrathyroidal extension and, therefore, with advanced AJCC III/IV stage. Furthermore, BRAF-mutated PTCs have shown to have decreased response to RAI I-131 treatment due to loss of radioiodine avidity. Currently, BRAF-inhibitors may be used as an alternative treatment in advanced carcinomas; however, most patients develop resistance. Potential therapeutic strategies including combination of BRAF-inhibitors with other targeted agents and immunotherapy may be promising.

The identification of TC-PTC regards a difficult problem in terms of nomenclature. What proportion of cells need to be described as 'tall-cell' to define the cutoff for predicting outcomes and whether the tall cell features represent an independent prognostic factor for PTC are still a matter of debate.

## References

1. Hawk WA, Hazard JB. The many appearances of papillary carcinoma of the thyroid. *Cleve Clin Q* 1976; 43: 207- 215.
2. Bongers PJ, Kluijfhout WP, Verzijl R, et al. Papillary thyroid cancers with focal tall cell change are as aggressive as tall cell variants and should not be considered as low-risk disease. *Ann Surg Oncol* 2019; 26: 2533-2539.
3. Ho AS, Luu M, Barrios L, et al. Incidence and mortality risk spectrum across aggressive variants of papillary thyroid carcinoma. *JAMA Oncol* 2020; 6: 706-713.
4. Ito Y, Hirokawa M, Miyauchi A, et al. Prognostic significance of the proportion of tall cell components in papillary thyroid carcinoma. *World J Surg* 2017; 41: 742-747.
5. Johnson TL, Lloyd RV, Thompson NW, et al. Prognostic implications of the tall cell variant of papillary thyroid carcinoma. *Am J Surg Pathol* 1988; 12: 22-27.
6. Kazaure HS, Roman SA, Sosa JA. Aggressive variants of papillary thyroid cancer: incidence, characteristics and predictors of survival among 43,738 patients. *Ann Surg Oncol* 2012; 19: 1874- 1880.
7. Morris LG, Shaha AR, Tuttle RM, et al. Tall-cell variant of papillary thyroid carcinoma: a matched-pair analysis of survival. *Thyroid* 2010; 20: 153-158.
8. Shi X, Liu R, Basolo F, et al. Differential clinicopathological risk and prognosis of major papillary thyroid cancer variants. *J Clin Endocrinol Metab* 2016; 101: 264-274.
9. Xu B, Ibrahimasic T, Wang L, et al. Clinicopathologic features of fatal non-anaplastic follicular cell-derived thyroid carcinomas. *Thyroid* 2016; 26: 1588-1597.
10. Akslen LA, LiVolsi VA. Prognostic significance of histologic grading compared with subclassification of papillary thyroid carcinoma. *Cancer* 2000; 88: 1902- 1908.
11. Axelsson TA, Hrafnkelsson J, Olafsdottir EJ, et al. Tall cell variant of papillary thyroid carcinoma: a population-based study in Iceland. *Thyroid* 2015; 25: 216-220.
12. Ganly I, Ibrahimasic T, Rivera M, et al. Prognostic implications of papillary thyroid carcinoma with tall-cell features. *Thyroid* 2014; 24: 662-670.
13. Kim Y, Roh JL, Song DE, et al. Risk factors for posttreatment recurrence in patients with intermediate-risk papillary thyroid carcinoma. *Am J Surg* 2020; 220: 642-647.
14. Michels JJ, Jacques M, Henry-Amar M, et al. Prevalence and prognostic significance of tall cell variant of papillary thyroid carcinoma. *Hum Pathol* 2007; 38: 212-219.
15. Prendiville S, Burman KD, Ringel MD, et al. Tall cell variant: an aggressive form of papillary thyroid carcinoma. *Otolaryngol Head Neck Surg* 2000; 122: 352-357.
16. Regalbuto C, Malandrino P, Frasca F, et al. The tall cell variant of papillary thyroid carcinoma: clinical and pathological features and outcomes. *J Endocrinol Invest* 2013; 36: 249- 254.

17. Song E, Jeon MJ, Oh HS, et al. Do aggressive variants of papillary thyroid carcinoma have worse clinical outcome than classic papillary thyroid carcinoma? *Eur J Endocrinol* 2018; 179: 135- 142.
18. Wong KS, Higgins SE, Marqusee E, et al. Tall cell variant of papillary thyroid carcinoma: impact of change in WHO definition and molecular analysis. *Endocr Pathol* 2019; 30: 43-48.
19. Yanhua B et al. Updates in the Pathologic Classification of Thyroid Neoplasms: A Review of the World Health Organization Classification. *Endocrinol Metab.* 2020; 35(4):696-715. Published online December 2, 2020.
20. WHO Classification of Tumours Editorial Board. Endocrine and Neuroendocrine tumours [Internet]. Lyon (France): International Agency for Research on Cancer; 2022 [cited YYYY Mmm D]. (WHO classification of tumours series, 5th ed.; vol. 8). Available from: <https://tumourclassification.iarc.who.int/chapters/36>.

## Case 63

**Paul. E. Wakely, Jr., M.D., Department of Pathology, The Ohio State University, Wexner Medical Center, James Cancer Hospital, Columbus, OH. USA**

---

### History:

A 36-year-old woman presented with left lower flank point tenderness without a prior history of trauma to the area. In February 2017, an incidental 4.0 cm. left adrenal mass was noted by CT scan. In March 2018, the mass measured 4.6 cm. and was described as a complex cyst. A year later, in January, 2019 the mass was 4.9 cm. in maximum dimension. Serum levels of metanephrines, aldosterone, renin, and 24-hour urinary cortisol were all within normal limits. Most recent CT scan showed peripheral calcifications and internal layering with fluid-fluid levels. Although she was largely asymptomatic, the patient agreed to a robotic adrenalectomy.

### Pathology:

The specimen consisted of a left adrenal gland with adherent hemorrhagic soft tissue. The adrenal gland itself weighed 41.0 grams and measured 6.0 x 4.0 x 1.7 cm. Serial sections revealed a circumscribed, homogenous extremely spongy, red-brown mass measuring 3.6 cm. Within the mass mottled, gritty, tan calcifications ranged from 0.2-0.5 cm. The unremarkable yellow adrenal cortex had an average cortical thickness of 0.1 cm. Microscopic examination showed a thin rim of adrenal cortex surrounding an angiomatous lesion comprised of papillae of varying lengths (some markedly elongated) covered by a single layer of cytologically bland but hyperchromatic endothelial cells and small amounts of fibrin. The overall appearance at low power imitated that of placental chorionic villi. Immunostains confirmed the endothelial nature of cells with positive CD34, CD31, and ERG staining. Mitotic figures were absent.

**Diagnosis: Primary Papillary Endothelial Hyperplasia, Adrenal Gland**

## Discussion:

Papillary endothelial hyperplasia (PEH), so named by P. Masson in a 1923 case report *Hémangioendothéliome végétant intra-vasculaire. Bull Mem Soc Anat Paris 1923;93:517-23* where he described it in a 68 y/o man who had a painful rapidly growing hemorrhoid, is a benign proliferation of endothelium associated with vascular hemorrhage/ thrombosis, hemangioma, or other vascular malformations. It is not a neoplasm. Subsequent to his report, the lesion has been variously termed intravascular papillary endothelial hyperplasia, vegetant intravascular hemangioendothelioma, Masson lesion, and Masson pseudoangiosarcoma. PEH is almost always intravascular, often associated with a fibrin thrombus, hemorrhagic, and consists of a well-circumscribed mass containing papillary projections with hyalinized cores that mimic sclerotic chorionic villi. No anastomosing channels are present, but the endothelial cells lining these papillae can appear hyperplastic and hyperchromatic. In most instances, PEH is a straightforward diagnosis. Its appearance as a primary adrenal mass is distinctly unusual, having been reported in < 10 instances in the English literature. Its importance lies in not mistaking it for angiosarcoma, which has infrequently occurred. Kuo T. et al. Several years ago Chan et al. described a vascular lesion in lymph nodes that he and his co-authors named polymorphous hemangioendothelioma. Although not sanctioned by the WHO classification, this neoplasm has strikingly similar features to PEH. Whether it truly exists as a distinct entity is currently unknown.

## References:

1. Constantinou C, Sheldon D. Papillary endothelial hyperplasia of the adrenal gland: report of a case and review of the literature. *Am Surg.* 2008;74:813-6.
2. Wenig BM, Abbondanzo SL, Heffess CS. Epithelioid angiosarcoma of the adrenal glands. A clinicopathologic study of nine cases with a discussion of the implications of finding "epithelial-specific" markers. *Am J Surg Pathol.* 1994; 18:62-73.
3. Grajales-Cruz A, Baco-Viera F, Rive-Mora E, et al. Primary Adrenal Angiosarcoma: A rare and potentially misdiagnosed tumor. *Cancer Control.* 2017; 24:198-201.
4. DiIombi ML, Khani F, Epstein JI. Diagnostic dilemmas in enlarged and diffusely hemorrhagic adrenal glands. *Hum Pathol.* 2016;53:63-72.
5. Steffen C. The man behind the eponym: C. L. Pierre Masson. *Am J Dermatopathol.* 2003;25:71-76.

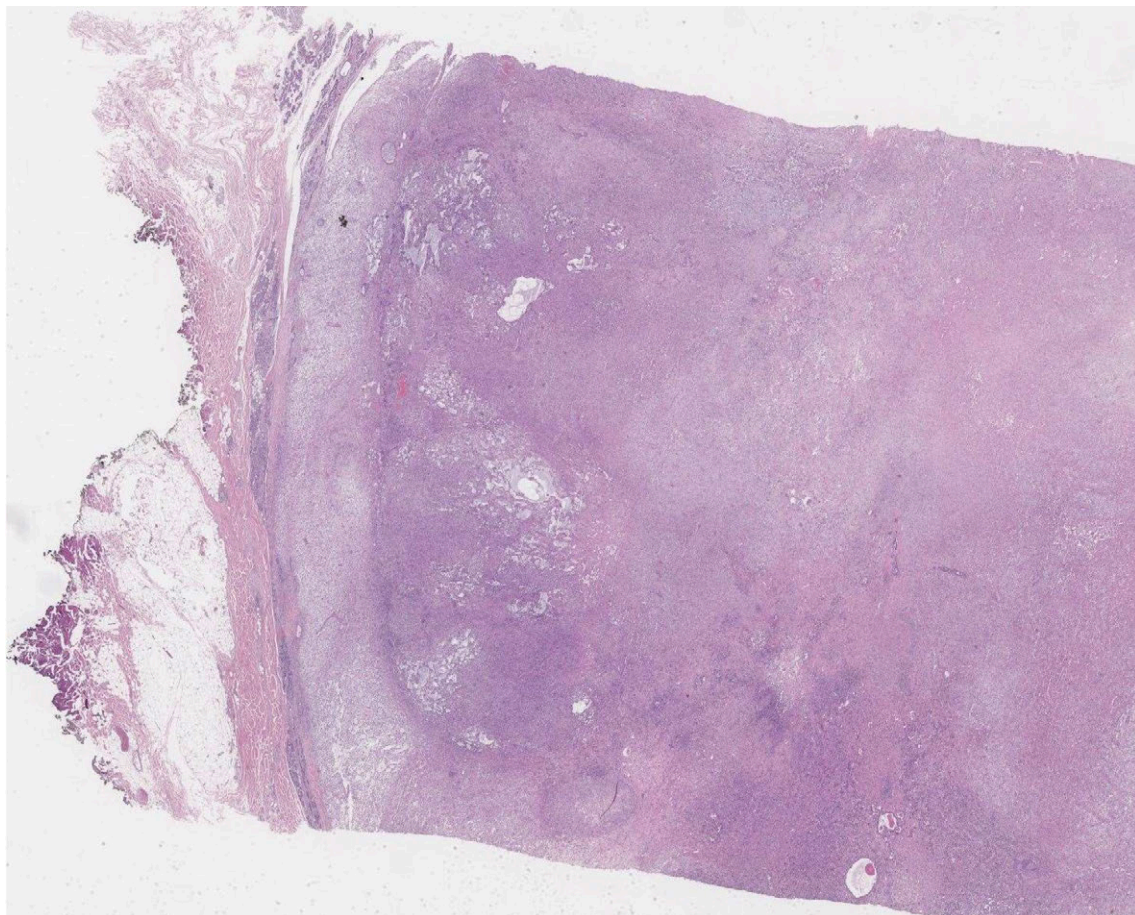
6. Kuo T, Sayers CP, Rosai J. Masson's "vegetant intravascular hemangioendothelioma:" a lesion often mistaken for angiosarcoma: study of seventeen cases located in the skin and soft tissues. *Cancer* 1976;38:1227-36.
7. Chan JK, Frizzera G, Fletcher CD, Rosai J. Primary vascular tumors of lymph nodes other than Kaposi's sarcoma. Analysis of 39 cases and delineation of two new entities. *Am J Surg Pathol.* 1992; 16:335-50.

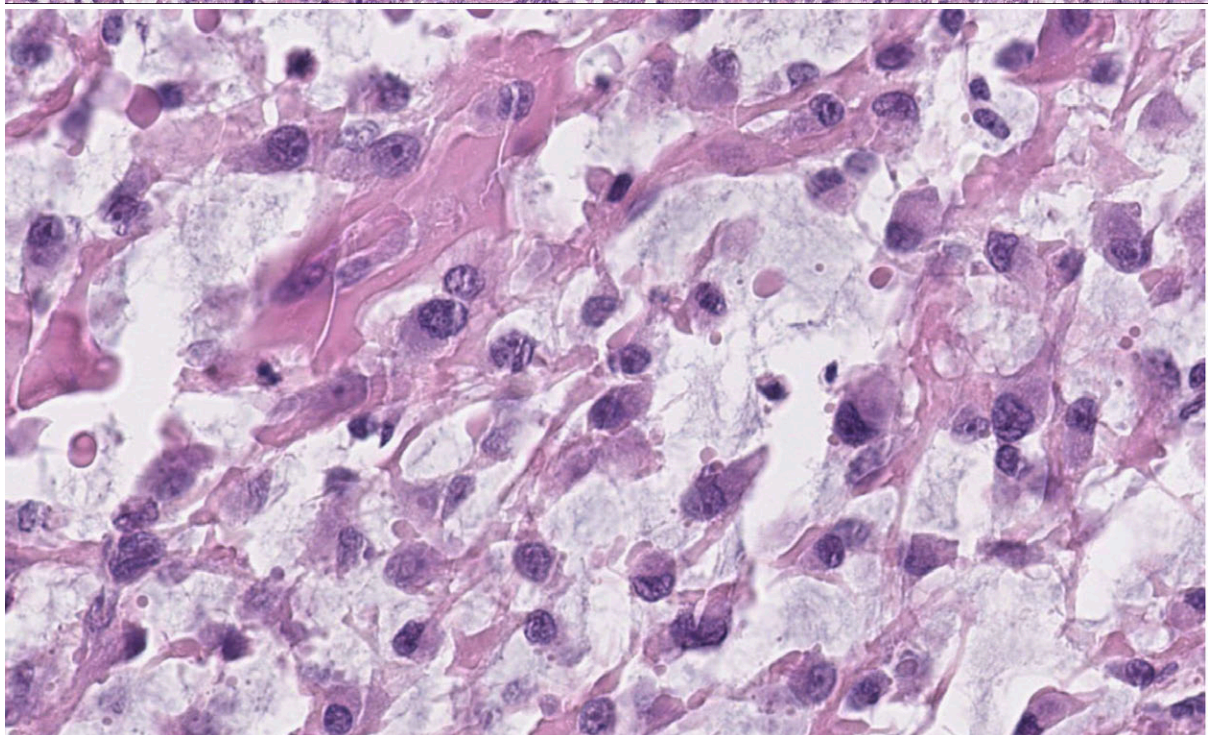
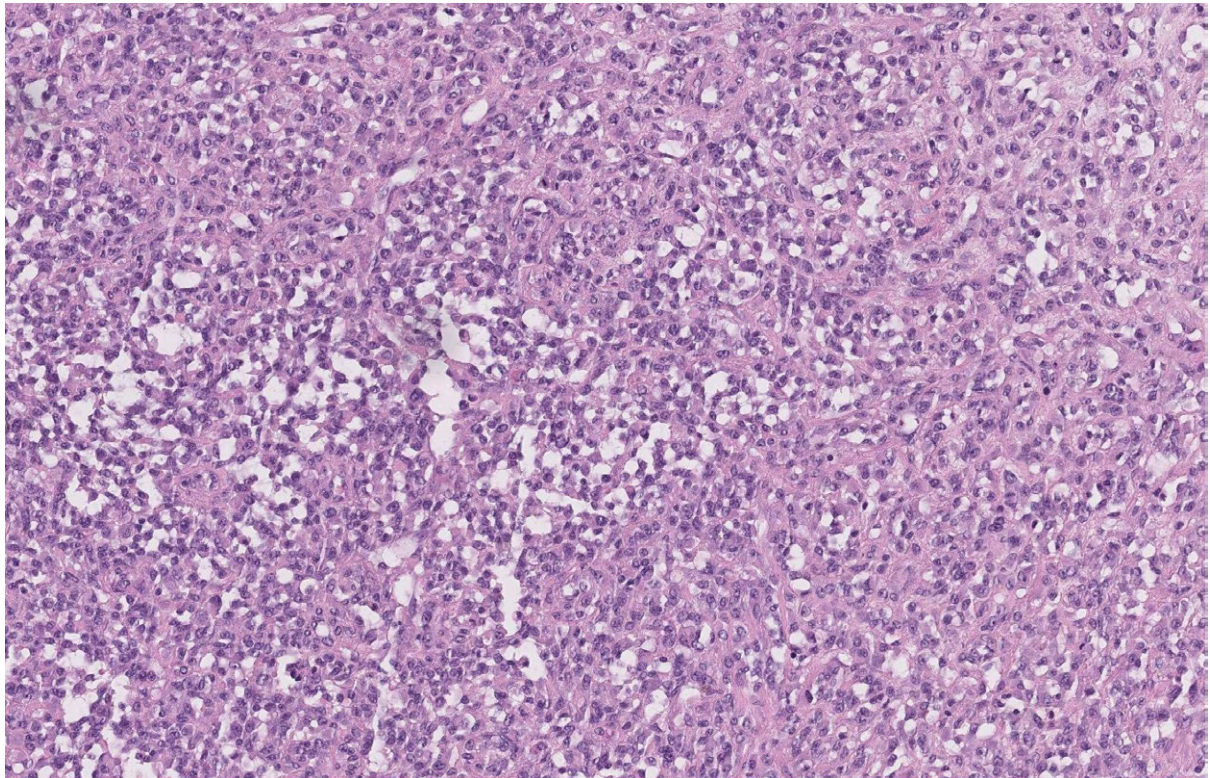
## Case 64

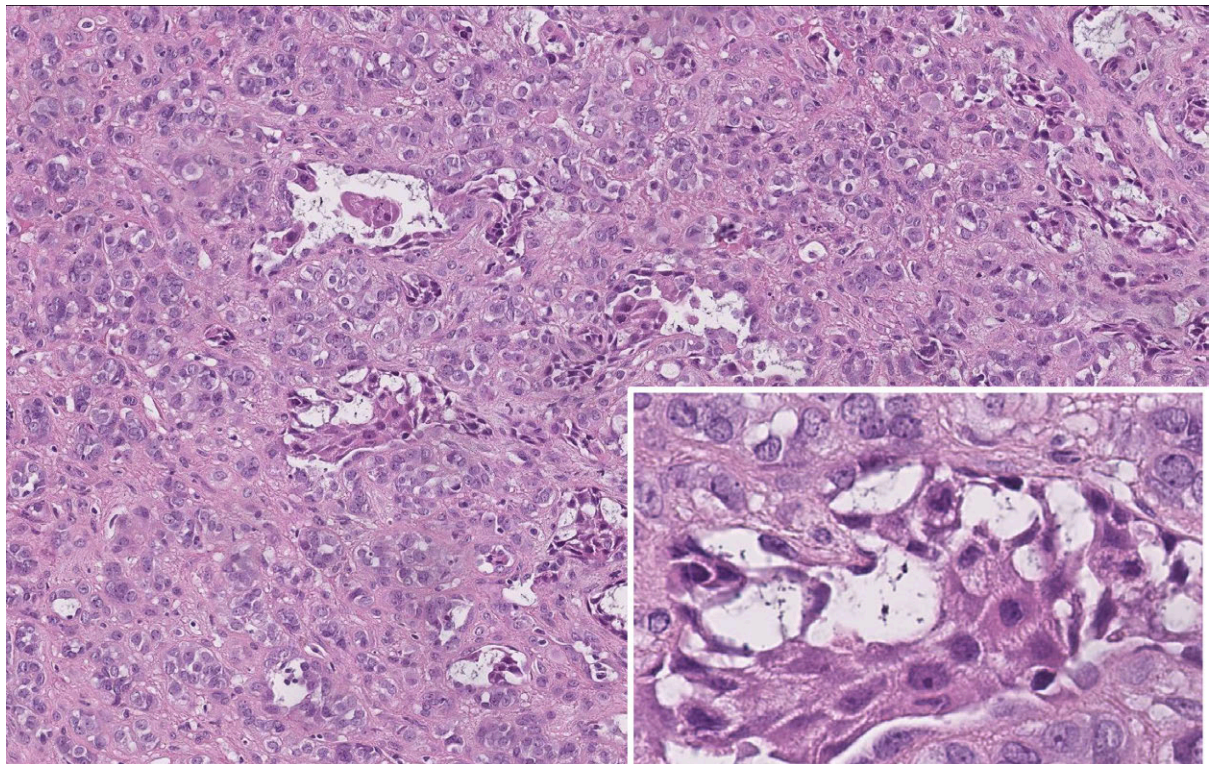
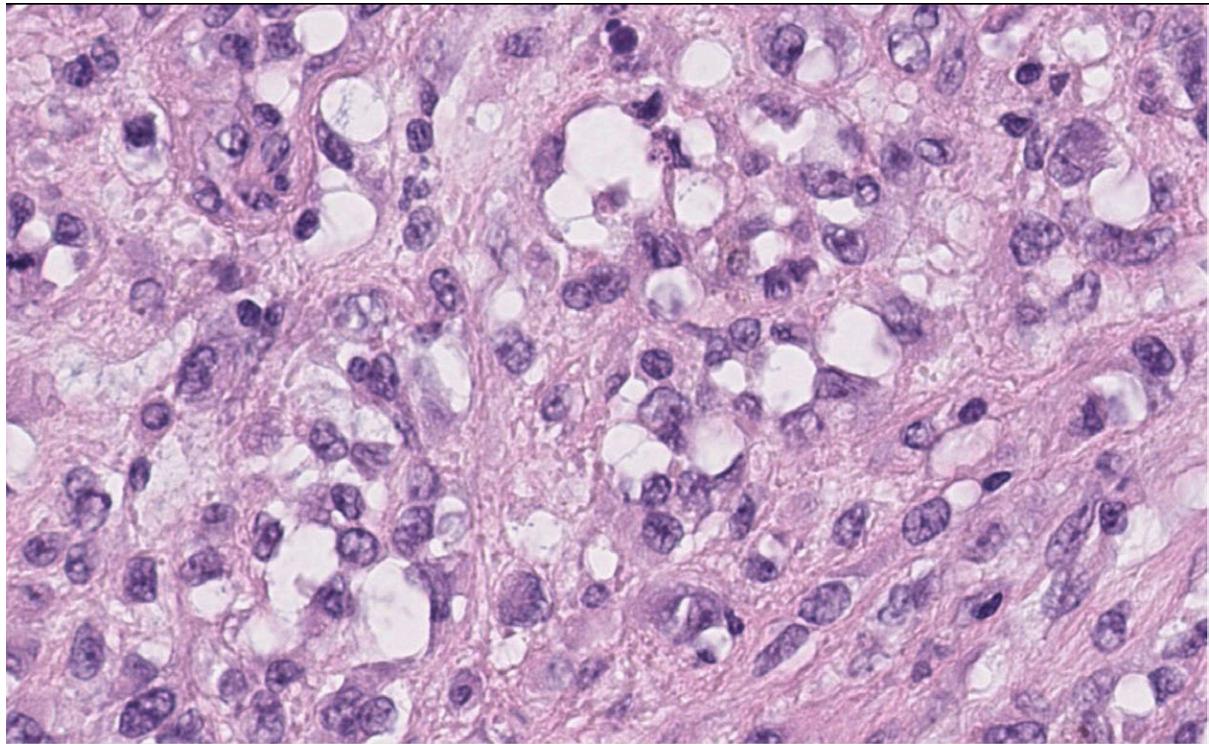
**Isabel Fonseca, Instituto de Anatomia Patológica, Faculdade, de Medicina da Universidade de Lisboa | lost-in-transformation**

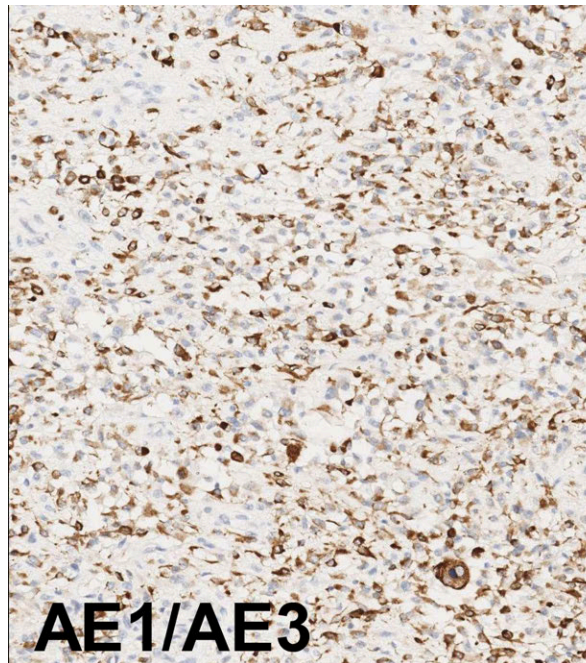
---

An 89-year-old woman presented with a left parotid gland mass that she defines was present for “a long time but had increased in size in recent months”. She underwent surgery (superficial parotidectomy) for an 8cm tumour, that was poorly-circumscribed, elastic and had a whitish cut-surface. She was treated with post-operative radiotherapy and refused any further treatment. She is currently well, without recurrence (refusing treatment, but not follow-up consultations).









## ? malignant myoepithelioma

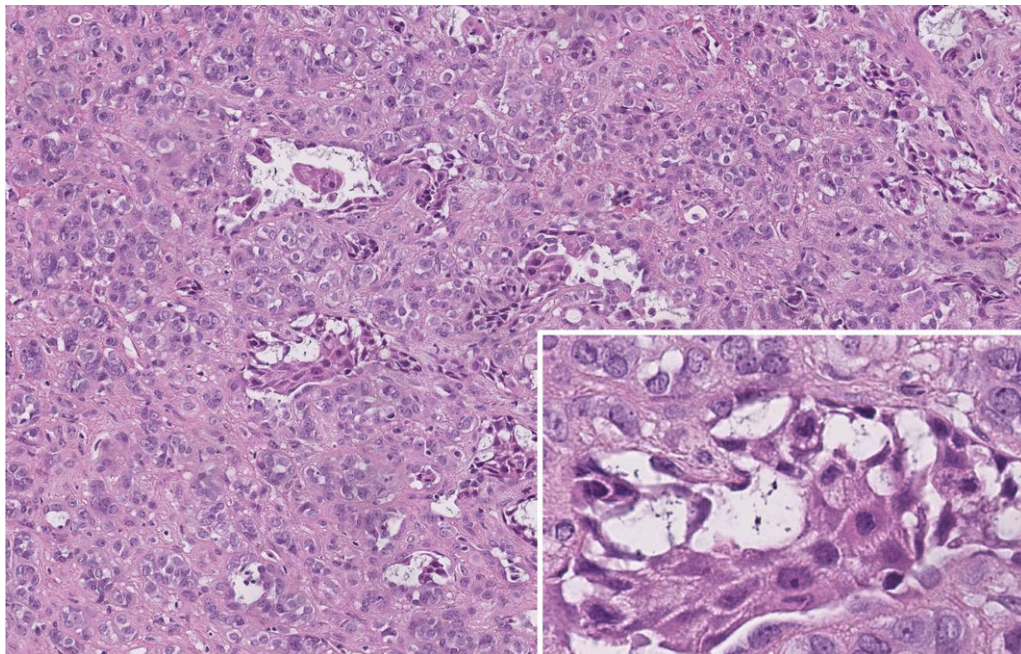
- hypo- and hypercellular areas
- multilobulated, expansive growth with infiltrative areas
- monotonous (solid, trabecular)
- necrosis
- formed by myoepithelial cells
  - spindle, epithelioid, plasmacytoid, clear
- myxoid stroma
- focal duct formation and squamous differentiation

## what do we know?

- undifferentiated carcinomas are exceedingly rare in salivary glands
- high-grade transformation occurs in salivary gland tumours
- in some cases, the "genetic markers" are not "lost-in-transformation"
- ? malignant myoepithelioma
  - ? originating in carcinoma ex-pleomorphic adenoma
  - ? can genetic markers be useful in this cases

## undifferentiated carcinoma (with myoepithelial markers)

- ? originating in carcinoma ex-pleomorphic adenoma
- ? can genetic markers be useful in this cases
- malignant myoepithelioma
- ? originating in carcinoma ex-pleomorphic adenoma
- sample more, looking for the pleomorphic adenoma area
- ? can genetic markers be useful in this cases
- let's see...



## High-grade Transformation/Dedifferentiation in Salivary Gland Carcinomas: Occurrence Across Subtypes and Clinical Significance

*Alena Skalova, MD, PhD,\* Ilmo Leivo, MD, PhD,†‡  
Henrik Hellquist, MD, PhD,§ Abbas Agaimy, MD,||  
Roderick H.W. Simpson, MD,¶|| Göran Stenman, DMD, PhD,#  
Vincent Vander Poorten, MD, PhD, MSc,\*\*†† Justin A. Bishop, MD,‡‡  
Alessandro Franchi, MD,§§ Juan C. Hernandez-Prera, MD,||||  
David Slouka, MD, PhD,¶¶ Stefan M. Willems, MD, PhD, MBA,##  
Kerry D. Olsen, MD,\*\*\* and  
Alfio Ferlito, MD, DLO, DPath, FRCSEd, FRCS, FDSRCS, FACS,  
FHKCORL, FRCPath, FASCP, IFCAP†††*

*Adv Anat Pathol • Volume 28, Number 3, May 2021*

### Dedifferentiation high-grade progression

- transformation of a salivary gland carcinoma into a highgrade carcinoma in which the original line of differentiation may be no longer apparent
- when present, increases the probability of lymph node and distant metastasis
- has been described in acinic cell carcinoma, adenoid cystic carcinoma, epithelial-myoepithelial carcinoma, polymorphous (low-grade) adenocarcinoma, ...

#### Dedifferentiated acinic cell (acinous) carcinoma of the parotid gland

ROBERT J. STANLEY, MD, LOUIS H. WEILAND, MD, KERRY D. OLSEN, MD, and BRUCE W. PEARSON, MD,  
Rochester, Minnesota, and Jacksonville, Florida

Otolaryngologists—head and neck surgeons and surgical pathologists should be aware of the potential for acinic cell carcinomas to dedifferentiate so that adequate histologic tumor sampling can be performed. Dedifferentiated acinic cell carcinoma is a highly malignant, newly recognized parotid malignancy. Clinical clues that may help identify this more ominous lesion must be recognized. (OTOLOGY/HEAD NECK SURG 1288-08-155)

HUMAN PATHOLOGY Volume 34, No. 10 (October 2003)

#### DEDIFFERENTIATION IN LOW-GRADE MUCOEPIDERMOID CARCINOMA OF THE PAROTID GLAND

TOSHITAKA NAGAO, MD, THOMAS A. GAFFY, MD, PAUL A. KAY, MD, KRISHNAN K. UNNI, MD,  
ANTONIO G. NASCIMENTO, MD, THOMAS J. SEBO, MD, HIROMI SERIZAWA, MD,  
HIROSHI MINATO, MD, AND JEAN E. LEWIS, MD

Virchows Arch (1999) 434:291–299

© Springer-Verlag 1999

#### Adenoid Cystic Carcinoma With High-grade Transformation

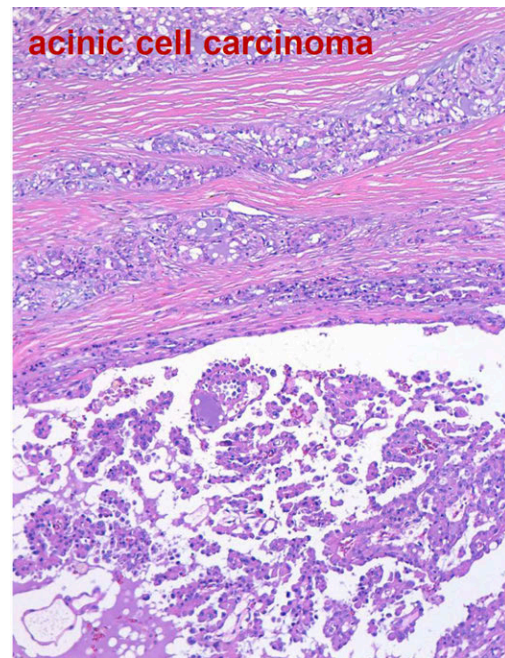
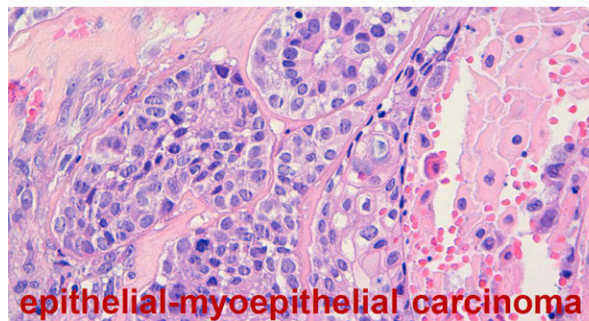
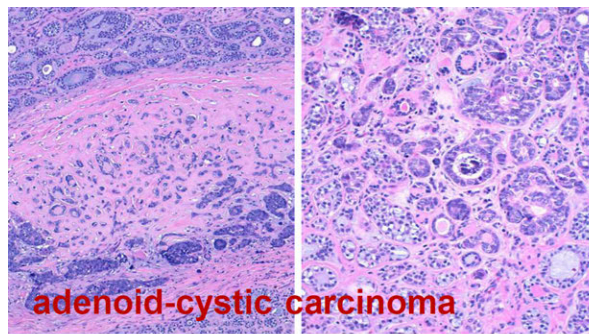
*A Report of 11 Cases and a Review of the Literature*

Raja R. Seethala, MD,\* Jennifer L. Hunt, MD, MEd,† Zubair W. Baloch, MD, PhD,‡  
Virginia A. LiVolsi, MD,§ and E. Leon Barnes, MD\*

ORIGINAL ARTICLE

L. Alos · R. Carrillo · J. Ramos · J.M. Baez  
C. Mallofre · P.L. Fernandez · A. Cardesa

**High-grade carcinoma component in epithelial-myoepithelial carcinoma of salivary glands clinicopathological, immunohistochemical and flow-cytometric study of three cases**



Case Report

**Dedifferentiated malignant myoepithelioma of the parotid gland**

Ikuo Ogawa,<sup>1</sup> Toshihiro Nishida,<sup>2</sup> Mutsumi Miyuchi,<sup>3</sup> Sunao Sato<sup>2</sup> and Takashi Takata<sup>1,4</sup>

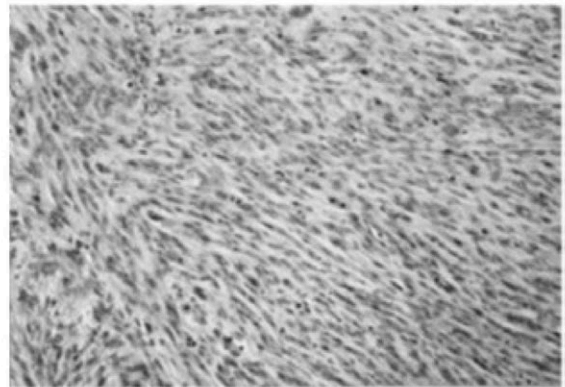


**Table 1.** Genetic alterations in salivary gland tumors

Tumor type	Chromosomal region	Gene and mechanism	Prevalence
Pleomorphic adenoma	8q12	<i>PLAG1</i> fusions/amplification	>50% (46)
	12q13-15	<i>HMG42</i> fusions/amplification	~15% (46)
Carcinoma ex pleomorphic adenoma	8q12	<i>PLAG1</i> fusions/amplification	72.7% (191)
	12q13-15	<i>HMG42</i> fusions/amplification	13.6% (191)
Myoepithelial carcinoma	8q12	<i>PLAG1</i> fusions <sup>1</sup>	37.5% (192)
	t(12;22)(q21;q12)	<i>EWSR1-ATF1</i> <sup>1</sup>	12.5% (192)
Clear cell carcinoma	t(12;22)(q21;q12)	<i>EWSR1-ATF1</i>	93% (193)
		<i>EWSR1-CREM</i>	<5% (194)
Tubulotrabeular basal cell adenoma	3p22.1	<i>CTNNB1</i> hotspot mutation	37.5–80% (195, 196)
Membranous basal cell adenoma	16q12.1	<i>CYLD</i> mutation	36% (197)
Basal cell adenocarcinoma	16q12.1	<i>CYLD</i> mutation	29% (197)
Mucoepidermoid carcinoma	t(11;19)(q21;p13)	<i>CRTC1-MAML2</i>	56% (198)
	t(11;15)(q21;q26)	<i>CRTC3-MAML2</i>	6% (199)
	9p21.3	<i>CDKN2A</i> deletion	25% (54)
Secretory carcinoma	t(12;15)(p13;q25)	<i>ETV6-NTRK3</i>	~95–98% (19)
	t(12;10)(p13;q11)	<i>ETV6-RET</i>	~2–5% (91)
	t(12;7)(p13;q31)	<i>ETV6-MET</i>	<1% (200)
Intraductal carcinoma, intercalated duct type	10q11.21	<i>RET</i> fusions	46.7% (23)
Intraductal carcinoma, apocrine type	3q26.32	<i>PIK3CA</i> mutations (apocrine type)	High <sup>2</sup> (23)
	11p15.5	<i>HRAS</i> mutations (apocrine type)	High <sup>2</sup> (23)
Epithelial-myoepithelial carcinoma	11p15.5	<i>HRAS</i> hotspot mutation <sup>1</sup>	77.8% (201)
Salivary duct carcinoma	17q21.1	<i>HER2</i> amplification	31% (45)
	8p11.23	<i>FGFR1</i> amplification	10.3% (45)
	17p13.1	<i>TP53</i> mutation	56% (45)
	3q26.32	<i>PIK3CA</i> mutation	33.3% (45)
	11p15.5	<i>HRAS</i> mutation	33.3% (45)
	Xq12	<i>AR</i> copy gain	35% (202)
	10q23.31	<i>PTEN</i> loss	38% (45)
		<i>CDKN2A</i> loss	10% (45)
Adenoid cystic carcinoma	6q22-23	<i>MYB</i> fusion/activation/amplification	~80% (203, 204)
	8q13	<i>MYBL1</i> fusion/activation/amplification	~10% (205)
	9q34.3	<i>NOTCH</i> mutations (solid type)	13.7% (40)
PAC, classic type	14q12	<i>PRKDI</i> hotspot mutation	73% (35)
PAC, cribriform type	14q12	<i>PRKDI</i> fusions <sup>3</sup>	38% (206)
	19q13.2	<i>PRKD2</i> fusions <sup>4</sup>	14.3% (206)
	2p22.2	<i>PRKD3</i> fusions <sup>4</sup>	19% (206)
Acinic cell carcinoma	19q31.1	<i>MSANTD3</i> fusion/amplification	4.4% (37)
	9q31	<i>NR4A3</i> fusion/activation	86% (207)

NDA, no data available.

<sup>1</sup>Not as the malignant component of carcinoma ex pleomorphic adenoma, i.e., only in *de novo* carcinomas.

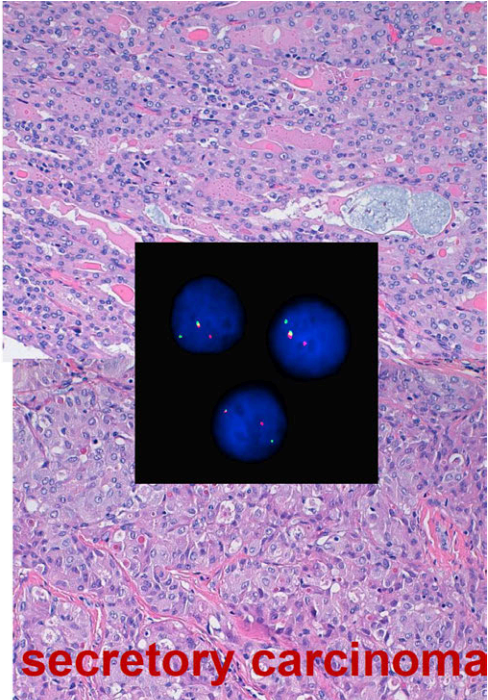
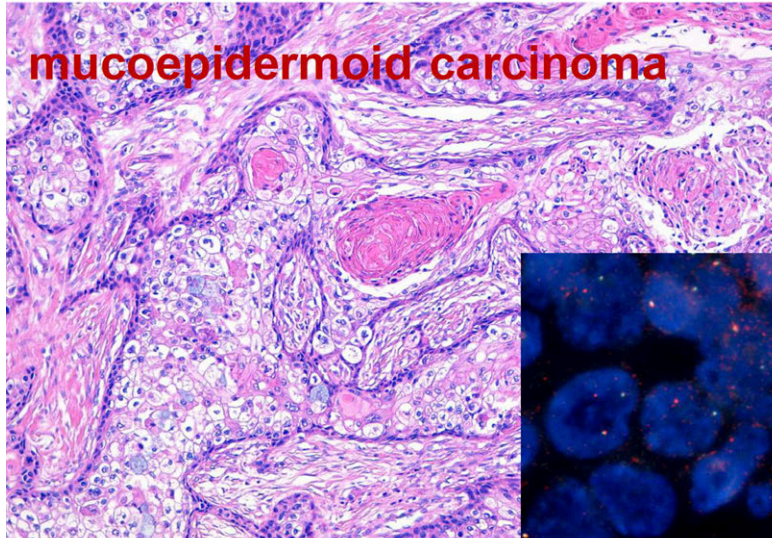
<sup>2</sup>Only very few cases tested.

<sup>3</sup>3/8 cases tested had *ARID1A-PRKDI* fusion, 1/8 had *DDX33-PRKDI* fusion, and 4/8 had unknown fusion partners.

<sup>4</sup>Unknown fusion partners.



some genetic markers are not  
“lost-in-transformation”



**FISH**

A análise por FISH, em secções de parafina, revelou que:  
Com sondas break-apart para o gene **EW5** não há rearranjo do gene  
Com sondas break-apart para o gene **ETV6** não há rearranjo do gene  
Com sondas break-apart para o gene **HMG2** não há rearranjo do gene.  
Com sondas break-apart para o gene **PLG1**, 53% dos núcleos têm ganho de 1 cópia de ambas as sondas mas não há rearranjo do gene.  
Com sondas break-apart para o gene **FGFR1**, 44% dos núcleos têm ganho de 1 cópia de ambas as sondas mas não há rearranjo do gene.

**CGH**

A análise por CGH revelou em cerca de 30% das células a presença das seguintes alterações cromossómicas:  
Ganho total dos cromossomas: 8,11,16,19,20.  
Perdas parciais das regiões cromossómicas: 1p32-p22,1q24-q42.1,6q15-q27,12q12-q15,14q31-q32.1,Xq23-q27.

**RELATÓRIO DE DIAGNÓSTICO GENÉTICO**  
Grupo de Citogenética de Tumores Sólidos  
INSTITUTO PORTUGUÊS DE ONCOLOGIA DE LISBOA FRANCISCO GENTIL, EPE  
UNIDADE DE INVESTIGAÇÃO EM PATOLOGIA MOLECULAR (UIPM)

Nome: [REDACTED] Médico requisitante: Professora Isabel Fonseca  
Sexo: [REDACTED] Serviço requisitante: Anatomia Patológica  
Data de nascimento: [REDACTED] Material enviado: secções de parafina 818-1662386  
Nº Observ./Processo: [REDACTED] Hospital: IPO Data de entrada: 06-02-2019/19-03-2019  
Informação clínica: Carcinoma mioepitelial Data de saída: 02-04-2019  
Exame requisitado: Análise genética Nº Laboratório: [REDACTED]

Metodologia: FISH e CGH

**Resultados:**  
FISH  
A análise por FISH, em secções de parafina, revelou que:  
Com sondas break-apart para o gene **EW5** não há rearranjo do gene  
Com sondas break-apart para o gene **ETV6** não há rearranjo do gene  
Com sondas break-apart para o gene **HMG2** não há rearranjo do gene.  
Com sondas break-apart para o gene **PLG1**, 53% dos núcleos têm ganho de 1 cópia de ambas as sondas mas não há rearranjo do gene.  
Com sondas break-apart para o gene **FGFR1**, 44% dos núcleos têm ganho de 1 cópia de ambas as sondas mas não há rearranjo do gene.

CGH  
A análise por CGH revelou em cerca de 30% das células a presença das seguintes alterações cromossómicas:  
Ganho total dos cromossomas: 8,11,16,19,20.  
Perdas parciais das regiões cromossómicas: 1p32-p22,1q24-q42.1,6q15-q27,12q12-q15,14q31-q32.1,Xq23-q27.

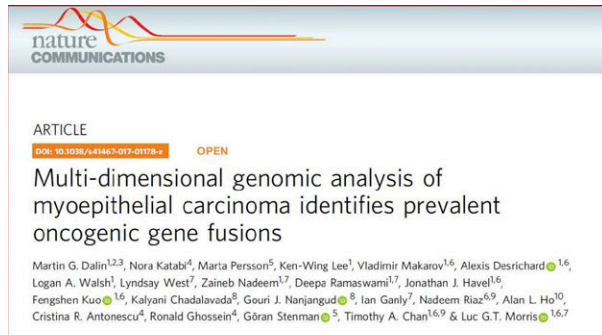
Realizado/Validado por: \_\_\_\_\_

Assumo em nome verdadeiro a declaração relativa à identidade do doente e à validade e identificação dos produtos biológicos analisados. No entanto, não é de excluir a possibilidade de um eventual erro que possa influenciar o resultado.

Unidade de Investigação em Patologia Molecular  
Grupo de Citogenética de Tumores Sólidos  
Tel: 217229188  
UIPM-Citogenética@ipolbica.min-saude.pt

O Citogenético Genético  
realizado na UIPM dispõe de um  
sistema de controlo de qualidade  
certificado

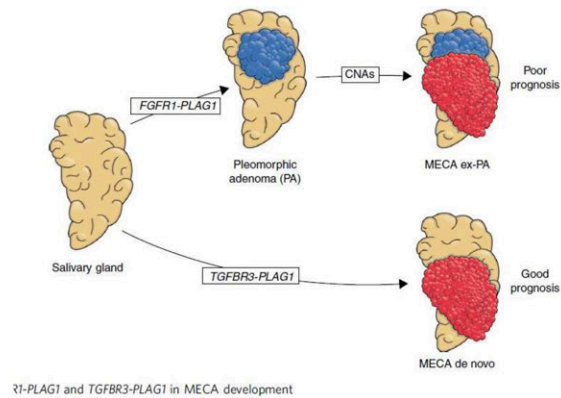
UIPM-CTGOL-MOD. 12.2



**Supplementary Table 6.** Significant CNAs in MECA de novo and MECA ex-PA tumors.

Chromosome region	Alteration	MECA (n=37)	MECA de novo (n=15)	MECA Ex-PA (n=22)	P-value**
1pccn-p32.3	Loss	6 (16%)	0 (0%)	6 (27%)	ns.
1qccn-qter	Gain	11 (30%)	1 (6.7%)	10 (45%)	0.014
5pter-pcen	Gain	7 (19%)	3 (20%)	4 (18%)	ns.
6qccn-qter	Loss	8 (22%)	0 (0%)	8 (36%)	0.012
8*	Gain	16 (43%)	2 (13%)	14 (64%)	0.003
11pter-pcen	Loss	7 (19%)	1 (6.7%)	6 (27%)	ns.
16qccn-qter	Gain	7 (19%)	2 (13%)	5 (23%)	ns.

\* Gain of whole chromosome 8 or complex rearrangements (including ring formation).  
 \*\*Fisher's exact test.



## back to the case...

and with the great and qualified help of Carmo Martins, PhD (and so that you do not get lost in translation!)

### FISH

- With break-apart probes for the EWS gene there is no gene rearrangement
- With break-apart probes for the ETV6 gene there is no gene rearrangement
- With break-apart probes for the HMGA2 gene there is no gene rearrangement
- With break-apart probes for the PLAG1 gene, 53% of the nuclei have gained 1 copy of both probes but there is no gene rearrangement.
- With break-apart probes for the FGFR1 gene, 44% of nuclei have gained 1 copy of both probes but there is no gene rearrangement.

### CGH

Total chromosome gain: 8, 11, 16, 19, 20.  
 Partial losses of chromosomal regions: 1p32-p22, 1q24-q42.1, 6q15-q27, 12q12-q15, 14q31- q32.1, Xq23-q27.

### SO.

- undifferentiated carcinomas are exceedingly rare in salivary glands - but myoepithelial carcinoma is also very rare

- if you have the resources, “dig in” and try to find molecular or genetic alterations to help interpret morphological findings
- (this is, of course, more of an academic issue: the patient should be treated and followed-up in a similar way)

**Diagnosis: myoepithelial carcinoma with genetic alterations compatible with origin in pleomorphic adenoma**

# Case 65

## Michal Michal, Czech Republic | Cases M72855/10

---

64 year old female had a neoplasm that obliterated the both nasal regions. The tumor was excised several pieces. The tumor was originally classified as membranous variety of basal cell carcinoma and after HPV genotyping, which revealed presence of HPV 56, the tumor was reclassified as HPV related multiphenotypic sinonasal adenoid cystic like carcinoma.

**Diagnosis: HPV related multiphenotypic sinonasal adenoid cystic like carcinoma.**

## Reference

1. J.A.Bishop, S.Andreasen, J.-F.Hang, M.J.Bullock, T.Y.Chen, A.Franchi, J.J.Garcia, D.R.Gnepp, C.R.Gomez-Fernandez, S.Ihrler, Y.-J.Kuo, J.S.Lewis, K.R.Magliocca, S.Pambuccian, A.Sandison, E.Uro-Coste. HPV-related multiphenotypic sinonasal carcinoma. An expanded series of 49 cases of the tumor formerly known as HPV-related carcinoma with adenoid cystic carcinoma-like features. *Am J Surg Pathol* 217:41:1690-1701.

## Case 66

Fredrik Petersson

---

### Clinical History:

The patient was a 23 year old woman with a few months history of increasing left sided nasal obstruction. On clinical examination, a large fleshy tumor occupying the whole (left) nasal cavity was seen. The tumor did not involve the right nasal cavity. On MRI a tumor in the left nasal cavity was confirmed. The tumor extended from the anterior nasal cavity into the nasopharynx and from the anterior skull base to the inferior aspect of the inferior turbinate. Tumor extended into the left maxillary sinus and bulged into the orbit. This lesion has obstructed the sphenoidal recess and the ostiomeatal unit resulting in fluid retention and mucosal thickening in the left frontal, ethmoid and sphenoid sinuses. The overall radiological impression was that of a benign or low grade malignant tumor. The possibility of an inverted papilloma was raised. The patient underwent a biopsy under general anaesthesia.

After resection of the tumor, the patient underwent 6 weeks of chemo-radiation. There has been no evidence of local recurrence or metastatic disease with a follow-up of 4.5 years.

### Histopathology and immunohistochemistry:

The tumor was composed of variably sized nests set in a desmoplastic-type stroma. The neoplastic cells displayed rather monotonous, enlarged nuclei with vesicular chromatin and one to several frequently fairly large nucleoli. The N/C-ratio was high (i.e. the amount of cytoplasm was limited). The mitotic activity was brisk. No light-microscopical glandular or squamous differentiation was discerned. On IHC, there was strong and diffuse expression of broad spectrum cytokeratins (AE1-3), CK5/6, p40 and p63. There was significant expression of p16. No expression of INI-1 was detected in any of the tumor cells (with good internal control). There was no expression of desmin, synaptophysin or chromogranin A.

**Diagnosis: *SMARCB1 (INI-1) Deficient Sinonasal Carcinoma***

## Comments:

This tumor was first characterized in 2014 (1, 2) and belongs to an ever growing list of neoplasms with basic genetic alterations (homozygous deletions, inactivating mutations or epigenetic mechanisms) in the SWI/SNF/Sucrose Nonfermentable (SWI/SNF) chromatin remodeling complex, which is composed of >20 closely related proteins that function to regulate chromatin remodeling and regulate gene expression, cell proliferation and differentiation. SWI/SNF deficient malignancies commonly display undifferentiated anaplastic and/or rhabdoid morphology, including small (blue) cell and large epithelioid cell "types". Over time, the spectrum of light-microscopical appearances of these tumors has been expanded (3). The most common histopathologic pattern encountered is a neoplasm composed of tumor cells with rather monomorphic cytology and with a predominance of basaloid or plasmacytoid/rhabdoid cells. In most cases, scattered plasmacytoid/rhabdoid cells may be identified among the basaloid tumor cells. Focal, limited glandular differentiation is a very rare event. Limited areas of clear cells are seen in a few cases. Conventional dysplasia or carcinoma in situ of the surface epithelium is lacking, but pagetoid spread along the surface epithelium is often identified.

Immunohistochemically, sinonasal SMARCB1-deficient carcinomas are immunoreactive with pankeratins in majority of cases with variable expression of CK5, p63 and CK7. The tumor cells are negative for EBV, HPV, NUT and neuroendocrine markers.

There is a slight predominance of males with a mean age of approximately 50 years. The tumors tend to present with locally advanced disease (T3/4). In most cases paranasal sinuses (mainly ethmoid) are involved with variable involvement of the nasal cavity.

Despite aggressive treatment, this tumor pursues an aggressive clinical course with >50% of patients dying within a few years after diagnosis.

In the H&N region, the main entities in the differential diagnosis can be divided into (1) high-grade tumors with a basaloid/"blue cell" pattern and those with (2) deficient expression of *INI-1/SMARCB1*. Most entities in (1) can be resolved by IHC/CISH studies.

(1):

*Non-keratinizing squamous cell carcinoma (HPV+/-)*

*Sinonasal non-keratinizing squamous cell carcinoma with DEK-AFF2 fusion*

*High-grade neuroendocrine carcinoma*

*Undifferentiated nasopharyngeal carcinoma (EBV+)*

*Rhabdomyosarcoma*

*Small cell synovial sarcoma*

*Mucosal melanoma*

*(Adamantinoma-like) Ewing sarcoma*

*NUT-carcinoma*

*De-differentiated salivary gland carcinoma*

*SMARCA4-deficient sinonasal carcinoma/*

*(SMARCA4-deficient) sinonasal teratocarcinosarcoma (small biopsies)*

*Lymphoma (small biopsies)*

*Sinonasal undifferentiated carcinoma (diagnosis of exclusion)*

(2):

*Malignant rhabdoid tumor* (extra-cranial counterpart of the highly aggressive atypical teratoid and rhabdoid tumor of the central nervous system; arises in soft tissue, mainly affects infants and young children). Of note is that up to 30% of all cases are hereditary -

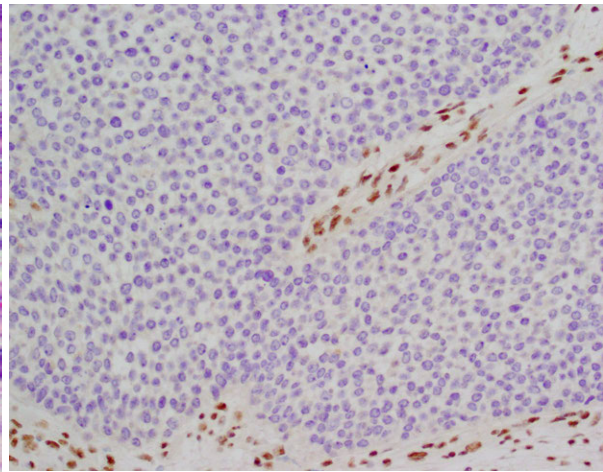
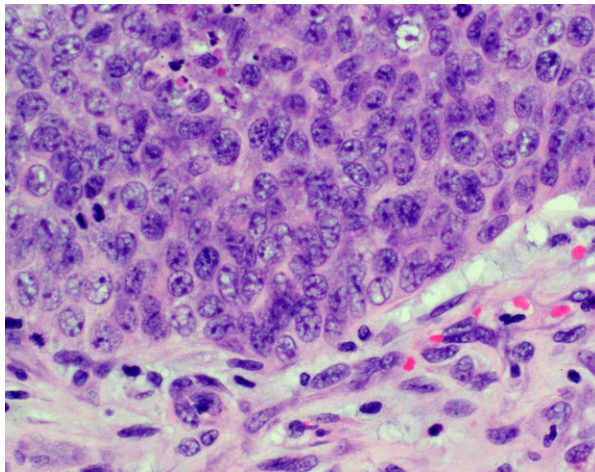
SMARCB1 germline mutations (rhabdoid tumor predisposition syndrome type 1).

*Epithelioid sarcoma* (soft tissue; classical/distal type composed of bland-looking epithelioid or histiocytoid cells arranged in granuloma-like nodular aggregates while the proximal type is made up of diffuse sheets of large anaplastic variably rhabdoid cells).

*SMARCB1-deficient sinonasal adenocarcinoma* (oncocytoïd/plasmacytoïd morphology with prominent, albeit variable gland formation; well formed tubules, cribriform structures, areas of intracellular and/or intraluminal mucin; focal yolk sac tumor-like structures; high-grade cytology with significant nuclear pleomorphism).

*Poorly differentiated chordoma* (brachyury and S100 immunohistochemistry).

## **Figures**



Left sided nasal tumor bulging into the periorbital tissue. Neoplastic cells displayed rather monotonous, enlarged nuclei with vesicular chromatin and one to several nucleoli. No expression of INI-1 was detected in any of the tumor cells (with good internal control).

## References:

1. Agaimy A, Koch M, Lell M, et al. SMARCB1(INI1)-deficient sinonasal basaloid carcinoma: a novel member of the expanding family of SMARCB1-deficient neoplasms. *Am J Surg Pathol.* 2014;38:1274-1281.
2. Bishop JA, Antonescu CR, Westra WH. SMARCB1 (INI-1)-deficient carcinomas of the sinonasal tract. *Am J Surg Pathol.* 2014;38:1282-1289.
3. Agaimy A, Hartmann A, Antonescu CR, et al. SMARCB1 (INI-1)-deficient Sinonasal Carcinoma: A Series of 39 Cases Expanding the Morphologic and Clinicopathologic Spectrum of a Recently Described Entity. *Am J Surg Pathol.* 2017;41:458-471.

## Case 67

**Paul E. Wakely, Jr., M.D., Department of Pathology, The Ohio State University, Wexner, Medical Center, James Cancer Hospital, Columbus, OH. USA**

---

### History:

A 50-year-old woman presented to ENT clinic with a 3 cm. firm, non-tender rapidly enlarging right parotid mass that appeared 4 weeks earlier. She now has lip weakness. Fine needle aspiration biopsy was interpreted as suspicious for lymphoma. CT of the neck revealed a 3.6 cm. mass of the right parotid. She denies fever/chills, and has no issues with swallowing. She has a history of invasive breast cancer treated with CRT 12 years earlier and no recurrence. A right parotid debulking was performed.

### Pathology:

The resected specimen consisted of an unoriented 6.5 x 3.5 x 2.4 cm. 19.8 gram yellow-red, lobulated partially cauterized piece of soft tissue. Serial sectioning revealed a 5.2 x 1.8 x 1.3 cm. tan-white, indurated, and well-demarcated mass with indistinct borders abutting the inked external surface. Microscopically, a monotonous population of basaloid malignant cells obliterated the normal parotid parenchyma, infiltrating the adjacent fibroadipose tissue and skeletal muscle. Malignant cells were mostly solidly arranged with peripheral infiltrative areas showing a trabecular and irregularly contoured nested pattern associated with desmoplastic fibrosis. Geographic foci of necrosis were seen throughout the tumor. Individual cells had rounded, angulated, and slightly pleomorphic nuclei, coarsely granular chromatin lacking distinct nucleoli, and only a minimal amount of visible cytoplasm.

Immunoprofile: positive staining with vimentin, cytokeratin AE1/3, TLE-1, PAX-7, and cytokeratin 20 (focal scattered); negative staining with CD45, cytokeratin 7, cytokeratin 5/6, GATA3, mammaglobin, GATA3, S-100, SOX-10, CD34, androgen receptor, synaptophysin, chromogranin and TTF-1. Ki-67 proliferative index: 80-90% nuclear

staining. FISH testing for *EWSR1* gene rearrangement was positive, and for SS18 (*SYT*) was negative.

## Diagnosis: ADAMANTINOMA-LIKE EWING SARCOMA, PAROTID

### Discussion:

Adamantinoma-like Ewing sarcoma is classified as a Ewing sarcoma (ES) variant with epithelial differentiation. Initially described in the long bones and thorax, several cases have been reported in the head and neck region including the sinonasal tract, soft tissues of the neck and thyroid gland. While conventional ES is rare in salivary gland (SG), this adamantinoma-like variant appears to have a predilection for the salivary glands. Of 10 SG cases reported by Rooper et al., 8 involved the parotid and 2 the submandibular gland. All cases occurred in adults, (x = 52 years). The histopathology closely recapitulates that of conventional ES. Necrosis is common, and mitotic rates are exceptionally high. ES markers CD99 and NKX2.2 are positive, and so is synaptophysin in a high percentage of cases. Finally, all cases harbor *EWSR1-FLI1* translocation by FISH. The adamantinoma-like variant also exhibits overt squamous differentiation with diffuse positivity for pan-cytokeratin and p40, and sometimes foci showing keratin pearl formation. Differential diagnosis includes basal cell adenocarcinoma, NUT carcinoma, adenoid cystic carcinoma, basaloid squamous carcinoma, and neuroendocrine carcinoma. The infiltrative growth of this tumor contrasts with the typical pushing border and low-grade cellular features of most basal cell adenocarcinomas. Co-expression of both squamous and neuroendocrine markers is a highly unusual pattern not seen in other SG tumors. Most cases are treated with ES chemotherapy and radiation, and have shown indolent behavior.

## References:

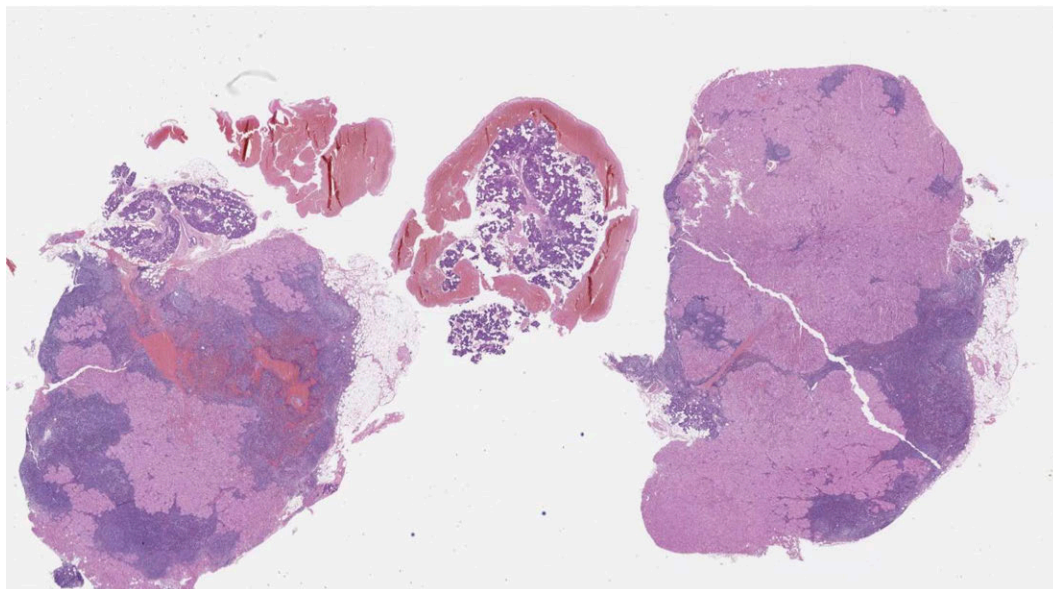
1. Bridge JA, Fidler ME, Neff JR, et al. Adamantinoma-like Ewing's sarcoma: genomic confirmation, phenotypic drift. *Am J Surg Pathol.* 1999;23:159-65.
2. Lezcano C, Clarke MR, Zhang L, et al. Adamantinoma-like Ewing sarcoma mimicking basal cell adenocarcinoma of the parotid gland: a case report and review of the literature. *Head Neck Pathol.* 2015; 9:280-285.
3. Bishop JA, Alaggio R, Zhang L, et al. Adamantinoma-like Ewing family tumors of the head and neck: a pitfall in the differential diagnosis of basaloid and myoepithelial carcinomas. *Am J Surg Pathol.* 2015;39:1267-1274.
4. Lilo MT, Bishop JA, Olson MT, et al. Adamantinoma-like Ewing sarcoma of the parotid gland: cytopathologic findings and differential diagnosis. *Diagn Cytopathol.* 2018;46:263-266.
5. Rooper LM, Jo VY, Antonescu CR, et al. Adamantinoma-like Ewing sarcoma of the salivary glands: a newly recognized mimicker of basaloid salivary carcinomas. *Am J Surg Pathol.* 2019; 43:187-194.

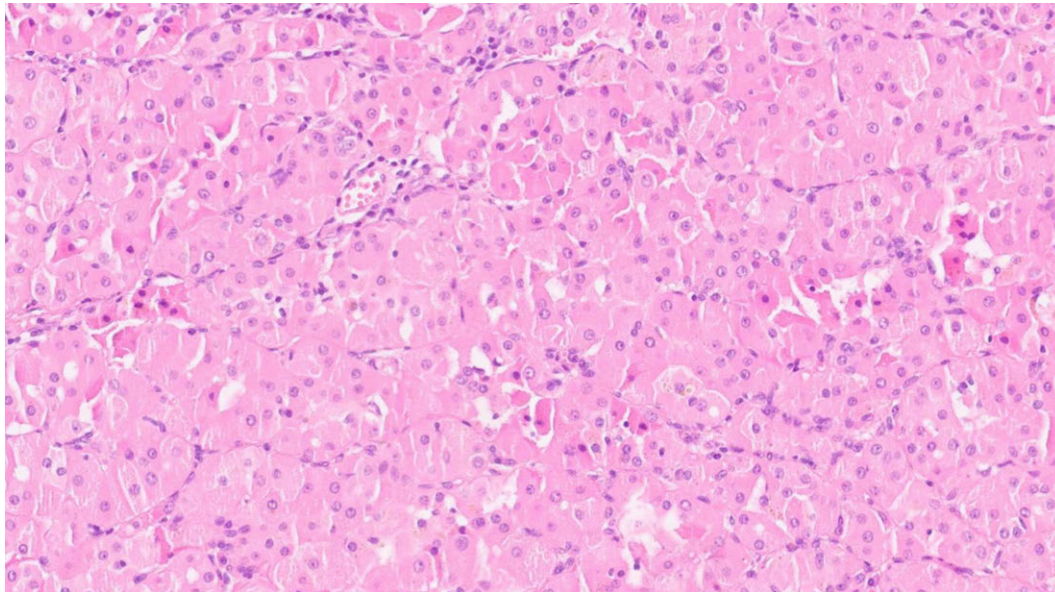
## Case 68

Isabel Fonseca, Instituto de Anatomia Patológica, Faculdade de Medicina da Universidade de Lisboa

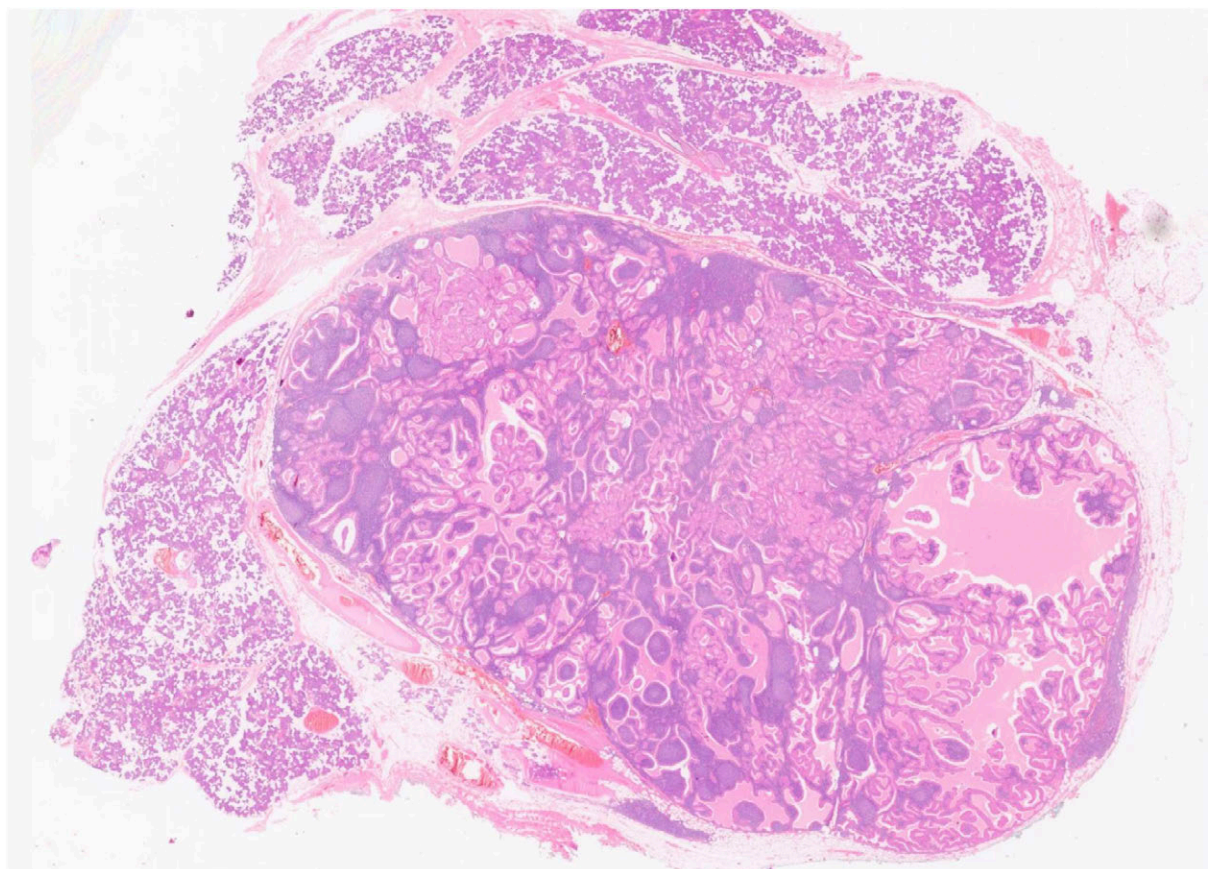
---

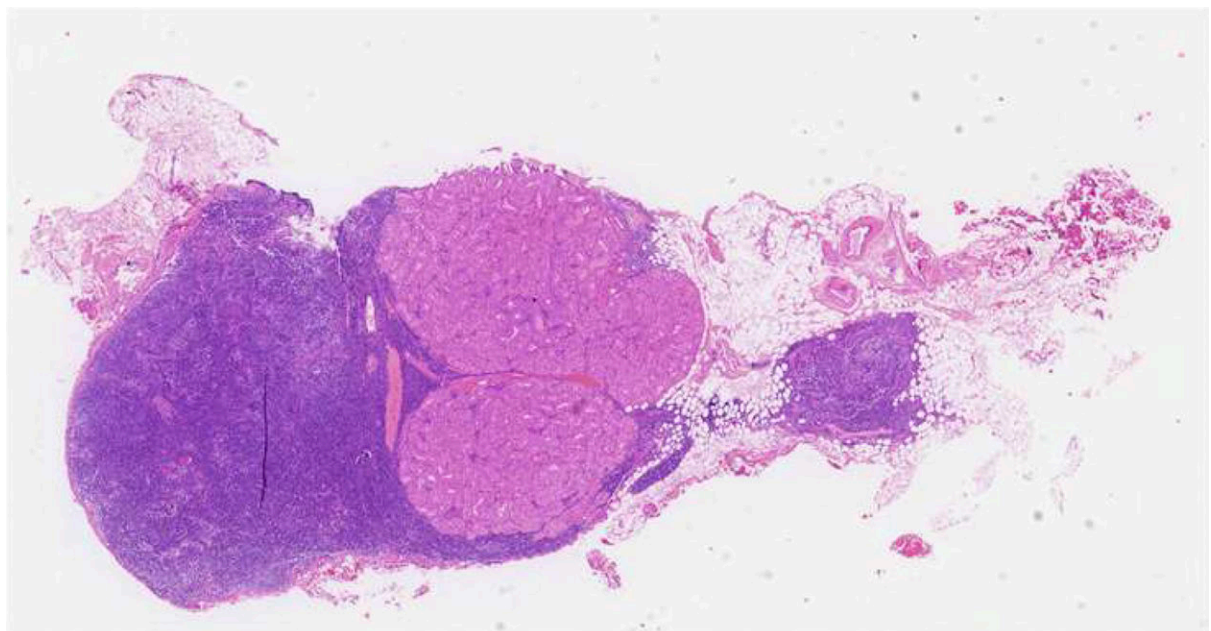
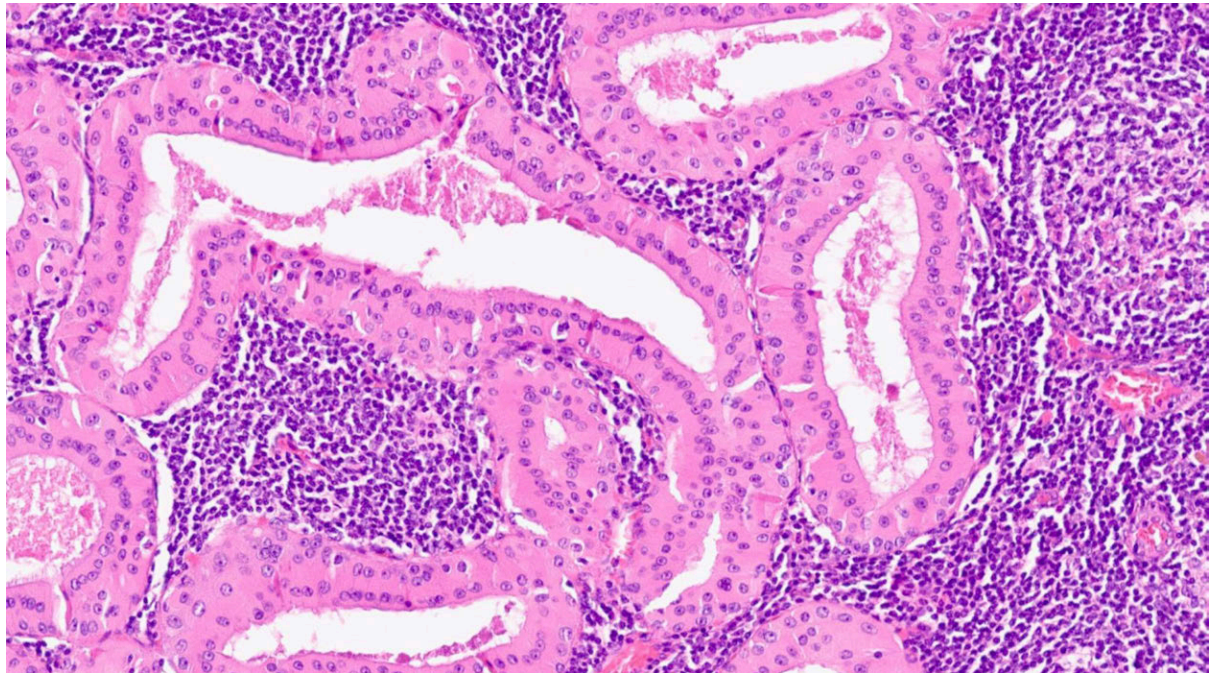
An 82-years old gentleman was referred because of a parotid gland nodule, 3cm in largest dimension. He had enlarged lymph nodes at levels I and II. The homolateral lacrimal gland was also enlarged (*biopsy showed chronic inflammation*). He underwent surgery (the slides are from one of the lymph nodes). The patient died of unrelated causes in 2021.

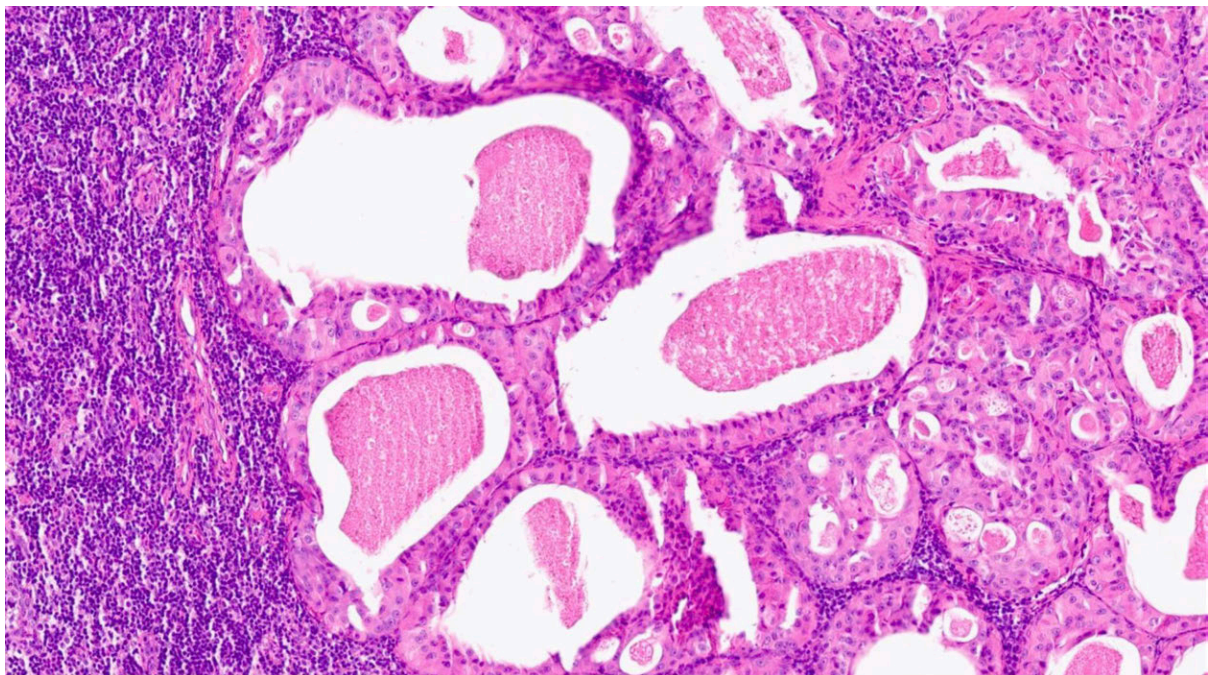
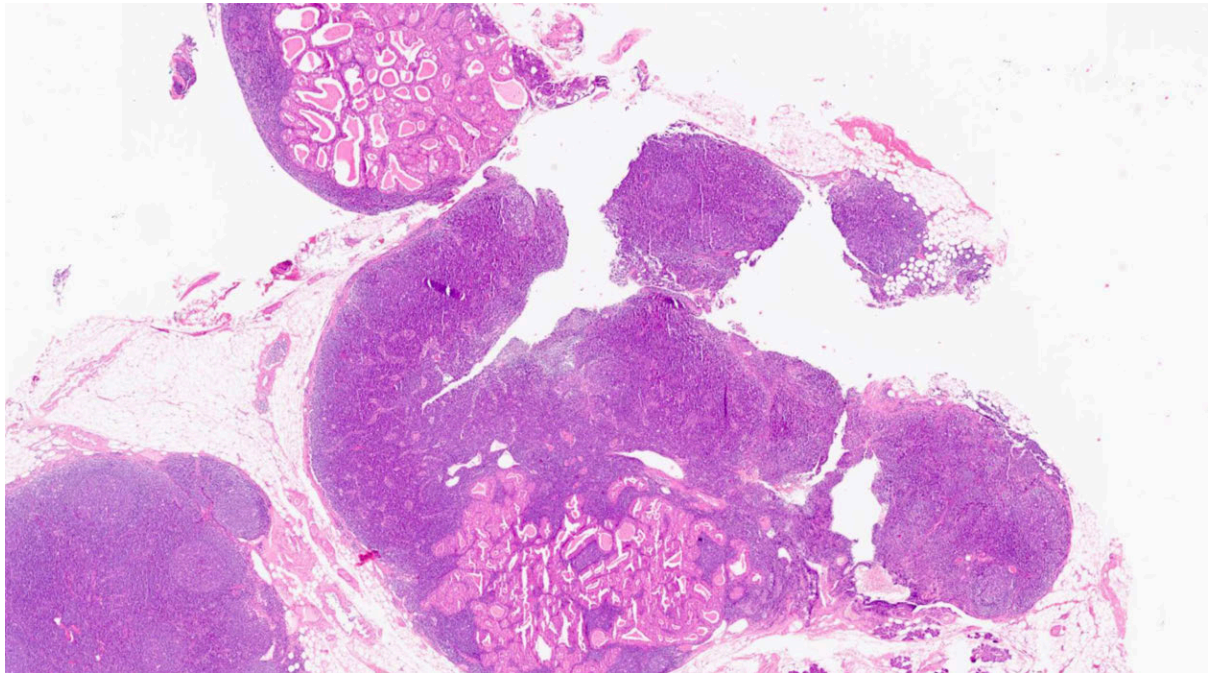




- but there were other lymph nodes and keep in mind that the patient had an ipsilateral parotid gland tumour
- and that he was a senior citizen



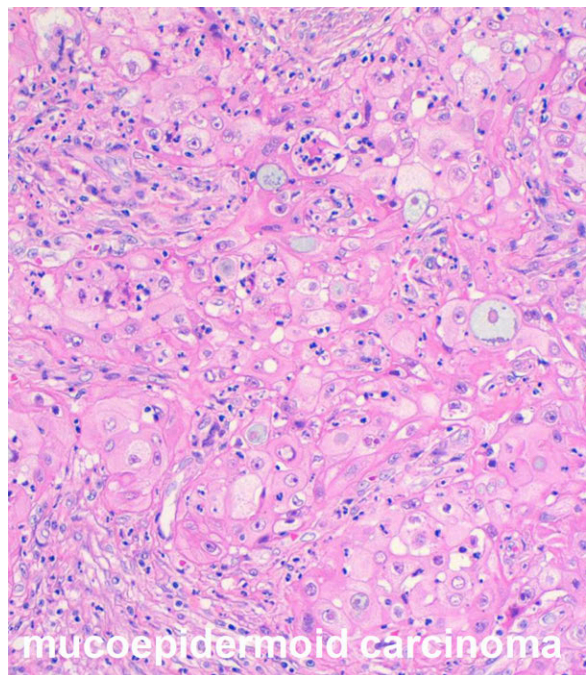




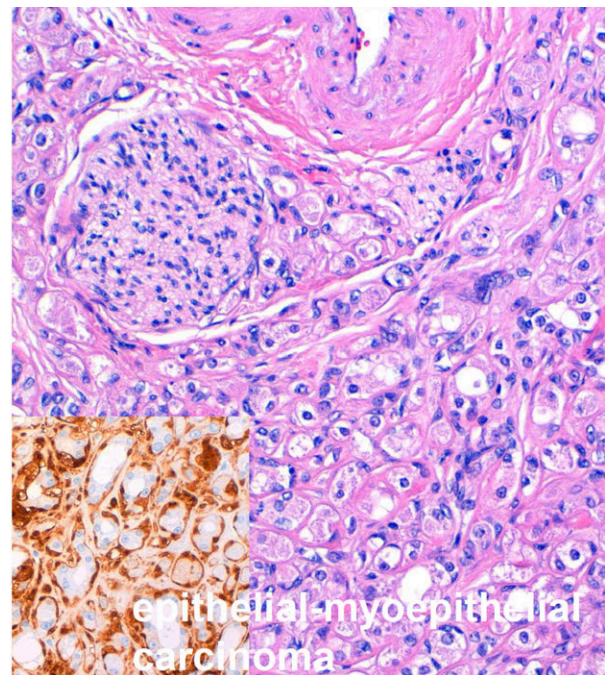
- multiple nodules (parotid and lymph nodes)
- metastatic lesion at the LN?
- all lesions have oncocytic features
- which salivary glands can have oncocytic features?

## oncocytic lesions of salivary glands

- oncocytoma
- Warthin tumour
  
- oncocytic variants
  - acinic cell carcinoma
  - mucoepidermoid carcinoma
  - salivary duct carcinoma
  - ...



Am J Surg Pathol • Volume 44, Number 12, December 2020



Molecular Profiling of Salivary OMEC

TABLE 4. Clinicopathologic Features of 22 Cases of OMEC

Case No.	Age (y)/Sex	Original Diagnosis	Site	AFIP Grade	Brandwein Grade	Outcome (mo)
1	48/female	Oncocytic neoplasm of uncertain malignant potential	Parotid	G1	G2	7 NED
2	53/male	Oncocytic neoplasm	Parotid	G2	G2	*
3	45/female	Recurrent oncocytoma	Sublingual	G1	G3	18 NED
4	74/male	Oncocytic neoplasm, possibly OMEC	Parotid	G2	G3	*
5	83/female	PA with oncocytic metaplasia	Parotid	G1	G2	*
6	41/female	Oncocytic neoplasm of uncertain malignant potential	Parotid	G1	G3	8 NED
7	46/male	Benign mucinous oncocytoma	Parotid	G1	G2	34 NED
8	71/female	Multifocal oncocytoma	Parotid	G1	G1	31 NED
9	13/female	OMEC	Palate	G1	G2	184 NED
10	59/female	Adenocarcinoma oncocytic NOS	Parotid	G2	G3	96 NED
11	13/male	Cystic sialometaplasia	Parotid	G1	G2	48 NED
12	74/female	Adenocarcinoma oncocytic, low grade	Parotid	G1	G1	60 NED
13	51/female	Oncocytic neoplasm	Palate	G2	G2	48 NED
14	72/male	Myoepithelial carcinoma	Tongue	G2	G3	20 DOD, lymph node metastasis
15	67/female	OMEC, low grade oncocytic tumor	Sublingual	G1	G2	24 NED
16	74/male	OMEC	Submandibular	G1	G1	*
17	57/male	Clear cell oncocytoma/PA/MEC	Parotid	G1	G1	2 NED
18	63/female	OMEC without mucinous cells	Parotid	G1	G2	2 NED
19	71/male	OMEC	Parotid	G1	G2	5 NED
20	70/female	Cystic intranodal oncocytic inclusion/cystic sialometaplasia	Parotid	G1	G1	72 NED
21	54/male	OMEC	Parotid	G2	G2	24 NED
22	56/male	Oncocytoma benign	Base of tongue	G1	G2	6 NED

Case 16 has been published earlier.<sup>3</sup>

\*Not known.

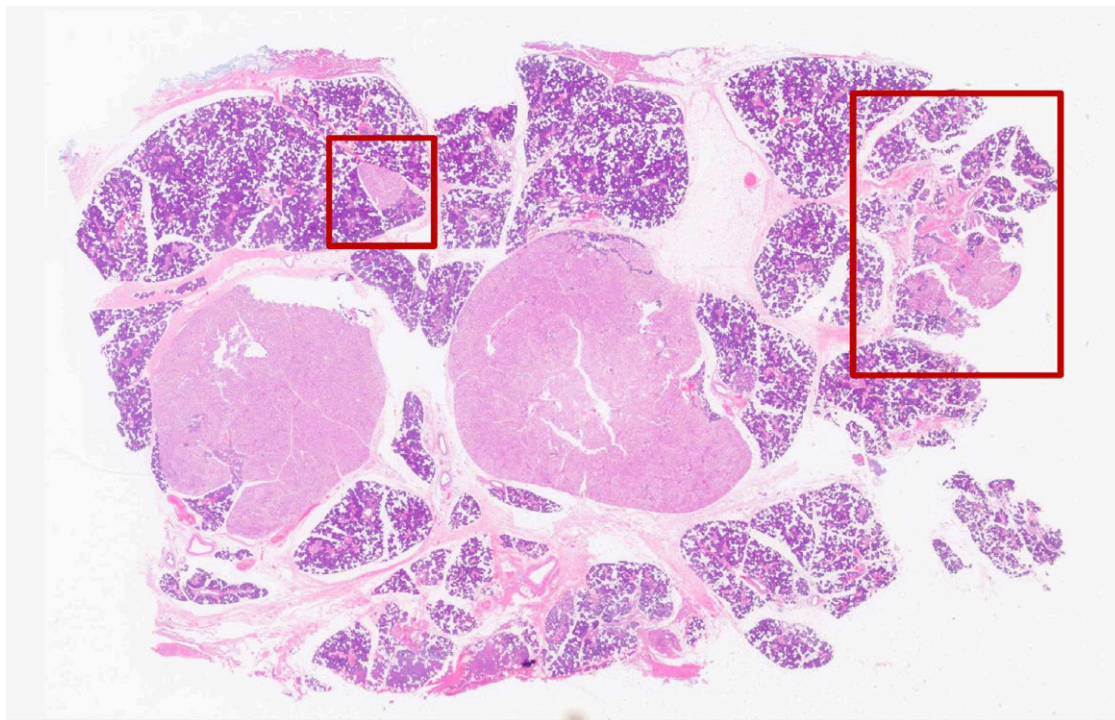
NED indicates no evidence of disease; NOS, not otherwise specified; PA, pleomorphic adenoma.

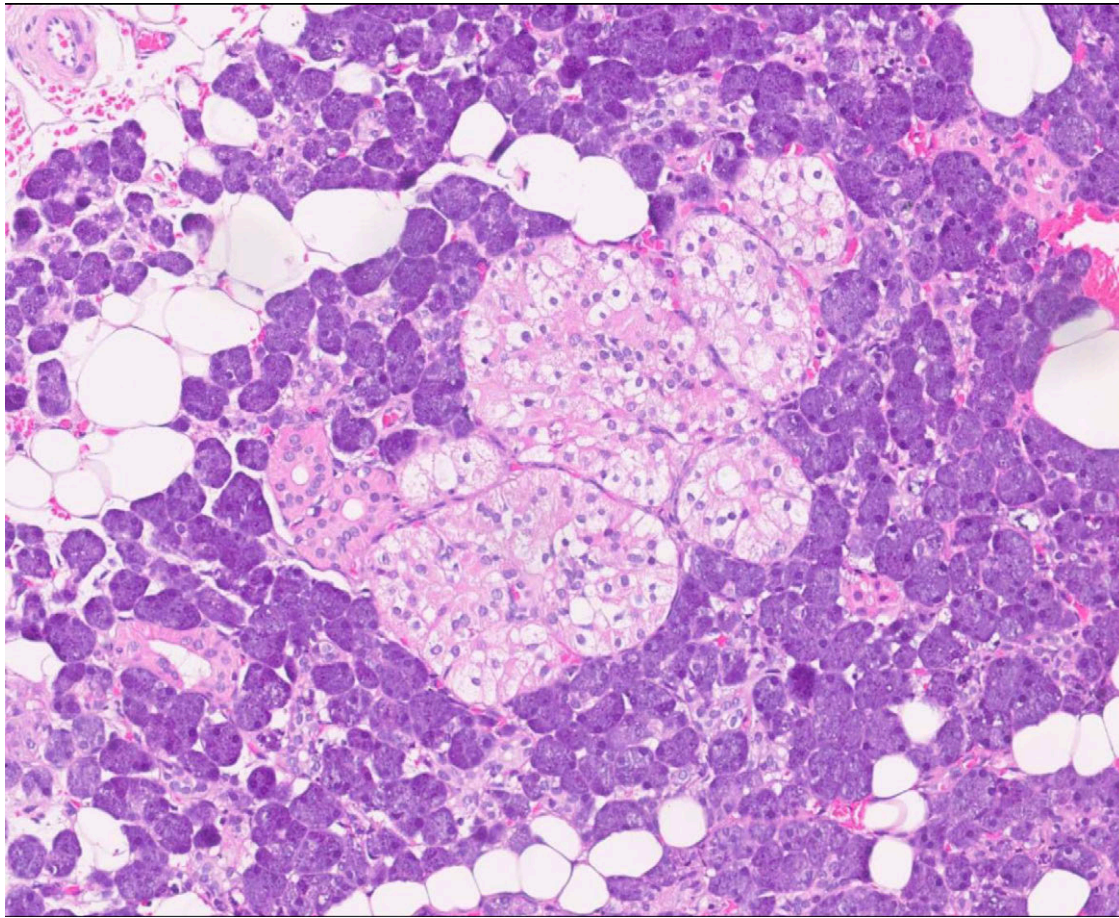
Skálová A, Agaimy A, Stanowska O, et al. Molecular Profiling of Salivary Oncocytic Mucoepidermoid Carcinomas Helps to Resolve Differential Diagnostic Dilemma With Low-grade Oncocytic Lesions. *Am J Surg Pathol.* 2020 Dec;44(12):1612-1622. doi: 10.1097/PAS.0000000000001590. PMID: 33002921.

ANTICANCER RESEARCH 37: 5263-5267 (2017)  
doi:10.21873/anticancerres.11951

## Are Multiple Tumors of the Parotid Gland Uncommon or Underestimated?

ACHIM M. FRANZEN<sup>1</sup>, ANNEKATRIN COORDES<sup>2</sup>, CHRISTIANE KAUP FRANZEN<sup>3</sup> and THOMAS GUENZEL<sup>4</sup>





**Intercalated Duct Lesions of Salivary Gland**  
*A Morphologic Spectrum From Hyperplasia to Adenoma*

Ilan Weinreb, MD,\*† Raja R. Seethala, MD,‡ Jennifer L. Hunt, MD,§  
 Ranjan Chetty, MB BCH, FRCPath, DPhil,\*† Irving Dardick, MD,\*†  
 and Bayardo Perez-Ordóñez, MD\*†

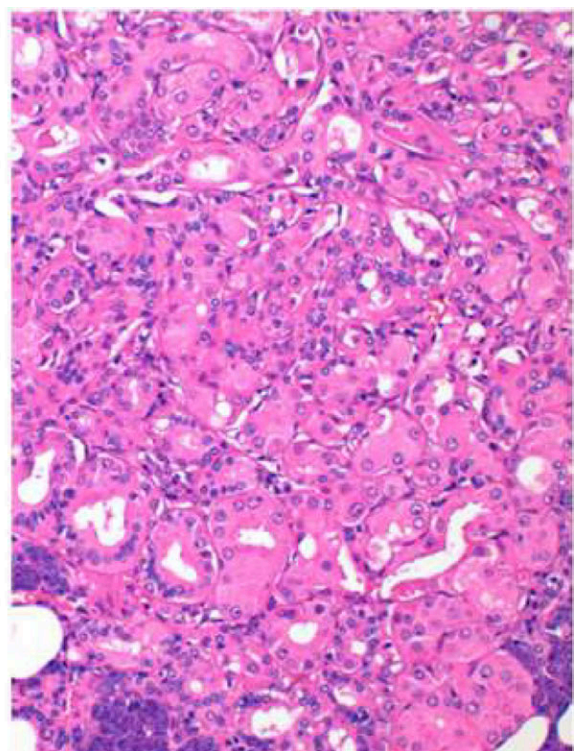
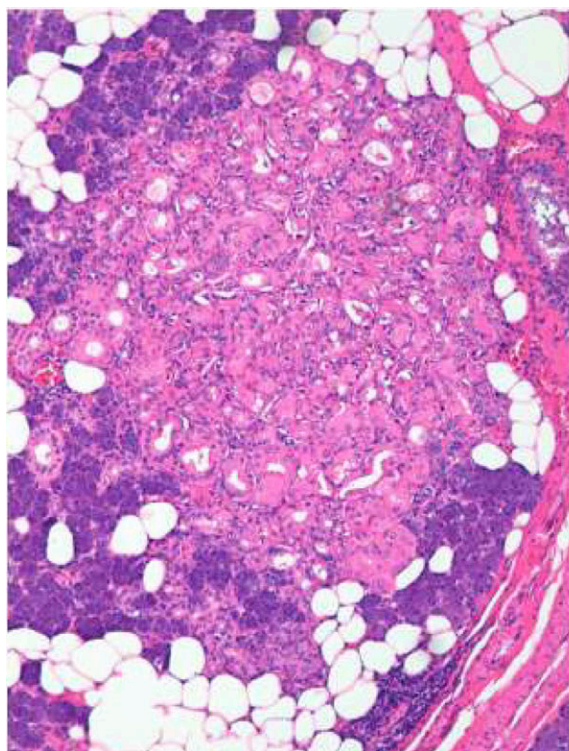
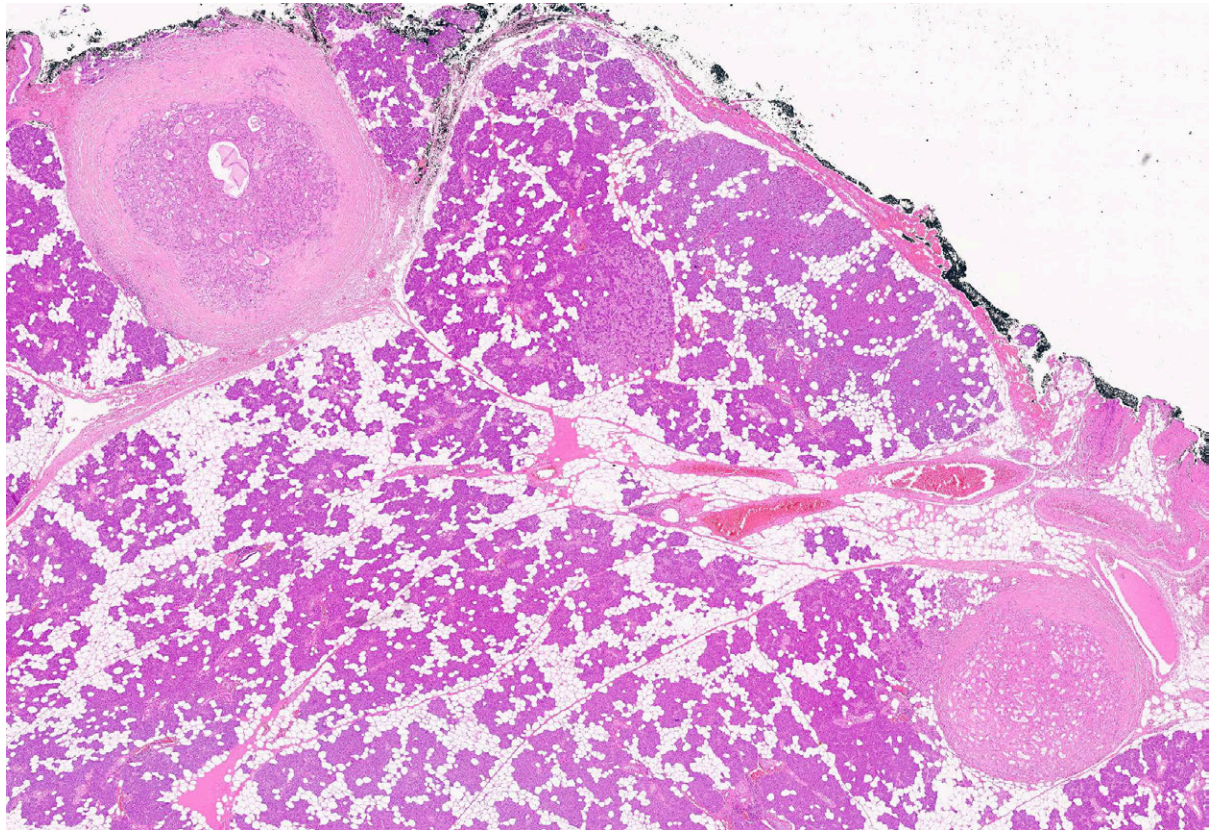
CHARACTERISTIC LESIONS, MOST OF WHICH OCCUR IN PAROTID AND do not infiltrate surrounding tissues.

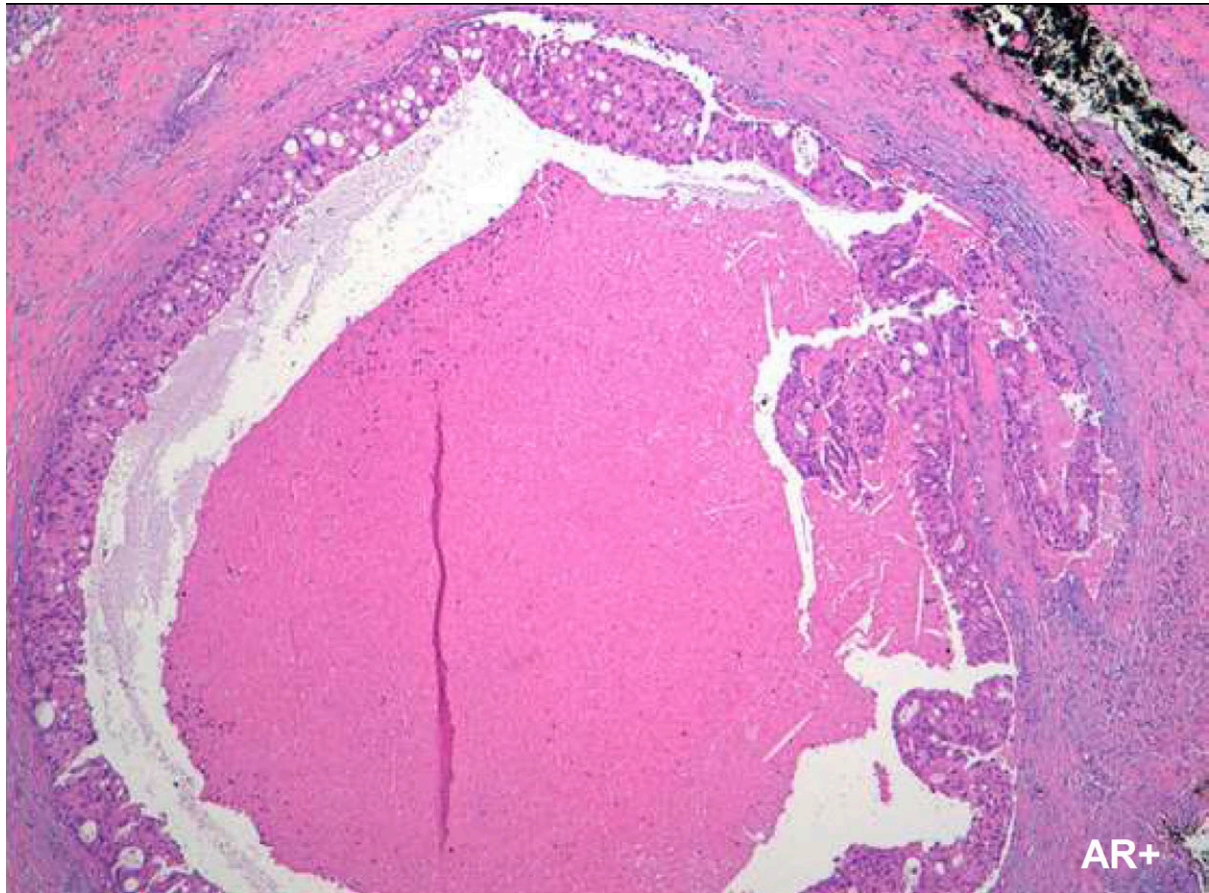
In summary, we have described 34 IDLs in 32 patients that morphologically and immunohistochemically recapitulate normal intercalated ducts. Architecturally, they range from hyperplasia to encapsulated adenomas with hybrid patterns. They can be associated with other salivary gland tumors especially basal cell neoplasms and EMC, suggesting that they may represent a precursor lesion of at least some of these neoplasms.

TABLE 1. Summary of Findings for Intercalated Duct Lesions

Patient	Sex/Age	Site	Size of Discrete Lesion (mm)		Type	Associated Tumor/Disease	Other Findings	
			Foci	Lesion (mm)				
1	78F	R parotid	1	1	IDH	Epithelial-myoeithelial carcinoma	—	
2	70F	L parotid	1	2	IDH	Pleomorphic adenoma	Nerve entrapped, clear myoeithelial cells	
3	70M	L parotid	1	4	Hybrid	None	—	
4	65M	R parotid	1	3	IDA	Melanoma	—	
5	74M	R parotid	1	4	IDA	Squamous cell carcinoma	Capsular clear myoeithelial cells	
6	59M	R parotid	1	5	IDA	None	Capsular clear myoeithelial cells	
7	36F	R parotid	1	8	IDA	None	Capsular clear myoeithelial cells	
8	79F	R parotid	1	3	Hybrid	BCA	—	
9	65F	R parotid	1	3	IDH	Squamous cell carcinoma	—	
10	65M	R parotid	2	1/1	IDH and IDH	BCA	Hyalinization—band-like	
11	74F	L parotid	1	2	IDH	BCA	—	
12	32F	L parotid	1	1	IDH	BCA	—	
13	52M	L parotid	1	2	IDH	Warthin tumor	—	
14	60F	R parotid	1	2	IDH	Epithelial-myoeithelial carcinoma	Hyalinization—dense, lymphoid stroma, clear myoeithelial cells	
8.	15	49F	R parotid	1	3	IDH	Squamous cell carcinoma	Clear intercalated ducts
16	20M	L parotid	1	2	IDH	None-parotid pain	—	
17	47M	Parotid	1	5	IDH	Skin basal cell carcinoma	—	
18	33F	Parotid	1	5	IDH/BCA	BCA	BM-like material and cribriform pattern	
19	46F	Parotid	1	2	IDH	Acinic cell carcinoma	Transition from IDH to BCA	
20	62F	Parotid	1	7	IDA	None	Hyalinization—band-like	
21	80F	Parotid	2	2/2	IDA and Hybrid	Pleomorphic adenoma	BM-like material and cribriform pattern	
22	59F	Parotid	1	4	IDA	Basal cell adenocarcinoma	—	
23	—	Parotid	1	2	IDH	Epithelial-myoeithelial carcinoma	—	
24	—	Parotid	1	5	IDA	None	—	
25	42F	L submandibular	D	—	IDH	Osteosarcoma of jaw	—	
26	19F	L submandibular	D	—	IDH	Mucocystic carcinoma	—	
27	79F	Submandibular	D	—	IDH	Squamous cell carcinoma	—	
28	59F	R parotid	1	3	Hybrid	BCA	—	
29	58F	Submandibular	D	—	IDH	Basal cell adenocarcinoma	—	
30	21M	Parotid	D	—	IDH	Mucocystic carcinoma	—	
31	—	Oral cavity	1	1	IDH	BCA	—	
32	67M	Buccal	1	1	IDH	BCA	—	

BCA indicates basal cell adenoma; BM, basement membrane; D, diffuse/multifocal; F, female; IDA, intercalated duct adenoma; IDH, intercalated duct hyperplasia; L, left; M, male; R, right.





**Table 1.** Criteria used for the diagnosis of the principal oncocytic lesion

Histopathology 1990; 16, 487-491

**Oncocytic adenomas and oncocytic hyperplasia of salivary glands: a clinicopathological study of 26 cases**

T.J.PALMER, M.J.GLEESON, J.W.EVESON\* & R.A.CAWSON

**Oncocytoma**

- Nodule entirely of oncocytic cells
- Solid trabecular/acinar growth pattern without a prominent peripheral palisade
- Light and dark cells
- Fibrous capsule, not necessarily complete
- Little internal fibrous stroma
- No included ducts
- Single central (degenerative) cyst or acinar lumina

**Multifocal nodular oncocytic hyperplasia (MNOH)**

- Multiple nodules of oncocytic cells in gland
- Typically clear cells with few light and dark cells
- No capsule around nodules
- Nodules in lobular distribution

**Diffuse oncocytosis**

- All acini affected
- Light and dark cells
- No nodules or tumour formation

The screenshot shows the WHO Classification of Tumours online page for 'Oncocytic carcinoma'. The page is titled 'WHO Classification of Tumours online' and includes a navigation path: 'Head and neck tumours // Tumours of salivary glands // Malignant tumours // Oncocytic carcinoma'. The main content area is titled 'Oncocytic carcinoma' and includes a definition, ICD-O coding (8290/3), related terminology (Malignant oncocytoma; oncocytic adenocarcinoma), localization (Most reported cases have been located in the parotid gland...), clinical features (Patients usually present with painless, slow-growing swellings.), epidemiology (Oncocytic carcinoma is an extremely rare salivary gland malignancy.), macroscopic appearance (The tumour is generally described as a grey-yellow, irregular but well-defined mass.), and histopathology (Oncocytic carcinoma is characterized by large polyhedral cells...).

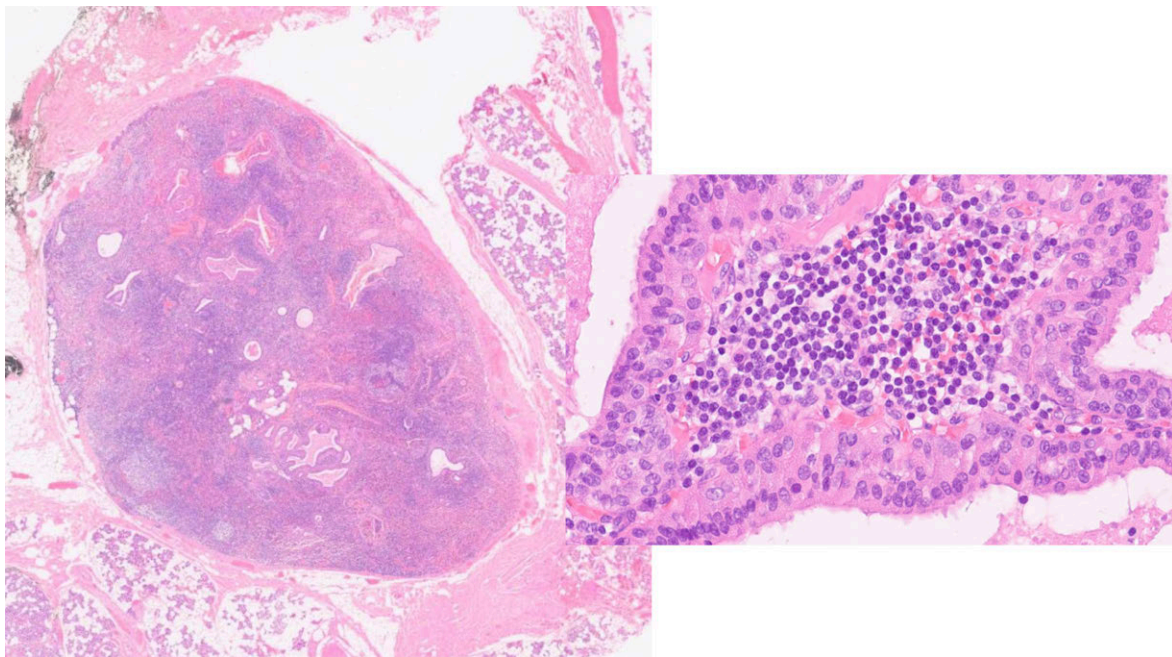
**4<sup>th</sup> edition**

*Malignant epithelial tumours*

- Mucoepidermoid carcinoma
- Adenoid cystic carcinoma
- Acinic cell carcinoma
- Secretory carcinoma
- Microsecretory adenocarcinoma
- Polymorphous adenocarcinoma
- Hyalinizing clear cell carcinoma
- Basal cell adenocarcinoma
- Intraductal carcinoma
- Salivary duct carcinoma
- Myoepithelial carcinoma
- Epithelial-myoepithelial carcinoma
- Mucinous adenocarcinoma
- Sclerosing microcystic adenocarcinoma
- Carcinoma ex pleomorphic adenoma
- Carcinosarcoma of the salivary glands
- Sebaceous adenocarcinoma
- Lymphoepithelial carcinoma
- Squamous cell carcinoma
- Sialoblastoma
- Salivary carcinoma, NOS and emerging entities

WHO Classification of Tumours Editorial Board. Head and neck tumours. Lyon (France): International Agency for Research on Cancer; forthcoming. (WHO classification of tumours series, 5th ed.; vol. 9). <https://publications.iarc.fr>.

- multiple nodules (parotid and lymph nodes)
  - metastatic lesion at the LN?
  - no, these oncocytic lesions probably arise from glandular inclusions which are very common in cervical level I and II LN
- all lesions have oncocytic features
- which salivary glands can have oncocytic features?
  - mostly all... (I showed some examples)



**Diagnosis: Warthin tumour; multifocal nodular oncocytic hyperplasia**

# Case 69

Michal Michal, Czech Republic | Case M71787/20

---

50 year old male had slightly enlarged thyroid with focally macroscopically fibrous white nodules.

**Diagnosis: Multifocal Fibrosing Thyroiditis**

## References:

1. Giovanni F, Rosai J. Multifocal Fibrosing Thyroiditis. Report of 55 Cases of a Poorly Recognized Entity. *Am J Surg Pathol* 2015;39:416-424

## Case 70

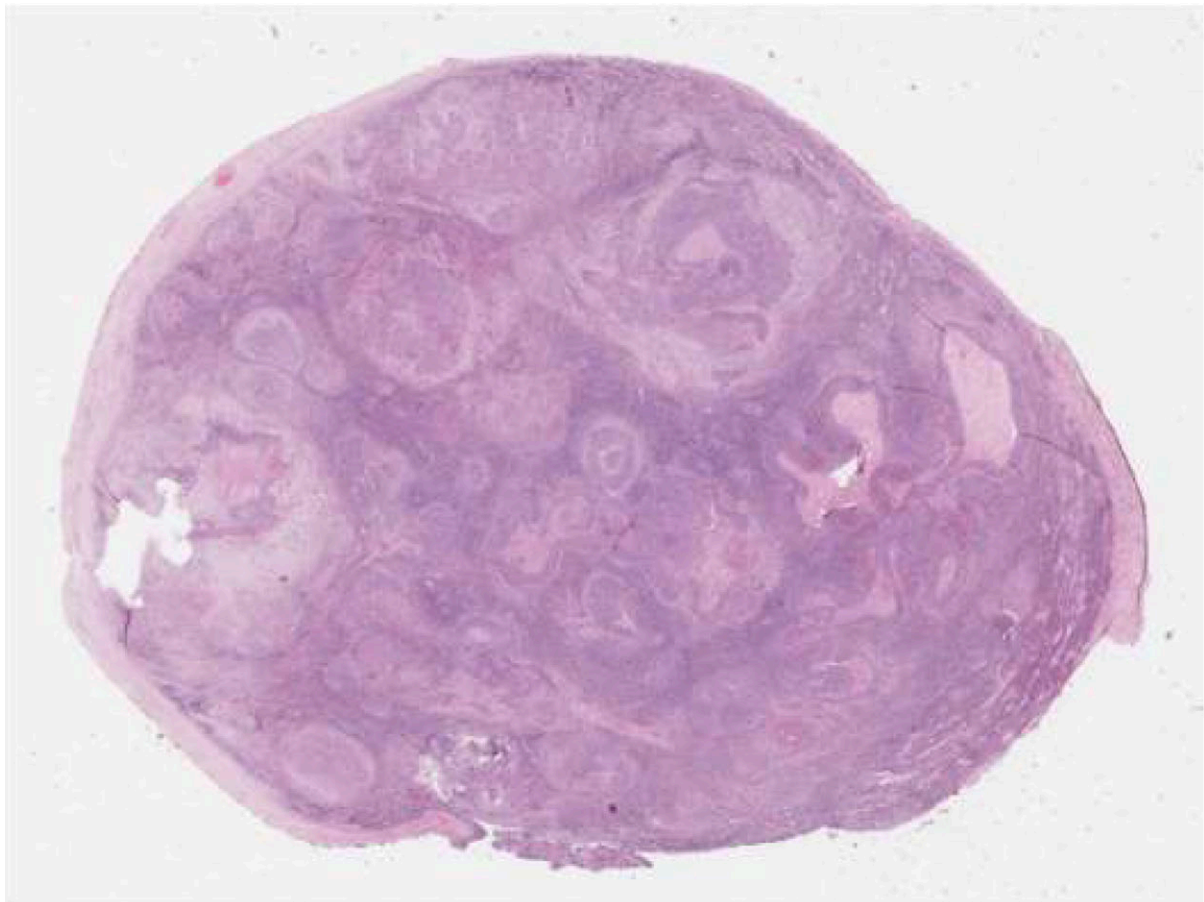
Isabel Fonseca, Faculdade de Medicina - ULisboa

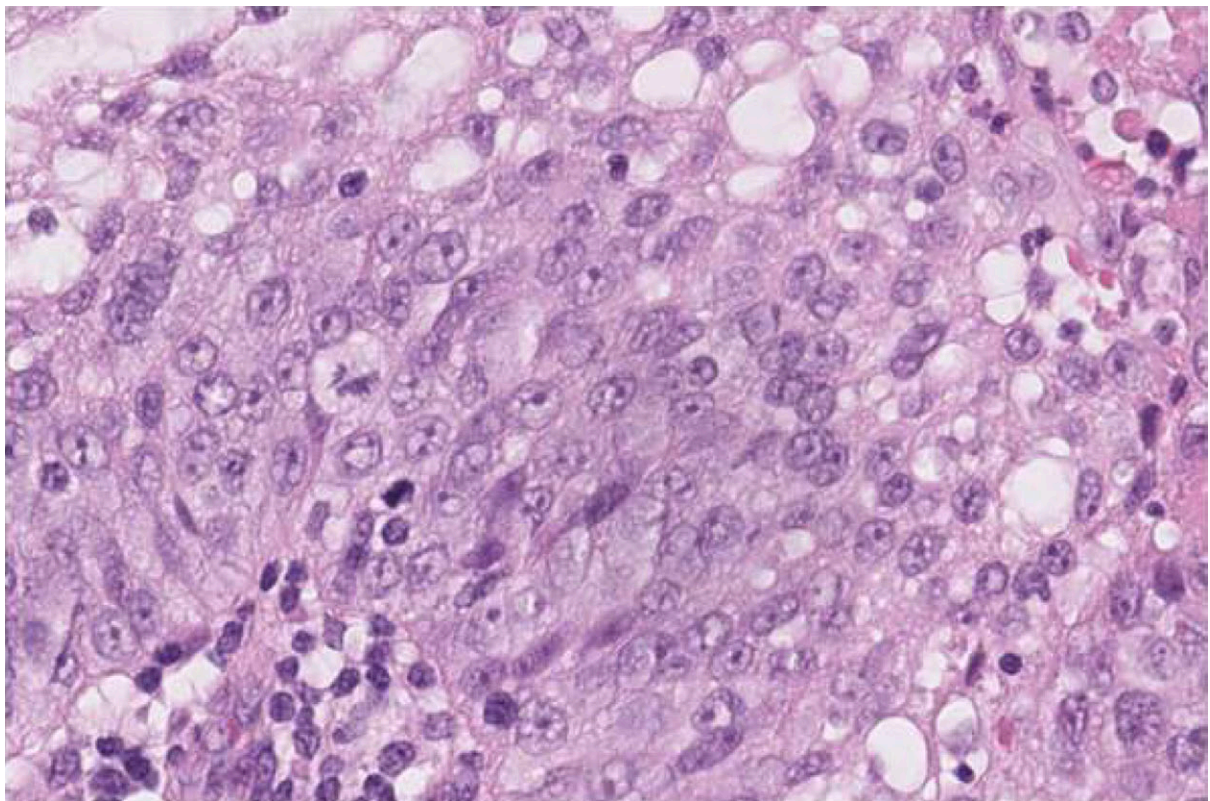
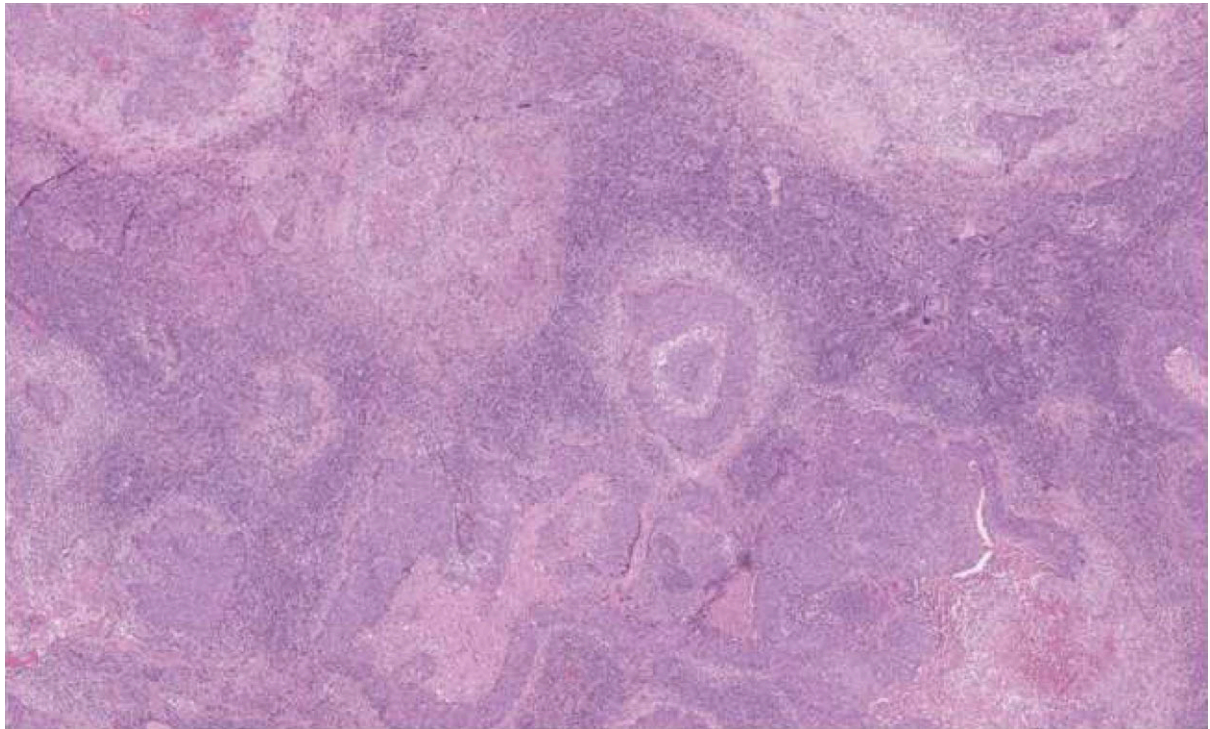
---

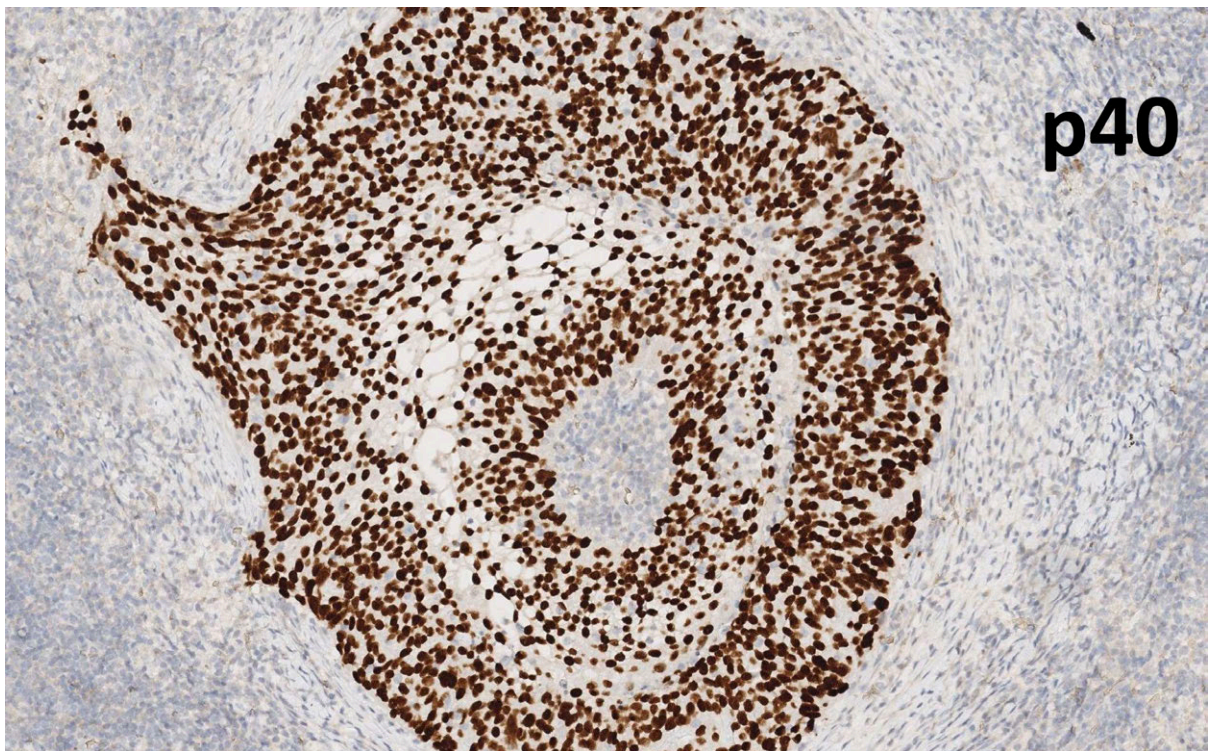
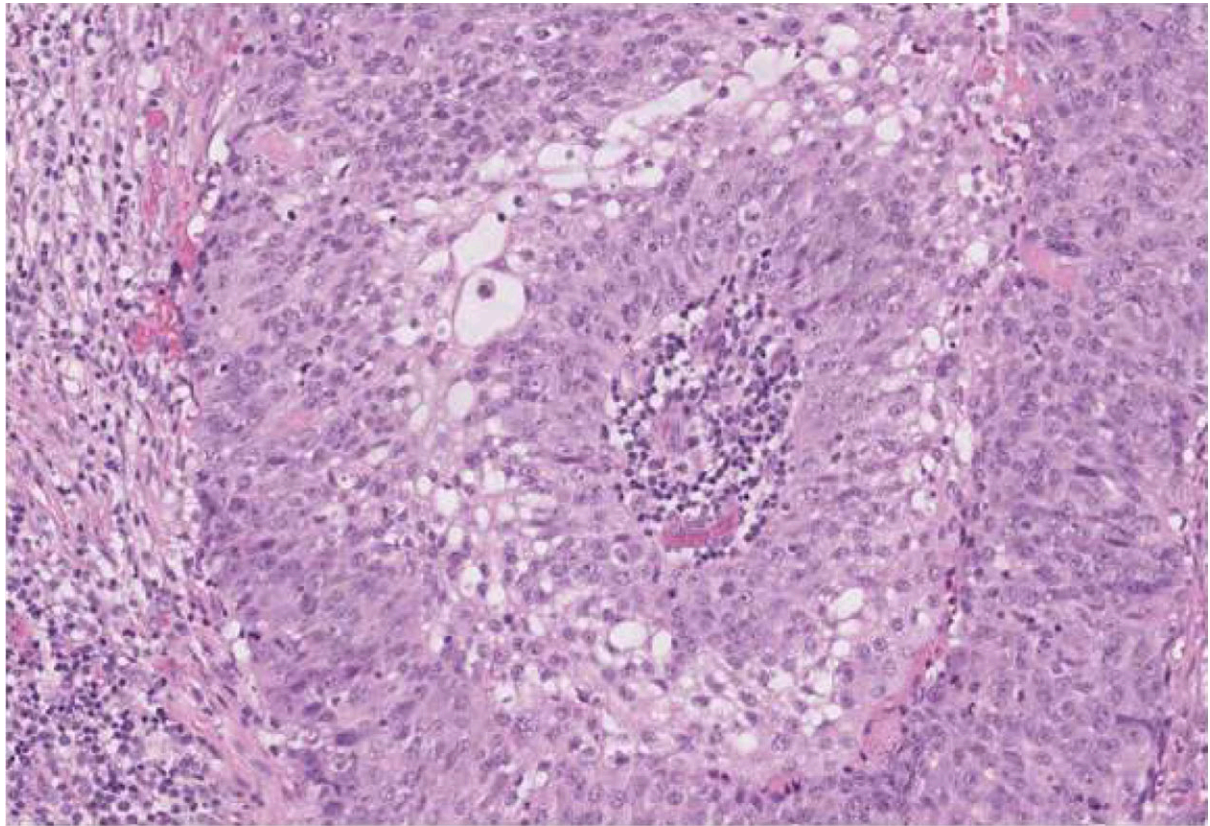
disclaimer: sorry, but back in 2019, this was a "burning issue", maybe not anymore!

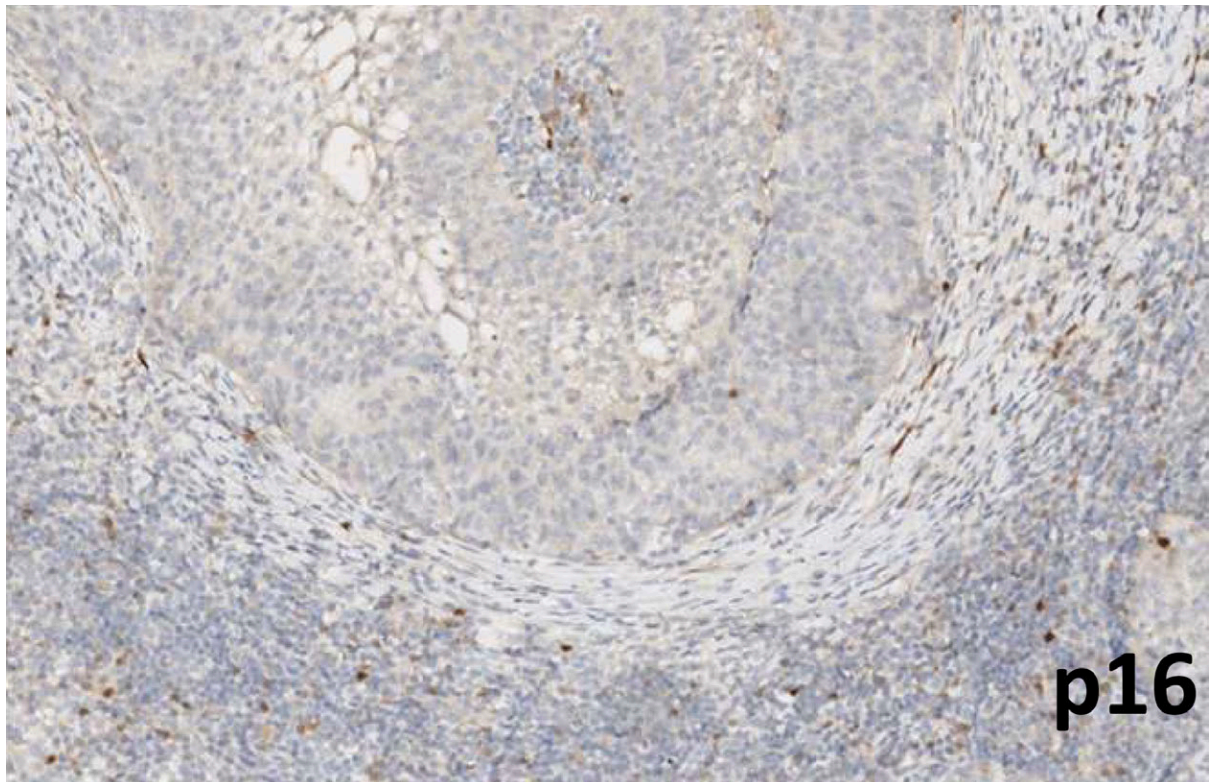
### Case history

A 40-year-old man was referenced with cervical (levels I and II) lumps. He was otherwise healthy. To note that he was a smoker (~25 cigarettes a day) and had a brother undergoing therapy for Hodgkin's lymphoma. He is currently well (having had COVID in 2021, times changed since 2019-2020...), without recurrence of the neoplastic disease. The slide is from a level II lymph node.



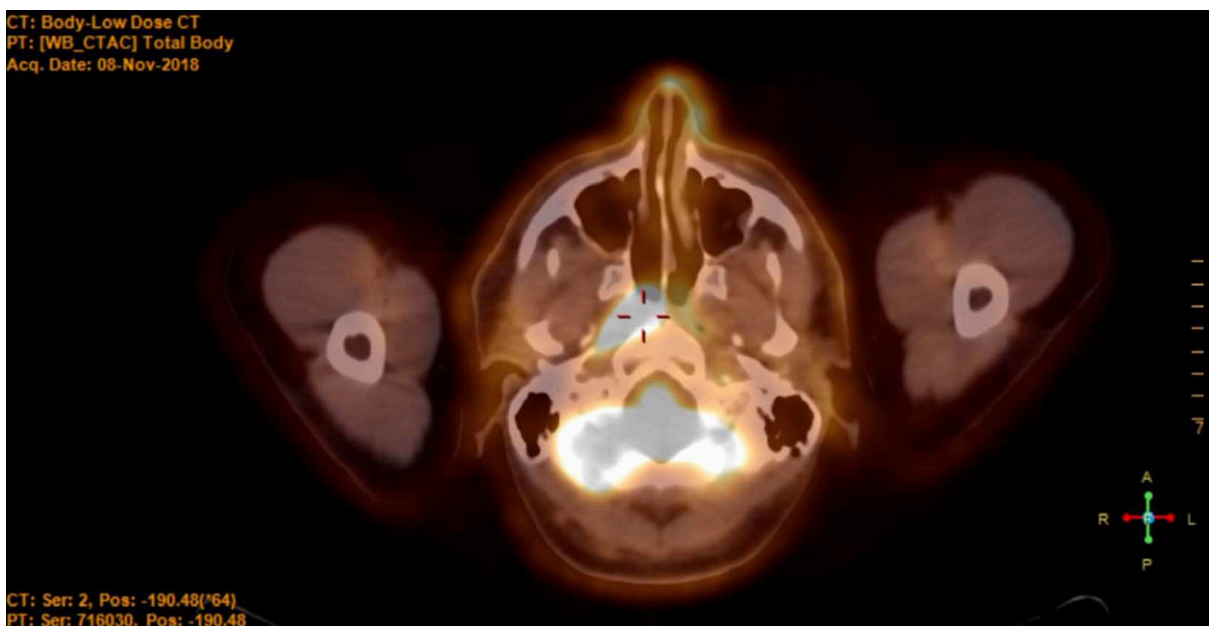






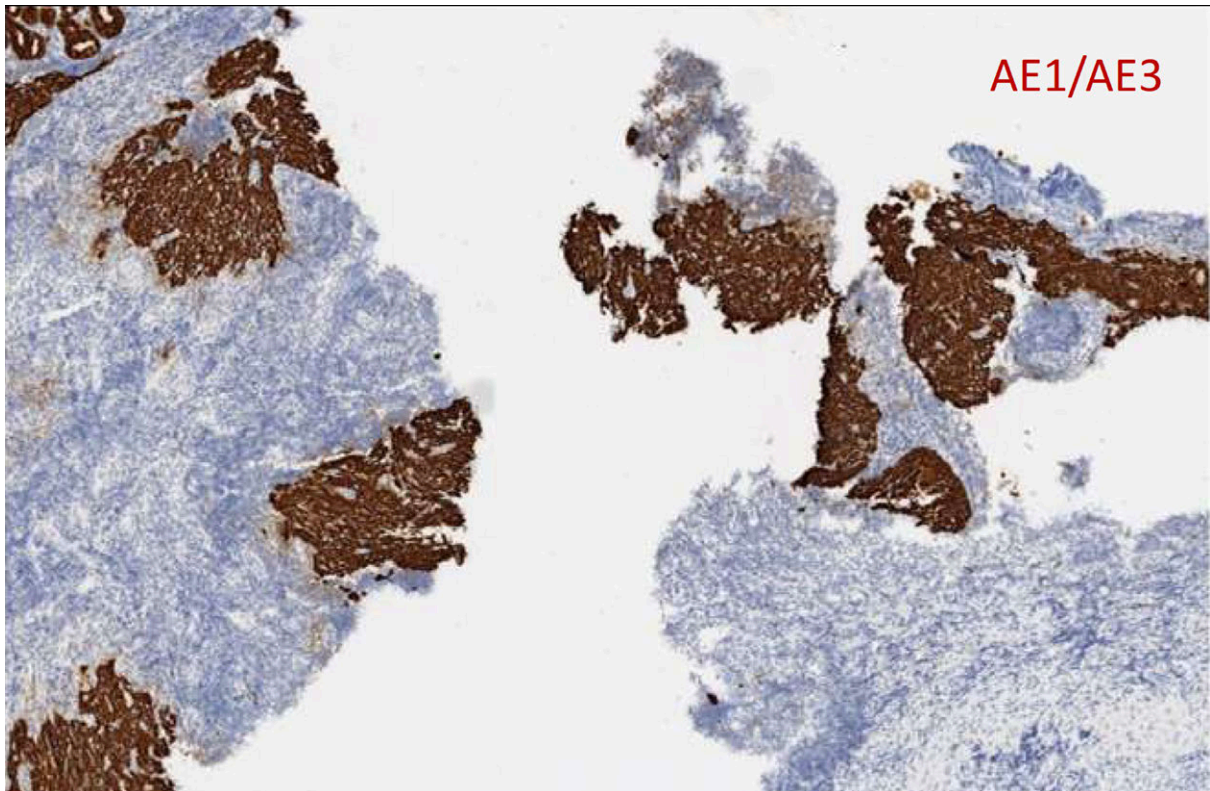
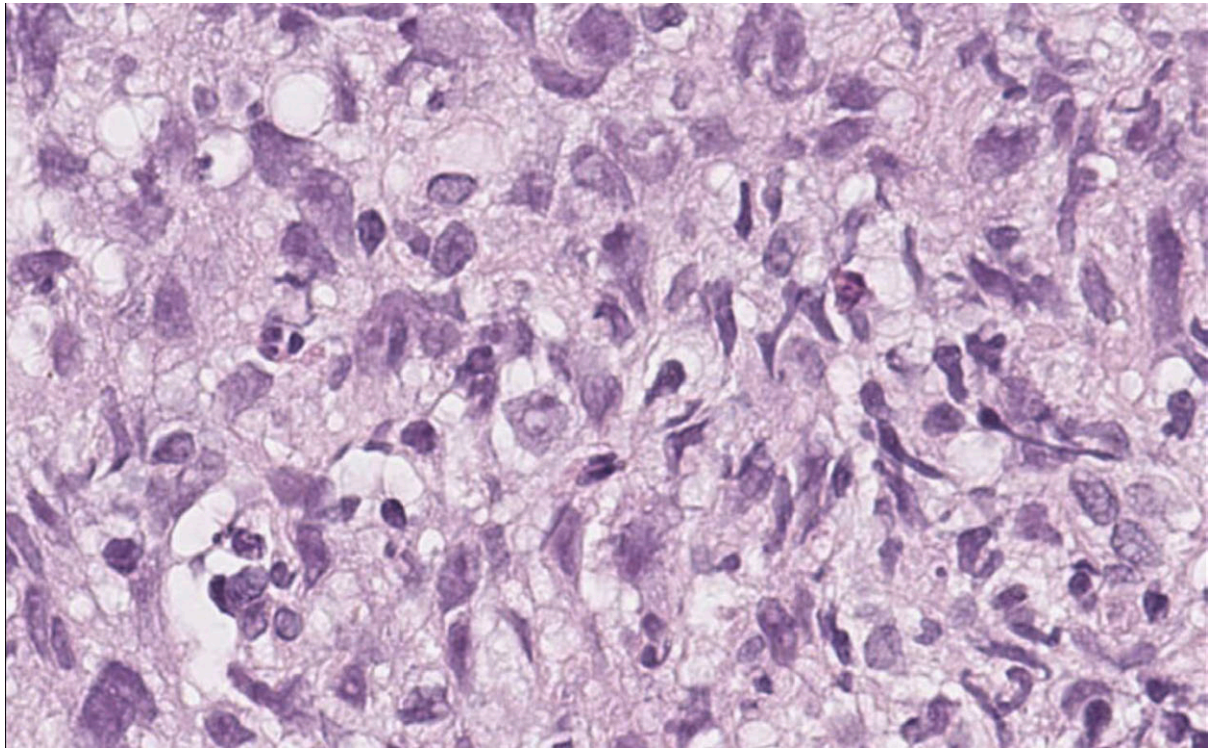
dx (october 2018)

- poorly differentiated squamous cell carcinoma, metastatic
- p16 negative



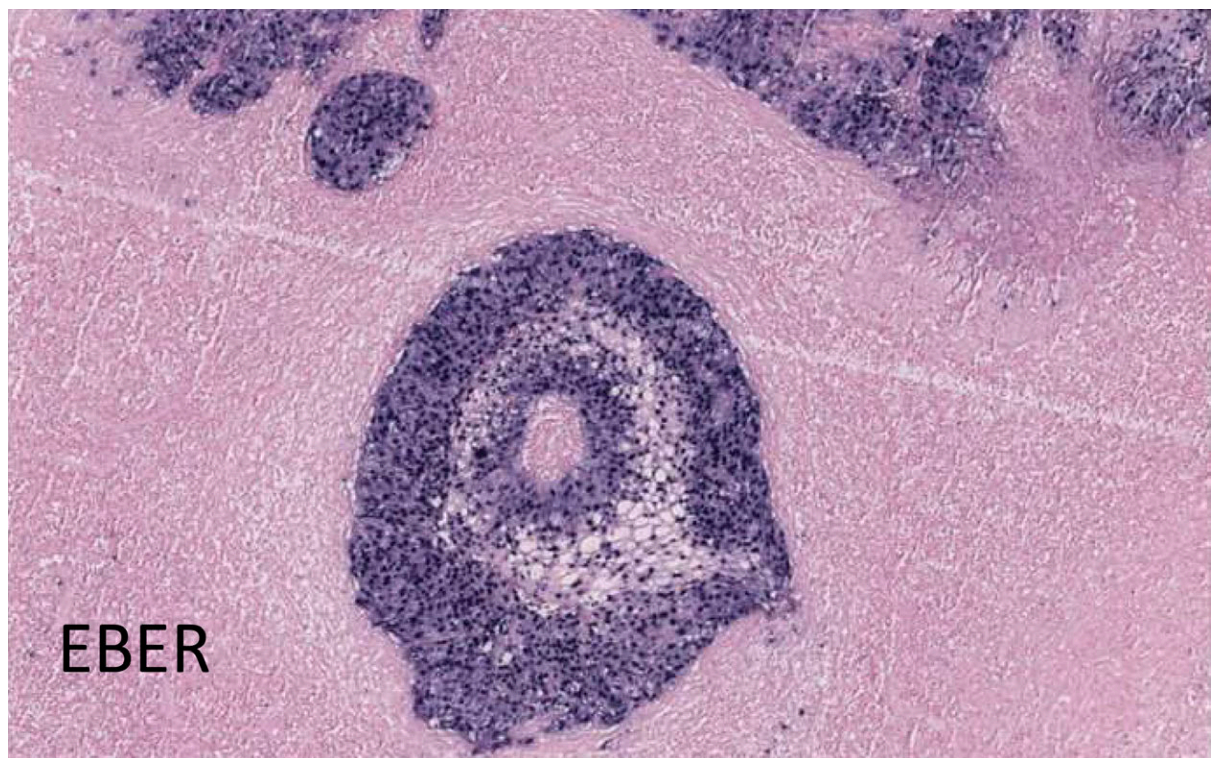
1 month later...a nasopharyngeal open biopsy was performed (the clinicians still "believed" in HL)

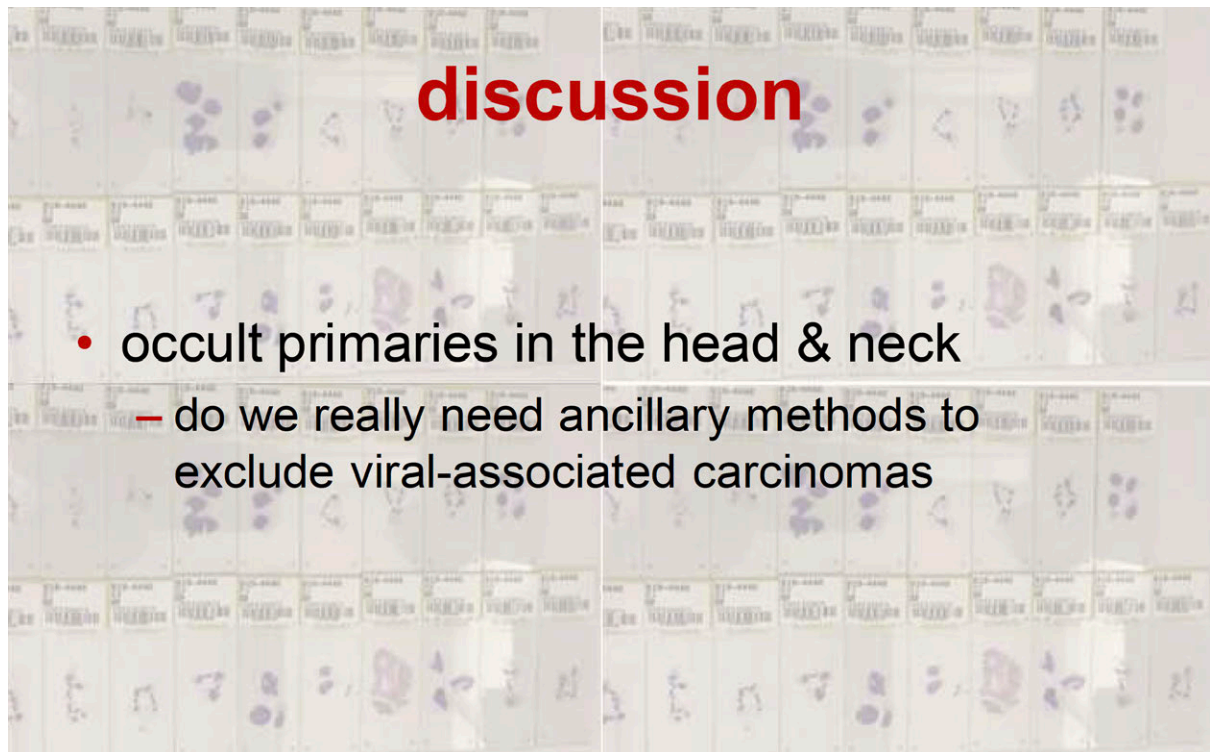






...and we went back to the LN





## EBV

### **EBV DNA in Biopsies of Burkitt Tumours and Anaplastic Carcinomas of the Nasopharynx**

A TEST system involving DNA-DNA hybridization has recently been described which makes possible the detection of Epstein-Barr virus (EBV) nucleic acid in tumour cells<sup>1</sup>. This method has been used to demonstrate EB viral genome equivalents in the "virus-free" Raji line of Burkitt tumour origin<sup>1</sup>. The presence of viral nucleic acid in these non-virus producing cells revealed that EBV can persist in a masked form, thus exhibiting characteristic

HARALD ZUR HAUSEN  
HEINRICH SCHULTE-HOLTHAUSEN

Institut für Virologie der Universität Würzburg,  
Luitpoldkrankenhaus,  
8700 Würzburg.

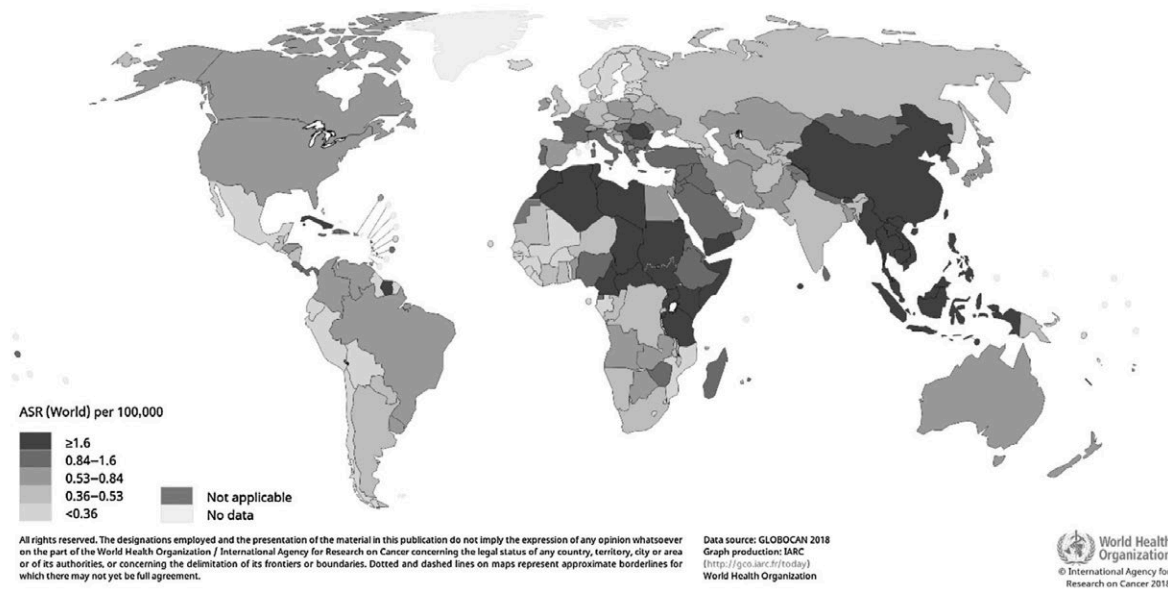
NATURE VOL. 228 DECEMBER 12 1970



From: **The Evolving Epidemiology of Nasopharyngeal Carcinoma**

Cancer Epidemiol Biomarkers Prev. 2021;30(6):1035-1047. doi:10.1158/1055-9965.EPI-20-1702

Estimated age-standardized incidence rates (World) in 2018, nasopharynx, males, all ages



Date of Download: 4/15/2022

Copyright © 2022 American Association for Cancer Research. All rights reserved.

# HPV

## Human Papillomavirus and Survival of Patients with Oropharyngeal Cancer

K. Kian Ang, M.D., Ph.D., Jonathan Harris, M.S., Richard Wheeler, M.D., Randal Weber, M.D., David I. Rosenthal, M.D., Phuc Felix Nguyen-Tân, M.D., William H. Westra, M.D., Christine H. Chung, M.D., Richard C. Jordan, D.D.S., Ph.D., Charles Lu, M.D., Harold Kim, M.D., Rita Axelrod, M.D., C. Craig Silverman, M.D., Kevin P. Redmond, M.D., and Maura L. Gillison, M.D., Ph.D.

N Engl J Med 2010;363:24-35.  
Copyright © 2010 Massachusetts Medical Society.

### HPV-associated head and neck cancer: a virus-related cancer epidemic

Shantti Morar, Gyorgyember D'Souza, William H Westra, Arlene A Forastiere

A rise in incidence of oropharyngeal squamous cell cancer—specifically of the lingual and palatine tonsils—in white men over 50 years who have a history of alcohol use has been recorded over the past decade.

VOLUME 33 • NUMBER 20 • OCTOBER 10 2015

JOURNAL OF CLINICAL ONCOLOGY

REVIEW ARTICLE

### Epidemiology of Human Papillomavirus–Positive Head and Neck Squamous Cell Carcinoma

Maura L. Gillison, Anil K. Chaturvedi, William F. Anderson, and Carole Fakhry

Publication of J Clin Oncol: 2015;33:2077  
https://doi.org/10.1200/JCO.2015.33.2077

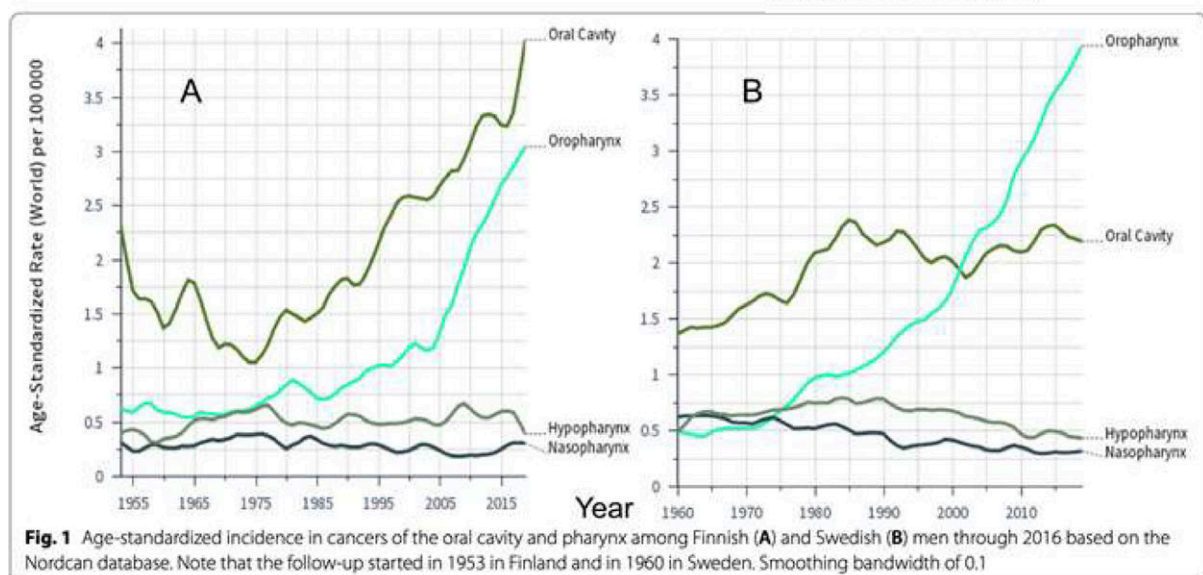
BMC Cancer

RESEARCH

Open Access

### Incidence and survival in oral and pharyngeal cancers in Finland and Sweden through half century

Anni K. Koskenvuo<sup>1</sup>, Otto Hemminki<sup>1\*</sup>, Aida Forsell<sup>2†</sup> and Karri Hemminki<sup>2†\*</sup>



## Morphologic diversity in human papillomavirus-related oropharyngeal squamous cell carcinoma: Catch Me If You Can!

James S Lewis Jr

**Table 1** Morphologic spectrum of oropharyngeal squamous cell carcinoma (SCC)

- ➔ Nonkeratinizing SCC
- Anaplastic and/or multinucleated tumor cells
- Tonsillar crypt tumor mimicking *in situ* disease
- Variants of SCC
  - ➔ Basaloid
  - ➔ Papillary
  - ➔ Lymphoepithelial
  - Adenosquamous
  - Spindle cell
  - Cystic cervical nodal metastases
  - Ciliated tumor cells
  - Small cell (high grade neuroendocrine) carcinoma

**Table 1** Comparison of certain features in viral +/- head and neck cancers

	EBV+ NPC	EBV- NPC	HPV+ HNSCC (most oropharyngeal)	HPV- HNSCC
Trigger	DS-DNA virus	Sporadic, likely tobacco/alcohol/other carcinogens	DS-DNA virus	Tobacco/alcohol/other carcinogens
WHO carcinogen group	Group 1 carcinogen	Group 1 carcinogens	Group 1 carcinogen	Group 1 carcinogens
Virus genome size	Size ~172 kb	NA	Size ~8 kb	NA
Virus location in cell	Episomal genome	NA	Mostly integrated into cellular genome (some episomal)	NA
Differentiation	Non-keratinising or undifferentiated SCC	Moderate to well differentiated SCC	Basaloid or undifferentiated SCC	Mostly moderate to well-differentiated SCC
Age at diagnosis	~ 50 years	~ >65 years	~ 53 years	~ > 65 years
Endemicity	High incidence rates in Southern China, South-East Asia, moderate rates in North Africa (Maghreb)	>100 fold lower in non-endemic areas	30–70% of annual oropharyngeal SCCs in Northern, Western Europe, North America	Dominant fraction of non-oropharyngeal cancers, and other head and neck anatomical sites
Sensitivity to treatment	Sensitive to radiochemotherapy (wtTP53)	Less sensitive	Sensitive to radiochemotherapy (wtTP53)	Less sensitive
Gender ratio	Male preponderance	Male preponderance	Male preponderance	Male preponderance
Targeted therapy potential	Viral (foreign) antigens and some endogenous mutations may be suitable as targets for screening or therapy	NA	Viral (foreign) antigens suitable as targets for screening or therapy	NA
Vaccine	Prophylactic vaccine not available (NA)	NA	Prophylactic vaccine available	NA

Copyright © 2017 Wolters Kluwer Health | Lippincott Williams & Wilkins  
 Head and Neck Cancers (5th Edition)  
 Viral and Clinical Oncology of Head and Neck Cancers  
 Peter G. Henson, Barbara Schuchman, Felix Ozyurt, Loretta Shaw, Simon Schreiber, Christopher P. Miller, Roy Teich, Frank Bracci, Lars Olsson, Robert H. Thaler, Robert S. Hittelman

# Human Papillomavirus Testing in Head and Neck Carcinomas

## Guideline From the College of American Pathologists

James S. Lewis Jr, MD; Beth Beadle, MD, PhD; Justin A. Bishop, MD; Rebecca D. Chernock, MD; Carol Colasacco, MLIS, SCT(ASCP); Christina Lacchetti, MHS; Joel Todd Moncur, MD, PhD; James W. Rocco, MD, PhD; Mary R. Schwartz, MD; Raja R. Seethala, MD; Nicole E. Thomas, MPH, CT(ASCP)<sup>CM</sup>; William H. Westra, MD; William C. Faquin, MD, PhD

• **Context.**—Human papillomavirus (HPV) is a major cause of oropharyngeal squamous cell carcinomas, and HPV (and/or surrogate marker p16) status has emerged as a prognostic marker that significantly impacts clinical management. There is no current consensus on when to test oropharyngeal squamous cell carcinomas for HPV/p16 or on which tests to choose.

**Objective.**—To develop evidence-based recommendations for the testing, application, interpretation, and reporting of HPV and surrogate marker tests in head and neck carcinomas.

**Design.**—The College of American Pathologists convened a panel of experts in head and neck and molecular pathology, as well as surgical, medical, and radiation oncology, to develop recommendations. A systematic review of the literature was conducted to address 6 key questions. Final recommendations were derived from

strength of evidence, open comment period feedback, and expert panel consensus.

**Results.**—The major recommendations include (1) testing newly diagnosed oropharyngeal squamous cell carcinoma patients for high-risk HPV, either from the primary tumor or from cervical nodal metastases, using p16 immunohistochemistry with a 70% nuclear and cytoplasmic staining cutoff, and (2) not routinely testing non-squamous oropharyngeal carcinomas or nonoropharyngeal carcinomas for HPV. Pathologists are to report tumors as HPV positive or p16 positive. Guidelines are provided for testing cytologic samples and handling of locoregional and distant recurrence specimens.

**Conclusions.**—Based on the systematic review and on expert panel consensus, high-risk HPV testing is recommended for all new oropharyngeal squamous cell carcinoma patients, but not routinely recommended for other head and neck carcinomas.

(*Arch Pathol Lab Med.* 2018;142:559–597; doi: 10.5858/arpa.2017-0286-CP)

Accepted for publication October 23, 2017

Sponsored by



**Nodal Excisions and Neck Dissection Specimens for Head & Neck Tumours Histopathology Reporting Guide**



### Note 3 – Histological tumour type (Core and Non-core)

#### Reason/Evidentiary Support

Identification of the histological tumour type is crucial for several reasons, including: 1) confirmation that a metastasis is of the same type as the resected primary tumour 2) facilitating a clinical search in cases of unknown primary tumours 3) determining the correct T and N categories (see below) 4) guiding treatment, which varies by tumour type and lymph node status.<sup>12</sup>

Histological type and grade is typically determined from the histology of the primary site, but this is not possible for tumours of unknown origin. Tissue from a neck metastasis may be required for ancillary testing (e.g. p16 immunohistochemistry, in situ hybridization for high-risk human papilloma virus (HPV), in situ hybridization for Epstein Barr virus encoded RNA/EBER). For patients with occult primary squamous cell carcinoma in level II or III, the cN or pN categories are influenced by EBV and HPV status.<sup>13</sup> EBV-related and HPV-related carcinomas are given the N category that applies to nasopharyngeal and HPV-related oropharyngeal carcinomas, respectively.<sup>1</sup>

## **Diagnosis:**

### **metastatic nasopharyngeal carcinoma**

- remember: in occult primaries in younger patients
- the most common primary location are the tonsils
- the second most common is nasopharynx
- so: for the detection of viral-related disease use p16 as a surrogate for HPV and EBER for EBV and you might solve most of the cases

# Case 71

(M20020/98)

---

48-year-old female with solitary renal tumor, size 2.5 x 3 x 2 cm, dark tan to brown in color, solid. No necrosis or hemorrhage.

## Pathologic findings

Architecture of the tumor is mostly solid, admixed with few nested areas. Thick-walled vessels are prominent at the periphery, as well as entrapped non-neoplastic tubules. The cells have large intracytoplasmic irregular vacuoles. The nuclei are round to oval, with enlarged nucleoli, WHO2016/ISUP grade 3. Neoplastic cells are packed in oval aggregates, cytoplasmic membranes surrounding these aggregates are thick and prominent.

Immunohistochemistry: Tumor was positive for PAX 8, AE1-AE3, CD117 (KIT), antimitochondrial antigen antibody, and cathepsin K. Strong positivity for CK7 was noted in scattered cells (up to 5-10%). Fumarate hydratase and SDHB were both retained.

Vimentin, HMB45, and Melan A were negative.

Mutation in *TSC2* gene was found in this case.

## Diagnosis: Eosinophilic vacuolated tumor

For many years, tumors with overlapping features between renal oncocytoma and chromophobe renal cell carcinoma posed a problem for daily routine pathology. In ISUP Vancouver Classification 2012 and in WHO 2016, these tumors were provisionally placed into the category of atypical chromophobe RCCs. Two perspective entities called "Eosinophilic Vacuolated Tumor" (EVT) and "Low-grade Oncocytic Tumor" (LOT) emerged from this overlapping chromophobe-oncocytic tumor group. EVT was initially described as "high-grade oncocytic tumor" by He et al. and as "sporadic RCC with eosinophilic and vacuolated cytoplasm" by Chen et al. In the recent GUPS update, a unifying name EVT was accepted for this tumor.

At the beginning, EVT was considered to be sporadic, however, later it was found also in patients with tuberous sclerosis complex (TSC).

EVT is typically detected incidentally, there are no specific clinical signs. Vast majority of documented cases are small tumors, rarely exceeding pT1 stage (UICC and IJCC). It occurs in slight female predominance. Age range is broad: 25 to 73 years.

However, the number of the reported cases is not high and follow up period is not very long, there is no single case with documented aggressive behavior.

Typically, EVT is solitary and sporadic tumor, however rare case reports described multifocal tumors were published (in rare patients with TSC). On gross section, EVT is typically solid, gray, tan or brown. Necrosis or extensive hemorrhage have not been so far documented grossly.

EVT typically has solid and nested architecture. Rarely, tubulocystic areas were reported. Thick-walled vessels are virtually always found at the periphery as well as entrapped non-neoplastic tubules. Cells are voluminous, pale to eosinophilic with vacuoles. Size of vacuoles is variable, however, large voluminous intracytoplasmic vacuoles are more typical. The nuclei are round to oval, with enlarged nucleoli, WHO2016/ISUP grade 3. EVT is diffusely positive for CD117 (KIT), CD10, antimitochondrial antigen antibody, PAX8, AE1-AE3, and cathepsin K, however single cases demonstrated more focal distribution of positivity. CK7 expression pattern and vimentin reactivity follow patterns known from renal oncocytoma, ie occasional single positive cells.

Loss of chromosome 1, along with concurrent TSC/MTOR mutations are typical and diagnostic feature for EVT. Based on the current knowledge, EVT is a renal tumor associated with either germline or somatic mutations leading to mTORC1 activation. In differential diagnostic list, the most important entity is eosinophilic variant of chromophobe RCC (eCHRCC). On morphologic level, the most important sign is the presence of prominent nuclear irregularities (classic raisinoid shape). Cytoplasm of eCHRCC is compact, oncocytic without voluminous vacuoles, however perinuclear clearing is always present. eCHRCC is positive diffusely for CK7 and CD117, which is not typically seen in EVT.

Renal oncocytoma (RO) differs mostly on morphology. However, RO tends to be solid, usually there are areas of fibrotic stroma with small islands of oncocytic cells. The most important difference is presence of large intracytoplasmic vacuoles in EVT, presence of thick basal membranes surrounding groups of neoplastic cells, the feature, which is absent in RO. Immunohistochemical positivity for cathepsin K favors diagnosis of EVT. Also

on molecular genetic level, presence of mTOR pathway genes speaks against diagnosis of RO.

Despite the fact, that for EVT are characteristic abnormalities in MTOR pathway genes, molecular testing is not necessary in typical cases. However, in cases with uncertain morphology, genetic testing would be useful for establishing of correct diagnosis.

## Selected references:

1. He H, Trpkov K, Martinek P, Isikci OT, Maggi-Galuzzi C, Alaghebandan R, et al. "High-grade oncocytic renal tumor": morphologic, immunohistochemical, and molecular genetic study of 14 cases. *Virchow Arch* 473,725-38(2018)
2. Chen YB, Mirsadraei L, Jayakumaran G, Al-Ahmadie HA, Fine SW, Gopalan A, et al. Somatic Mutations of TSC2 or MTOR Characterize a Morphologically Distinct Subset of Sporadic Renal Cell Carcinoma With Eosinophilic and Vacuolated Cytoplasm. *Am J Surg Pathol* 43,121-31(2019)
3. Trpkov K, Williamson SR, Gill AJ, Adeniran AJ, Agaimy A, Alaghebandan R, et al. Novel, emerging and provisional renal entities: The Genitourinary Pathology Society (GUPS) update on renal neoplasia. *Mod Pathol* 34, 1392-424 (2021)
4. Petersson F, Gatalica Z, Grossmann P, Perez Montiel MD, Alvarado Cabrero I, Bulimbasic S, et al. Sporadic hybrid oncocytic/chromophobe tumor of the kidney: a clinicopathologic, histomorphologic, immunohistochemical, ultrastructural, and molecular cytogenetic study of 14 cases. *Virchows Arch* 456,355-65, (2010)
5. Trpkov K, Bonert M, Gao Y, Kapoor A, He H, Yilmaz A, et al. High-grade oncocytic tumour (HOT) of kidney in a patient with tuberous sclerosis complex. *Histopathology* 75,440-2 (2019)
6. Lerma LA, Schade GR, Tretiakova MS. Co-existence of ESC-RCC, EVT, and LOT as synchronous and metachronous tumors in six patients with multifocal neoplasia but without clinical features of tuberous sclerosis complex. *Hum Pathol* 116,1-11 (2021)
7. Ruiz-Cordero R, Rao P, Li L, Qi Y, Atherton D, Peng B, et al. Hybrid oncocytic/chromophobe renal tumors are molecularly distinct from oncocytoma and chromophobe renal cell carcinoma. *Mod Pathol* 32,1698-707(2019)
8. Kapur P, Gao M, Zhong H, Rakheja D, Cai Q, Pedrosa I, et al. Eosinophilic Vacuolated Tumor of the Kidney: A Review of Evolving Concepts in This Novel Subtype With Additional Insights From a Case With MTOR Mutation and Concomitant Chromosome 1 Loss. *Adv Anat Pathol* 28,251-7(2021)
9. Gupta S, Jimenez RE, Herrera-Hernandez L, Lohse CM, Thompson RH, Boorjian SA, et al. Renal Neoplasia in Tuberous Sclerosis: A Study of 41 Patients. *Mayo Clin Proc* 96,1470-89(2021)

10. Kapur P, Gao M, Zhong H, Chintalapati S, Mitui M, Barnes SD, et al. Germline and sporadic mTOR pathway mutations in low-grade oncocytic tumor of the kidney. *Mod Pathol* online ahead of print (2021)
11. Farcas M, Gatalica Z, Trpkov K, Swensen J, Zhou M, Alaghebandan R, et al. Eosinophilic vacuolated tumor (EVT) of kidney demonstrates sporadic TSC/MTOR mutations: next-generation sequencing multi-institutional study of 19 cases. *Mod Pathol* online ahead of print (2021)
12. Siadat F, Trpkov K. ESC, ALK, HOT and LOT: Three Letter Acronyms of Emerging Renal Entities Knocking on the Door of the WHO Classification. *Cancers* 12, 168 (2021)

# Case 72

(M70420/15)

---

67-year-old female with renal tumor located in the central part of the kidney. Diameter was 6 cm, tumor infiltrated renal sinus.

## Pathologic findings

On gross section, tumor showed yellow golden color with regressive changes, hemorrhages and foci of firm gray tissue on cut surface. Necrotic areas were minimal. Histologically, majority of cells showed predominantly clear cytoplasm, arranged mainly in alveolar, nested, and trabecular patterns, separated by fibrovascular septae. Papillary/tubulopapillary pattern was present in approximately 70% of the tumor volume. Fibrovascular cores were populated by lymphocytic inflammatory cells. Foamy macrophages were not observed. The ISUP/WHO2016 histologic grade was up to 3. CK7 was negative in non-papillary areas, focally positive in papillary structures. In papillary areas, AMACR was focally positive, negative in solid-alveolar part of the tumor. CAIX was positive, however positivity was focal and weaker, comparing with the classic type of clear cell RCC. Vimentin was positive. TFE3, Melan A, and HMB45 were all negative.

Unfortunately, case had low DNA quality and we were not able to finish NGS analysis.

## Diagnosis: Clear cell renal cell carcinoma with papillary pattern

Clear cell RCC (CCRCC) usually shows a solid, alveolar or acinar growth pattern, composed of clear or eosinophilic neoplastic cells. However, substantial part of CCRCCs is highly heterogeneous. Variability in both architectural growth patterns and morphologic features is very common. Focal pseudopapillary features with large cells with bizarre nuclei and eosinophilic rhabdoid-like cytoplasm were already documented in the literature.

Other less common morphologic variants of CCRCCs have been described, including mucin-secreting CCRCC, CCRCC with low-grade spindle cell proliferation, CCRCC with syncytial giant cell component, and CCRCCs with prominent emperipolesis.

According to the World Health Organization (WHO) Classification of Genitourinary tumors 2016 and 2022, "focal" papillary areas can be seen in CCRCCs.

However, in consultation practice, such cases are not entirely rare and constantly posing problem for routine daily diagnostic work. CCRCCs can have rather voluminous papillary areas with well-formed true papillae, including fibrovascular core and epithelial lining of such structures. A couple of studies described CCRCC with papillary pattern have been published so far. The papillary area could constitute a substantial portion of the CCRCCs demonstrating between 50-90% of tumor volume composed of papillary areas. However, CCRCC with papillary pattern are not common, focally, papillary areas are not entirely rare.

Fuzesi et al., Salama et al., and Jia et al. described exactly such RCCs. Authors used classic cytogenetics, FISH and data from TCGA. All 3 studies demonstrate papillary pattern in CCRCC. Recently, Alaghehbandan et al. also analyzed CCRCC with papillary pattern by NGS. Comprehensive cancer panel showed large spectrum of variants with mostly unknown pathogenicity. Most frequently mutated gene was *VHL* followed by *PRBM1* and other different mutations in various genes. Five of the most commonly mutated genes in ccRCCs including *VHL*, *PRBM1*, *PTEN*, *PIK3CA*, and *KDM5C*, were mutated in this study. The two most common differential diagnoses for RCCs with papillary architecture and clear cell morphology would include MiT family, particularly *TFE3* translocation RCC, and clear cell papillary RCC.

RCCs associated with Xp11.2 translocation, demonstrate variable morphological features. However, morphology is dependent on *TFE3* gene partner. These tumors are mostly arranged in papillary architecture with large, weakly eosinophilic or clear neoplastic cells with psammoma bodies and eosinophilic hyaline nodules. However, morphology might be substantially different from "classic, textbook examples". Immunohistochemically, these tumors usually express TFE3 protein, however IHC is not reliable in many cases. Thus, *TFE3* break-apart fluorescence in situ hybridisation assay or better NGS are the most reliable method of detection.

Clear cell papillary RCC (according WHO 2022 clear cell papillary tumor), the other main differential diagnosis, is easily recognizable morphologically, including tubopapillary architecture, variable presence of leiomyomatous stroma, so-called "shark smiles," and apical "blister" feature and low-grade basally located nuclei. Unlike CCRCCs, which are mostly CK7 negative/focally positive, these tumors are strongly and diffusely positive for

CK7. However, some CCPRCCs resemble *TFE3-NONO* RCC, which can mimic closely CCPRCC. Analysis of *VHL* gene (abnormalities like mutation, hypermethylation or LOH3p) is helpful in differential diagnosis CCPRCC versus CCRCC.

## Conclusions

Papillary growth pattern in CCRCC is not uncommon and in fact, it can constitute a substantial portion the tumor. Clear cell papillary RCC/tumor and MiT family (*TFE3/XP11.2*) translocation RCCs are the major differential diagnostic considerations, which can be resolved with help of morphology, immunohistochemistry, and basic FISH/NGS testing if needed.

## Selected references:

1. Val-Bernal JF, Salcedo W, Val D, Parra A, Garijo MF. Mucin-secreting clear cell renal cell carcinoma. A rare variant of conventional renal cell carcinoma. *Ann Diagn Pathol.* 2013;17:226-229.
2. Williamson SR, Kum JB, Goheen MP, Cheng L, Grignon DJ, Idrees MT. Clear cell renal cell carcinoma with a syncytial-type multinucleated giant tumor cell component: implications for differential diagnosis. *Hum Pathol.* 2014;45:735-744.
3. Tanas Isikci O, He H, Grossmann P, Alaghebandan R, Ulamec M, Michalova K, et al. Low-grade spindle cell proliferation in clear cell renal cell carcinoma is unlikely to be an initial step in sarcomatoid differentiation. *Histopathology.* 2018;72:804-813.
4. de Peralta-Venturina M, Moch H, Amin M, Tamboli P, Hailemariam S, Mihatsch M, et al.. Sarcomatoid differentiation in renal cell carcinoma: a study of 101 cases. *Am J Surg Pathol.* 2001;25:275-284.
5. Lopez JI, Angulo JC. Pathological Bases and Clinical Impact of Intratumor Heterogeneity in Clear Cell Renal Cell Carcinoma. *Curr Urol Rep.* 2018;19:3.
6. Salama ME, Worsham MJ, DePeralta-Venturina M. Malignant papillary renal tumors with extensive clear cell change: a molecular analysis by microsatellite analysis and fluorescence in situ hybridization. *Arch Pathol Lab Med.* 2003;127:1176-1181.
7. Klatte T, Said JW, Seligson DB, Rao PN, de Martino M, Shuch B, Zomorodian N, Kabbinar FF, Belldegrun AS, Pantuck AJ. Pathological, immunohistochemical and cytogenetic features of papillary renal cell carcinoma with clear cell features. *J Urol.* 2011;185:30-35.
8. Haudebourg J, Hoch B, Fabas T, Cardot-Leccia N, Burel-Vandenbos F, Vieillefond A, et al. Strength of molecular cytogenetic analyses for adjusting the diagnosis of renal cell carcinomas with both clear cells and papillary features: a study of three cases. *Virchows Arch.* 2010;457:397-404.

9. Rotterova P, Martinek P, Alaghebandan R, Prochazkova K, Damjanov I, Rogala J, et al. High-grade renal cell carcinoma with emperipolesis: Clinicopathological, immunohistochemical and molecular-genetic analysis of 14 cases. *Histol Histopathol.* 2018;33:277-287.
10. Fuzesi L, Gunawan B, Bergmann F, Tack S, Braun S, Jakse G. Papillary renal cell carcinoma with clear cell cytomorphology and chromosomal loss of 3p. *Histopathology.* 1999;35:157-161.
11. Moch H, Humphrey PA, Ulbright TM, Reuter VE: WHO classification of tumours of the urinary system and male genital organs. Lyon, IARC; 2016.
12. Amin MB, Berney D, Comperat EM eds WHO Classification of Tumours. Urinary and male genital tumours [Internet]. Lyon (France): International Agency for Research on Cancer; 2022
13. Jia L JG, Al-Ahmadie H, Fine SW, Gopalan A, Sirintrapun SJ, Tickoo S, Reuter V, Chen YB. Clear Cell Renal Cell Carcinoma with Prominent Papillary Architecture: a Rare Morphologic Variant Supported by Molecular Evidence. *Laboratory Investigation.* 2018;98:353.
14. Alaghebandan R, Ulamec M, Martinek P, Pivovarcikova P, Michalova K, Skenderi F, et al. Papillary pattern in clear cell renal cell carcinoma: Clinicopathologic, morphologic, immunohistochemical and molecular genetic analysis of 23 cases *Annals Diagn Pathol.* 2019;41:96-101

# Case 73

Fredrik Petersson

---

## Clinical History:

A 48 year old female with hypertension and previous hysterectomy (leiomyomas), presented with unintentional loss of weight 2-3 months, loss of appetite and upper abdominal - left hypochondrium discomfort. She also had fever and anemia. She underwent a CT scan of the abdomen which revealed a 14.9 x 10.5 x 9.2 cm heterogeneous left renal mass, which was inseparable from the left psoas, para-renal fascias, pancreatic tail, spleen, left ovarian vessels as well as adjacent small bowel and large bowel loops. There were nodular left perinephric deposits and a tumour thrombus left renal vein. Surgery (nephrectomy + extended anterior resection) was performed and the intraoperative findings were those of a large renal tumour involving the mesentery of the descending colon with tumor rupture. Four months after the surgery a bone scan showed multiple bone metastases and she developed lung metastasis and non-ischemic cardiomyopathy. The patient received palliative chemotherapy.

## Gross Features:

The surgical specimen contained a partly necrotic, white-grayish 12 x 10 x 9.5 cm ruptured tumor. The tumor showed invasion into perinephric tissues, beyond Gerota's fascia, into the adherent large bowel mesentery. There was extension into the renal sinus and into major veins. There was metastasis in multiple hilar lymph node.

## Histology:

The tumor was predominantly composed of elongated and anastomosing tubular structures that transitioned to spindle cells within a variably mucinous stroma. The tubular cells and spindle cells generally showed low grade nuclear atypia. However, there were areas of the tumor which were more cohesive/solid, where the tumor cells exhibited high-grade features, including large, irregular vesicular nuclei and prominent nucleoli. Areas with necrosis were present.

## Immunohistochemistry:

The neoplastic cells expressed vimentin and were focally positive for Pax-8, AMACR and CD10. Few cells were positive for CAM5.2 and EMA. AE1/3, CD117, CK7 and HMB45 were negative.

## Diagnosis: *Mucinous tubular and spindle cell carcinoma with high-grade features*

## Comments:

Mucinous tubular and spindle cell carcinoma (MTSCC) is a rare neoplasm. This tumor was originally reported by Ordonez and Mackay (1) and MacLennan et al (2) and labelled as "renal cell carcinoma with unusual differentiation, originating in loop of Henle" and "low grade collecting duct carcinoma", respectively. This entity was subsequently published in a series of 4 cases of low-grade renal tumors with myxoid appearance and distal nephron differentiation by Parwani et al. (3) and the term mucinous tubular and spindle cell carcinoma was introduced in the 2004 edition of the WHO classification (4) and was kept in the recent edition (5). Not more than 100 cases have been reported in the literature (6). As the name implies, MTSCC is composed of 3 elements, namely spindle cells, tubular structures, and extracellular mucoid material. It accounts for < 1% of all renal tumors and is most commonly encountered in adults (mean age 58 years). There is a female preponderance (female to male ratio 3:1). A majority of cases are incidentally detected on imaging for other unrelated causes, but some patients have presented with hematuria, flank pain, and a palpable abdominal mass (7,8). The tumor is generally found in the cortex, and very rarely arise in the medulla (5). The imaging features of MTSCC are different from those of clear cell RCC but similar to papillary RCC (9). CT scan of MTSCC characteristically presents as a well-demarcated rounded mass. Tumors less than 5 cm usually demonstrate a homogenous pattern of enhancement, whereas those larger than 5 cm are heterogeneous (6,10). On contrast-enhanced ultrasonography and contrast-enhanced computed tomography, MTSCC shows a hypovascular pattern similar to papillary and chromophobe RCC (11).

Histologically, the tumor is comprised of a mixture of tubular and spindle cells separated by variable amounts of mucoid material. The tubules are round, ovoid, or elongated and anastomosing, often with a collapsed lumen; often tightly packed and arranged in parallel, occasionally with formation of cords and may even form a solid areas. The tubular

epithelium can display clear cells, oncocytic change or vacuolated cytoplasm. Originally MTSCC was characterized as a histologically low-grade neoplasm featuring round relatively isomorphic nuclei with evenly dispersed chromatin, and occasional small nucleoli. However, infrequently tumors with high-grade nuclei features and even sarcomatoid change have been reported (4,7). In some cases, the spindle cells is the predominant component, thus imparting a mesenchymal appearance. The extracellular mucoid material may be basophilic or, uncommonly eosinophilic, often with a bubbly appearance. Fine et al (12) have expanded the histologic spectrum of MTSCC and suggest 2 variants: classic and mucin poor. Other reported histologic features include aggregates of foamy histiocytes, papillations (7) (projecting epithelial tufts into the tubular lumina, necrosis, a cuff of lymphoplasmacytic cells surrounding tumor cell nests, psammomatous calcifications, and heterotopic bone formation. The mitotic activity is most commonly very low. However, this is in contrast to high-grade tumors including those MTSCC with sarcomatoid change, which not surprisingly, may contain atypical mitotic figures (in addition to marked cytologic atypia and tumor necrosis) (13).

On immunohistochemistry, both the tubular and spindle neoplastic express PAX2, PAX8, low-molecular-weight cytokeratin (CK8/18, CK19 and CK7), EMA, alpha-methylacyl coenzyme A and E-cadherin. 34bE12 and other high-molecular-weight keratins and vimentin show variable expression. CD10, CD15, and RCC marker are often negative. Carbonic anhydrase IX, p63, CK20, GATA3, and smooth muscle actin are negative. Increased Ki-67 proliferation index and nuclear p53 accumulation has been observed in high-grade tumors (14).

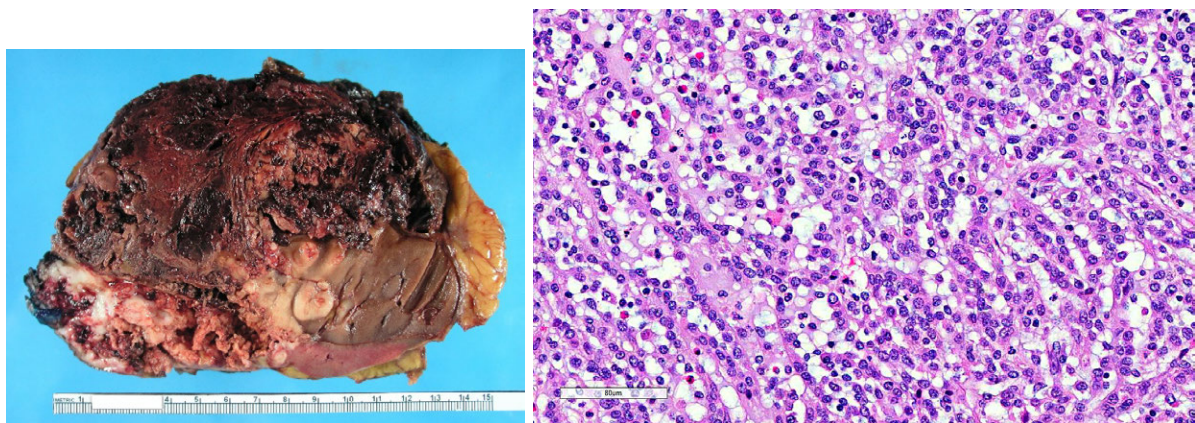
Multiple numerical aberrations involving chromosomes 1, 4, 6, 8, 9, 11, 13, 14, 15, 18, 22, and X have been observed on comparative genomic hybridization, cytogenetics, and fluorescent in situ hybridization studies on MTSCC. In a large series of comparative genomic hybridization studies on MTSCC, Peckova et al (14) reported that the tumors with classic morphology showed loss of chromosomes 1, 4, 6, 8, 9, 13, 14, 15, and 22, whereas tumors with overlapping features with papillary RCC showed variable losses and gains, including gain of chromosomes 7 and 17. Notwithstanding this, subsequent FISH studies revealed no gains of 7 and 17 (15). Whole-exome and transcriptome sequencing of MTSCC showed biallelic loss of Hippo signaling pathway tumor suppressor genes; PTPN14, NF2, and SAV1.

Mucinous tubular and spindle cell carcinoma with classic (low-grade) morphology has mostly very good prognosis (5). Most reported cases that have shown recurrence, regional lymph nodal and distant metastases were high-grade examples, including cases with sarcomatoid transformation. However, low-grade tumors (with classic morphology)

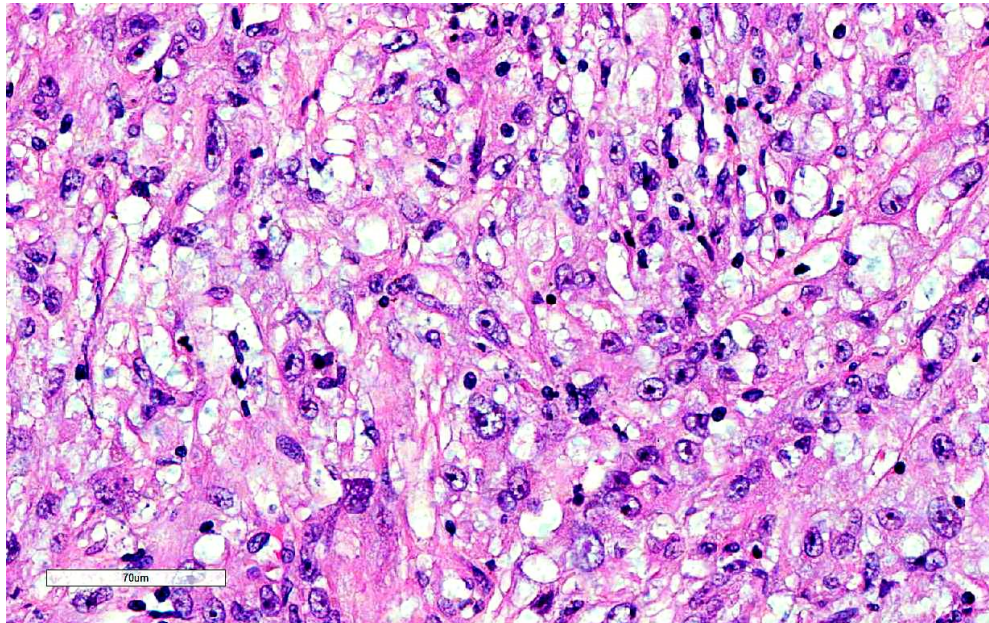
have shown metastatic behaviour (lymph nodes and liver) (16), also with low-grade histological features in the metastatic neoplastic tissue. Hence, follow-up is warranted in all cases irrespective of histology.

The differential diagnosis of mucinous tubular and spindle cell carcinoma depends on whether one is dealing with a classical or mucin-poor variant or a tumor that has undergone high-grade (including sarcomatoid) transformation. In the latter case, finding a low-grade component (sampling!) should help to resolve this. In the former scenario, the main differential diagnosis is a papillary renal cell carcinoma, which very rarely may contain mucinous material (17). However, no spindle cell component is present in these tumors and a molecular genetic/cytogenetic study focusing on chromosomes 7, 17 (gains) and Y (loss) would be helpful.

**Figures:**



Large, partially necrotic tumor that widely extended beyond the perinephric fat. Large part of the tumor was made up of anastomosing tubular structures composed of neoplastic cells with low-grade nuclear features and variable mucoid stroma.



In some areas the tumor cells showed high-grade nuclear features; increased nuclear size, pleomorphism and prominent nucleoli.

## References:

1. Ordonez NG, Mackay B. Renal cell carcinoma with unusual differentiation. *Ultrastruct Pathol.* 1996;20(1):27-30.
2. MacLennan GT, Farrow GM, Bostwick DG. Low-grade collecting duct carcinoma of the kidney: report of 13 cases of low-grade mucinous tubulocystic renal carcinoma of possible collecting duct origin. *Urology.* 1997;50(5):679-684.
3. Parwani AV, Husain AN, Epstein JI, Beckwith JB, Argani P. Low-grade myxoid renal epithelial neoplasms with distal nephron differentiation. *Hum Pathol.* 2001;32(5):506-512.
4. Lopez-Beltran A, Scarpelli M, Montironi R, Kirkali Z. 2004 WHO classification of the renal tumors of the adults. *Eur Urol.* 2006;49(5):798-805.
5. Moch H, Cubilla AL, Humphrey PA, Reuter VE, Ulbright TM. The 2016 WHO Classification of tumours of the urinary system and male genital organs– part A: renal, penile, and testicular tumours. *Eur Urol.* 2016;70(1):93-105.
6. Sadimin ET, Chen Y-B, Wang L, Argani P, Epstein JI. Chromosomal abnormalities of high-grade mucinous tubular and spindle cell carcinoma of the kidney. *Histopathology.* 2017;71(5):719-724.

7. Zhao M, He X-L, Teng X-D. Mucinous tubular and spindle cell renal cell carcinoma: a review of clinicopathologic aspects. *Diagn Pathol.* 2015;10(1):168.
8. Sun N, Fu Y, Wang Y, Tian T, An W, Yuan T. Mucinous tubular and spindle cell carcinoma of the kidney: a case report and review of the literature. *Oncol Lett.* 2014;7(3):811-814.
9. Kenney PA, Vikram R, Prasad SR, et al. Mucinous tubular and spindle cell carcinoma (MTSCC) of the kidney: a detailed study of radiological, pathological and clinical outcomes. *BJU Int.* 2015;116(1):85-92.
10. Nouh MA, Kuroda N, Yamashita M, et al. Renal cell carcinoma in patients with end-stage renal disease: the relationship between histological type and duration of dialysis. *BJU Int.* 2010;105(5):620-627.
11. Zhang Q, Wang W, Zhang S, et al. Mucinous tubular and spindle cell carcinoma of the kidney: the contrast-enhanced ultrasonography and CT features of six cases and review of the literature. *Int Urol Nephrol.* 2014;46(12):2311-2317.
12. Fine SW, Argani P, DeMarzo AM, et al. Expanding the histologic spectrum of mucinous tubular and spindle cell carcinoma of the kidney. *Am J Surg Pathol.* 2006;30(12):1554-1560.
13. Arafah M, Zaidi SN. Mucinous tubular and spindle cell carcinoma of the kidney with sarcomatoid transformation. *Saudi J Kidney Dis Transplant.* 2013; 24(3):557-560.
14. Peckova K, Martinek P, Sperga M, et al. Mucinous spindle and tubular renal cell carcinoma: analysis of chromosomal aberration pattern of low-grade, highgrade, and an overlapping morphologic variant with papillary renal. *Ann Diagn Pathol.* 2015;19(4):226-231.
15. Alexiev BA, Burke AP, Drachenberg CB, Richards SM, Zou YS. Mucinous tubular and spindle cell carcinoma of the kidney with prominent papillary component, a non-classic morphologic variant: a histologic, immunohistochemical, electron microscopic and fluorescence in situ hybridization study. *Pathol Res Pract.* 2014;210(7):454-458.
16. Ursani NA, Robertson AR, Schieman SM, Bainbridge T, Srigley JR. Mucinous tubular and spindle cell carcinoma of the kidney without sarcomatoid change showing metastases to liver and retroperitoneal lymph node. *Hum Pathol.* 2011;42(3):444-448.
17. "Mucin"-secreting papillary renal cell carcinoma: clinicopathological, immunohistochemical, and molecular genetic analysis of seven cases. Pivovarcikova K, Peckova K, Martinek P, Montiel DP, Kalusova K, Pitra T, Hora M, Skenderi F, Ulamec M, Daum O, Rotterova P, Ondic O, Dubova M, Curik R, Dunatov A, Svoboda T, Michal M, Hes O. *Virchows Arch.* 2016 Jul;469(1):71-80

## Case 74

Contributed by: Kyle Perry, M.D.

---

63 y/o female with a kidney mass

### Clinical history and Radiology:

A 63 y/o female underwent a CT scan of the abdomen and pelvis for previous endometrial carcinoma and was incidentally found to have a 2.7 cm mass in the anterior interpolar region of the left kidney that was not appreciated during the previous year. The patient and urologist decided to perform a nephrectomy for definitive removal of the tumor.

Grossly, the resection specimen contained an approximately 3.0 cm tumor which abutted the collecting system and renal vein. Microscopically, the lesion was composed of haphazardly arranged spindled cells which involved the renal parenchyma (Fig. A). There were varying amounts of background hyalinized fibrosis in association with the tumor cells (Fig. B). On high power examination, the cells contained plump and vesicular nuclei without substantial areas of nuclear atypia or atypical mitoses (Fig. C). Immunohistochemical stains showed the tumor cells to be positive for smooth muscle actin and Alk. Overall, the findings were considered diagnostic for an inflammatory myofibroblastic tumor.

**Diagnosis: Inflammatory myofibroblastic tumor involving the kidney**

### Comment:

Inflammatory myofibroblastic tumor has rarely been described in the kidney in limited case series. The tumor can exhibit a range of histologic appearances but is principally characterized by spindled cells arranged in a vague fascicular architecture. The nuclei typically exhibit a vesicular chromatin pattern and contain small nucleoli. The background stroma can show varying degrees of fibrous or myxoid changes. Background inflammation is also typically seen. These tumors typically stain for

smooth muscle actin (membranous staining pattern) and variably express desmin. Up to 60% will stain positive for ALK (membranous, cytoplasmic or nuclear membranous). Although a majority (50-70%) of tumors will exhibit a fusion involving the ALK gene, alterations of additional genes, such as *ROS1* and *PDGFRB* have also been identified. (1)

In the context of the kidney, the differential diagnosis would include other spindle cell neoplasms such as solitary fibrous tumor, leiomyoma, leiomyosarcoma, sarcomatoid renal cell carcinoma and a renomedullary interstitial tumor. Solitary fibrous tumor will typically exhibit positive staining for STAT6. Leiomyoma and leiomyosarcoma will usually show a more diffuse and strong staining pattern with smooth muscle actin. Sarcomatoid renal cell carcinoma will typically exhibit a portion of tumor with a more conventional epithelioid morphology. Renomedullary interstitial tumor typically has a limited size and has more limited expression of smooth muscle actin.

Approximately about a third of inflammatory myofibroblastic tumors of the abdomen and retroperitoneum have been noted to recur. Metastasis is a relatively rare event for conventional inflammatory myofibroblastic tumors. In a previous case series of inflammatory myofibroblastic tumor of the kidney, no recurrence or metastasis was identified, though the number of patients was limited. (2, 3)

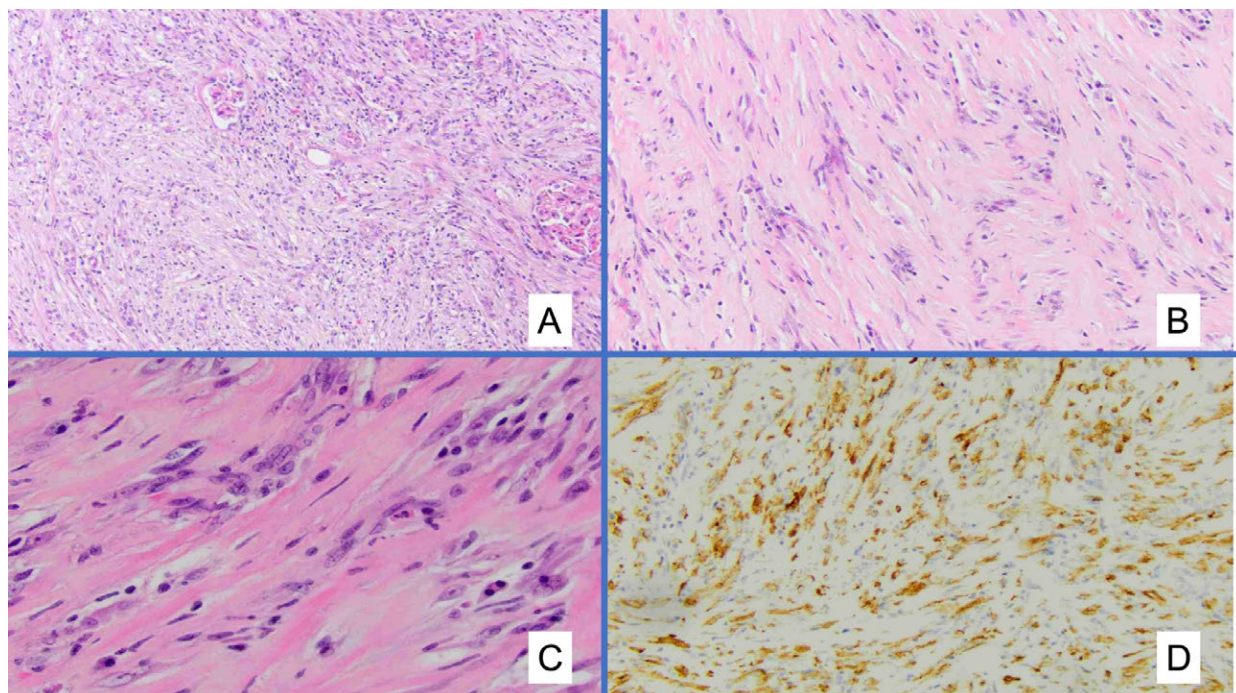


**Figure 1:** Inflammatory myofibroblastic tumor intimately involving the renal parenchyma (A). The tumor shows areas of variably hyalinized stroma (B). Higher power examination shows bland appearing nuclei with vesicular chromatin (C). The tumor cells were diffusely positive for Alk1(D).

## References

1. Yamamoto H, Yoshida A, Taguchi K, Kohashi K, Hatanaka Y, Yamashita A, et al. ALK, ROS1 and NTRK3 gene rearrangements in inflammatory myofibroblastic tumours. *Histopathology*. 2016;69(1):72-83.
2. Coffin CM, Watterson J, Priest JR, Dehner LP. Extrapulmonary inflammatory myofibroblastic tumor (inflammatory pseudotumor). A clinicopathologic and immunohistochemical study of 84 cases. *The American journal of surgical pathology*. 1995;19(8):859-72.
3. Kapusta LR, Weiss MA, Ramsay J, Lopez-Beltran A, Srigley JR. Inflammatory myofibroblastic tumors of the kidney: a clinicopathologic and immunohistochemical study of 12 cases. *The American journal of surgical pathology*. 2003;27(5):658-66.

# Case 75

(M27221/18)

---

67-year-old male with tumor replacing majority of the kidney parenchyma. Metastases in regional lymph nodes and in adrenal gland were documented. Family anamnesis was unknown.

## Pathologic finding

Grossly tumor was composed of spongy whorls and solid areas. Invasion into the renal vein was detected grossly. Histologically, tumor is composed of tubulocystic structures. Focally cribriform pattern was present as well as short papillary structures. True solid areas are very rarely present; in fact, grossly visible "solid" areas are composed of small cyst/tubules. Larger cyst are also focally present. Neoplastic cells are large, voluminous with prominent nuclei with easily visible nucleoli. Majority of nucleoli are large, prominent, deep red with perinucleolar clearing. Epithelial lining of larger cyst show hobnail morphology.

Immunohistochemically, tumor was diffusely positive for AMACR and vimentin. CK 7 was focally positive. Fumarate hydratase staining was negative.

Molecular genetic analysis showed mutation c.1158\_1160delAGT / p.(Gln386\_Val387delinsHis) of *FH* gene

LOH of *FH* gene was not present.

## Diagnosis: Fumarate hydrogenase deficient RCC (FHD RCC)

## Discussion

FHD RCC is characteristic by presence of multiple admixed growth patterns. The most common pattern is papillary, however combination of solid, tubulocystic, cribriform/sieve-like, and cystic architecture is frequently encountered. The classic morphologic feature, besides architecture, is the presence of deep red macronucleoli. However, it is a nonspecific but common feature, which might be found only focally. The presence of

deep red macronucleoli is not reserved for FHD RCC only, they can be found even in papillary RCC, translocation RCC, etc. The spectrum of architecture is much broader and even cases with clearly tubulocystic pattern were described. Moreover, tumors resembling SDH deficient RCC with low-grade oncocytic appearance were also rarely documented.

Negative immunohistochemical staining for FH in tumor cells, in the presence of positive FH staining in internal non-neoplastic cells, is highly specific for FH-deficient RCC but typically not sensitive. In contrast, aberrant staining for 2SC is highly sensitive for FH-deficient RCC but less specific. However, majority of commercially available 2SC antibodies are not very robust and evaluation of stains is sometimes difficult. A low threshold for immunohistochemical screening for FH is recommended. I would recommend to use FH antibody as screening tool for every "unclassifiable" unusual or unknown renal tumors (together with SDHB, ALK, etc). For final diagnosis, genetic testing is strongly recommended. We always should look not only for *FH* gene mutations, but also for LOH of *FH* gene. Of course, further genetic testing of patients and their relatives for potentially present germline mutation is reserved for clinical genetic laboratories.

## Differential diagnosis:

There is broad spectrum of tumors, which should be taken into the consideration.

Traditionally, high-grade papillary RCC is differential diagnosis no 1. In my opinion, majority of suspect FHD RCC are in fact high-grade papillary RCCs (NOS). Sometimes, without precise diagnostic approach, it is not possible to sort out these two entities. Deep red macronucleoli might be frequently present in papillary RCC as well as in FHD RCC. Even non-specific FH staining doesn't help. Only genetic testing can give the definitive answer.

Tubulocystic RCC is another mimicker of FHD RCC. All "high-grade tubulocystic RCC" should be considered as potential FHD RCC. Minimum is screening with FH antibody and in case of clinically suspect case or morphologic worries, genetic testing bring the answer. Collecting duct carcinoma is always diagnosis per exclusionem. FHD RCC is always one of entities, which should be questioned.

Urothelial carcinoma is the last in the differential diagnostic list. In all high-grade RCCs, urothelial carcinoma should be, at least briefly, considered. Good sampling usually brings the answer and correct diagnosis, however in limited material it might be problematic.

## Prognosis and prediction

FH-deficient RCCs are often aggressive, however cases with favorable prognosis were reported. Based on WHO 2022, histological grading is not recommended.

For *FH* mutation carriers is recommended surveillance.

## Selected references:

1. Smith SC, Trpkov K, Chen YB, et al. Tubulocystic Carcinoma of the Kidney With Poorly Differentiated Foci: A Frequent Morphologic Pattern of Fumarate Hydratase-deficient Renal Cell Carcinoma. *Am J Surg Pathol* 2016;40:1457-72.
2. Chen YB, Brannon AR, Toubaji A, et al. Hereditary leiomyomatosis and renal cell carcinoma syndrome-associated renal cancer: recognition of the syndrome by pathologic features and the utility of detecting aberrant succination by immunohistochemistry. *Am J Surg Pathol* 2014;38:627-37.
3. Trpkov K, Hes O, Agaimy A, et al. Fumarate Hydratase-deficient Renal Cell Carcinoma Is Strongly Correlated With Fumarate Hydratase Mutation and Hereditary Leiomyomatosis and Renal Cell Carcinoma Syndrome. *Am J Surg Pathol* 2016;40:865-75.
4. Muller M, Guillaud-Bataille M, Salleron J, et al. Pattern multiplicity and fumarate hydratase (FH)/S-(2-succino)-cysteine (2SC) staining but not eosinophilic nucleoli with perinucleolar halos differentiate hereditary leiomyomatosis and renal cell carcinoma-associated renal cell carcinomas from kidney tumors without FH gene alteration. *Mod Pathol* 2018;31:974-83.
5. Ohe C, Smith SC, Sirohi D, et al. Reappraisal of Morphologic Differences Between Renal Medullary Carcinoma, Collecting Duct Carcinoma, and Fumarate Hydratase-deficient Renal Cell Carcinoma. *Am J Surg Pathol* 2018;42:279-92.
6. Agaimy A, Amin MB, Gill AJ, et al. SWI/SNF Protein Expression Status in Fumarate Hydratase-deficient Renal Cell Carcinoma: Immunohistochemical Analysis of 32 Tumors from 28 Patients. *Hum Pathol* 2018
7. Lau HD, Chan E, Fan AC, et al. A Clinicopathologic and Molecular Analysis of Fumarate Hydratase-deficient Renal Cell Carcinoma in 32 Patients. *Am J Surg Pathol* 2020;44:98-110.
8. Merino MJ, Torres-Cabala C, Pinto P, Linehan WM. The morphologic spectrum of kidney tumors in hereditary leiomyomatosis and renal cell carcinoma (HLRCC) syndrome. *Am J Surg Pathol* 2007;31:1578-85.
9. Muller M, Ferlicot S, Guillaud-Bataille M, et al. Reassessing the clinical spectrum associated with hereditary leiomyomatosis and renal cell carcinoma syndrome in French FH mutation carriers. *Clin Genet* 2017;92:606-15.

10. Moch H, Humphrey PA, Ulbright TM, Reuter VE: WHO classification of tumours of the urinary system and male genital organs. Lyon, IARC; 2016.
11. Amin MB, Berney D, Comperat EM eds WHO Classification of Tumours. Urinary and male genital tumours [Internet]. Lyon (France): International Agency for Research on Cancer; 2022
12. Trpkov K, Hes O, Williamson SR, Adeniran AJ, Agaimy A, Alaghehbandan R, et al. New developments in existing WHO entities and evolving molecular concepts: The Genitourinary Pathology Society (GUPS) update on renal neoplasia. *Mod Pathol* 2021;34,1392-424.

## Case 76

Contributed by: Kyle Perry, M.D.

---

69 y/o female who presented with "enlargement of the belly"

### Clinical history and Radiology:

After a patient presented with abdominal enlargement, a CT scan showed a septated cystic mass that was ultimately excised and found to be a seromucinous cystadenofibroma of the left ovary. During the procedure, an incidental mass was seen in the wall of the distal small bowel. Frozen sections showed a spindle cell proliferation. Given a clinical concern for gastrointestinal stromal tumor, the remainder of the lesion was resected.

A segment of small bowel with associated mesentery was received. Within the mesentery, there was a multinodular mass which measured approximately 4.5 cm in greatest dimension. Microscopically, the lesion was composed of a subserosal proliferation of bland spindled to stellate cells that was centered just beneath the muscularis propria (Fig. A). Some areas of the tumor showed a septated architecture or exhibited fat trapping in a "honey-comb" like appearance (Fig B). Significant cytologic atypia, increased mitoses, or necrosis were not identified (Fig C). Multiple areas of the tumor exhibited dense collagen deposition (Fig D).

The tumor cells were positive for ER and MUC4 and were negative for GLUT-1, SMA, desmin, CD34, and STAT6. MDM2 did not show definitive staining. Next generation sequencing was performed and showed the tumor cells to exhibit a *FUS-CREB3L2* fusion transcript.

**Diagnosis: Low-grade fibromyxoid sarcoma confirmed by *FUS-CREB3L2* fusion transcript, forming a mesenteric mass**

## Comment:

Low-grade fibromyxoid sarcoma typically arises as a deep-seated soft tissue mass in the extremities of adults. The histologic appearance of these tumors can vary considerably but are mostly characterized by bland appearing spindled cells in the background of alternating collagenous and myxoid stroma. There are usually areas of background branching vessels. Increased areas of collagen deposition can be seen, sometimes forming a rosette like architecture (i.e. hyalinizing spindle cell tumor with giant rosettes).

This tumor exhibits a few histologic features which could be misleading in a mesenteric presentation. It's septated pattern and intimate association with surrounding adipose tissue could mimic a well-differentiated liposarcoma, which would be a more common entity in this location. Unlike well-differentiated liposarcoma, low-grade fibromyxoid sarcoma would not exhibit *MDM2* gene amplification. The areas of extensive collagen deposition could perhaps be mistaken for deep/desmoid fibromatosis. Deep fibromatosis will often stain positive for beta catenin or be positive for a mutation in the *CTNNB1* gene. Other potential considerations include gastrointestinal stromal tumor (which would be positive for CD117), solitary fibrous tumor with considerable adipocytic metaplasia (which would be positive for STAT6), among other possibilities.

There recently has been increasing documentation of low-grade fibromyxoid sarcoma in historically unconventional anatomic locations, including cases in the head and neck and abdomen/retroperitoneum. (1, 2)

As utilization of next generation sequencing becomes more common, there will likely be increased recognition of "atypical" presentations of low grade fibromyxoid sarcoma.

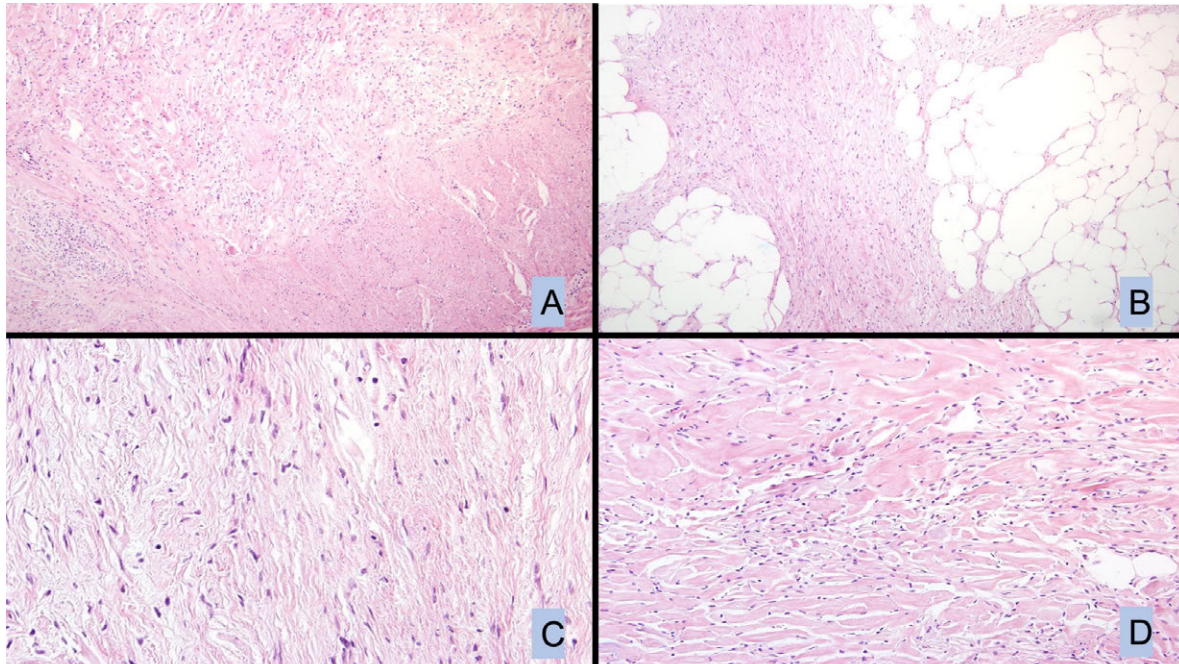


**Figure 1:** Low grade fibromyxoid sarcoma is centered in the tissue just deep to the muscularis propria which is in the lower right-hand corner (A). Some areas of the tumor exhibited a septated architecture in the background of adipose tissue (B). Higher power examination shows relatively bland appearing spindled cells without over nuclear atypia or increased mitoses, consistent with the diagnosis (C). Blatant areas of myxoid stroma were not identified, but prominent areas of background collagen deposition were noted (D).

## References

1. Gjorgova Gjeorgjievski S, Fritchie K, Thangaiah JJ, Folpe AL, Din NU. Head and Neck Low-Grade Fibromyxoid Sarcoma: A Clinicopathologic Study of 15 Cases. *Head Neck Pathol.* 2021.
2. Ud Din N, Ahmad Z, Zreik R, Horvai A, Folpe AL, Fritchie K. Abdominopelvic and Retroperitoneal Low-Grade Fibromyxoid Sarcoma: A Clinicopathologic Study of 13 Cases. *Am J Clin Pathol.* 2018;149(2):128-34.

## Case 77

Contributed by Franco Fedeli, MD, Malpighi Pathology Academy

---

[www.malpighipathologyacademy.org](http://www.malpighipathologyacademy.org)

### Clinical History:

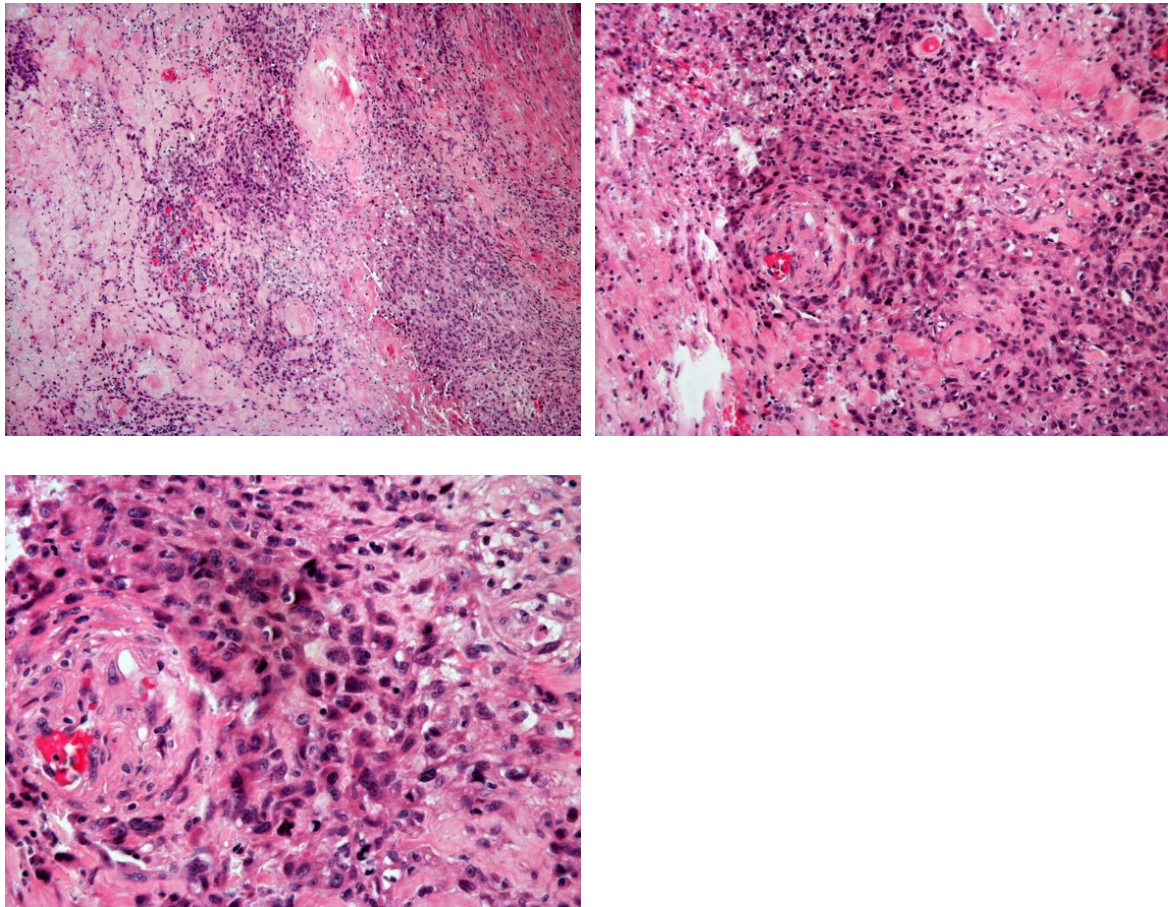
42 years old male with sovraorbital paresthesia and diplopia in 2007. CT scan revealed an intraorbital mass. This tumor was resected in another institution and relapsed in 2011, 2013 and 2018 after radiation therapy. The patient died after 1 year with diffuse metastasis.

### Macroscopic findings:

The 2018 recurred tumor mass was 4 cm in size. Macroscopically, the tumor was grayish and diffusely infiltrated the soft tissue of the orbital space and maxillary and zygomatic bone.

### Histological Findings:

The tumor was composed of multinodular distribution and sheets of large polygonal cells with mildly to moderately pleomorphic vesicular nuclei and prominent nucleoli. Rhabdoid morphology and pleomorphic cells were easily seen. In some areas a minor spindle cell component was present. The neoplastic cells showed eosinophilic cytoplasm. Hemorrhage and necrotic changes were common findings and the mitotic count was 7 per 10 high-power fields.



## Immunohistochemical Findings:

Immunohistochemically the tumor cells were positive for Vimentin, Cytokeratin (Cam5.2), CD34 and displayed moderate to intense cell membrane-based reactivity for EMA. There was also loss of SMARCB1 (INI-1) expression. Additional immunoreactivity was negative for CK5/6, TTF-1, D2-40, Napsin-A, p63, p40, Ber-EP4, S100, CD30, CD31, SOX10 and Desmin.

## Diagnosis: Proximal type epithelioid sarcoma

## Comments:

In 1961, Laskowski described cases of “aponeurotic sarcoma” in the Polish (and subsequently English) literature (1). Subsequently epithelioid sarcoma was described by Enzinger in 1970; usually arises in the distal extremities in adolescents and young adults,

with male prevalence (2). The proximal-type variant, first described in 1997, is an aggressive form of sarcoma with a great ability to metastasize and high capacity of recurrence, even after surgery with radical surgical margins and propensity for early metastasis (3). Proximal-type epithelioid sarcoma occurs 94% in the chest wall, inguinal region, thigh and perineum. Its size at presentation varies from 0.5 to 19 cm. (4) To date, there are only 7 previously reported cases of epithelioid sarcoma of the orbit to our knowledge. Of the seven primary orbital epithelioid sarcoma cases reported, two patients were treated with orbital exenteration (5)

Histologically distinctive features are prominence of the epithelioid cell component, a sheet-like growth pattern of large cells with vesicular nuclei and prominent nucleoli, and a frequent rhabdoid morphology (6). Proximal type epithelioid sarcomas can show a typical granuloma-like pattern. Occasionally a pseudoangiomatous architecture may be present. Immunohistochemically, irrespective of the tumor types, the proximal-type epithelioid sarcomas

are clearly epithelial-like, with cytokeratin and EMA commonly present. These tumors show cell membrane-based reactivity for EMA. Just over half of proximal type epithelioid sarcoma express CD34 which is an important factor in distinguishing them from carcinomas, which are virtually always CD34 negative. Ninety-six percent of epithelioid sarcoma have been shown to express cyclin D1 in nuclei, and there may be variable expression of smooth muscle actin (SMA) (particularly in the spindle cells), muscle-specific actin (HHF35), neurofilament, claudin-1, podoplanin (D2-40), and FLI1. In addition, ERG is expressed in 38%, usually uniformly, similarly to the expression pattern seen in angiosarcoma and GLUT-1 is positive in 40% to 50% of cases. Proximal type of epithelioid sarcoma is generally negative for S-100 protein. INI1 (SMARCB1) is deficient in approximately 90% of epithelioid sarcoma of both classic and proximal type, and its loss can be detected by immunohistochemistry or with fluorescence in situ hybridization. The differential diagnosis of proximal type epithelioid sarcoma encompasses several malignant conditions with INI1 loss, which often show epithelioid or rhabdoid morphology. Malignant rhabdoid tumor is also composed of sheets of large rounded cells that are usually CK positive, but malignant rhabdoid tumor predominantly arises in children younger than 3 years. Malignant rhabdoid tumor is typically poorly defined and infiltrative; the majority of its cells show eccentrically oriented vesicular nuclei and eosinophilic intracytoplasmic inclusions comprising aggregates of intermediate filaments characteristic of rhabdoid morphology. CK expression in malignant rhabdoid tumor is frequently in a dot-like pattern. In addition, malignant rhabdoid tumor do not typically express CD34. INI1 is lost in approximately 50% of epithelioid MPNST; these can occur in

both superficial and deep soft tissues of the extremities, and are composed of vague nodules comprising clusters, strands or cords of large, rounded cells with prominent nucleoli. These typically show diffuse and strong expression of S100 protein.

Nuclear INI1 loss occurs in about 10% of soft-tissue myoepithelial carcinomas in adults.

Myoepithelial tumors of soft tissue can arise at similar sites to proximal type of epithelioid sarcoma. They show a wide histologic spectrum but can be composed of sheets of polygonal or rounded cells.

Other epithelioid neoplasms in the differential diagnosis of proximal type epithelioid sarcoma include epithelioid angiosarcomas, epithelioid hemangioendothelioma, pseudomyogenic hemangioendothelioma, epithelioid schwannoma and malignant melanoma.

In conclusion proximal type epithelioid sarcoma is an extremely rare tumor with a well characterized histology and immunohistochemistry. It is difficult to treat in the head and neck region and the associated mortality rate is high. Aggressive surgical therapy with intensive follow-up is recommended. The prognosis depends on the resection status.

## References

1. Laskowski J. Sarcoma aponeuroticum. *Noworotwy*. 1961;11: 61-67.
2. Enzinger FM. Epithelioid sarcoma: A sarcoma simulating a granuloma or a carcinoma. *Cancer*. 1970(5); 26:1029-1041.
3. Chase DR, Enzinger FM. Epithelioid sarcoma. Diagnosis, prognostic indicators, and treatment. *Am J Surg Pathol*. 1985;9:241-263.
4. Hasegawa T, Matsuno Y, Shimoda T, Umeda T, Yokoyama R, Hirohashi S. Proximal-type epithelioid sarcoma: A clinicopathologic study of 20 cases. *Mod Pathol*. 2001; 14(7): 655-63.
5. Guillou L, Wadden C, Coindre JM, Krausz T, Fletcher CM. "Proximal-type" epithelioid sarcoma, a distinctive aggressive neoplasm showing rhabdoid features. *Am J Surg Pathol*. 1997; 21(2):130-46.
6. V. A. White, J. G. Heathcote, J. J. Hurwitz, J. L. Freeman, and J. Rootman, "Epithelioid sarcoma of the orbit," *Ophthalmology*, vol. 101, no. 10, pp. 1680-1687, 1994.

# Case 78

presented by Ricardo R. Lastra, University of Chicago

---

## Clinical History:

17-year-old woman with a history of multinodular goiter presented in 2011 with acute onset of heavy vaginal bleeding and was found to have an 8.5 cm hemorrhagic mass protruding from the vaginal introitus. The polypoid mass was originating from the cervix and surgically excised. 6 years later (2017) the patient re-presented with a cervical polypoid lesion (2.5 cm) and a left adnexal mass (7.5 cm). Representative blocks from the original cervical mass (2011) were submitted for this seminar.

## Pathology:

Gross findings: The specimen consisted of a rubbery, polypoid mass measuring 8.5 x 8.3 x 6.0 cm and weighing 217 g. It had a nodular but smooth outer surface and a tan, focally hemorrhagic cut surface.

Microscopic: It is a deeply invasive, variably cellular, primitive, round to spindle cell neoplasm entrapping endocervical glands with focal subepithelial condensation. The tumor cells are relatively small, hyperchromatic, and demonstrated brisk mitotic activity as well as some apoptotic bodies. Islands of cartilaginous differentiation are present in some blocks (not submitted for the seminar).

## Differential diagnosis:

Adenosarcoma with sarcomatous overgrowth *versus* embryonal rhabdomyosarcoma of the cervix

*Immunohistochemical study:* Diffuse strong positivity for myogenic markers desmin and myogenin. No immunoreactivity for various cytokeratins, EMA, S100, SOX10, ER, PR, CD10, CD99, FLI1, CyclinD1.

**Diagnosis (2011): Embryonal rhabdomyosarcoma of the cervix (stage I)**

## Follow up:

Following surgery (partial trachelectomy), the patient received combination chemotherapy and continued with no evidence of disease for several years, until 2017 (6 years after diagnosis) when an endocervical polypoid lesion (2.5 cm) was excised and diagnosed as "recurrent" cervical embryonal rhabdomyosarcoma. At the same time, a 7.5 cm left ovarian mass was identified and assumed to be metastatic rhabdomyosarcoma. However, in this clinicopathologic context, an alternative possibility: DICER1 syndrome with ovarian Sertoli-Leydig cell tumor was suggested. The ovarian mass was excised and indeed it was a Sertoli-Leydig cell tumor with intermediate differentiation, with heterologous mucinous epithelial components.

*Molecular studies* confirmed *DICER1* mutation in both the Sertoli-Leydig cell tumor (c.904-1G> C, splice acceptor and c.5439G > A p.E1813D) and in the cervical embryonal rhabdomyosarcoma (c.904-1G, splice acceptor and c.5425G > A p.G1809R). Patient was referred for genetic counseling where germline *DICER1* mutation (c.904-1G > C, splice acceptor) was also detected. Molecular study of the "recurrent" cervical rhabdomyosarcoma (2017) revealed a partly different *DICER1* gene mutation (c.904-1G > C splice acceptor and c.5439G > A p.E1813N) than the one identified in the original rhabdomyosarcoma (2011) suggesting a metachronous second primary cervical embryonal rhabdomyosarcoma (Cowan M et al, 2018). Currently (2020), the patient is well without disease.

## **Final Diagnosis: Cervical embryonal rhabdomyosarcoma and ovarian Sertoli-Leydig cell tumor, in the setting of germline DICER1 syndrome**

*Embryonal rhabdomyosarcoma of the cervix (2011), metachronous second primary embryonal rhabdomyosarcoma of the cervix (2017) and Sertoli-Leydig cell tumor of ovary (2017) with heterologous mucinous epithelial differentiation*

## Comments:

The original diagnosis of the 2011 cervical mass was that of a cervical rhabdomyosarcoma with both embryonal and alveolar patterns. However, molecular cytogenetic studies were negative for *PAX3* (2q36.1) and for *FOXO1* (13q14) rearrangement. The presence of

islands of cartilaginous differentiation was not appreciated and possible syndrome-association was not considered in 2011 (not too surprising as *DICER1* gene mutation causing pleuropulmonary blastoma was described only in 2009 by Hill et al., and various other lesions/tumors as manifestation of DICER1 syndrome described later on).

Rhabdomyosarcoma is the most common soft tissue sarcoma of childhood. Unlike soft tissue sarcomas of adulthood, rhabdomyosarcomas in children preferentially occur in the head and neck region (35%) and genitourinary tract (25%). In the genital tract, the vagina is the most common site (Kirsch CH et al. 2014). Rhabdomyosarcomas of the uterine cervix are exceedingly rare, and documented only in small case series and reports (Dehner LP et al. 2012; Daya DA, Scully RE 1988). Unlike vaginal rhabdomyosarcomas, they tend to occur in older children, adolescents and young adults, with a mean age of 13-18 years old at the time of presentation. As the number of reported cases of cervical rhabdomyosarcomas have grown over the years, the link between this rare tumor to another rare disorder, DICER1 syndrome, has become more solidified (Foulkes WD et al, 2011; Witkowski L et al, 2016; Bennett et al, 2021).

DICER1 syndrome is a familial tumor susceptibility syndrome first described in 2009 in patients with pleuropulmonary blastoma (Hill DA et al. 2009). It is caused by a germline mutation in the *DICER1* gene and is inherited in an autosomal dominant manner. The penetrance is variable, reported to be around 15% for any of the associated manifestations, with fewer than half of mutation carriers affected (Slade I et al, 2011). *DICER1* gene encodes for a highly conserved, multi-domain RNase III enzyme that plays a critical role in the biogenesis of microRNA, which help to regulate gene expression. Most gene mutations involved in DICER1 syndrome lead to an abnormally short DICER protein that is unable to aid in the production of microRNA; without appropriate regulation of microRNA, genes are more likely to be expressed abnormally, potentially leading to abnormal cellular proliferation, differentiation and tumor formation (Foulkes WD et al, 2014).

The mutation pattern in DICER1 syndrome is unique among tumor suppressor genes in that the "first hit" in the germline is widely distributed, typically truncating, inactivation mutations, whereas the "second hit" consists of hotspot somatic missense mutations highly focused to exon 24 and 25, which encode the RNAase IIIb domain, responsible for cleaving precursor microRNAs to their final mature length. These alterations result in the formation of a mutant DICER1 protein with altered microRNA processing ability, rather than loss of the protein, as seen in other tumor suppressor genes such as retinoblastoma. Heterozygous germline *DICER1* mutations, in the context of tissue-specific mutations, on the other allele, predispose a patient to various tumors. The most well-defined association

is pleuropulmonary blastoma, with approximately 66% of patients testing positive for a germline pathogenetic variant in *DICER1*. Other high-frequency phenotypes include nodular hyperplasia of thyroid, cystic nephroma of the kidney, Sertoli-Leydig cell tumor of the ovary, and cervical embryonal rhabdomyosarcoma. Sertoli-Leydig cell tumors are the most common gynecological manifestation of *DICER1* syndrome; approximately 56-88% of cases and *virtually all of moderately and poorly differentiated types*, have been shown to harbor germline mutations in *DICER1*, compared to approximately 20-30% for cervical rhabdomyosarcomas (Garg K et al, 2018, Stewart CJR et al, 2016). Less frequent phenotypes include nasal chondromesenchymal hamartoma, ciliary body medulloepithelioma, and pineoblastoma/pituitary blastoma.

*DICER1*-related extracranial rhabdomyosarcomas primarily involve the female genital tract. Within the uterus (cervix or corpus), embryonal rhabdomyosarcomas exhibit morphologic overlap with adenocarcinomas, especially when adenocarcinoma shows rhabdomyoblastic differentiation or sarcomatous overgrowth. There are published cases of cervical embryonal rhabdomyosarcoma having been misdiagnosed as adenocarcinoma (de Kock L et al, 2020). *DICER1* mutation has also been described in genuine Mullerian adenocarcinomas (Bean GR et al, 2018), though with less frequency than in cervical rhabdomyosarcomas.

There is a high association of cervical embryonal rhabdomyosarcoma and Sertoli-Leydig cell tumor of the ovary with *DICER1* syndrome; hence, such diagnoses should prompt genetic risk assessment referral. An additional interesting finding in the presented case is the development of a metachronous second primary cervical rhabdomyosarcoma with a different *DICER1* alteration (Cowan M et al, 2018).

## References:

1. Bennett et al. Embryonal rhabdomyosarcoma of the uterine corpus: a clinicopathological and molecular analysis of 21 cases highlighting a frequent association with *DICER1* mutations. *Modern Pathol.* 2021; Sep;34(9):1750-1762
2. De Kock L et al. Significantly greater prevalence of *DICER1* alterations in uterine embryonal rhabdomyosarcoma compared to adenocarcinoma. *Modern Pathol.* 2020 Jun;33(6):1207-1219
3. Garg K et al. Uncommon hereditary gynaecological tumour syndromes: pathological features in tumours that may predict for germline mutation. *Pathology.* 2018 Feb;50(2):238-256
4. Bean GR et al. *DICER1* mutations are frequent in mullerian adenocarcinomas and are independent of rhabdomyosarcomatous differentiation. *Mod Pathol.* 2018 Feb;32(2):280-289

5. Cowan M et al. Second primary rhabdomyosarcoma of the uterine cervix presenting with synchronous ovarian Sertoli-Leydig cell tumor: An illustrative case of DICER1 syndrome. *Gynecol Oncol Rep.* 2018 Jun 15;25:94-97
6. Stewart CJR et al. Gynecologic manifestations of the DICER1 syndrome. *Surg Pathol Clin.* 2016 Jun;9(2):227-41
7. Witkowski L et al. Recently characterized molecular events in uncommon gynecological neoplasms and their clinical importance. *Histopathology.* 2016 Dec;69(6):903-913
8. Kirsch CH et al. Outcome of female pediatric patients diagnosed with genital tract rhabdomyosarcoma based on analysis of cases registered in SEER database between 1973-2006. *Am J Clin Oncol.* 2014 Feb;37(1):47-50
9. Foulkes WD et al. DICER1: mutations, microRNAs and mechanisms. *Nat Rev Cancer.* 2014 Oct;14(10):662-72
10. Foulkes WD et al. Extending the phenotypes associated with DICER1 mutations. *Hum Mutat.* 2011 Dec;32(12):1381-4
11. Dehner LP et al. Embryonal rhabdomyosarcoma of the uterine cervix: a case report of 14 cases and a discussion of its unusual clinicopathological associations. *Mod Pathol.* 2012 Apr;25(4):602-614
12. Slade I et al. DICER1 syndrome: clarifying the diagnosis, clinical features and management implications of a pleiotropic tumor predisposition syndrome. *J Med Gen.* 2011 Apr;48(4):273-278
13. Hill DA et al. DICER1 mutations in familial pleuropulmonary blastoma. *Science.* 2009 Aug 21;325(5943):965
14. Daya DA, Scully RE. Sarcoma botryoides of the uterine cervix in young women: a clinicopathological study of 13 cases. *Gynecol Oncol.* 1988 Mar;29(3):290-304

## Case 79

### Clinical History

A 61-year-old female patient developed a 9.0 x 7.0 x 5.0 cm measuring neoplasm at the vulva that has been marginally excised.

### Pathological Findings

Histologically, a variable cellular neoplasm is seen that is composed of two components that are either irregularly admixed or sharply demarcated. One component is composed of bland, spindle-shaped tumour cells associated with numerous narrow and dilated vessels set in a collagenous, focally myxoid stroma with scattered mast cells. In addition, there is an abrupt or gradual transformation to a cellular tumour component. The cellular tumour component is composed of highly atypical spindle-shaped, polygonal and pleomorphic tumour cells including numerous multinucleated tumour giant cells. Tumour cell nuclei are enlarged, irregular and hyperchromatic. In some areas lipogenic cells with variations in size and shape and enlarged hyperchromatic nuclei are seen. Immunohistochemically, tumour cells stain positively for CD34, whereas ASMA, desmin, MDM2, CDK4 and p16 are all negative.

### Diagnosis: Cellular Angiofibroma with multifocal sarcomatous transformation

### Comments

Cellular angiofibroma represents a rare mesenchymal neoplasm occurring predominantly in the superficial soft tissue of the genital region of middle-aged adults. Cellular angiofibroma affects female and male patients (here these lesions have been reported also as "angiofibroblastoma-like tumour") but male patients tend to be older and lesions in males tend to be larger than in female patients. Most patients present with a well-circumscribed, painless mass often with a long preoperative duration. The well-circumscribed neoplasms are composed of short, intersecting fascicles of bland, spindle-shaped tumour cells and numerous small to medium sized, thick-walled, often hyalinized blood vessels. Tumour cells are set in a hyalinized or edematous stroma with scattered mast cells, and in many cases a lipomatous component is seen. Mitoses are seen but nuclear

atypia and necrosis are absent. Immunohistochemically, spindled tumour cells stain positively for CD34 in about two third of the cases, whereas ASMA and desmin are more rarely and rather focally positive. An expression of estrogen and progesterone receptors may be seen, whereas S-100 protein and cytokeratins are negative. Tumour cells show loss of expression of Rb1, and loss of chromosome 13q14 similar as in spindle cell lipoma and mammary myofibroblastoma has been reported. Very rarely, cases of cellular angiofibroma contain an atypical or sarcoma-like component with features of pleomorphic sarcoma, atypical lipomatous tumour or pleomorphic liposarcoma. In addition to strong and diffuse p16 expression TP53 gene mutations have been detected in several cases. Despite worrisome morphological features no increased rate of local recurrences or metastases have been reported, and the prognostic significance of this phenomenon is uncertain.

In the past malignant transformation in benign mesenchymal tumours has been denied with the exception of transformation of neurofibroma to malignant peripheral nerve sheath tumour especially in patients with known neurofibromatosis type 1. However, in the last decades it has been shown convincingly, that, although rare, malignant transformation may occur also in other mesenchymal neoplasms as it is the case for angiosarcoma arising within preexisting haemangioma or schwannoma, liposarcoma arising in preexisting lipoma or malignant transformation in dermatofibroma.

## References

1. Chan Chien YC, Mokanszki A, Huang HY et al. First glance of molecular profile of atypical cellular angiofibroma/cellular angiofibroma with sarcomatous transformation by next generation sequencing. *Diagnostics Basel* 2020; 10 (1)
2. Chen E, Fletcher CDM. Cellular angiofibroma with atypia or sarcomatous transformation: clinicopathologic analysis of 13 cases. *Am J Surg Pathol* 2010; 34: 707-714
3. Clarke LE, Julian KG, Clarke JT, Ioffreda MD. Reactive angioendotheliomatosis in association with a well-differentiated angiosarcoma. *Am J Dermatopathol* 2005; 27: 422-427
4. Creytens D. Cellular angiofibroma with sarcomatous transformation showing pleomorphic liposarcoma-like and atypical lipomatous tumour-like features. *Am J Dermatopathol* 2016; 38: 712-714
5. Damiani S, Corti B, Neri F, Collina G, Bertoni F. Primary angiosarcoma of the parotid gland arising from benign congenital hemangioma. *Oral Surg Oral Med Oral Pathol Oral Radiol Endod* 2003; 96: 66-69

6. Dei Tos AP, Doglioni C, Piccinin S, Sciot R, Furlanetto A, Boiocchi M, Dal Cin P, Maestro R, Fletcher CD, Tallini G. Coordinated expression and amplification of the MDM2, CDK4, and HMGI-C genes in atypical lipomatous tumours. *J Pathol* 2000; 190: 531-536
7. Doyle LA, Fletcher CD. Metastasizing "benign" cutaneous fibrous histiocytoma: a clinicopathologic analysis of 16 cases. *Am J Surg Pathol* 2013; 37: 484-495
8. Flucke U, Han J, van Krieken JM, Mentzel T. Cellular angiofibroma: analysis of 25 cases emphasizing its relationship to spindle cell lipoma and mammary-type myofibroblastoma. *Mod Pathol* 2011; 24: 82-89
9. Kandil DH, Kida M, Laub DR, Cooper K. Sarcomatous transformation in a cellular angiofibroma: a case report. *J Clin Pathol* 2009; 62: 945-947
10. Kuhnen C, Mentzel T, Lehnhardt M, Homann HH, Sciot R, Debiec-Rychter M. Lipoma and atypical lipomatous tumor within the same neoplasia: Evidence for a continuous transition. *Pathologie* 2010; 31: 129-134
11. Laskin WB, Fetsch JF, Mostofi FK. Angiomyofibroblastoma-like tumor of the male genital tract: analysis of 11 cases with comparison to female angiomyofibroblastoma and spindle cell lipoma. *Am J Surg Pathol* 1998; 22: 6-16
12. Mentzel T, Katenkamp D. Intranural angiosarcoma and angiosarcoma arising in benign and malignant peripheral nerve sheath tumours: clinicopathological and immunohistochemical analysis of four cases. *Histopathology* 1999; 35: 114-120
13. Mentzel T. Biological continuum of benign, atypical, and malignant mesenchymal neoplasms - does it exist? *J Pathol* 2000; 190: 523-525
14. Mentzel T, Wiesner T, Cerroni L, Hantschke M, Kutzner H, Rütten A, Häberle M, Bisceglia M, Chibon F, Coindre JM. Malignant dermatofibroma: clinicopathological, immunohistochemical, and molecular analysis of seven cases. *Mod Pathol* 2013; 26: 256-267
15. Nathenson MJ, Molavi D, Aboulafia A. Angiosarcoma arising in a patient with a 10-year-old hemangioma. *Case Rep Oncol Med* 2014; 185323
16. Nucci MR, Granter SR, Fletcher CDM. Cellular angiofibroma: a benign neoplasm distinct from angiomyofibroblastoma and spindle cell lipoma. *Am J Surg Pathol* 1997; 21: 636-644
17. Ptaszynski K, Szumera-Cieckiewicz A, Bartczak A. Cellular angiofibroma with atypia or sarcomatous transformation - case description with literature review. *Pol J Pathol* 2012; 63: 207-211
18. Rossi S, Fletcher CDM. Angiosarcoma arising in hemangioma/vascular malformation: report of four cases and review of the literature. *Am J Surg Pathol*. 2002; 26: 1319-1329

## Case 80

### Case presentation:

28-year-old male with abdominal pain who was found to have retroperitoneal mass. Excision of the mass was performed. The patient was treated with 3 different lines of chemotherapy, however, he never achieved complete remission and died of disease approximately 2 years after diagnosis.

### Gross description:

Resected mass was 12x10.5x9 cm and weighed 770 gm, with an attached 10 cm segment of bowel. On sectioning, mass appeared completely encapsulated and was tan and predominantly solid with multiple areas of hemorrhage, cystic degeneration and prominent necrosis. Some of the cystic spaces were filled with a clear serous fluid. Seven lymph nodes were found and were not involved by tumor.

### Microscopic description and immunohistochemical stains:

Morphologically, tumor was composed of sheets of pleomorphic histiocytic cells with round to slightly irregular nuclei, open chromatin, small nucleoli, and abundant eosinophilic cytoplasm. Scattered inflammatory cells, including small lymphocytes and plasma cells are seen admixed with malignant cells. The tumor infiltrated full thickness of the bowel wall.

By immunohistochemistry, the tumor was positive for CD4, CD68, PU.1, lysozyme, CD163, CD33, clusterin (weak), fascin (weak), and were negative for cytokeratin cocktail, melan A, S100, CD1a, CD45, CD20, CD3, CD43, CD21, CD23, CD117, myeloperoxidase, CD34, CD30, CD15, ALK-1, BRAF, chromogranin, OCT-4, and SALL-4.

Molecular studies were negative for *BRAF* V600E and V600K mutations. FISH study was negative for *BRAF* (7q34) rearrangement.

## Discussion:

Histiocytic sarcoma (HS) is a rare malignant neoplasm derived from histiocytes. It most commonly occurs in the sixth decade of life with a broad age range, and no gender predominance. Most common sites of involvement are extranodal locations such as soft tissue, skin and gastrointestinal tract, but it can also involve lymph nodes. Histologically, the malignant cells are usually large, reminiscent of histiocytic with mild to severe pleomorphism. Admixed, there are inflammatory cells (small lymphocytes, histiocytes, plasma cells, and eosinophils). Immunophenotype is typical of histiocytic neoplasm including the positivity for CD4, CD11c, CD14, CD63, CD163, lysozyme, and CD45. S100 is positive in a subset of cases. Subset of cases carry *BRAF* V600E mutation.

Differential diagnosis includes hematopoietic tumors (large cell lymphomas of B and T cell lineage, classic Hodgkin lymphoma, myeloid sarcoma), dendritic cell neoplasms (follicular and interdigitating dendritic cell sarcoma), Langerhans cell sarcoma, Rosai-Dorfman disease. Furthermore, non-hematopoietic neoplasm such as carcinoma and melanoma with histiocytic features should be excluded. Mesenchymal neoplasms that should be considered in differential diagnosis include inflammatory myofibroblastic tumor, liposarcoma (inflammatory or dedifferentiated), myxoinflammatory fibroblastic sarcoma, histiocytic variant of angiosarcoma, etc.

Patients are usually treated with a CHOP (cyclophosphamide, doxorubicin, vincristine, and prednisone) chemotherapy protocol, which is used for variety of lymphoma.

Histiocytic sarcoma is an aggressive neoplasm with median survival of approximately 2.5 years.

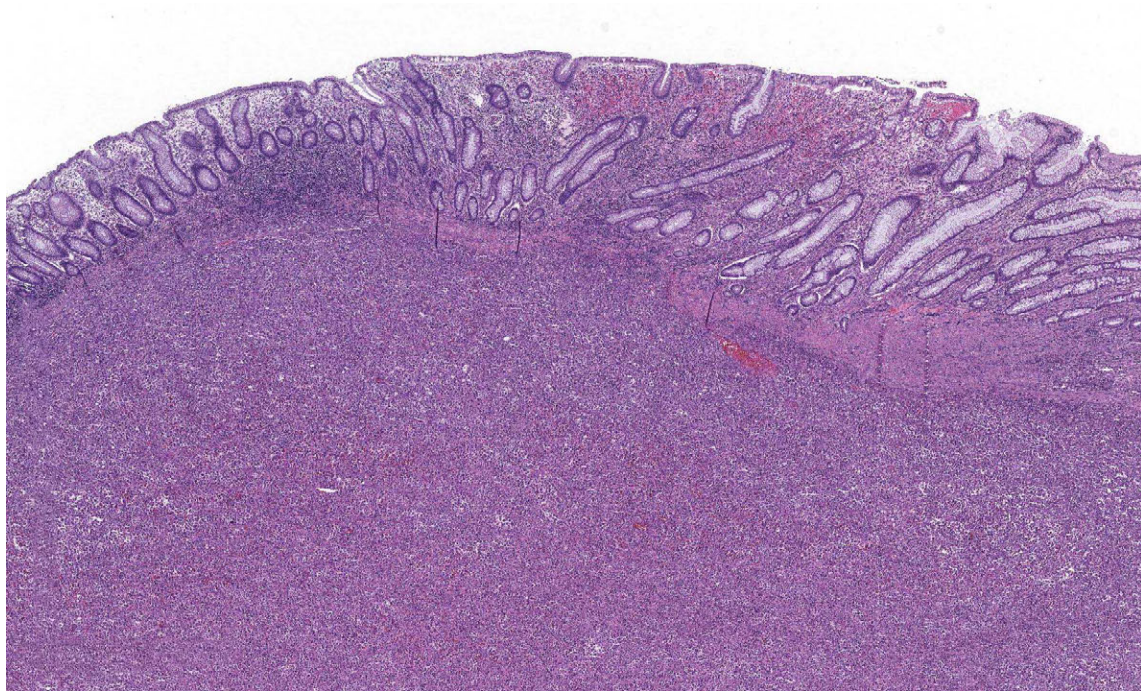


**Figure 1.** Colon infiltrated by histiocytic sarcoma

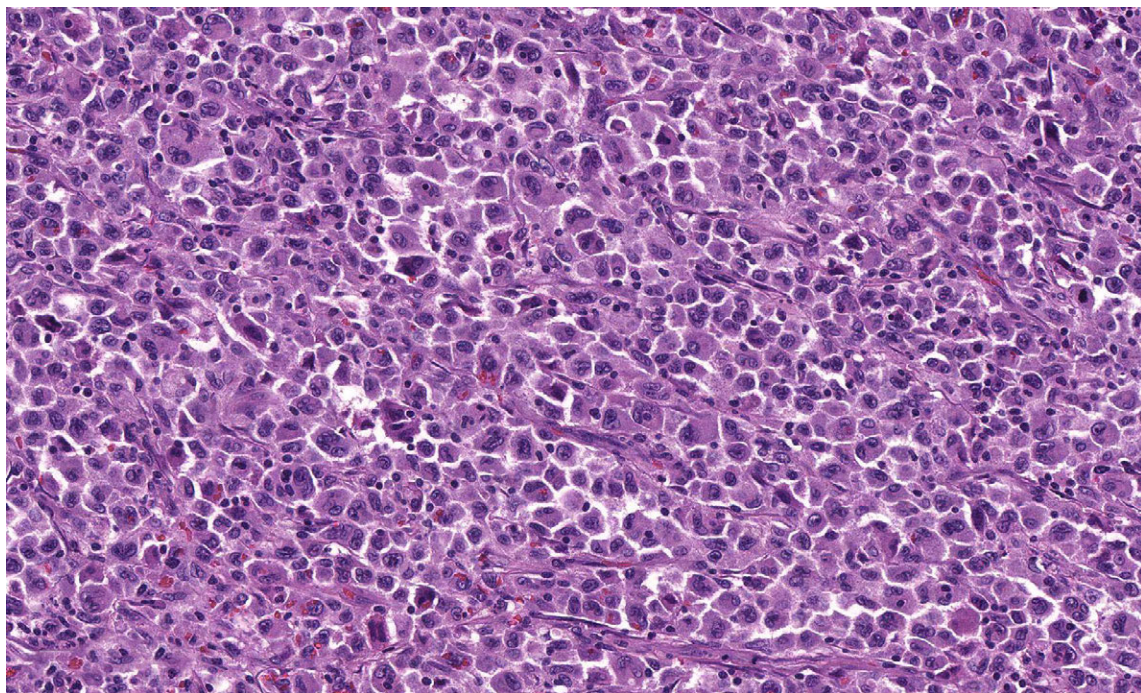


**Figure 2.** Sheets of malignant histiocytic cells

## References:

1. Hornick JL, Jaffe ES, Fletcher CDM. Extranodal histiocytic sarcoma: clinicopathologic analysis of 14 cases of a rare epithelioid malignancy. *Am J Surg Pathol*. 2004; 28 (9): 1133- 1144.
2. Swerdlow SH, Campo E, Harris NL, et al. (eds). *WHO Classification of Tumours of Haematopoietic and Lymphoid Tissues*. Revised 4th ed. Lyon, France: International Agency for Research on Cancer; 2017.
3. Facchetti F, Pileri SA, Lorenzi L, et al. Histiocytic and dendritic cell neoplasms: what have we learnt by studying 67 cases. *Virchows Arch*. 2017; 471 (4): 467- 489.

# Case 81

Contributed by Franco Fedeli, MD, Malpighi Pathology Academy

---

[www.malpighipathologyacademy.org](http://www.malpighipathologyacademy.org)

## Clinical History:

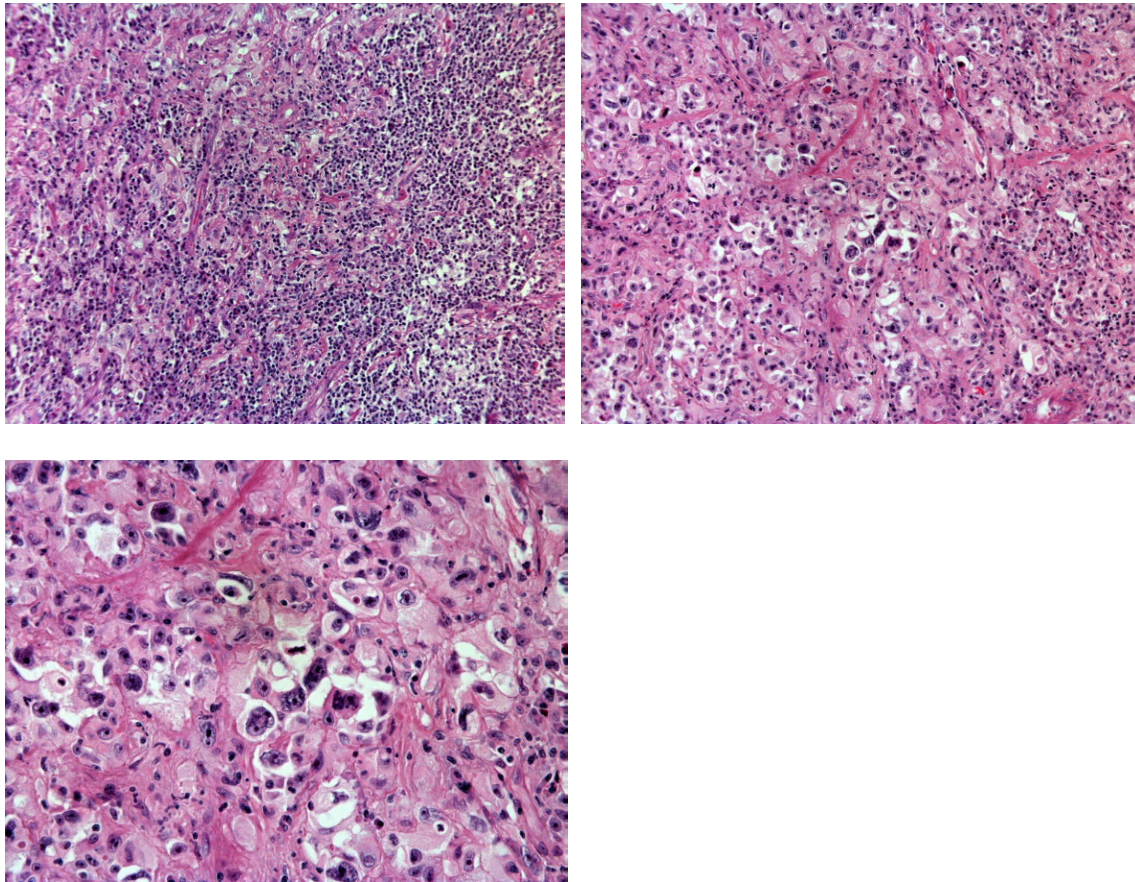
71 years old male with tumor in the left kidney of 6,5 cm in size. The patient lacked family history of sickle cell trait or other hemoglobinopathies. Radical nephrectomy with regional lymphadenectomy was performed. Multiple metastatic sites were apparent at bone CT scan. The patient died 3 months later.

## Macroscopic findings:

At gross examination, the specimen revealed a yellowish-white mass with extensive central cystic degeneration in the upper renal pole, 5.5 cm in diameter, with invasion of both perirenal and renal sinus fat.

## Histological Findings:

The architectural pattern was non-glandular, including areas of solid, nested and cord like growth. The cytology of the tumor was composed by cells with rhabdoid and spindle sarcomatoid differentiation. Giant pleomorphic and multinucleate tumor cells were present in some foci. Stroma showed marked inflammatory reaction. In other areas, pools of myxoid extracellular fluid were seen among sheets of plump, atypical cells with prominent nucleoli. Rare hyaline globules were also present. Focally, metaplastic bone was identified.



## Immunohistochemical Findings:

The tumor cells were positive for Vimentin, Cytokeratin (Cam5.2), EMA, CD10, PAX8 and OCT 3/4 and negative for Racemase, GATA 3. Fumarate Hydratase expression was diffusely retained. In addition the tumor cells had shown loss of SMARCB1 (INI-1).

## Diagnosis: Renal cell carcinoma, unclassified with medullary phenotype

## Comments:

Renal medullary carcinoma is a renal neoplasms occurring in association with sickle cell trait and, less frequently, with sickle cell disease. The existence of renal medullary carcinoma without a concomitant hemoglobinopathy is a controversial subject (1,2). According to the 4th edition of the World Health Organization's "Classification of Tumours of the Urinary System and Male Genital Organs", high-grade renal adenocarcinoma with

histologic and immunophenotypic findings consistent with those of medullary carcinoma occurring in a patient with no evidence of a hemoglobinopathy, is best categorized as unclassified renal cell carcinoma (RCC) with medullary phenotype. Sirohi et al (2) describe a series of 5 such patients (the second case is presented here) with no history of sickle cell disease or trait in which all tumors showed a poorly differentiated renal adenocarcinoma with aggressive behavior and morphologic and immunophenotypic characteristics identical to those of renal medullary carcinoma.

These are tumors commonly present in young individuals, mostly in the third decade, with a range of 5 to 69 years. They show a male predilection with a male-to-female ratio of 2:1. Renal medullary carcinoma is an aggressive tumor, frequently with metastatic lesions at the time of presentation and dismal outcomes, with the longest reported survival of 15 months.

Histologic studies show poorly differentiated, high-grade infiltrative adenocarcinomas, frequently with reticular or microcystic patterns reminiscent of yolk sac tumor, and cribriform, adenoid cystic-like, solid, or trabecular architecture eliciting a desmoplastic stromal response. They often show areas with rhabdoid cytomorphology and stromal inflammation is common. Hemorrhage and extensive necrosis are frequently present. The necrosis pattern is most commonly suppurative, resembling microabscesses within the epithelial aggregates.

Renal medullary carcinoma may be positive for CAM 5.2, pancytokeratin (AE1/AE3), vimentin, PAX-8, EMA, hypoxia-inducible factor (HIF), and vascular endothelial growth factor (VEGF). More recently, staining for a germ cell tumor marker, octamer-binding transcription factor 3/4 (OCT3/4), has shown positivity in most cases. OCT3/4 staining was notably absent in all cases of collecting duct carcinoma (CDC) and urothelial carcinoma (3,4). Renal medullary carcinoma has been shown to have a complete loss of tumor suppressor gene integrase interactor 1 (INI1), being similar to that seen in the malignant rhabdoid tumor of the kidney (5). In contrast, all renal cell carcinoma or urothelial cell carcinomas, including those with rhabdoid features, expressed INI1.

## References

1. Colombo P, Smith SC, Massa S, Renne SL, Brambilla S, Peschechera R, et al. Unclassified renal cell carcinoma with medullary phenotype versus renal medullary

- carcinoma: lessons from diagnosis in an Italian man found to harbor sickle cell trait. *Urol Case Rep.* 2015;3(6):215-8.
2. Sirohi D, Smith SC, Ohe C et al. Renal cell carcinoma, unclassified with medullary phenotype: Poorly differentiated adenocarcinomas overlapping with renal medullary carcinoma. *Hum Pathol* 2017; 67: 134-45.
  3. Ohe C, Smith SC, Sirohi D et al. Reappraisal of morphologic differences between renal medullary carcinoma, collecting duct carcinoma, and fumarate hydratase-deficient renal cell carcinoma. *Am J Surg Pathol* 2018; 42: 279-92.
  4. Amin MB, Smith SC, Agaimy A et al. Collecting duct carcinoma versus renal medullary carcinoma: An appeal for nosologic and biological clarity. *Am J Surg Pathol* 2014; 38: 871-74.
  5. Cheng JX, Tretiakova M, Gong C, Mandal S, Krausz T, Taxy JB. Renal medullary carcinoma: Rhabdoid features and the absence of INI1 expression as markers of aggressive behavior. *Mod Pathol* 2008; 21: 647-52.

